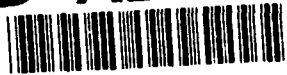


AD-A239 949



2

NAVAL POSTGRADUATE SCHOOL

Monterey, California



DTIC
ELECTE
AUG 27 1991
S B D

THESIS

NUMERICAL INVESTIGATION OF THE
EFFECT OF LEADING EDGE GEOMETRY
ON DYNAMIC STALL OF AIRFOILS

by

Lt. Col. Steven P. Grohsmeyer
September 1990

Thesis Advisor: Dr. J. A. Ekaterinaris
Thesis Co-Advisor: Dr. M. F. Platzer

Approved for public release; distribution is unlimited

91 8 26 010

10

91-08868



UNCLASSIFIED

SECURITY CLASSIFICATION OF THIS PAGE

REPORT DOCUMENTATION PAGE				Form Approved OMB No 0704-0188	
1a REPORT SECURITY CLASSIFICATION Unclassified			1b RESTRICTIVE MARKINGS		
2a SECURITY CLASSIFICATION AUTHORITY			3 DISTRIBUTION/AVAILABILITY OF REPORT		
2b DECLASSIFICATION/DOWNGRADING SCHEDULE			Approved for public release; distribution is unlimited		
4. PERFORMING ORGANIZATION REPORT NUMBER(S)			5 MONITORING ORGANIZATION REPORT NUMBER(S)		
6a NAME OF PERFORMING ORGANIZATION Naval Postgraduate School		6b OFFICE SYMBOL (If applicable) 31	7a NAME OF MONITORING ORGANIZATION Naval Postgraduate School		
6c ADDRESS (City, State, and ZIP Code) Monterey, CA 93943-5000			7b ADDRESS (City, State, and ZIP Code) Monterey, CA 93943-5000		
8a. NAME OF FUNDING / SPONSORING ORGANIZATION		8b. OFFICE SYMBOL (If applicable)	9 PROCUREMENT INSTRUMENT IDENTIFICATION NUMBER		
8c. ADDRESS (City, State, and ZIP Code)			10 SOURCE OF FUNDING NUMBERS		
			PROGRAM ELEMENT NO	PROJECT NO	TASK NO
					WORK UNIT ACCESSION NO
11 TITLE (Include Security Classification) NUMERICAL INVESTIGATION OF THE EFFECT OF LEADING EDGE GEOMETRY ON THE DYNAMIC STALL OF AIRFOILS					
12 PERSONAL AUTHOR(S) GROHSMeyer, STEVEN P.					
13a TYPE OF REPORT Master's Thesis		13b TIME COVERED FROM _____ TO _____		14 DATE OF REPORT (Year, Month, Day) 1990 September	
				15 PAGE COUNT 182	
16 SUPPLEMENTARY NOTATION The views expressed in this thesis are those of the author and do not reflect the official policy or position of the Department of Defence or the U.S. Government.					
17 COSATI CODES			18 SUBJECT TERMS (Continue on reverse if necessary and identify by block number)		
FIELD	GROUP	SUB-GROUP	Dynamic Stall, Oscillating Airfoil, Pitching Airfoil, Leading Edge Geometry, Pressure Gradient		
19 ABSTRACT (Continue on reverse if necessary and identify by block number) The dynamic stall of rapidly pitching and oscillating airfoils is investigated by the numerical solution of the full compressible unsteady two-dimensional Navier-Stokes equa- tions using an alternating-direction-implicit scheme. The flow is assumed to be fully turbulent, and the turbulent stresses are modelled by the Baldwin-Lomax eddy viscosity model. Three airfoils (NACA 0012, NACA 0012-33, and NACA 0012-63) are analyzed for the purpose of examining the influence of leading-edge geometry on unsteady flow separation. It is found that a larger leading edge radius, thicker contouring of the forward part of the airfoil, or increasing reduced frequency results in delaying flow separation and formation of the dynamic stall vortex to a higher angle of attack, yielding higher peak C _L . Within the scope of this study, the pressure gradient encountered by the flow at initial separation is found to be independent of reduced frequency and freestream speed. The critical pressure gradient is dependent on leading edge radius and increases for decreasing leading edge radius.					
20 DISTRIBUTION/AVAILABILITY OF ABSTRACT <input checked="" type="checkbox"/> UNCLASSIFIED/UNLIMITED <input type="checkbox"/> SAME AS PPT <input type="checkbox"/> DTIC USERS			21 ABSTRACT SECURITY CLASSIFICATION Unclassified		
22a NAME OF RESPONSIBLE INDIVIDUAL M.F. Platzler			22b TELEPHONE (Include Area Code) (408)646-2058		22c OFFICE SYMBOL Code 31AAPL

Approved for public release; distribution is unlimited.

Numerical Investigation of the
Effect of Leading Edge Geometry on
Dynamic Stall of Airfoils

by

Steven P. Grohsmeyer
Lieutenant Colonel, United States Marine Corps
E.S., Illinois Benedictine College, 1973

Submitted in partial fulfillment of the
requirements for the degrees of

AERONAUTICAL ENGINEER

and

MASTER OF SCIENCE IN AERONAUTICAL ENGINEERING

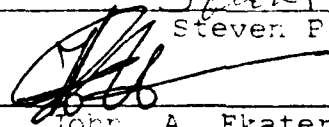
from the

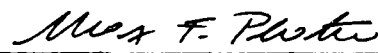
NAVAL POSTGRADUATE SCHOOL
September 1990

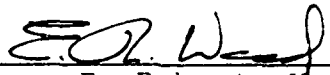
Author:


Steven P. Grohsmeyer

Approved by:


John A. Ekaterinaris, Thesis Advisor


Max F. Platzer, Thesis Co-Advisor


E. Roberts Wood, Chairman,
Department of Aeronautics and Astronautics


Richard S. Elster, Dean of Instruction

ABSTRACT

The dynamic stall of rapidly pitching and oscillating airfoils is investigated by the numerical solution of the full compressible unsteady two-dimensional Navier-Stokes equations using an alternating-direction-implicit scheme. The flow is assumed to be fully turbulent, and the turbulent stresses are modelled by the Baldwin-Lomax eddy viscosity model. Three airfoils (NACA 0012, NACA 0012-33, and NACA 0012-63) are analyzed for the purpose of examining the influence of leading-edge geometry on unsteady flow separation. It is found that a larger leading edge radius, thicker contouring of the forward part of the airfoil, or increasing reduced frequency results in delaying flow separation and formation of the dynamic stall vortex to a higher angle of attack, yielding higher peak C_L . Within the scope of this study, the pressure gradient encountered by the flow at initial separation is found to be independent of reduced frequency and freestream speed. The critical pressure gradient is dependent on leading edge radius and increases for decreasing leading edge radius.

TABLE OF CONTENTS

I. INTRODUCTION	1
A. BACKGROUND	1
B. PURPOSE	5
C. AIRFOIL SELECTION	6
II. GOVERNING EQUATIONS	9
A. CONTINUITY EQUATION	9
B. THE MOMENTUM (NAVIER-STOKES) EQUATIONS	10
C. THE ENERGY EQUATION	14
D. CONSERVATION LAW FORM OF THE GOVERNING EQUATIONS	17
III. NUMERICAL APPROACH	22
A. NUMERICAL PROCEDURE	22
B. THE BEAM-WARMING ALGORITHM	22
C. THE BALDWIN-LOMAX EDDY-VISCOSITY MODEL	31
D. BOUNDARY CONDITIONS	33
E. GRID GENERATION	34
1. Grid Generation Methods	34
2. Algebraic Grid Generation Method	35
IV. RESULTS AND DISCUSSION	40
A. INVESTIGATION METHOD	40
B. LIFT BEHAVIOR	43
1. Harmonically Oscillating Airfoil	43
2. Rapidly Pitching Airfoil	46

C.	VORTEX FLOW DEVELOPMENT	59
1.	Rapidly Pitching Airfoil	59
2.	Harmonically Oscillating Airfoil	91
D.	REDUCED FREQUENCY EFFECT	96
E.	EFFECT OF FREESTREAM MACH NUMBER	99
F.	PRESSURE GRADIENT AT FLOW SEPARATION	102
V.	CONCLUSIONS AND RECOMMENDATIONS	109
A.	CONCLUSIONS	109
B.	RECOMMENDATIONS	109
	LIST OF REFERENCES	111
	APPENDIX A - USING THE PROGRAM	113
	APPENDIX B - PROGRAM NSE2D.F	121
	APPENDIX C - PROGRAM AIRFGR.F	157
	INITIAL DISTRIBUTION LIST	167

LIST OF TABLES

TABLE 1.	AIRFOIL COORDINATES	7
TABLE 2.	RAPIDLY PITCHING AIRFOIL CASES, $Re = 4 \times 10^6$	40
TABLE 3.	PEAK LIFT COEFFICIENTS	42

LIST OF FIGURES

Figure 1.	Events of Dynamic Stall on NACA 0012 Airfoil	3
Figure 2.	Airfoil Profile Comparison	8
Figure 3.	Forces on a Fluid Element	11
Figure 4.	Strain on a Fluid Element	12
Figure 5.	Energy Fluxes on Fluid Element	15
Figure 6.	Airfoil Grid Unwrapping	36
Figure 7.	N0012 Global Grid	37
Figure 8.	N0012-63 Local Grid	38
Figure 9.	N0012-33 Local Grid	39
Figure 10.	Lift Behavior, NACA 0012, $M=0.3$, $k=0.1$. . .	44
Figure 11.	Lift Behavior, NACA 0012, $M=0.3$, $k=0.2$. . .	45
Figure 12.	Lift Comparison, $M=0.3$, $k=0.01$	47
Figure 13.	Lift Comparison, $M=0.3$, $k=0.02$	48
Figure 14.	Lift Comparison, $M=0.4$, $k=0.01$	49
Figure 15.	Lift Comparison, $M=0.4$, $k=0.02$	50
Figure 16.	Instantaneous Streamlines, NACA 0012, $M=0.4$, $k=0.01$, $\alpha=17^\circ$	54
Figure 17.	Leading Edge Instantaneous Streamlines, NACA 0012, $M=0.4$, $k=0.01$, $\alpha=17^\circ$	55
Figure 18.	Instantaneous Streamlines, NACA 0012-63, $M=0.4$, $k=0.01$, $\alpha=17^\circ$	56
Figure 19.	Leading Edge Instantaneous Streamlines, NACA 0012-63, $M=0.4$, $k=0.01$, $\alpha=17^\circ$	57

Figure 20.	Instantaneous Streamlines, NACA 0012-33, M=0.4, k=0.01, $\alpha=17^\circ$	58
Figure 21.	Velocity Field, NACA 0012-63, M=0.4, k=0.01, $\alpha=14.0^\circ$	62
Figure 22.	Vorticity Contours, NACA 0012-63, M=0.3, k=0.01, $\alpha=14.0^\circ$	63
Figure 23.	Velocity Field, NACA 0012-63, M=0.4, k=0.01, $\alpha=16.0^\circ$	64
Figure 24.	Vorticity Contours, NACA 0012-63, M=0.4, k=0.01, $\alpha=16.0^\circ$	65
Figure 25.	Velocity Field, NACA 0012-63, M=0.4, k=0.01, $\alpha=17.0^\circ$	66
Figure 26.	Vorticity Contours, NACA 0012-63, M=0.3, k=0.01, $\alpha=17.0^\circ$	67
Figure 27.	Velocity Field, NACA 0012-63, M=0.4, k=0.01, $\alpha=18.0^\circ$	68
Figure 28.	Velocity Field, NACA 0012-63, M=0.4, k=0.01, $\alpha=19.0^\circ$	69
Figure 29.	Vorticity Contours, NACA 0012-63, M=0.4, k=0.01, $\alpha=19.0^\circ$	70
Figure 30.	Velocity Field, NACA 0012-63, M=0.4, k=0.01, $\alpha=20.0^\circ$	71
Figure 31.	Vorticity Contours, NACA 0012-63, M=0.3, k=0.01, $\alpha=20.0^\circ$	72
Figure 32.	Velocity Field, NACA 0012-63, M=0.4, k=0.01, $\alpha=21.0^\circ$	73
Figure 33.	Vorticity Contours, NACA 0012-63, M=0.4, k=0.01, $\alpha=21.0^\circ$	74
Figure 34.	Surface Pressure, NACA 0012-63, M=0.4, k=0.01, $\alpha=14.0^\circ$	75
Figure 35.	Surface Pressure, NACA 0012-63, M=0.4, k=0.01, $\alpha=16.0^\circ$	76
Figure 36.	Surface Pressure, NACA 0012-63, M=0.4, k=0.01, $\alpha=17.0^\circ$	77

Figure 37.	Surface Pressure, NACA 0012-63, $M=0.4$, $k=0.01$, $\alpha=18.0^\circ$	78
Figure 38.	Surface Pressure, NACA 0012-63, $M=0.4$, $k=0.01$, $\alpha=19.0^\circ$	79
Figure 39.	Surface Pressure, NACA 0012-63, $M=0.4$, $k=0.01$, $\alpha=20.0^\circ$	80
Figure 40.	Surface Pressure, NACA 0012-63, $M=0.4$, $k=0.01$, $\alpha=21.0^\circ$	81
Figure 41.	Surface Temperature, NACA 0012-63, $M=0.4$, $k=0.01$, $\alpha=14.0^\circ$	82
Figure 42.	Surface Temperature, NACA 0012-63, $M=0.4$, $k=0.01$, $\alpha=16.0^\circ$	83
Figure 43.	Surface Temperature, NACA 0012-63, $M=0.4$, $k=0.01$, $\alpha=17.0^\circ$	84
Figure 44.	Surface Temperature, NACA 0012-63, $M=0.4$, $k=0.01$, $\alpha=18.0^\circ$	85
Figure 45.	Surface Temperature, NACA 0012-63, $M=0.4$, $k=0.01$, $\alpha=19.0^\circ$	86
Figure 46.	Surface Temperature, NACA 0012-63, $M=0.4$, $k=0.01$, $\alpha=20.0^\circ$	87
Figure 47.	Surface Temperature, NACA 0012-63, $M=0.4$, $k=0.01$, $\alpha=21.0^\circ$	88
Figure 48.	Velocity Field, NACA 0012-33, $M=0.3$, $k=0.02$, $\alpha=22.0^\circ$	89
Figure 49.	Vorticity Contours, NACA 0012-33, $M=0.3$, $k=0.02$, $\alpha=22.0^\circ$	90
Figure 50.	Velocity Field, NACA 0012, $M=0.3$, $k=0.1$, $\alpha=15.0^\circ$ downstroke	92
Figure 51.	Velocity Field, NACA 0012, $M=0.3$, $k=0.1$, $\alpha=13.0^\circ$ downstroke	93
Figure 52.	Velocity Field, NACA 0012, $M=0.3$, $k=0.1$, $\alpha=11.0^\circ$ downstroke	94
Figure 53.	Velocity Field, NACA 0012, $M=0.3$, $k=0.1$, $\alpha=10.0^\circ$ downstroke	95

Figure 54.	Reduced Frequency Effect, NACA 0012, $M=0.3$	97
Figure 55.	Reduced Frequency Effect, NACA 0012-33, $M=0.3$	99
Figure 56.	Freestream Speed Effect, NACA 0012, $k=0.02$	100
Figure 57.	Freestream Speed Effect, NACA 0012-33, $k=0.02$	101
Figure 58.	Pressure Gradients, NACA 0012-63	105
Figure 59.	Pressure Gradients, NACA 0012-33	106
Figure 60.	Pressure Gradient Comparison, $M=0.4$, $k=0.01$	107
Figure 61.	Flow Reversal Location, $M=0.4$, $k=0.01$. . .	108

ACKNOWLEDGEMENTS

I would like to acknowledge the instruction and support given by Dr. John Ekaterinaris in the use of advanced numerical computational facilities. In addition, his ability to link aerodynamic theory to the numerical techniques required in this investigation has been invaluable.

Likewise, over the past 18 months, Dr. Max Platzer has provided instruction and valued discussion in a number of areas of aerodynamic theory. In particular, his instruction on the full, unsteady, compressible Navier-Stokes equations and Boundary Layer theory have given me the theoretical background necessary for the completion of this study.

Finally, I would like to thank my wife Janeen for her patience and durability in typing the iterations required for this thesis.

I. INTRODUCTION

A. BACKGROUND

The aeronautical community has been aware of the phenomenon of dynamic stall for several decades. Dynamic stall is characterized by separated flow and shedding of the leading edge vortex from the upper surface of an airfoil which is rapidly pitched to angles of attack beyond the normal stalling angle of attack. The phenomenon results in significant temporary increases and decreases in lift, drag, and moment coefficients.

The scope of this work is the investigation of the phenomenon of dynamic stall for rapidly pitching and oscillating airfoils. The phenomenon of dynamic stall was observed for the first time for flows over the retreating blades of a helicopter. The dynamic stall resulting from the oscillatory motion of the rotor blade is associated with an increase in lift and the development of a severe nose down pitching moment. The effects of dynamic stall are usually undesirable for the helicopter, and where possible special care is taken to reduce its effects by special design of the rotor. On the other hand, interest has recently developed to exploit the increased lift obtained from the rapid pitch-up motion of an airfoil in order to enhance the maneuverability and extend the

flight envelope of the modern fighter aircraft to the high angle of attack regime, or to alleviate retreating blade stall for helicopters utilizing Higher Harmonic Control (HHC).

It is well known that for flow over an airfoil at fixed angle of attack the streamlined airflow is disrupted once a critical angle of attack is exceeded. At stall, the flow over the upper surface of the airfoil separates and the lift drops. It was observed, however, that rapid pitch-up motion of the airfoil delays static stall so that high lift can be maintained for angles of attack beyond the static stall angle.

As the pitch-up angle exceeds the static stalling angle of attack, a thin layer of reversed flow develops in the boundary layer. This reversed flow occurs in two types of stall: trailing edge stall and leading edge stall [Ref. 1]. In trailing edge stall, the reverse flow region begins near the trailing edge and traverses forward; in leading edge stall, the reverse flow region occurs near the suction peak just aft of the leading edge. In both cases, a vortex begins to form near the leading edge region, expands, and moves downstream. The angle of attack at which the vortex is formed depends on airfoil shape, pitch rate, mean angle and amplitude, Mach number, and Reynolds number.

The vortex formed at the leading edge is called the dynamic stall vortex, and moves with a speed of approximately 0.4 freestream speed relative to the airfoil as the pitch-up progresses. Lift, drag, and pitching moment increase signifi-

cantly until the vortex approaches the trailing edge, then drop sharply, but not simultaneously (Figure 1). The unsteady surface pressure increases, and the suction peak appears at different locations along the chord as the dynamic stall vortex moves over the airfoil. Secondary and tertiary vortices may also be present and produce additional suction peaks and fluctuations in airloads.

To date, most theoretical investigations on dynamic stall have focused on the effects of variations of reduced frequency ($k = \omega c / 2U_\infty$), angle of attack, free stream speed, and Reynolds number on a particular airfoil shape (usually the NACA 0012 airfoil). McCroskey [Ref. 1] documented the effects of reduced frequency, amplitude and

Mach number on different airfoils. These experi-

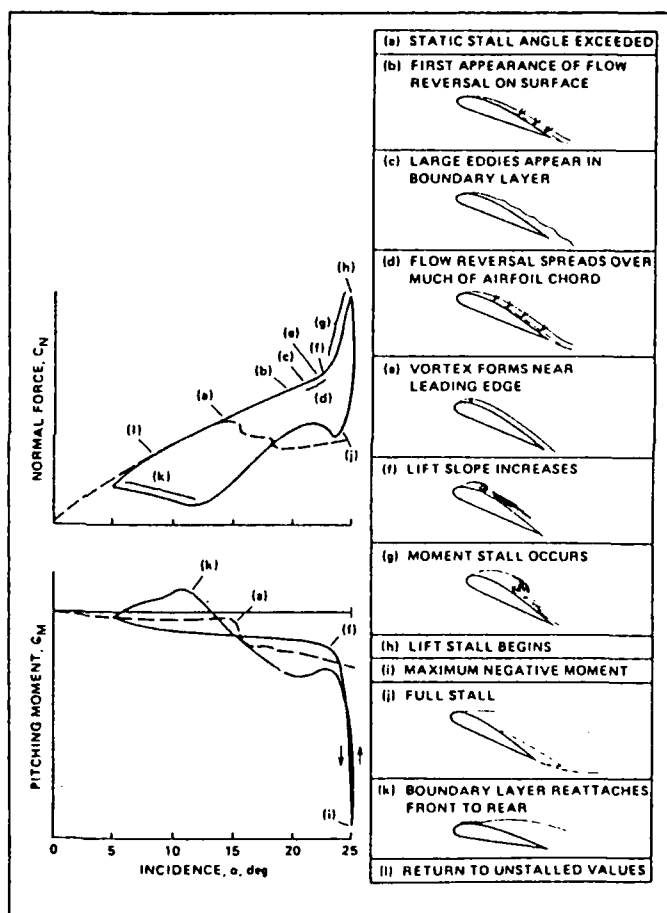


Figure 1. Events of Dynamic Stall on NACA 0012 Airfoil

occurrence of stall of an oscillating airfoil compared to a fixed angle of attack airfoil. McCroskey and Pucci [Ref. 2] identified varying regimes of viscous-inviscid interaction during varying degrees of unsteady flow separation. The conclusion of the experimental studies of Refs. 1 and 2 was that the reduced frequency has a dominant effect on the development and progression of the dynamic stall. Experimental work by Chandrasekhara and Carr [Ref. 3] using the NACA 0012 airfoil showed that a dynamic stall vortex always forms near the leading edge of an oscillating airfoil. Their study also documents the movement of the dynamic stall vortex. Chandrasekhara and Brydges [Ref. 4] documented the effects of increasing amplitude on an oscillating airfoil in both compressible and incompressible flow. They showed that larger amplitudes resulted in vortex retention at higher angles of attack for a given Mach number and reduced frequency.

Progress in computational fluid dynamics has made possible the study of dynamic stall by numerical solution of the unsteady Navier-Stokes equations. Mehta [Ref. 5] demonstrated that Navier-Stokes simulation of the unsteady incompressible flow around the airfoil in oscillatory motion can reproduce the experimentally observed results. Wu et al. [Ref. 6] presented solution procedures based on an integral formulation of the incompressible Navier-Stokes equations for the computation of unsteady flow over airfoils. Beddoes [Ref. 7] and Jang et al. [Ref. 8] presented viscous-inviscid computa-

tion methods for unsteady flows. Sankar and Tang [Ref. 9], Visbal [Ref. 10], and Ekaterinaris [Ref. 11] used ADI (Alternating Direction Implicit) numerical schemes for the solution of the compressible Navier-Stokes equations, and investigated the effects of compressibility on dynamic stall. The numerical solutions for both incompressible and compressible flows showed good agreement with experimental results, and predicted the events of dynamic stalls.

B. PURPOSE

As indicated, the aforementioned studies focused on the variation of flowfield parameters on the dynamic stall of a particular airfoil. The purpose of this study is the systematic investigation of the effect of leading edge geometry on the development of dynamic stall. It is expected that the effect of the leading edge geometry will have a significant effect on both the development of the dynamic stall vortex and its subsequent shedding. This numerical investigation is intended to provide a cost-effective means of quantifying which airfoil parameter variations should be analyzed in more expensive wind-tunnel tests. The numerical investigation of airfoil parameter variations offers the benefit of optimizing the utilization of more costly test facilities.

The investigation is conducted using a numerical solution of the full two-dimensional, Reynolds-averaged Navier-Stokes

Equations, and the Baldwin-Lomax eddy viscosity model of Ref. 16 is used to obtain the turbulent stresses.

C. AIRFOIL SELECTION

Modifications to the NACA 0012 airfoil were made forward of the point of maximum thickness (12% thick at 30%) chord by the method suggested in Ref. 12. The NACA 0012 profile was retained aft of 30% chord for the two new airfoils. In this manner, changes in the flow could be attributed directly to the changes in the forward part of the airfoil. The two airfoils consisted of the NACA 0012-63 and NACA 0012-33 airfoil section forward of 30% chord. The NACA 0012-63 has the same leading edge radius as the NACA 0012 (1.58% chord) but different curvature to the point of maximum thickness. The NACA 0012-33 has a smaller leading edge radius (0.39% chord) with curvature necessary to achieve the same 12% thickness ratio at 30% chord. Airfoil coordinates are provided in Table 1, and the resulting modified profiles are shown in Figure 2.

TABLE 1. AIRFOIL COORDINATES

<u>X/C</u>	<u>N0012</u>	<u>N0012-63</u>	<u>N0012-33</u>
.01	.01701	.01682	.01040
.02	.02360	.02320	.01550
.03	.02842	.02783	.01969
.04	.03232	.03160	.02332
.05	.03555	.03474	.02661
.06	.03840	.03750	.02962
.07	.04090	.03991	.03241
.08	.04313	.04210	.03500
.09	.04505	.04403	.03741
.10	.04681	.04580	.03966
.11	.04842	.04742	.04177
.12	.04990	.04890	.04374
.13	.05123	.05023	.04557
.14	.05242	.05147	.04734
.15	.05345	.05260	.04888
.16	.05441	.05362	.05035
.18	.05610	.05540	.05300
.20	.05742	.05686	.05515
.22	.05840	.05802	.05692
.24	.05903	.05890	.05830
.25	.05943	.05924	.05881
.26	.05964	.05952	.05925
.28	.05992	.05988	.05982
.30	.06000	.06000	.06000
.40	.05803	.05803	.05803
.50	.05294	.05294	.05294
.60	.04563	.04563	.04563
.70	.03664	.03664	.03664
.80	.02623	.02623	.02623
.90	.01448	.01448	.01448
.95	.00807	.00807	.00807
1.00	.00126	.00126	.00126

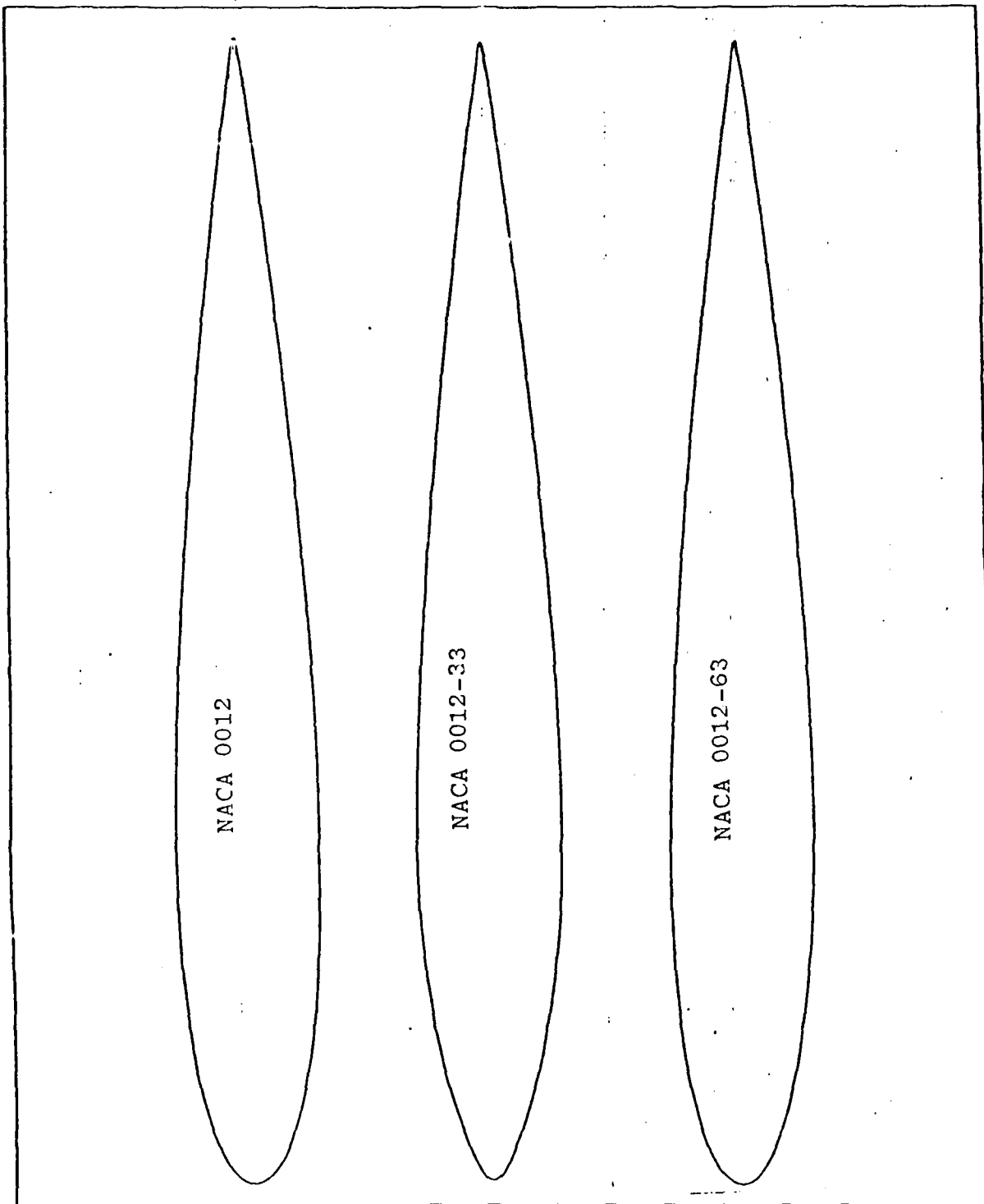


Figure 2. Airfoil Profile Comparison

II. GOVERNING EQUATIONS

The flow of a compressible, viscous fluid satisfies conservation of mass, momentum, and energy. The conservation of mass is expressed by the Continuity Equation, the conservation of momentum by the Navier-Stokes Equations, and the conservation of energy by the Energy Equation. The conservation equations are derived in the following section. The derivation is done in an Eulerian frame of reference.

A. CONTINUITY EQUATION

Consider a control volume in a flow field where flow properties vary with both time and space. Conservation of mass requires that the rate of change of mass inside the control volume equals net mass flux out of the control volume. This is expressed as:

$$\frac{\partial}{\partial t} \iiint_{vol} \rho \, d(vol) + \int_s \rho \vec{V} \cdot d\vec{s} = 0 \quad (1)$$

using Gauss's theorem for a surface integral, Eq. 1 becomes

$$\iiint_{vol} \frac{\partial \rho}{\partial t} \, d(vol) + \iiint_{vol} \nabla \cdot (\rho \vec{V}) \, d(vol) = 0 \quad (2)$$

or,

$$\iiint_{vol} \left[\frac{\partial \rho}{\partial t} + \nabla \cdot (\rho \vec{V}) \right] \, d(vol) = 0 \quad (3)$$

therefore, for an arbitrary control volume,

$$\frac{\partial \rho}{\partial t} + \nabla \cdot (\rho \vec{V}) = 0 \quad (4)$$

for any continuous flow. For a two-dimensional flow, and Cartesian coordinates, Eq. 4 reduces to

$$\frac{\partial \rho}{\partial t} + \frac{\partial (\rho u)}{\partial x} + \frac{\partial (\rho v)}{\partial y} = 0 \quad (5)$$

B. THE MOMENTUM (NAVIER-STOKES) EQUATIONS

Consider a fluid element in a rectangular Cartesian coordinate system. The stresses and pressures are shown in Figure 3, and body forces are neglected. Summation of forces in the x-direction yields:

$$\begin{aligned} F_x &= \rho \, dx \, dy \, dz \frac{Du}{Dt} \\ &= [p - (p + \frac{\partial p}{\partial x} dx)] \, dy \, dz + [(\tau_{xx} + \frac{\partial \tau_{xx}}{\partial x} dx) - \tau_{xx}] \, dy \, dz \\ &\quad + [(\tau_{yx} + \frac{\partial \tau_{yx}}{\partial y} dy) - \tau_{yx}] \, dx \, dz + [\tau_{zx} + \frac{\partial \tau_{zx}}{\partial z} dz - \tau_{zx}] \, dx \, dy \end{aligned} \quad (6)$$

or,

$$\rho \frac{Du}{Dt} = -\frac{\partial p}{\partial x} + \frac{\partial \tau_{xx}}{\partial x} + \frac{\partial \tau_{yx}}{\partial y} + \frac{\partial \tau_{zx}}{\partial z} \quad (7)$$

Similarly, summation of forces in the y- and z- directions yields:

$$\rho \frac{Dv}{Dt} = -\frac{\partial p}{\partial y} + \frac{\partial \tau_{xy}}{\partial x} + \frac{\partial \tau_{yy}}{\partial y} + \frac{\partial \tau_{zy}}{\partial z} \quad (8)$$

$$\rho \frac{Dw}{Dt} = -\frac{\partial p}{\partial z} + \frac{\partial \tau_{xz}}{\partial x} + \frac{\partial \tau_{yz}}{\partial y} + \frac{\partial \tau_{zz}}{\partial z} \quad (9)$$

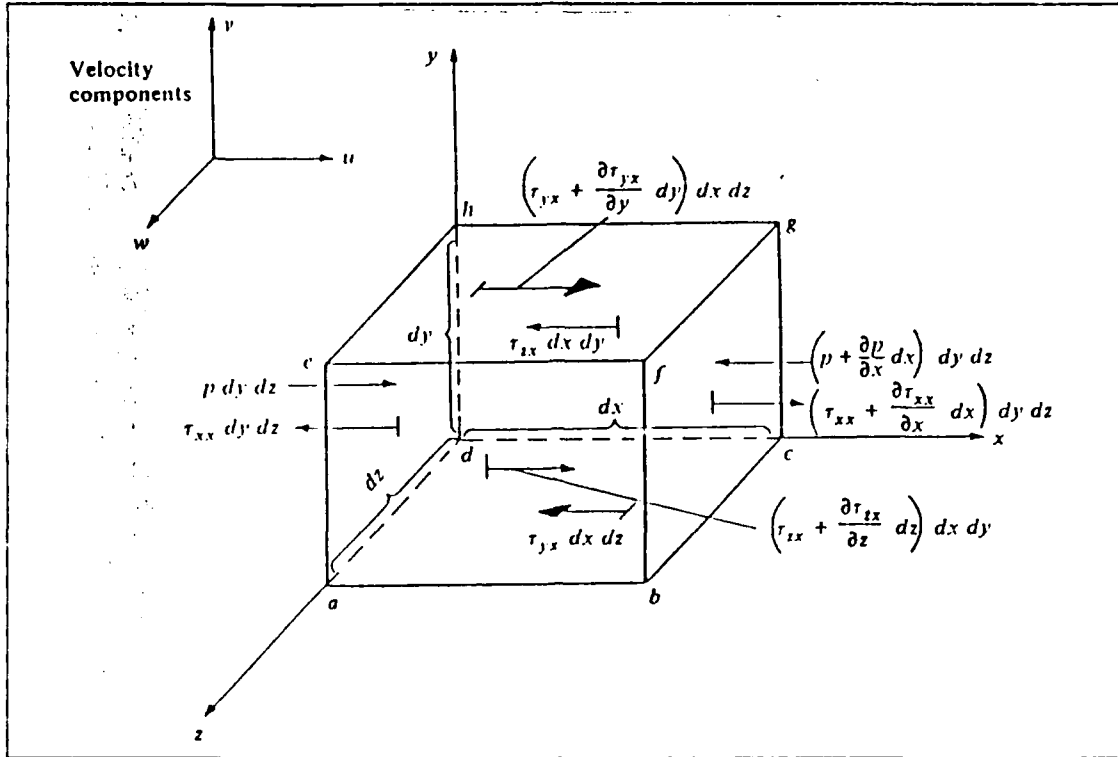


Figure 3. Forces on a Fluid Element

Using the Continuity Equation, the equations expressing the conservation of momentum for a two-dimensional flow are:

$$\frac{\partial(\rho u)}{\partial t} + \frac{\partial}{\partial x}(\rho u^2 + p) + \frac{\partial}{\partial y}(\rho uv) = \frac{\partial \tau_{xx}}{\partial x} + \frac{\partial \tau_{xy}}{\partial y} \quad (10)$$

$$\frac{\partial(\rho v)}{\partial t} + \frac{\partial}{\partial x}(\rho uv) + \frac{\partial}{\partial y}(\rho v^2 + p) = \frac{\partial \tau_{xy}}{\partial x} + \frac{\partial \tau_{yy}}{\partial y} \quad (11)$$

The relation of the viscous stresses τ_{xx} , τ_{yy} , and τ_{xy} to the independent variables is developed in the following discussion.

For a two-dimensional flow in Cartesian coordinates with an infinitesimal fluid element undergoing distortion due to

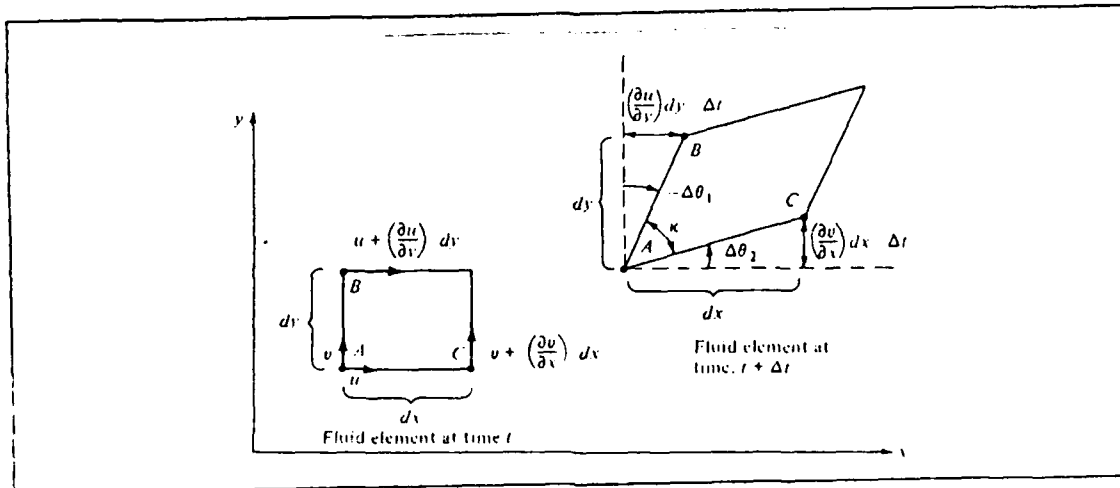


Figure 4. Strain on a Fluid Element

stresses as shown in Figure 4, the angular displacements $\Delta\theta_1$ and $\Delta\theta_2$ are:

$$\Delta\theta_2 = \frac{\partial v}{\partial x} \Delta t \quad \Delta\theta_1 = -\frac{\partial u}{\partial y} \Delta t \quad (12)$$

The strain increment is given by:

$$\Delta K = \Delta\theta_2 - \Delta\theta_1, \quad (13)$$

in the limit, the rate of strain is given by:

$$e_{xy} = \frac{dk}{dt} = \frac{d\theta_2}{dt} - \frac{d\theta_1}{dt} = \frac{\partial v}{\partial x} + \frac{\partial u}{\partial y} \quad (14)$$

Using Newton's Law of Fluid Friction (definition of viscosity),

$$\tau_{ij} = \mu \frac{\partial u_i}{\partial x_j} \quad (15)$$

then the rate of strain caused by the tangential shear stress is given by:

$$\tau_{xy} = \mu \epsilon_{xy} = \mu \left(\frac{\partial v}{\partial x} + \frac{\partial u}{\partial y} \right) \quad (16)$$

For large velocity gradients the normal stresses τ_{xx} and τ_{yy} can be significant and result in a viscous-induced normal force on the fluid element. For example, as documented by Schlichting [Ref. 13], in order for fluid isotropy to be maintained at every point, the principal axes of stress and rate-of-strain must coincide to avoid introducing a preferred rotation direction. With this concept, a normal stress must depend both on its respective component rate of strain as well as the shearing strain rates, with different weighting factors. Choosing the factor 2μ for the component direction factor, which causes Newton's Law of Friction to be satisfied for simple shear, obtain

$$\tau_{xx} = \lambda \left(\frac{\partial u}{\partial x} + \frac{\partial v}{\partial y} \right) + 2\mu \frac{\partial u}{\partial x} \quad (17)$$

$$\tau_{yy} = \lambda \left(\frac{\partial u}{\partial x} + \frac{\partial v}{\partial y} \right) + 2\mu \frac{\partial v}{\partial y} \quad (18)$$

where λ is the shearing stress proportionality factor. Using Stokes's hypothesis, $\lambda = -2/3 \mu$, obtain

$$\begin{aligned}
\tau_{xx} &= \frac{2}{3} \mu \left(2 \frac{\partial u}{\partial x} - \frac{\partial v}{\partial y} \right) \\
\tau_{yy} &= \frac{2}{3} \mu \left(2 \frac{\partial v}{\partial y} - \frac{\partial u}{\partial x} \right) \\
\tau_{xy} &= \mu \left(\frac{\partial v}{\partial x} + \frac{\partial u}{\partial y} \right)
\end{aligned} \tag{19}$$

C. THE ENERGY EQUATION

Conservation of energy is the manifestation of the First Law of Thermodynamics ($dE = dW + dQ$) to a moving fluid element in rectangular Cartesian coordinates. The First Law of Thermodynamics is applied to a control volume (Figure 5), where the energy fluxes are shown. The rate of change of energy inside the fluid element is equal to the net flux of heat into the element plus the rate of work done on the element by pressure and viscous stress.

The rate of change of energy of the fluid element having an instantaneous internal energy per unit mass e and speed V is

$$\rho \frac{\partial}{\partial t} \left(e + \frac{V^2}{2} \right) dx dy dz \tag{20}$$

where $V^2 = u^2 + v^2 + w^2$. The heat flux into the fluid element is the sum of external volumetric heating and heat transfer across the surface due to temperature gradients. Assuming no external heat addition, the volumetric heating is zero.

The net heat transferred out of the fluid element due to thermal conduction in the x -direction can be expressed as:

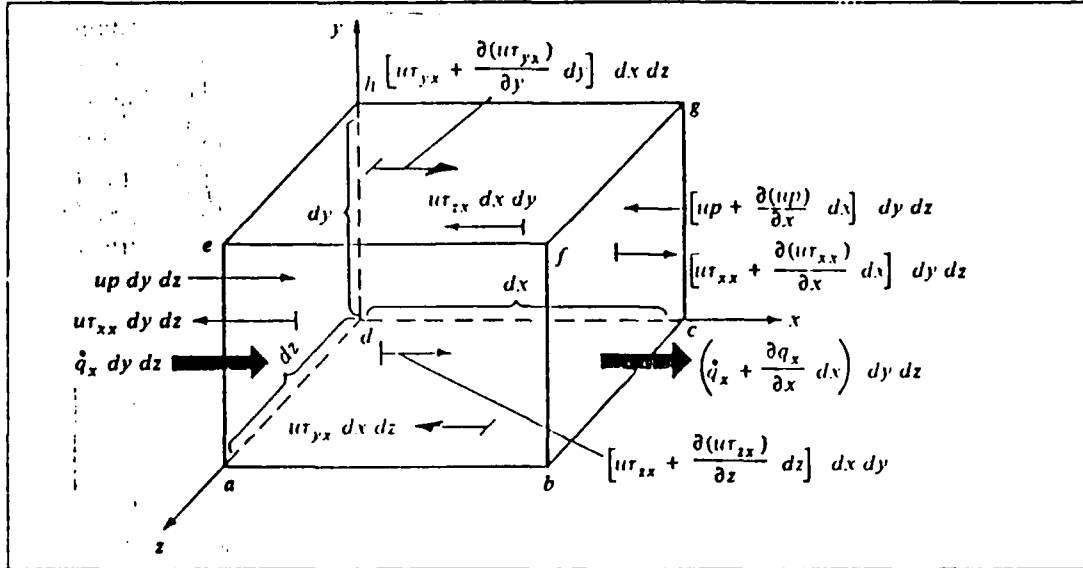


Figure 5. Energy Fluxes on Fluid Element

$$[\dot{q}_x - (\dot{q}_x + \frac{\partial \dot{q}_x}{\partial x} dx)] dy dz = - \frac{\partial \dot{q}_x}{\partial x} dx dy dz \quad (21)$$

Accounting for the y and z directions, the total heat transferred out of the fluid element is:

$$- (\frac{\partial \dot{q}_x}{\partial x} + \frac{\partial \dot{q}_y}{\partial y} + \frac{\partial \dot{q}_z}{\partial z}) dx dy dz = - (\nabla \cdot \vec{q}) dx dy dz \quad (22)$$

where the heat flux is expressed in terms of the temperature gradient according to Fourier's law of heat conduction as

$$\dot{q}_i = -k \frac{\partial T}{\partial x_i} \quad (23)$$

and k is the thermal conductivity, considered constant and independent of temperature.

The rate of work done on the fluid element in the x-direction by pressure and shear stresses is

$$\left[-\frac{\partial(u p)}{\partial x} + \frac{\partial(u \tau_{xx})}{\partial x} + \frac{\partial(u \tau_{yx})}{\partial y} + \frac{\partial(u \tau_{zx})}{\partial z} \right] dx dy dz \quad (24)$$

Accounting for the y and z direction pressure and shear stresses, the net rate of work done on the fluid element can be expressed as:

$$\begin{aligned} & \left[-\nabla \cdot p \vec{V} + \frac{\partial(u \tau_{xx})}{\partial x} + \frac{\partial(u \tau_{yx})}{\partial y} + \frac{\partial(u \tau_{zx})}{\partial z} \right. \\ & \quad + \frac{\partial(v \tau_{xy})}{\partial x} + \frac{\partial(v \tau_{yy})}{\partial y} + \frac{\partial(v \tau_{zy})}{\partial z} \\ & \quad \left. + \frac{\partial(w \tau_{xz})}{\partial x} + \frac{\partial(w \tau_{yz})}{\partial y} + \frac{\partial(w \tau_{zz})}{\partial z} \right] dx dy dz \end{aligned} \quad (25)$$

The complete energy equation for a viscous flow with no external heating can then be expressed as:

$$\begin{aligned} \rho \frac{d}{dt} \left(e + \frac{1}{2} V^2 \right) = & \left[-\nabla \cdot \vec{q} - \nabla \cdot p \vec{V} \right. \\ & + \frac{\partial(u \tau_{xx})}{\partial x} + \frac{\partial(u \tau_{yx})}{\partial y} + \frac{\partial(u \tau_{zx})}{\partial z} \\ & + \frac{\partial(v \tau_{xy})}{\partial x} + \frac{\partial(v \tau_{yy})}{\partial y} + \frac{\partial(v \tau_{zy})}{\partial z} \\ & \left. + \frac{\partial(w \tau_{xz})}{\partial x} + \frac{\partial(w \tau_{yz})}{\partial y} + \frac{\partial(w \tau_{zz})}{\partial z} \right] dx dy dz \end{aligned} \quad (26)$$

The two-dimensional compressible viscous flow energy equation reduces to:

$$\begin{aligned} & \rho \frac{d}{dt} \left(e + \frac{1}{2} V^2 \right) + \frac{\partial}{\partial x} (p u) + \frac{\partial}{\partial y} (p v) \\ & = \frac{\partial}{\partial x} (u \tau_{xx} + v \tau_{xy} - \dot{q}_x) + \frac{\partial}{\partial y} (u \tau_{yx} + v \tau_{yy} - \dot{q}_y) \end{aligned} \quad (27)$$

Using the continuity equation and setting

$$E = (e + \frac{1}{2} V^2) \rho , \quad (28)$$

the total energy per unit volume, the energy equation becomes

$$\begin{aligned} & \frac{\partial E}{\partial t} + \frac{\partial}{\partial x} [(E+p) u] + \frac{\partial}{\partial y} [(E+p) v] \\ & = \frac{\partial}{\partial x} (u \tau_{xx} + v \tau_{xy} - \dot{q}_x) + \frac{\partial}{\partial y} (u \tau_{xy} + v \tau_{yy} - \dot{q}_y) \end{aligned} \quad (29)$$

where τ_{xx} , τ_{yy} , and τ_{xy} are as previously derived (see Eq. 19).

D. CONSERVATION LAW FORM OF THE GOVERNING EQUATIONS

The conservation law form of the governing equations for the two-dimensional viscous compressible flows can be written as [Ref. 14]

$$\frac{\partial Q}{\partial t} + \frac{\partial F}{\partial x} + \frac{\partial G}{\partial y} = \frac{\partial R}{\partial x} + \frac{\partial S}{\partial y} \quad (30)$$

where Q is the vector of dependent variables, F and G are the inviscid fluxes along the x and y directions, respectively, and R and S are the viscous fluxes along the x and y directions, respectively. These terms are given by:

$$Q = \begin{bmatrix} \rho \\ \rho u \\ \rho v \\ E \end{bmatrix} \quad F = \begin{bmatrix} \rho u \\ \rho u^2 + p \\ \rho uv \\ (E+p) u \end{bmatrix} \quad G = \begin{bmatrix} \rho v \\ \rho uv \\ \rho v^2 + p \\ (E+p) v \end{bmatrix}$$

$$R = \begin{bmatrix} 0 \\ \tau_{xx} \\ \tau_{xy} \\ u\tau_{xx} + v\tau_{xy} - \dot{q}_x \end{bmatrix} \quad S = \begin{bmatrix} 0 \\ \tau_{xy} \\ \tau_{yy} \\ u\tau_{xy} + v\tau_{yy} - \dot{q}_y \end{bmatrix}$$

Non-dimensionalizing the equations with

$$\begin{aligned} x_i^* &= \frac{x_i}{L} & u_i^* &= \frac{u_i}{V_\infty} & \rho^* &= \frac{\rho}{\rho_\infty V_\infty^2} & p^* &= \frac{p}{\rho_\infty V_\infty^2} \\ T^* &= \frac{T}{T_\infty} & \mu^* &= \frac{\mu}{\mu_\infty} & e^* &= \frac{e}{V_\infty^2} & t^* &= \frac{t}{L/V_\infty} \end{aligned}$$

where L is the reference length, and setting

$$Re = \frac{\rho_\infty V_\infty L}{\mu_\infty} \quad (31)$$

the Reynolds number based on the reference length, obtain the non-dimensional form of the conservation law:

$$\frac{\partial Q}{\partial t} + \frac{\partial F}{\partial x} + \frac{\partial G}{\partial y} = \frac{1}{Re} \left(\frac{\partial R}{\partial x} + \frac{\partial S}{\partial y} \right) \quad (32)$$

with non-dimensional variable Q and the inviscid flux terms (F and G) as before, and the viscous terms given by:

$$R = \begin{bmatrix} 0 \\ \tau_{xx} \\ \tau_{xy} \\ u\tau_{xx} + v\tau_{xy} - \frac{\mu}{(\gamma-1)M^2 Pr} \frac{\partial T}{\partial x} \end{bmatrix} \quad (33)$$

$$S = \begin{bmatrix} 0 \\ \tau_{xy} \\ \tau_{yy} \\ u\tau_{xy} + v\tau_{yy} - \frac{\mu}{(\gamma-1)M^2 Pr} \frac{\partial T}{\partial y} \end{bmatrix} \quad (34)$$

Here $Pr = C_p \mu / K$ is the Prandtl number, and $M = |\nabla| / a_\infty$. In order to enable solution of the governing equation for arbitrary geometries, the governing equations are expressed for a curvilinear generalized coordinate system. The curvilinear coordinate system (ξ, η) is linked to the Cartesian coordinate system (x, y) by

$$\xi = \xi(x, y, t), \quad \eta = \eta(x, y, t) \quad (35)$$

The curvilinear coordinate space (ξ, η) is referred to as the computational domain and is linked to the physical domain (x, y) by the non-zero Jacobian of the coordinates transformation

$$J = \frac{\partial(\xi, \eta)}{\partial(x, y)} = \frac{\partial\xi}{\partial x} \frac{\partial\eta}{\partial y} - \frac{\partial\xi}{\partial y} \frac{\partial\eta}{\partial x} = \frac{1}{\frac{\partial x}{\partial\xi} \frac{\partial y}{\partial\eta} - \frac{\partial x}{\partial\eta} \frac{\partial y}{\partial\xi}} \quad (36)$$

It can be shown that the governing equations [Ref. 18] retain the strong conservation law form for a generalized coordinate system. The two-dimensional strong conservation law form for a generalized coordinate system is:

$$\frac{\partial Q}{\partial t} + \frac{\partial F}{\partial\xi} + \frac{\partial G}{\partial\eta} = \frac{1}{Re} \left(\frac{\partial R}{\partial\xi} + \frac{\partial S}{\partial\eta} \right) \quad (37)$$

where

$$Q = \frac{1}{J} \begin{bmatrix} \rho \\ \rho u \\ \rho v \\ E \end{bmatrix} \quad (38)$$

$$F = \frac{1}{J} \begin{bmatrix} \rho U \\ \rho u U + p \frac{\partial \xi}{\partial x} \\ \rho v U + p \frac{\partial \xi}{\partial y} \\ (E+p) U - p \frac{\partial \xi}{\partial t} \end{bmatrix} \quad G = \frac{1}{J} \begin{bmatrix} \rho V \\ \rho u V + p \frac{\partial \eta}{\partial x} \\ \rho v V + p \frac{\partial \eta}{\partial y} \\ (E+p) V - p \frac{\partial \eta}{\partial t} \end{bmatrix} \quad (39, 40)$$

and U and V are the contravariant velocity components along the ξ and η directions, respectively given by:

$$U = \frac{\partial \xi}{\partial t} + u \frac{\partial \xi}{\partial x} + v \frac{\partial \xi}{\partial y} \quad V = \frac{\partial \eta}{\partial t} + u \frac{\partial \eta}{\partial x} + v \frac{\partial \eta}{\partial y} \quad (41, 42)$$

The viscous terms are given by:

$$R = \frac{1}{J} \begin{bmatrix} 0 \\ \tau_{xx} \frac{\partial \xi}{\partial x} + \tau_{xy} \frac{\partial \xi}{\partial y} \\ \tau_{xy} \frac{\partial \xi}{\partial x} + \tau_{yy} \frac{\partial \xi}{\partial y} \\ \left[(u \tau_{xx} + v \tau_{xy} - \frac{\mu}{(\gamma-1) M^2 P_r} \frac{\partial T}{\partial x}) \frac{\partial \xi}{\partial x} \right. \\ \left. + (u \tau_{xy} + v \tau_{yy} - \frac{\mu}{(\gamma-1) m^2 P_r} \frac{\partial T}{\partial y}) \frac{\partial \xi}{\partial y} \right] \end{bmatrix} \quad (43)$$

and

$$S = \frac{1}{J} \begin{bmatrix} 0 \\ \tau_{xx} \frac{\partial \eta}{\partial x} + \tau_{xy} \frac{\partial \eta}{\partial y} \\ \tau_{xy} \frac{\partial \eta}{\partial x} + \tau_{yy} \frac{\partial \eta}{\partial y} \\ \left[(u\tau_{xy} + v\tau_{yy} - \frac{\mu}{(\gamma-1)M^2 Pr} \frac{\partial T}{\partial y}) \frac{\partial \eta}{\partial x} \right. \\ \left. + (u\tau_{xy} + v\tau_{yy} - \frac{\mu}{(\gamma-1)m^2 Pr} \frac{\partial T}{\partial y}) \frac{\partial \eta}{\partial y} \right] \end{bmatrix} \quad (44)$$

III. NUMERICAL APPROACH

A. NUMERICAL PROCEDURE

The strong conservation law form of the two-dimensional Continuity, Navier-Stokes, and Energy Equations in generalized coordinates presented in Chapter II provides a useable format for implementing a numerical solution technique. The numerical method used for the integration of the governing equations is a finite difference numerical scheme based on the Beam-Warming algorithm [Ref. 15]. The viscous terms are retained in both directions in order to enable capturing intense viscous effects encountered in massively separated flow regions at high angles of attack. The turbulent stresses were modeled using the Baldwin-Lomax eddy viscosity model [Ref. 16]. An algebraic C-type grid (157x58) was used for the computations. The boundary conditions were treated explicitly, and the unsteadiness was imposed by the motion of the grid.

B. THE BEAM-WARMING ALGORITHM

The strong conservation law form of the two-dimensional compressible Navier-Stokes equations in the vector notation is as follows:

$$\begin{aligned} \frac{\partial U}{\partial t} + \frac{\partial E(U)}{\partial x} + \frac{\partial F(U)}{\partial y} = & \frac{\partial V_1(U, U_x)}{\partial x} + \frac{\partial V_2(U, U_y)}{\partial x} \\ & + \frac{\partial W_1(U, U_x)}{\partial y} + \frac{\partial W_2(U, U_y)}{\partial y} \end{aligned} \quad (45)$$

here the vector U , the non-linear inviscid terms E and F , and the viscous terms R and S are given by:

$$\begin{aligned} U = \begin{bmatrix} \rho \\ \rho u \\ \rho v \\ E_t \end{bmatrix} \quad E(U) = \begin{bmatrix} \rho u \\ \rho u^2 + p \\ \rho uv \\ (E_t + p)u \end{bmatrix} \quad F(U) = \begin{bmatrix} \rho v \\ \rho uv \\ \rho v^2 + p \\ (E_t + p)v \end{bmatrix} \\ R = V_1 + V_2 = \begin{bmatrix} 0 \\ \frac{2}{3}\mu(2u_x - v_y) \\ \mu(u_y + v_x) \\ \mu v(u_y + v_x) + \frac{2}{3}\mu u(2u_x - v_y) + kT_x \end{bmatrix} \\ S = W_1 + W_2 = \begin{bmatrix} 0 \\ \mu(u_y + v_x) \\ \frac{2}{3}\mu(2v_y - u_x) \\ \mu u(u_y + v_x) + \frac{2}{3}\mu v(2v_y - u_x) + kT_y \end{bmatrix} \end{aligned} \quad (46)$$

The Beam-Warming numerical algorithm is an implicit finite difference scheme where the solution is marched in time using the difference formula

$$\begin{aligned} \Delta^n U = & \frac{\theta_1 \Delta t}{1 + \theta_2} \frac{\partial}{\partial t} (\Delta^n U) + \frac{\Delta t}{1 + \theta_2} \frac{\partial}{\partial t} (U^n) + \frac{\theta_2}{1 + \theta_2} \Delta^{n-1} U \\ & + O[(\theta_1 - \frac{1}{2} - \theta_2)(\Delta t)^2 + (\Delta t)^3] \end{aligned} \quad (47)$$

where $\Delta^n U = U^{n+1} - U^n$. By substituting Eq. (45) into Eq. (47), obtain

$$\begin{aligned} \Delta^n U = & \frac{\theta_1 \Delta t}{1 + \theta_2} \left[\frac{\partial}{\partial x} (-\Delta^n E + \Delta^n V_1 + \Delta^n V_2) + \frac{\partial}{\partial y} (-\Delta^n F + \Delta^n W_1 + \Delta^n W_2) \right] \\ & + \frac{\Delta t}{1 + \theta_2} \left[\frac{\partial}{\partial x} (-E^n + V_1^n + V_2^n) + \frac{\partial}{\partial y} (-F^n + W_1^n + W_2^n) \right] \\ & + \frac{\theta_2}{1 + \theta_2} \Delta^{n-1} U + O \left[\left(\theta_1 - \frac{1}{2} - \theta_2 \right) (\Delta t)^2 + (\Delta t)^3 \right] \end{aligned} \quad (48)$$

The delta terms are linearized using truncated Taylor series expansions, so that:

$$E^{n+1} = E^n + \left(\frac{\partial E}{\partial U} \right)^n (U^{n+1} - U^n) + O[(\Delta t)^2] \quad (49)$$

which can be rewritten as

$$\Delta^n E = [A]^n \Delta^n U + O[(\Delta t)^2] \quad (50)$$

where $[A]$ is the flux Jacobian matrix $\partial E / \partial U$ given by

$$[A] = - \begin{bmatrix} 0 & -1 & 0 & 0 \\ \frac{3-\gamma}{2} u^2 + \frac{1-\gamma}{2} v^2 & (\gamma-3)u & (\gamma-1)v & (1-\gamma) \\ uv & -v & -u & 0 \\ \frac{\gamma E_t u}{\rho} + (1-\gamma)u(u^2 + v^2) & -\frac{\gamma E_t}{\rho} + \frac{\gamma-1}{2}(3u^2 + v^2) & (\gamma-1)uv & -\gamma u \end{bmatrix} \quad (51)$$

In a like manner, $\Delta^n F$ can be linearized as

$$\Delta^n F = [B]^n \Delta^n U + O[(\Delta t)^2] \quad (52)$$

where $[B]$ is the Jacobian matrix $\partial F / \partial U$ given by

$$[B] = - \left[\begin{array}{ccc|ccc} 0 & 0 & -1 & 0 \\ uv & -v & -u & 0 \\ \frac{3-\gamma}{2}v^2 + \frac{1-\gamma}{2}u^2 & (\gamma-1)u & (\gamma-3)v & 1-\gamma \\ \frac{\gamma E_t v}{\rho} + (1-\gamma)v(u^2 + v^2) & (\gamma-1)uv & -\frac{\gamma E_t}{\rho} + \frac{\gamma-1}{2}(3v^2 + u^2) & -\gamma v \end{array} \right] \quad (53)$$

The viscous delta term $\Delta^n V_1(U, U_x)$ is linearized by writing

$$\begin{aligned} \Delta^n V_1 &= \left(\frac{\partial V_1}{\partial U} \right)^n \Delta^n U + \left(\frac{\partial V_1}{\partial U_x} \right)^n \Delta^n U_x + O[(\Delta t)^2] \\ &= [P]^n \Delta^n U + [R]^n \Delta^n U_x + O[(\Delta t)^2] \\ &= ([P] - [R_x])^n \Delta^n U + \frac{\partial}{\partial x} ([R]^n \Delta^n U) + O[(\Delta t)^2] \end{aligned} \quad (54)$$

where $[P]$ is the Jacobian $\partial V_1 / \partial U$, $[R]$ is the Jacobian $\partial V_1 / \partial U_x$, and $[R_x] = \partial [R] / \partial x$. These matrices can be written as

$$[P] - [R_x] = -\frac{1}{\rho} \left[\begin{array}{ccc|ccc} 0 & 0 & 0 & 0 \\ -u \left(\frac{4}{3} \mu \right)_x & \left(\frac{4}{3} \mu \right)_x & 0 & 0 \\ -v \mu_x & 0 & \mu_x & 0 \\ -u^2 \left(\frac{4}{3} \mu \right)_x - v^2 \mu_x & u \left(\frac{4}{3} \mu \right)_x & v \mu_x & 0 \end{array} \right] \quad (55)$$

$$[R] = \frac{1}{\rho} \left[\begin{array}{ccc|ccc} 0 & 0 & 0 & 0 \\ -\frac{4}{3} \mu u & \frac{4}{3} \mu & 0 & 0 \\ -\mu v & 0 & \mu & 0 \\ -\left(\frac{4}{3} \mu - \frac{k}{c_v} \right) u^2 - \left(\mu - \frac{k}{c_v} \right) v^2 - \frac{k}{c_v} \frac{E_t}{\rho} & \left(\frac{4}{3} \mu - \frac{k}{c_v} \right) u & \left(\mu - \frac{k}{c_v} \right) v & \frac{k}{c_v} \end{array} \right] \quad (56)$$

The matrix for $[P]-[R_x]$ is obtained by assuming that μ and k are locally independent of U . In a like manner, $\Delta^n W_2(U, U_y)$ is linearized as

$$\Delta^n W_2 = ([Q] - [S_y])^n \Delta^n U + \frac{\partial}{\partial y} ([S]^n \Delta^n U) + O[(\Delta t)^2] \quad (57)$$

where

$$[Q] - [S_y] = -\frac{1}{\rho} \left[\begin{array}{c|c|c|c} 0 & 0 & 0 & 0 \\ -u\mu_y & \mu_y & 0 & 0 \\ -v\left(\frac{4}{3}\mu\right)_y & 0 & \left(\frac{4}{3}\mu\right)_y & 0 \\ -v^2\left(\frac{4}{3}\mu\right)_y - u^2\mu_y & u\mu_y & v\left(\frac{4}{3}\mu\right)_y & 0 \end{array} \right] \quad (58)$$

and

$$[S] = \frac{1}{\rho} \left[\begin{array}{c|c|c|c} 0 & 0 & 0 & 0 \\ -\mu u & \mu & 0 & 0 \\ -\frac{4}{3}\mu v & 0 & \frac{4}{3}\mu & 0 \\ -\left(\frac{4}{3}\mu - \frac{k}{c_v}\right)v^2 - \left(\mu - \frac{k}{c_v}\right)u^2 - \frac{k}{c_v}\frac{E_t}{\rho} & \left(\mu - \frac{k}{c_v}\right)u & \left(\frac{4}{3}\mu - \frac{k}{c_v}\right)v & \frac{k}{c_v} \end{array} \right] \quad (59)$$

The cross-derivative terms can be evaluated explicitly without loss of accuracy by noting that

$$\begin{aligned}\Delta^n V^2 &= \Delta^{n-1} V_2 + O[(\Delta t)^2] \\ \Delta^n W^n &= \Delta^{n-1} W_1 + O[(\Delta t)^2]\end{aligned}\tag{60}$$

for a uniform time step Δt . By evaluating the cross-derivative terms in this manner, the block tridiagonal form of the final equations is maintained.

Substituting Eqs. (50), (52), (54), (57), and (59) into Eq. (48) yields

$$\begin{aligned}& \left\{ [I] + \frac{\theta_1 \Delta t}{1 + \theta_2} \left[\frac{\partial}{\partial x} ([A] - [P] + [R_x])^n - \frac{\partial^2}{\partial x^2} [R]^n \right. \right. \\& \quad \left. \left. + \frac{\partial}{\partial y} ([B] - [Q] + [S_y])^n - \frac{\partial^2}{\partial y^2} [S]^n \right] \right\} \Delta^n U \\&= \frac{\Delta t}{1 + \theta_2} \left[\frac{\partial}{\partial x} (-E + V_1 + V_2)^n + \frac{\partial}{\partial y} (-F + W_1 + W_2)^n \right] \\& \quad + \frac{\theta_1 \Delta t}{1 + \theta_2} \left[\frac{\partial}{\partial x} (\Delta^{n-1} V_2) + \frac{\partial}{\partial y} (\Delta^{n-1} W_1) \right] + \frac{\theta_2}{1 + \theta_2} \Delta^{n-1} U \\& \quad + O \left[\left(\theta_1 - \frac{1}{2} - \theta_2 \right) (\Delta t)^2, (\Delta t)^3 \right]\end{aligned}\tag{61}$$

where $[I]$ is the identity matrix. In Eq. (61), expressions such as

$$\left[\frac{\partial}{\partial x} ([A] - [P] + [R_x])^n \right] \Delta^n U\tag{62}$$

are equivalent to

$$\left[\frac{\partial}{\partial x} ([A] - [P] + [R_x])^n \Delta^n U \right]\tag{63}$$

The left-hand side of Eq. (60) is factorized in the following manner:

$$\begin{aligned}
 & \left([I] + \frac{\theta_1 \Delta t}{1 + \theta_2} \left[\frac{\partial}{\partial x} ([A] - [P] + [R_x])^n - \frac{\partial^2}{\partial x^2} [R]^n \right] \right) \\
 & \times \left([I] + \frac{\theta_1 \Delta t}{1 + \theta_2} \left[\frac{\partial}{\partial y} ([B] - [Q] + [S_y])^n - \frac{\partial^2}{\partial y^2} [S]^n \right] \right) \Delta^n U \quad (64) \\
 & = LHS(Eq. 60) + O[(\Delta t)^3]
 \end{aligned}$$

and the final form of the Beam-Warming Algorithm becomes

$$LHS[Eq. (64)] = RHS[Eq. (61)] \quad (65)$$

The partial derivatives in the algorithm are evaluated using second-order accurate central differences.

The Beam-Warming algorithm is implemented in the following manner:

Step 1:

$$\left([I] + \frac{\theta_1 \Delta t}{1 + \theta_2} \left[\frac{\partial}{\partial x} ([A] - [P] + [R_x])^n - \frac{\partial^2}{\partial x^2} [R]^n \right] \right) \Delta^n U_1 = RHS[61] \quad (66)$$

Step 2:

$$\left([I] + \frac{\theta_1 \Delta t}{1 + \theta_2} \left[\frac{\partial}{\partial y} ([B] - [Q] + [S_y])^n - \frac{\partial^2}{\partial y^2} [S]^n \right] \right) \Delta^n U = \Delta^n U_1 \quad (67)$$

Step 3:

$$U^{n+1} = U^n + \Delta^n U \quad (68)$$

In Step 1, $\Delta^n U_1$ represents the remaining terms on the left-hand side of Eq. (64). Equations (66) and (67) represent systems of equations which have a block tridiagonal structure.

For the two-dimensional compressible Navier-Stokes equations the block matrices have a dimension of 4x4. Central differencing is used for the second order space derivatives. Dissipation terms for numerical stability are added.

Warming and Beam [Ref. 15] have shown that the algorithm can be simplified by assuming that μ is locally constant so that $\partial\mu/\partial x=0$, $\partial\mu/\partial y=0$. Then $[P]-[R_x]=0$ and $[Q]-[S_y]=0$. Therefore, the algorithm for $\theta_1 = \frac{1}{2}$, $\theta_2 = 0$, implying second order accuracy in time, obtains the following form:

$$[I] + \frac{\Delta t}{2} \left[\frac{\partial}{\partial x} [A]^n - \frac{\partial}{\partial x} [R_x]^n \right] \Delta^n U_1 = RHS \quad (69)$$

$$[I] + \frac{\Delta t}{2} \left[\frac{\partial}{\partial x} [B]^n - \frac{\partial}{\partial y} [S_y]^n \right] \Delta^n U = \Delta^n U_1 \quad (70)$$

In the present work the viscous terms were treated explicitly in order to avoid the expensive computation of the matrices R_x and S_y . The Beam-Warming algorithm with explicit treatment of viscous terms in generalized coordinates (ξ, η) is written as

$$\begin{aligned} & \left([I] + \frac{\Delta t}{2} \left[\frac{\partial}{\partial \xi} A^n + \frac{\partial}{\partial \eta} B^n \right] \right) \Delta U^{n+1} = \\ & \Delta t \left(-\frac{\partial}{\partial \xi} F^n - \frac{\partial}{\partial \eta} G^n + \frac{\partial}{\partial \xi} R^n + \frac{\partial}{\partial \eta} S^n \right) = RHS^n \end{aligned} \quad (71)$$

The algorithm is further simplified by approximately factorizing the LHS(61) or LHS(71) operator in order to avoid integration of the full two-dimensional operator. The factored form of the algorithm is

$$\begin{aligned}
([I] + \frac{\Delta t}{2} \delta_{\xi} A_{i,k}^n) \Delta \bar{U}_{i,k}^{n+1} &= RHS(61)^n \\
([I] + \frac{\Delta t}{2} \delta_{\eta} B_{i,k}^n) \Delta U_{i,k}^{n+1} &= \Delta \bar{U}_{i,k}^{n+1}
\end{aligned} \tag{72}$$

In practice, implicit algorithms have stability limits due to nonlinearities. In addition, whenever discrete methods are used to compute high Reynolds number viscous behavior, small scales of motion appear which cannot be resolved by the numerics. These scales are brought about by the nonlinear interactions in the convective terms of the momentum equations. In any finite discrete mesh the small scales which cannot be resolved, result eventually in inaccuracy and contamination of the long wavelength, large scale phenomena. In order to dampen the high frequency numerical effects caused by the poor resolution of the small scales, implicit and explicit numerical dissipation is added to complete the algorithm. The numerical dissipation terms introduce an error level that does not interfere with the accuracy and resolution of any physical effects. The dissipation terms used in the present work are the ones suggested by Ref. 15. The complete factorized form of the numerical algorithms with the implicit and explicit dissipation terms is

$$\begin{aligned}
&[I + (\frac{\Delta t}{2}) (\partial_{\xi} A^n + (D_{impl})_{\xi})] \times [I + (\frac{\Delta t}{2}) (\partial_{\eta} B^n + (D_{impl})_{\eta})] \Delta^n Q \\
&= \Delta t (-\partial_{\xi} F^n - \partial_{\eta} G^n + \partial_{\eta} R^n + \partial_{\eta} S^n - \epsilon_{expl} D_n)
\end{aligned} \tag{73}$$

C. THE BALDWIN-LOMAX EDDY-VISCOSITY MODEL

The Baldwin-Lomax model [Ref. 16] is an algebraic eddy viscosity model for calculating two- and three-dimensional separated flows. As opposed to the classical boundary-layer approximation which assumes zero normal pressure gradient in the boundary layer, thereby neglecting the normal momentum equation, the Baldwin-Lomax Thin Layer model retains the momentum equations and makes no assumptions about the pressure gradient. The advantage of this model arises in application to high Reynolds number, separated turbulent flows, including reverse flow regions. The Baldwin-Lomax model is a two-layer algebraic eddy-viscosity model and avoids the difficulty of finding the edge of the boundary layer. The effects of turbulence are simulated in terms of an eddy viscosity coefficient μ_t , where $\mu + \mu_t$ replaces μ (the physical viscosity coefficient) in the stress terms of the governing equations. In the model, μ_t is given by

$$\mu_t = \begin{cases} (\mu_t)_{inner} & y \leq y_c \\ (\mu_t)_{outer} & y_c > y \end{cases} \quad (74)$$

where y is the normal distance from the wall and y_c is the smallest y where inner and outer values are equal. In the inner region, the Prandtl-Van Driest formula is used:

$$(\mu_t)_{inner} = \rho l^2 |\omega| \quad (75)$$

where $l = ky[1 - \exp(-y^+/A^+)]$ and $|\omega|$ is the magnitude of the vorticity. In two dimensions,

$$|\omega| = \left(\frac{\partial u}{\partial y} - \frac{\partial v}{\partial x} \right) \quad (76)$$

and

$$y^+ = \frac{\rho_w u_{\tau} y}{\mu_w} = \frac{\sqrt{\rho_w \tau_w} y}{\mu_w} \quad (77)$$

The subscript w indicates wall values.

For the outer region

$$(u_t)_{outer} = KC_{cp} \rho F_{WAKE} F_{KLEB}(y) \quad (78)$$

where K , C_{cp} are constants and

$$\begin{aligned} F_{WAKE} &= y_{MAX} F_{MAX} && \text{for boundary layers, or} \\ F_{WAKE} &= C_{wk} y_{MAX} u_{DIP}^2 / F_{MAX} && \text{for wakes and separated boundary layers.} \end{aligned}$$

The quantities y_{MAX} and F_{MAX} are determined from

$$F(y) = y|w|[1 - \exp(y^+/A^+)] \quad (79)$$

The exponential term in this equation is set equal to zero for wakes.

F_{MAX} is the maximum values of $F(y)$, which occurs at a value of $y = y_{MAX}$. The function $F_{KLEB}(y)$ is the Klebanoff intermittency factor given by

$$F_{KLEB}(y) = [1 + 5.5 \left(\frac{C_{KLEB} y}{y_{MAX}} \right)^6]^{-1} \quad (80)$$

The quantity U_{DIF} is the difference between $U = U|_{y=y_{MAX}}$ and minimum total velocity at a fixed flow-wise station:

$$U_{DIF} = (\sqrt{U^2 + V^2})_{y=y_{MAX}} - (\sqrt{U^2 + V^2})_{min} \quad (81)$$

where the second term is zero except in wakes.

In order to achieve agreement with Cebeci [Ref. 17], the values determined for the constants are:

A^+	$= 26$	k	$= 0.4$
C_{cp}	$= 1.6$	K	$= 0.0168$
C_{KLEB}	$= 0.3$	Pr	$= 0.72$
C_{WK}	$= 1.0$	Pr_t	≈ 0.9

D. BOUNDARY CONDITIONS

The following boundary conditions were used in the numerical implementation. A non-slip non-penetration boundary condition in terms of the contravariant velocity components was used on the airfoil solid boundary. The unsteady pitching motion was accomplished by rotating the grid about the quarter chord point at pitch rates determined by the desired reduced frequency. The inflow boundary was placed approximately eight chord lengths away from the body surface. Therefore, freestream conditions were specified at the grid inflow boundary. Simple first order extrapolation was used for the flow variables at the outflow boundary. For the wake, averaging of the flow variables on the upper and lower surfaces of the C-grid was used. The velocity on the surface

is given by $u_s = \dot{x} = \omega z$ and $v_s = \dot{z} = -\omega x$. The contravariant velocity components for viscous flow solutions are set equal to 0. Therefore, the non-slip condition in terms of the physical velocity components for moving grid is expressed by

$$\begin{bmatrix} u \\ v \end{bmatrix} = \frac{1}{J} \begin{bmatrix} \eta_y & -\xi_y \\ -\eta_x & \xi_x \end{bmatrix} \begin{bmatrix} \dot{x} \\ \dot{z} \end{bmatrix} \quad (82)$$

E. GRID GENERATION

1. Grid Generation Methods

In order to effectively compute complex flowfields, the physical domain of interest must be discretized with a finite mesh. The requirements of an efficient numerical grid are [Ref. 18]:

1. smooth grid lines so that the transformation derivatives (metrics) are continuous.
2. grid point spacing which varies inversely with expectation of large numerical errors.
3. minimizing grid skewness to avoid large truncation errors.

Several general grid generation techniques exist; among these the most common methods are:

1. Complex Variable methods, where the transformations are at least partly analytic; this method is restricted to two-dimensions.
2. Algebraic methods, usable in two- or three-dimensions.
3. Differential Equation methods, usable in two- or three-dimensions.

The grid generation method used in this study utilized the algebraic grid generation technique because of the computational efficiency and speed it provides.

2. Algebraic Grid Generation Method

The algebraic method used employs known, easily invertible, functions to map arbitrarily shaped regions (in this case, the airfoil contour) into a simpler computational domain. The airfoil surface is unwrapped to form a simple curve in the computational plane as in Figure 6. In the computational domain lines are first drawn normal to this curve, and the grid points in the normal direction are subsequently generated. In the case of airfoil grid generation, consideration must be given for the clustering of grid points near the airfoil in order to adequately resolve the near surface viscous layers. An algebraic function is used to provide a uniform stretching normal to the airfoil in the computational plane. The resulting computational domain grid is wrapped back to the initial physical grid using inverse transformations.

The grid generation program used in this study yielded a 157x58 C-type grid. The program is listed in Appendix C. Grids for the airfoils under consideration are displayed in Figures 7-9. Figure 7 displays the global grid including wake for the NACA 0012 airfoil. Figures 8 and 9 show the body-fitted grid in more detail for the two modified airfoils. Grid clustering near the airfoils is shown for resolving the

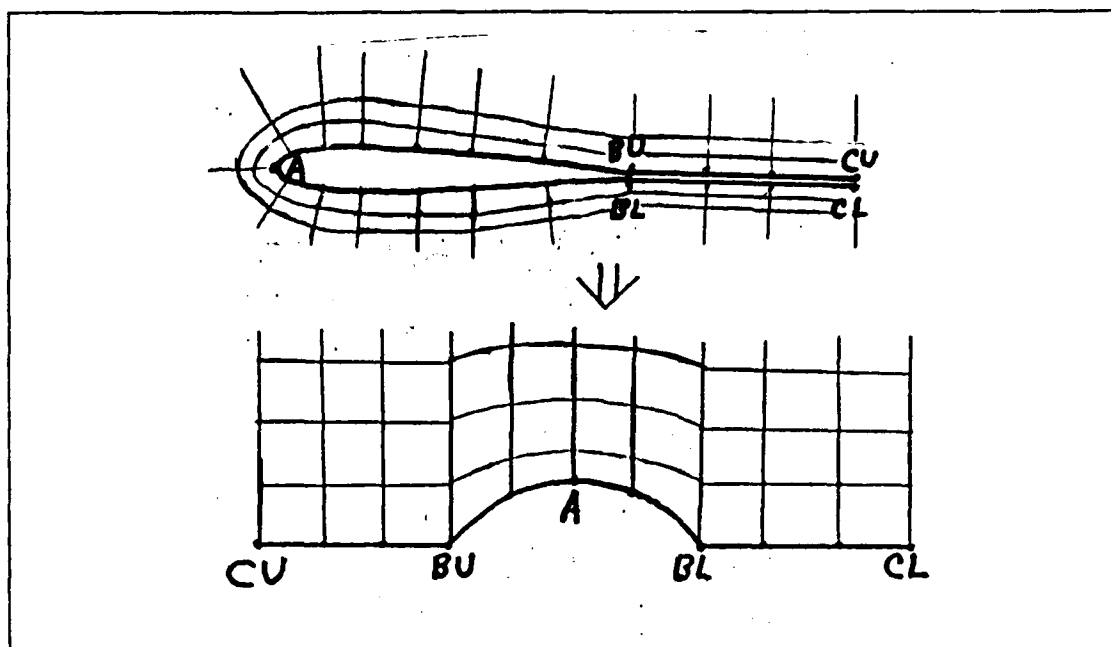


Figure 6. Airfoil Grid Unwrapping

boundary layer flow in turbulent and separated flow conditions.

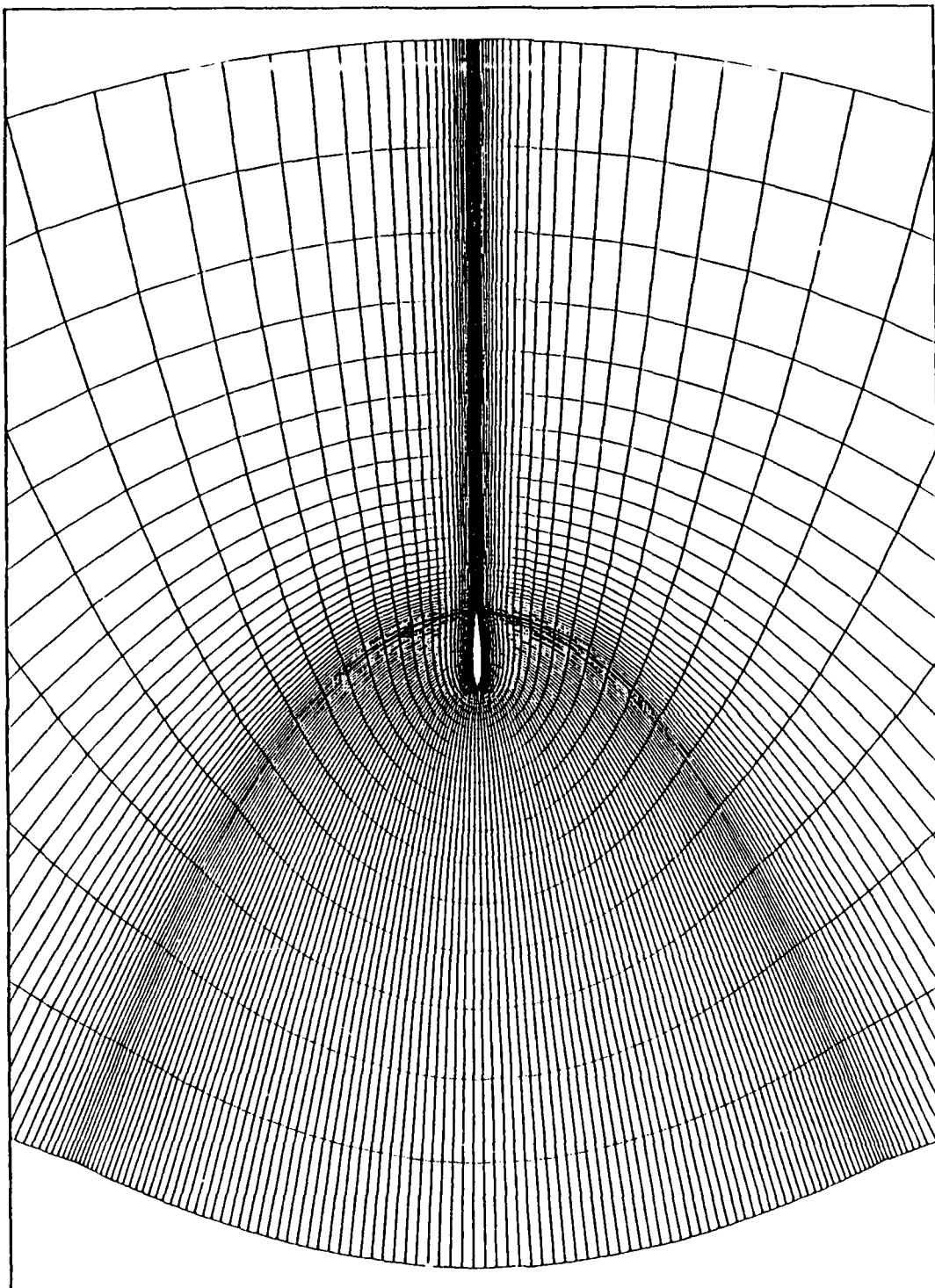


Figure 7. N0012 Global Grid

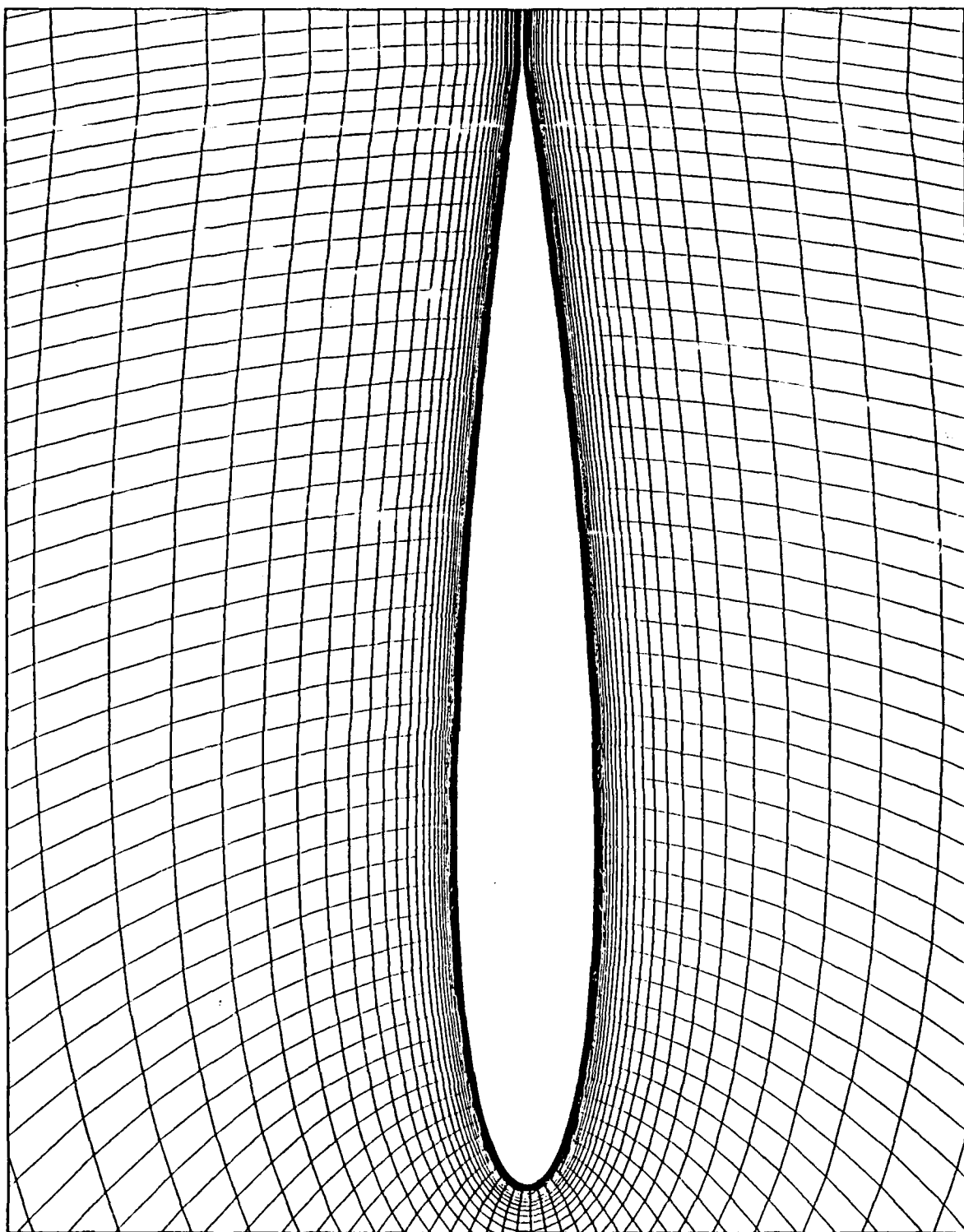


Figure 8. N0012-63 Local Grid

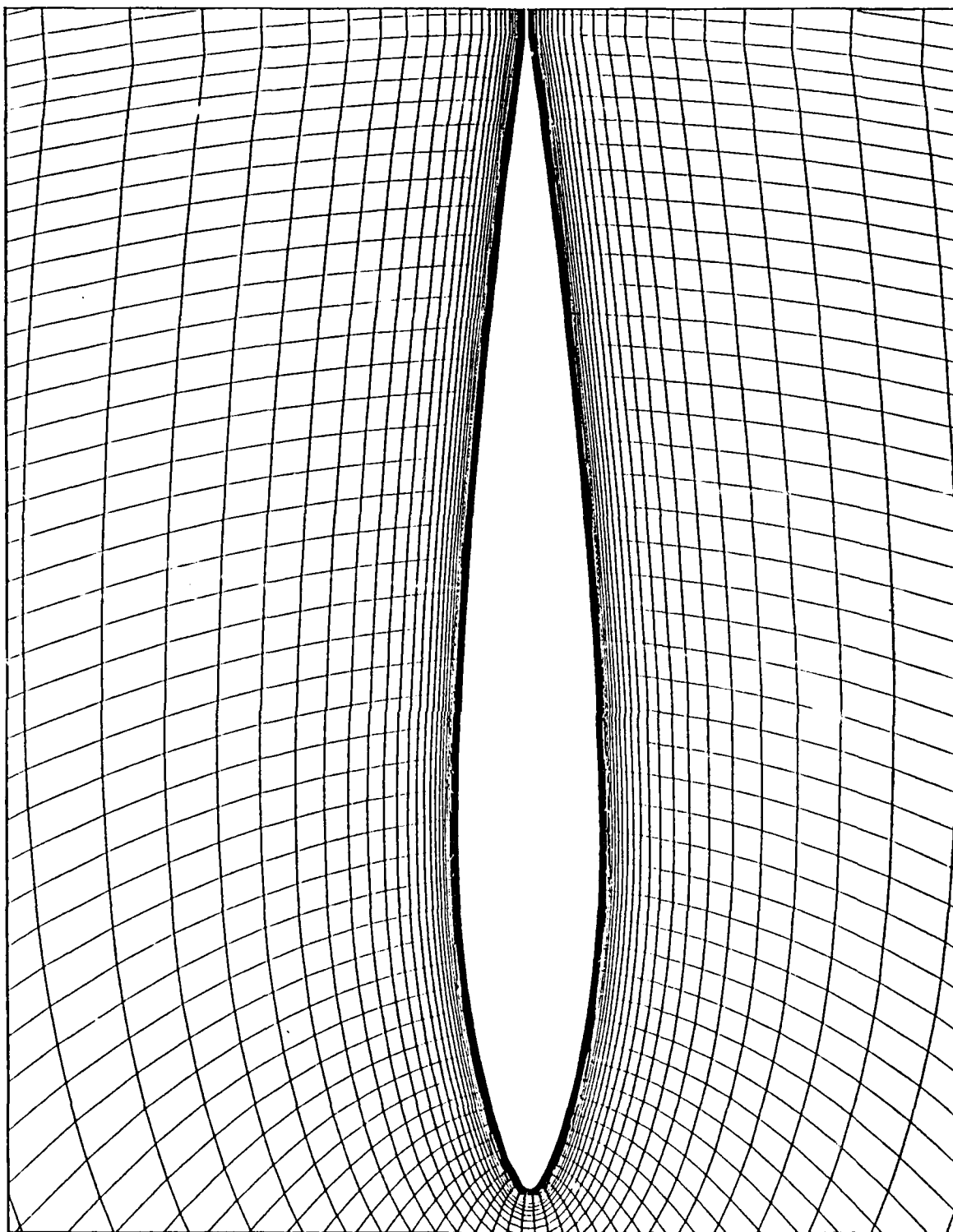


Figure 9. N0012-33 Local Grid

IV. RESULTS AND DISCUSSION

A. INVESTIGATION METHOD

Two-dimensional unsteady flows involving both harmonically oscillating and rapidly pitching (ramp pitch-up) airfoils were investigated. Studies for the oscillatory cases were conducted using the NACA 0012 airfoil in order to enable comparisons with previously conducted experimental measurements. Flows over all three airfoils rapidly pitched from 0° to 30° angle of attack with the reduced frequencies and Mach numbers (shown in Table 2) were subsequently investigated.

TABLE 2. RAPIDLY PITCHING AIRFOIL CASES, $Re = 4 \times 10^6$

AIRFOIL	0.3 Mach		0.4 Mach	
	$k=.01$	$k=.02$	$k=.01$	$k=.02$
NACA 0012	X	X	X	X
NACA 0012-63	X	X	X	X
NACA 0012-33	X	X	X	X

Solutions for the harmonically oscillating NACA 0012 airfoil were obtained for flows at a freestream Mach number of 0.3, Reynolds number based on the root chord $Re_c = 4 \times 10^6$ and for two reduced frequencies of $k=0.1$ and $k=0.2$. The reduced frequency is defined as $k=\omega c/2U_\infty$ for the oscillatory case where $\alpha(t)=\alpha_0 + a_1 \sin(\omega t)$. In terms of nondimensional quantities k is given by $k=\omega/2M_\infty$, and $\alpha(t)=a_1 \omega \cos(\omega t)$ is the

instantaneous pitch-up rate which varies during the cycle with $\omega = 2kM_\infty$ for a unit chord length. The present computations were conducted for a variation of the angle of attack as $\alpha(t) = 10^\circ + 6\sin(t)$. Experimental test conditions for the same freestream Mach and Reynolds numbers were for $\alpha(t) = 10^\circ + 5\sin(t)$. Because the airfoil stalled just at 15° for the experiment, the computed flow for the same conditions did not yield a hysteresis loop. Therefore, as McCroskey suggested, the oscillation was increased by one degree and a hysteresis loop was obtained. The computed lift behavior shown in Figures 10 and 11 exhibits the well-known hysteresis loop of a harmonically oscillating airfoil experiencing dynamic stall. The computation was initiated from a steady-state solution at $\alpha = 5^\circ$ and was carried out for two cycles. Figures 10 and 11 display the results of the second cycle from the two-cycle computation.

Flow solutions for a rapidly pitching airfoil were obtained by pitching the airfoil at a constant rate from a zero angle of attack and steady-state flow conditions to an angle of attack of 30° at the desired reduced frequency and freestream Mach number. For the case where ramp motion was imposed, the reduced frequency k is given by $k = \dot{\alpha}c/2U_\infty$ where $\dot{\alpha}$ is the constant pitch-up rate. In terms of nondimensional quantities $k = \omega/2M_\infty$, or $\omega = 2kM_\infty = \text{constant}$, and $\alpha(t) = \alpha_0 + (\alpha_f - \alpha_0)\omega t$, where in this study $\alpha_0 = 0^\circ$ and $\alpha_f = 30^\circ$ and $\omega = \dot{\alpha}(t)$. A summary of

the computed results for the rapidly pitching airfoils is provided in Table 3.

TABLE 3. PEAK LIFT COEFFICIENTS

AIRFOIL	Mach No.	Reduced Frequency	Peak C_l	Angle of Attack
N0012	0.3	.01	1.90	19.40°
		.02	2.10	23.40°
	0.4	.01	1.97	21.08°
		.02	2.24	25.21°
N0012-63	0.3	.01	1.84	18.50°
		.02	2.09	23.00°
	0.4	.01	1.93	20.60°
		.02	2.22	25.00°
N0012-33	0.3	.01	1.65	15.80°
		.02	1.94	19.60°
	0.4	.01	1.74	17.10°
		.02	2.09	23.15°

A general observation on the computed solution is that the modified NACA 0012-63 airfoil exhibited comparable lift behavior to the baseline NACA 0012 airfoil. A slight angle of attack versus lift curve shift was observed between the two airfoils at all reduced frequency/Mach number combinations. However, for the same flow parameters the NACA 0012-33 airfoil consistently underperformed the larger leading edge radius airfoils. The difference in the unsteady lift behavior with increasing angle of attack resulted from the different flow character at the leading edge region as will be shown later in detail. In the following sections, detailed comparison of the lift behavior of the three airfoils is presented at the various flow conditions. The flow characteristics and the

development and progression of the dynamic stall process are examined. The effects of reduced frequency and freestream Mach number are also discussed.

B. LIFT BEHAVIOR

1. Harmonically Oscillating Airfoil

Although hysteresis loops characteristic of an oscillating airfoil undergoing dynamic stall were observed for reduced frequencies of both 0.1 and 0.2, agreement with experimental results varied. At a reduced frequency of 0.1, the response agreed well with McCroskey's experimental results (Figure 10) during the upstroke. Maximum lift coefficient was 1.52 at an angle of attack of 15.8° . The lift behavior continues to agree well with the experimental data during the upstroke of the hysteresis loop and during the initial part of the downstroke. As the downstroke continues and the flow reattaches, however, the numerical solution displays significantly greater oscillations in lift coefficient compared to experimental data, which were obtained as an average over several cycles of oscillation.

At a reduced frequency of 0.2 (Figure 11), the numerical solution exhibited a much smaller hysteresis loop than the respective experimental data. In this case, maximum lift coefficient in the numerical solution occurred just prior to the downstroke, so that flow reattachment occurred almost

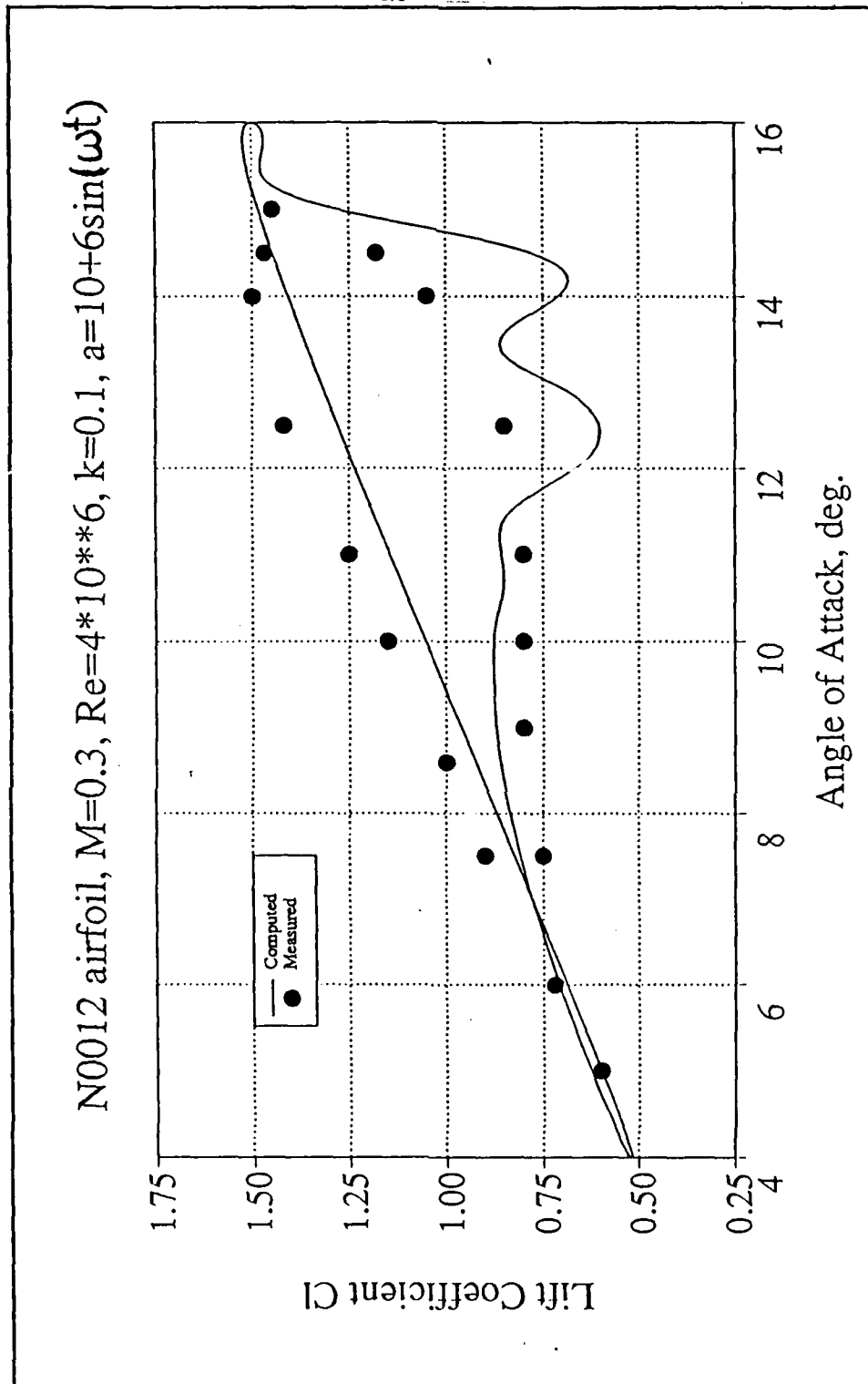


Figure 10. Lift Behavior, NACA 0012, $M=0.3$, $k=0.1$

N0012 airfoil, $M=0.3$, $Re=4 \times 10^6$, $k=0.2$, $a=10+6\sin(\omega t)$

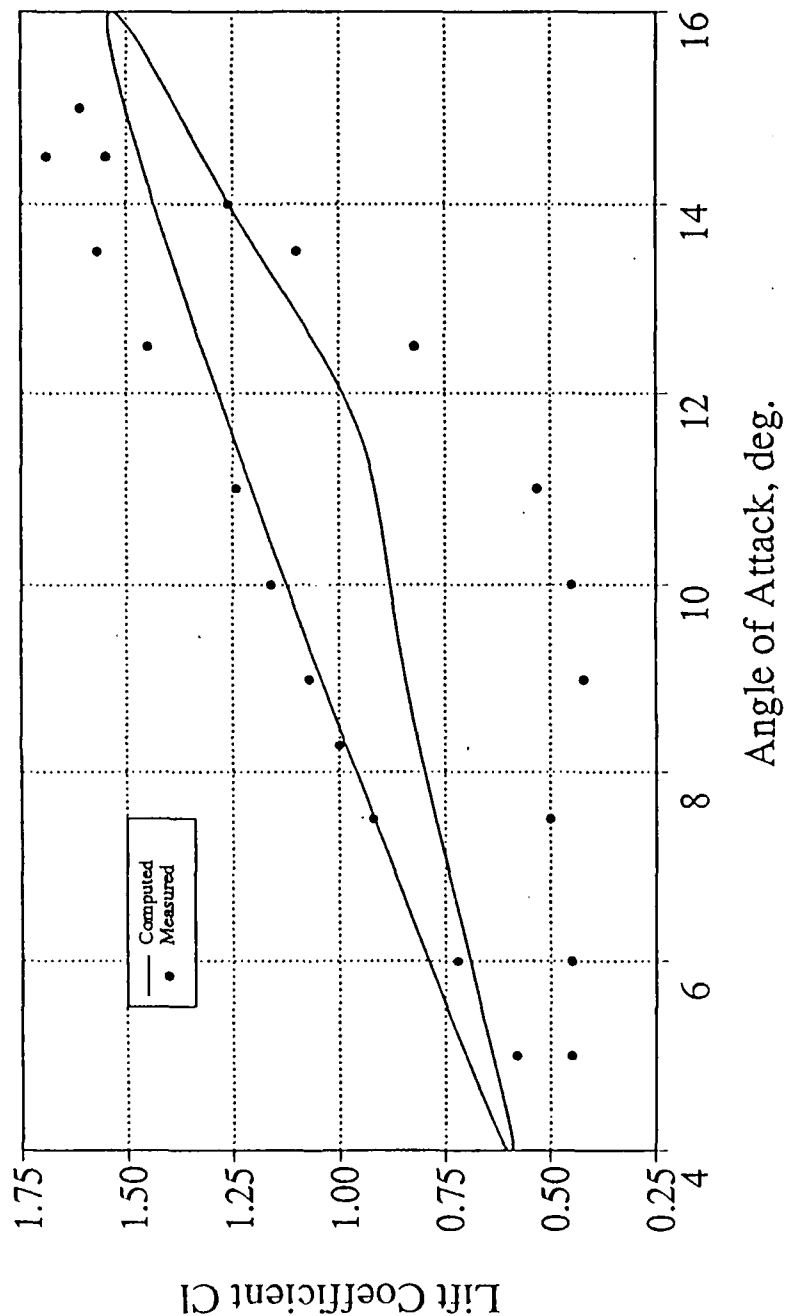


Figure 11. Lift Behavior, NACA 0012, $M=0.3$, $k=0.2$

immediately. Maximum lift coefficient at $k=0.2$ was only slightly higher than at the $k=0.1$ case.

The lack of agreement with experimental data at a reduced frequency of 0.2 and during the flow reattachment process at $k=0.1$ may be indicative of the poor behavior of the eddy-viscosity model (which is suitable for steady flows). Higher values of the reduced frequency resulted in larger discrepancies from the measured lift values.

2. Rapidly Pitching Airfoil

Lift coefficient vs. angle of attack comparison of the three airfoils is presented in Figures 12-15 for the Mach number/reduced frequency combinations listed in Table 2. For the same flow parameters, all three airfoils have nearly the same lift curve slope until the onset of dynamic stall. Along with the aforementioned angle of attack shift of the lift curves between the NACA 0012 and -63 airfoils after stall occurs, the peak lift coefficients for the NACA 0012 airfoil are slightly higher than for the -63 airfoil. The peak lift coefficient for the NACA 0012 occurred 0.2 to 0.9 degrees angle of attack higher than the peak C_l for the -63 airfoil for the same flow conditions. With both airfoils having the same leading edge radius, the small difference in performance may be attributed to the slightly thicker contouring of the forward part of the baseline NACA 0012 airfoil (Table 1).

Ramp pitch-up from 0 to 30 deg, $M=0.3$, $Re=4 \times 10^6$, $k=0.01$

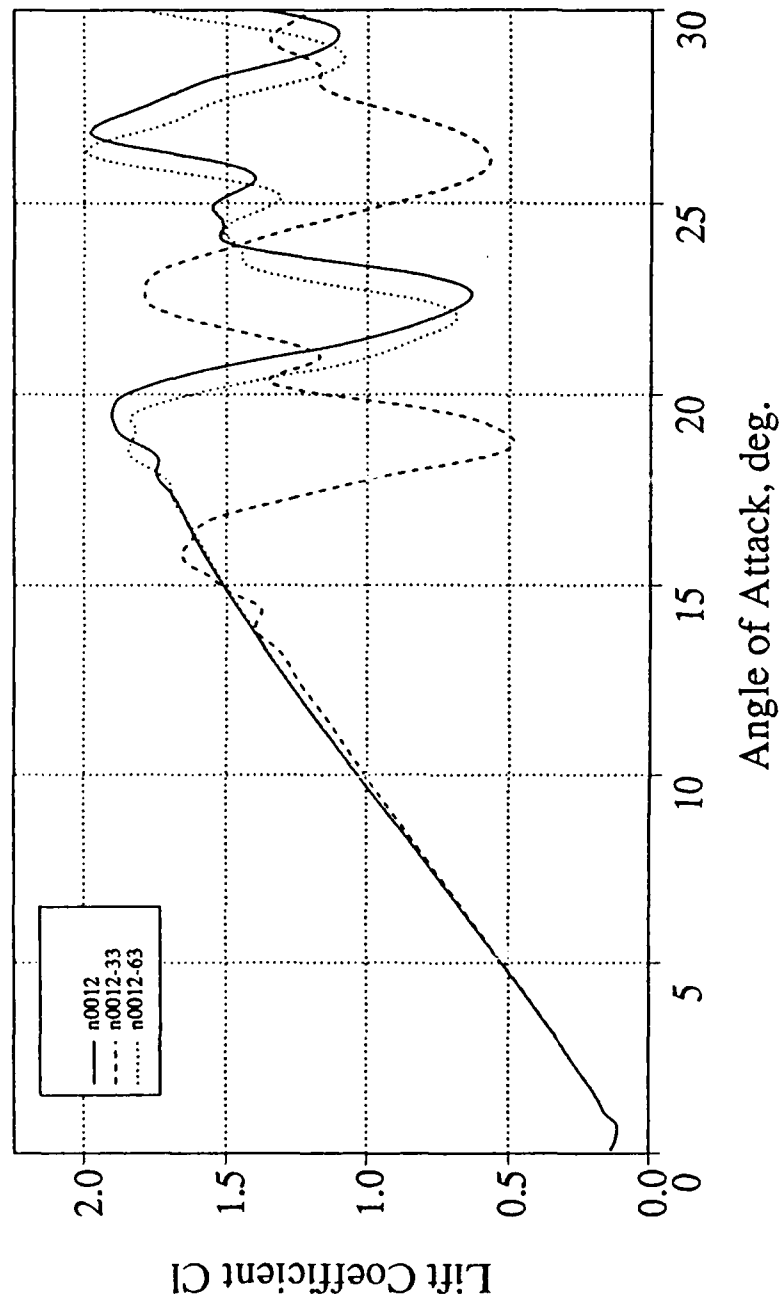


Figure 12. Lift Comparison, $M=0.3$, $k=0.01$

Ramp pitch-up from 0 to 30 deg, $M=0.3$, $Re=4 \times 10^6$, $k=0.02$

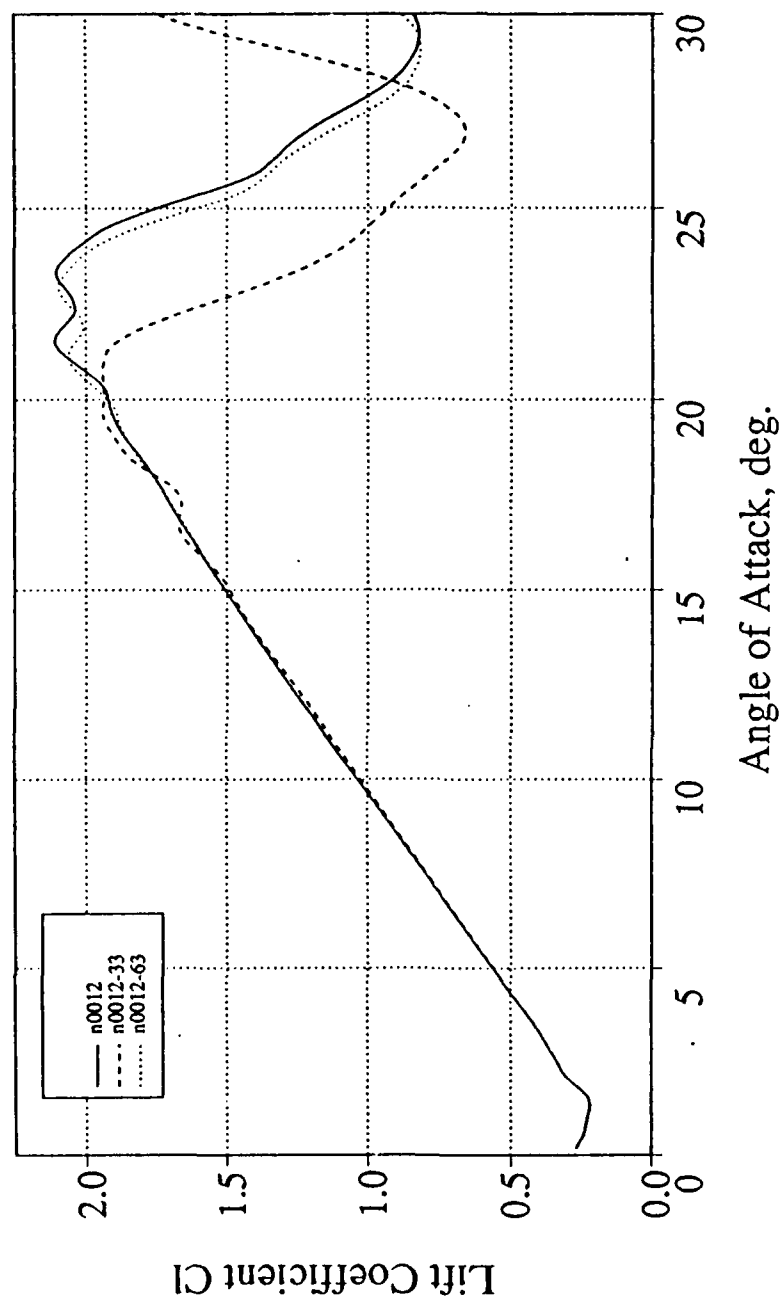


Figure 13. Lift Comparison, $M=0.3$, $k=0.02$

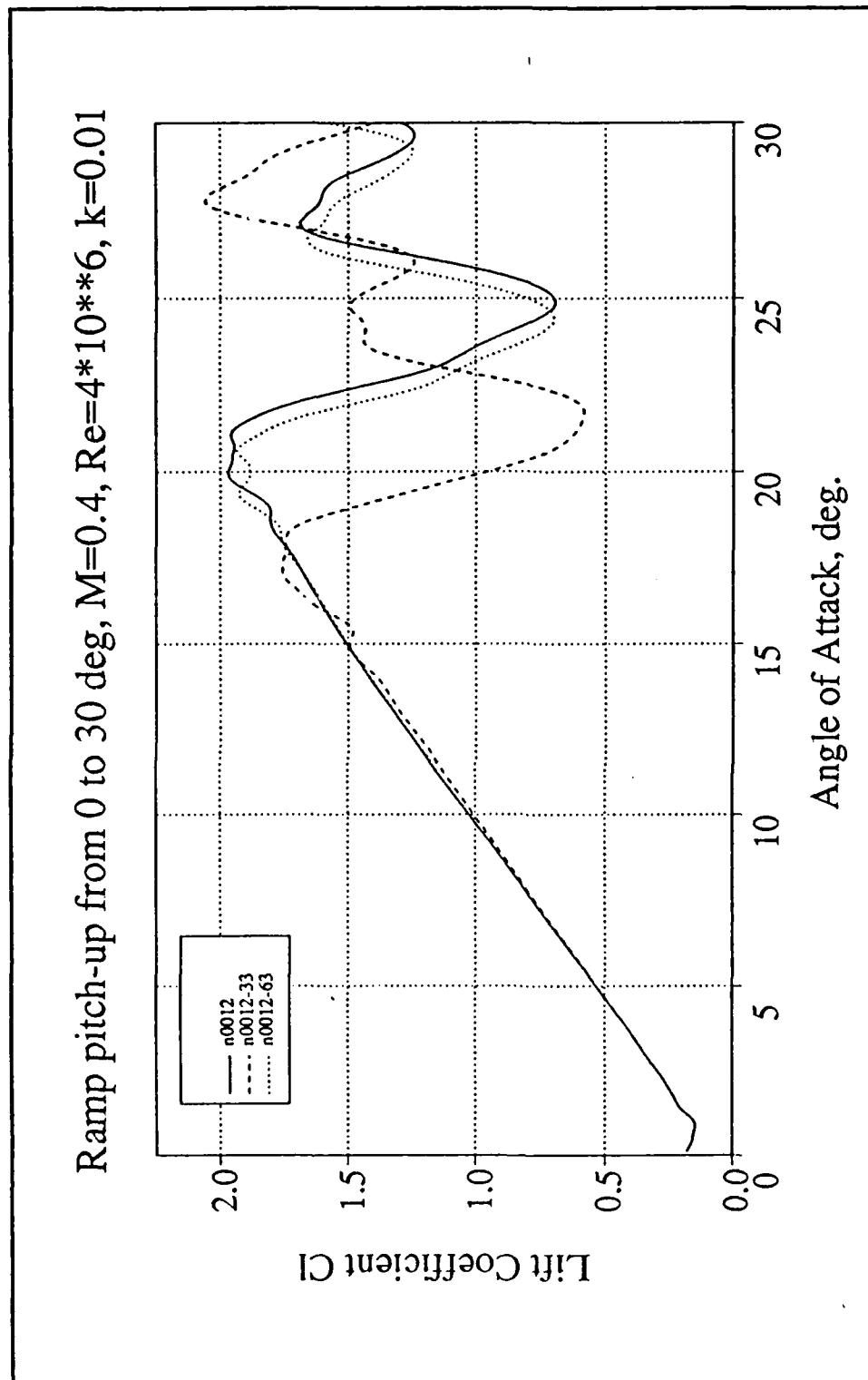


Figure 14. Lift Comparison, $M=0.4$, $k=0.01$

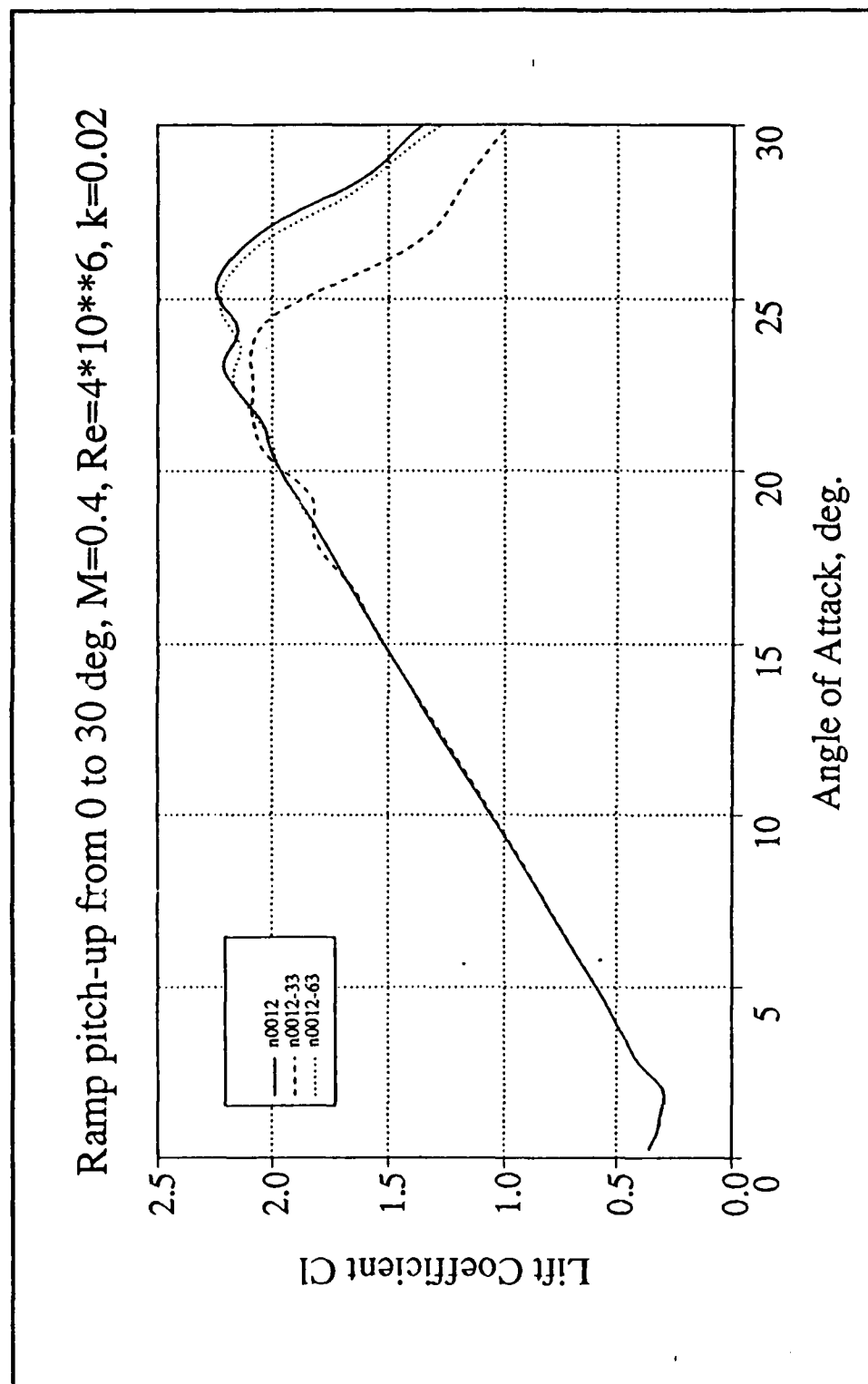


Figure 15. Lift Comparison, $M=0.4$, $k=0.02$

The maximum lift coefficient obtained with the NACA 0012-33 airfoil was lower than that obtained with the other two airfoils and occurred at 1.8 to 4.0 degrees lower angle of attack. At a reduced frequency of $k=0.01$ and freestream Mach number of 0.3, the initial leading edge vortex originated at an angle of attack of 12° for the -33 airfoil. Under the same flow conditions, formation of the vortex occurred at 17° and 16.5° for the baseline 0012 and -63 airfoils, respectively. Similar differences occurred at all other flow conditions investigated. The smaller leading edge radius of the NACA 0012-33 airfoil promoted earlier development of the dynamic stall vortex from the leading edge upper surface.

As will be shown, the dynamic stall vortex originates as a result of the combination of the accelerated flow over the leading edge with the boundary layer reverse flow behind the leading edge. An adverse pressure gradient is encountered by the flow as it passes the suction peak just downstream of the airfoil leading edge. This adverse pressure gradient causes flow deceleration just aft of the suction peak, leading eventually to the boundary layer separating at a critical value of the adverse pressure gradient. The momentum of the flow, however, is increased as the flow accelerates around the leading edge and opposes the tendency of the flow to separate. Eventually, depending on the airfoil shape characteristics, the boundary layer separates, reversed flow occurs, and combines with the freestream to form the leading edge vortex.

As observed in this investigation, the size of the leading edge radius is of primary importance in determining the angle of attack at which the boundary layer separates and rolls to form the dynamic stall vortex. For the same flow parameters and angle of attack during pitch-up, the critical pressure gradient for flow separation occurred earlier on the airfoil with smaller leading edge radius (NACA 0012-33). Stated otherwise, at a given angle of attack during pitch-up, the adverse pressure gradient aft of the suction peak is greater for the smaller leading edge airfoil.

The contouring of the forward part of the airfoil is of secondary importance in alleviating development of the adverse pressure gradient. The effect of contouring is indicated by the slightly earlier development of leading edge reverse flow on the NACA 0012-63 airfoil compared to the baseline 0012 airfoil.

In summary, enlarging the leading edge radius and thickening the contouring of the forward part of the airfoil results in decreasing the adverse pressure gradient encountered by the flow, with resulting delay in separation. This is shown graphically in Figures 16-20 where instantaneous streamlines are shown for the three airfoils at the same 17° angle of attack, 0.4 Mach, and $k=0.01$. Reversed boundary layer flow has just begun on the NACA 0012 airfoil aft of the suction peak, whereas initiation of the dynamic stall vortex has already occurred on the NACA 0012-63 airfoil which has

thinner contouring. The NACA 0012-33 airfoil with the small leading edge radius has a fully developed dynamic stall vortex and is 0.6° angle of attack prior to dynamic stall. A detailed discussion of the vortical flow development follows.

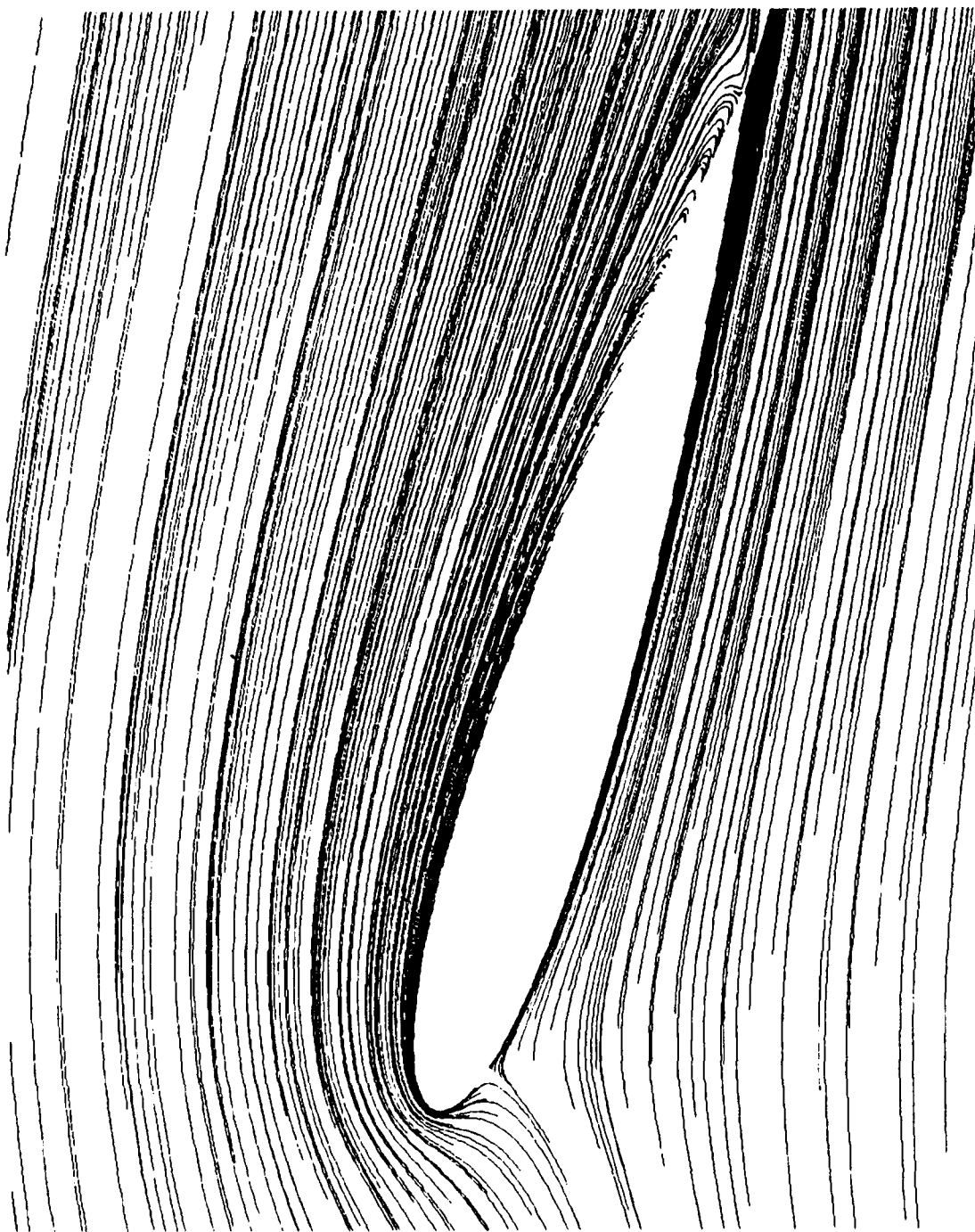


Figure 16. Instantaneous Streamlines, NACA 0012, $M=0.4$, $k=0.01$, $\alpha=17^\circ$

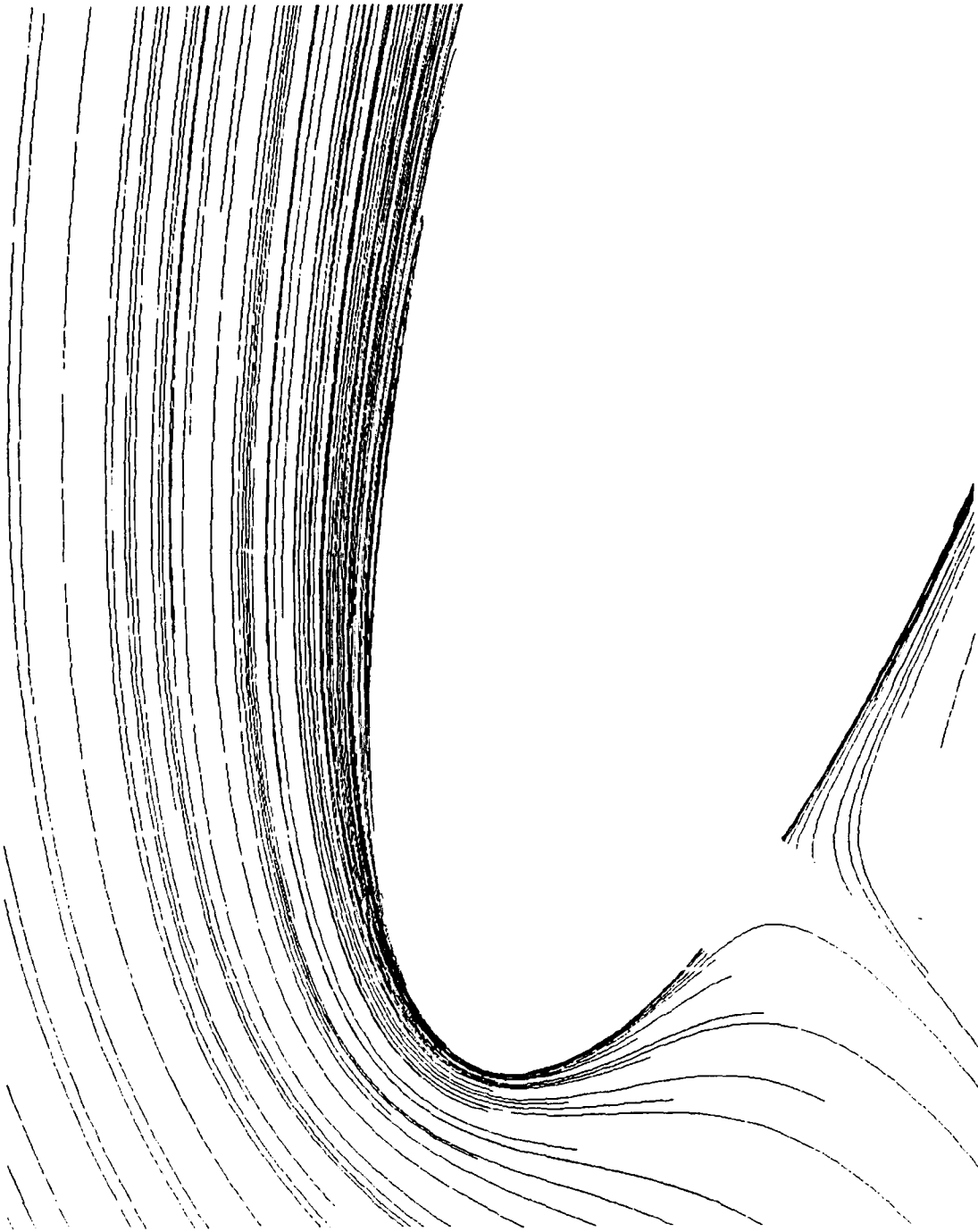


Figure 17. Leading Edge Instantaneous Streamlines, NACA 0012,
 $M=0.4$, $k=0.01$, $\alpha=17^\circ$

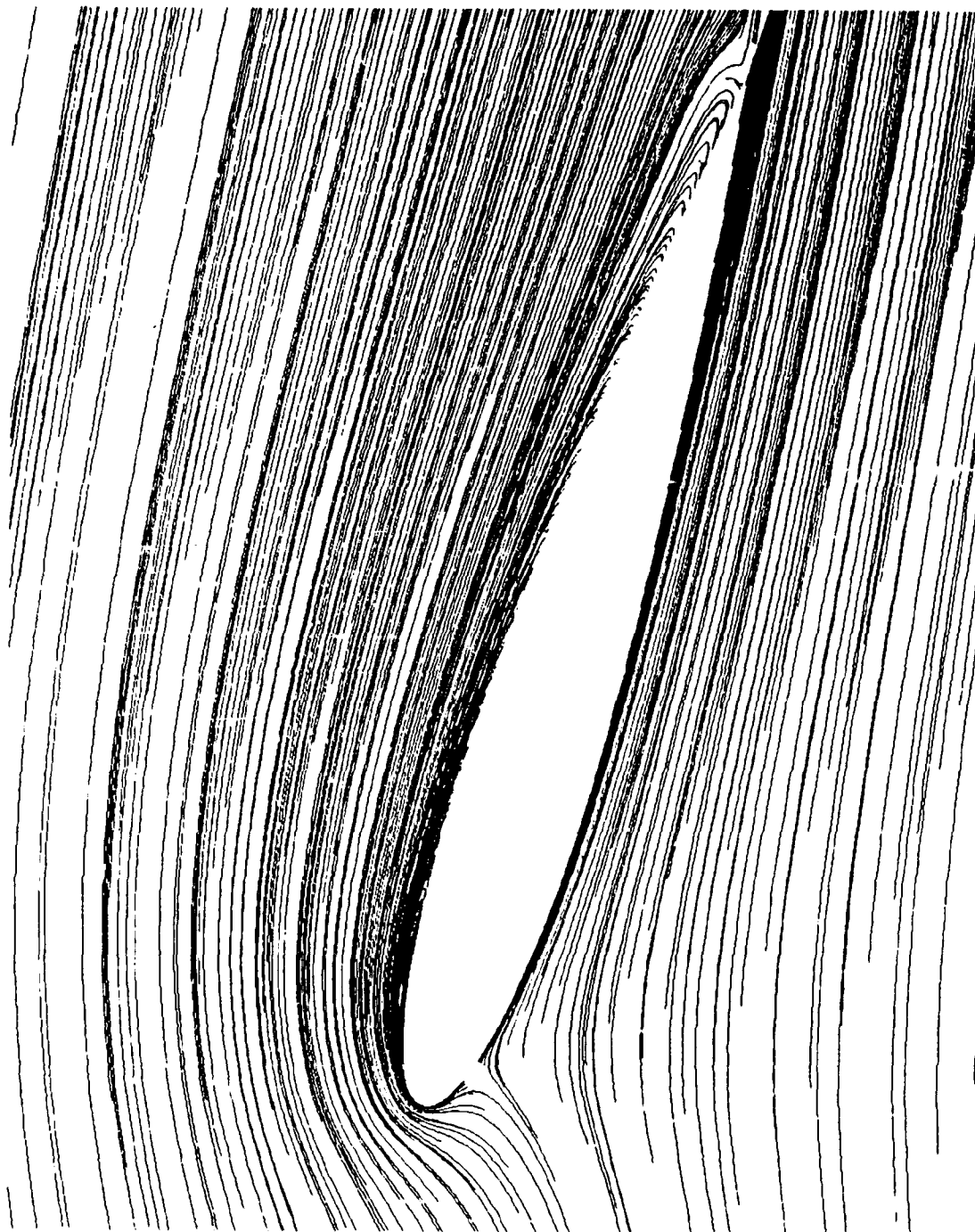


Figure 18. Instantaneous Streamlines, NACA 0012-63, $M=0.4$, $k=0.01$, $\alpha=17^\circ$



Figure 19. Leading Edge Instantaneous Streamlines, NACA 0012-63, $M=0.4$, $k=0.01$, $\alpha=17^\circ$

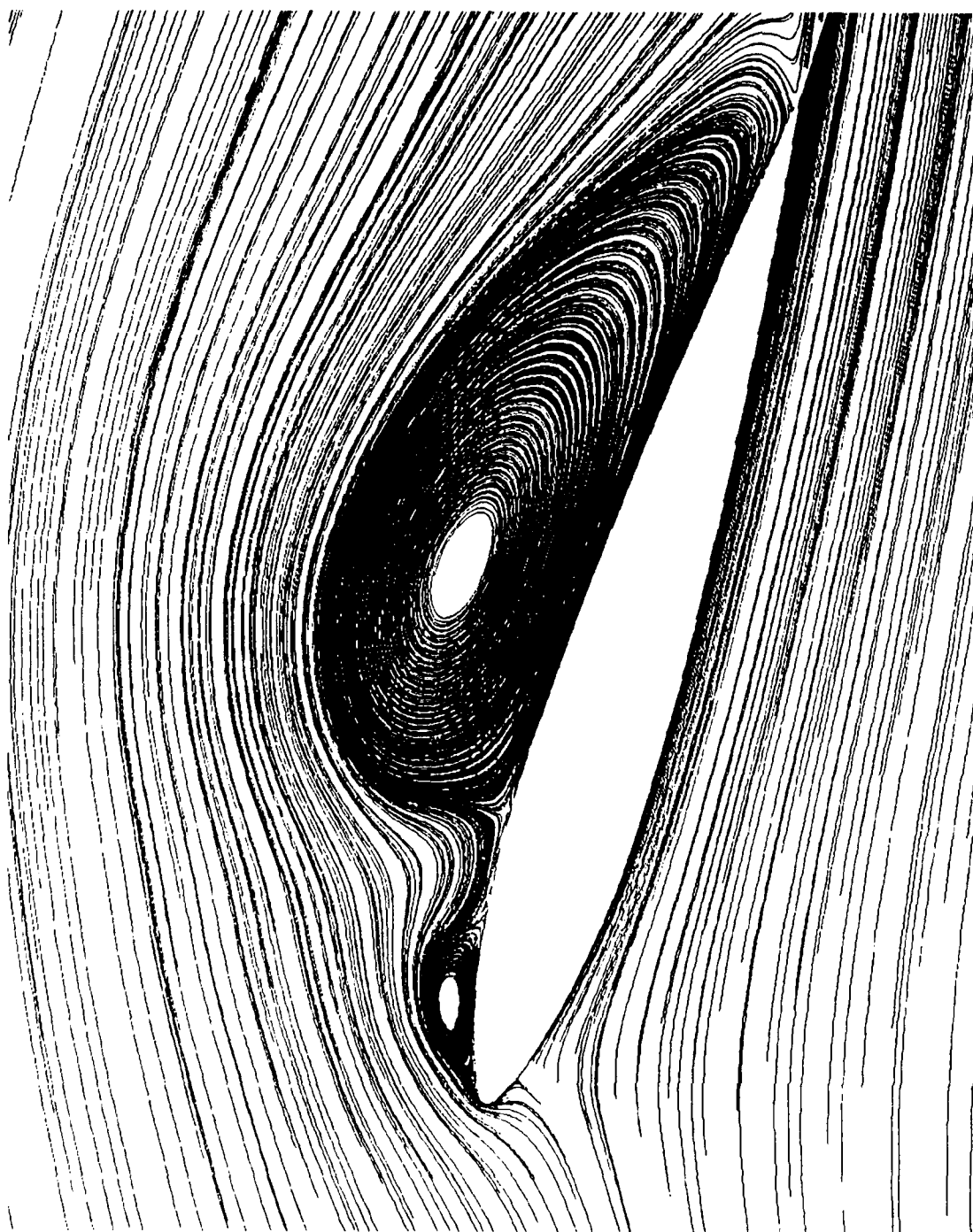


Figure 20. Instantaneous Streamlines, NACA 0012-33, $M=0.4$,
 $k=0.01$, $\alpha=17^\circ$

C. VORTEX FLOW DEVELOPMENT

1. Rapidly Pitching Airfoil

The development of the vortical flowfield as the angle of attack is increasing follows a consistent, general sequence of events. This sequence of events requires examination of the variation of several flow quantities as angle of attack is increased. Figures 21-33 illustrate the flow development stages using the velocity vector field, the pressure, and vorticity field contours for the NACA 0012-63 airfoil at $M=0.4$ and $k=0.01$. Figures 34-47 display the associated surface pressures and temperatures of the developing flow.

Initially, smooth streamlined flow is observed over the airfoil leading edge (Figures 21-22). As angle of attack increases beyond a certain critical limit depending on pitching rate, freestream Mach number, airfoil shape, and Reynolds number, small reverse flow regions develop on the upper surface aft of the suction peak and forward of the trailing edge due to the adverse pressure gradients encountered by the flow. Figure 23 shows the reversed boundary layer flow near the airfoil surface. Figure 24 displays the developing leading edge vortex.

The developing vortex forms on the upper surface just aft of the leading edge as a result of the combination of the accelerated flow near the suction peak and the reverse flow just aft of the suction peak. It is observed that the dynamic stall vortex initiates as a separated flow bubble, and rapidly

grows in size to form the characteristic leading edge dynamic stall vortical structure as the angle of attack increases. During this initiation process the primary vortex has a oval shape and becomes more rounded as the angle of attack increases. Figure 25 shows the oval dynamic stall vortex taking shape. Figure 26 displays the relative strength of the developing vortex.

The vortex grows in size and strengthens, becoming approximately circular as angle of attack increases, and moves away from the airfoil. Figure 27 shows the development of the vortex as it moves downstream. Passage of the dynamic stall vortex over the airfoil surface induces reverse velocities and significantly contributes to the development of reversed flows. A secondary vortex originates near the leading edge and also grows as angle of attack increases. Figures 28 and 29 show the development of a secondary vortex as the primary vortex moves downstream and promotes reverse flow over the whole upper airfoil surface.

At the trailing edge, flow separation is initiated at approximately the same time as at the leading edge, and a pressure gradient exists between the lower and upper surfaces. The upper surface reverse flow combines with the high pressure flow from the lower surface to form a counter-clockwise vortex at the trailing edge shortly before dynamic stall occurs. Figures 30 and 31 show the developed trailing edge vortex 0.6° angle of attack before peak lift coefficient is obtained. As

the primary vortex grows and moves downstream past approximately 60-70% chord, dynamic stall occurs, usually accompanied by development of a small, tertiary vortex at the leading edge. Figures 32 and 33 display the position of the dynamic stall vortex 0.4° angle of attack after attainment of peak lift coefficient.

By this time, the primary vortex is centered at a distance greater than the airfoil maximum thickness from the airfoil and combines with lower surface high pressure flow to energize the counter-clockwise vortex at the trailing edge.

With further increase in angle of attack, the airfoil enters the deep stall regime, and the freestream flow has no effect on the upper surface flow characteristics. In this case, the aerodynamic behavior of the airfoil is greatly determined by the vortical flow field formed by the shed vortices, and the strength of the vortices themselves determine the flow over the upper surface. Figures 48 and 49 show the NACA 0012-33 airfoil in deep stall at 0.3 Mach, $k=0.02$, $\alpha=22.0^\circ$ and demonstrate that the vortices can combine to form a large vortical region and entrain other secondary flows. In this case a counterclockwise vortex was formed between the paired primary and secondary vortices and the airfoil.

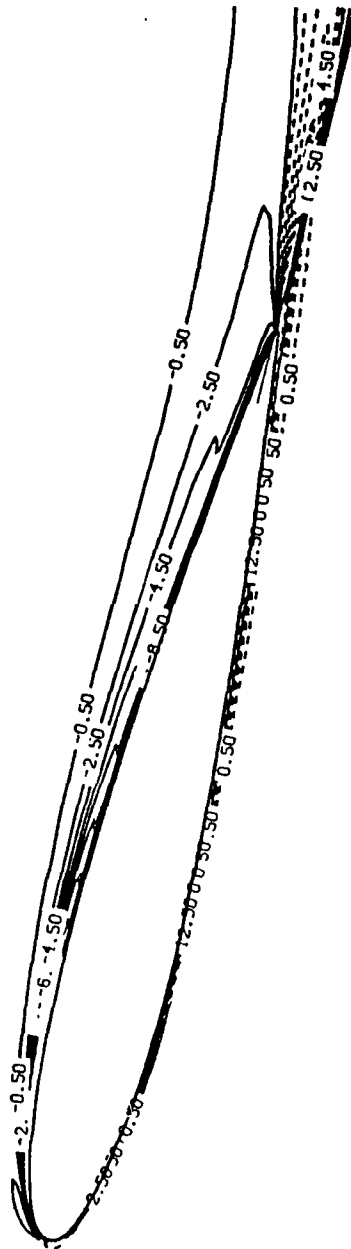


Figure 22. Vorticity Contours, NACA 0012-63, $M=0.3$, $k=0.01$, $\alpha=14.0^\circ$

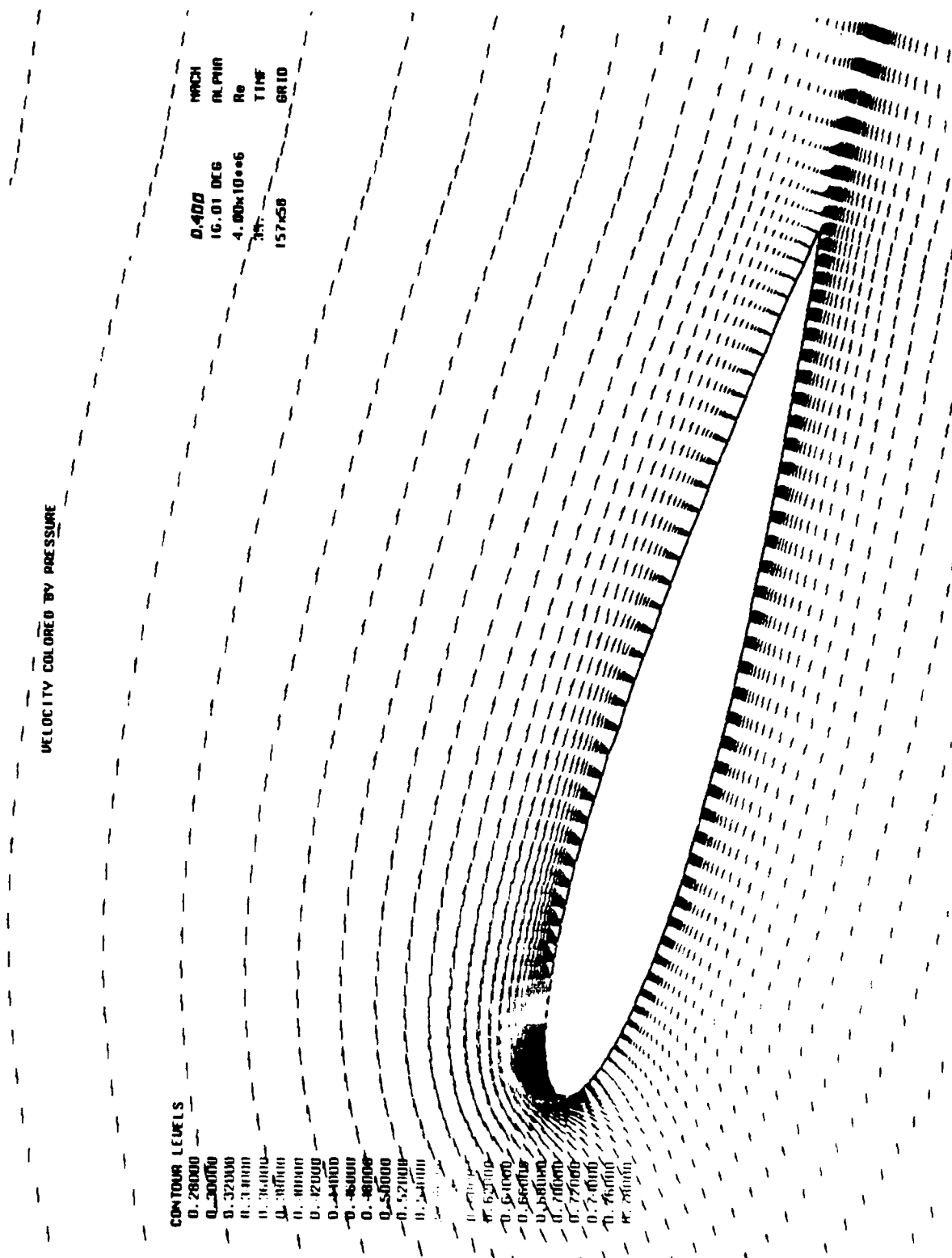


Figure 23. Velocity Field, NACA 0012-63, $M=0.4$, $k=0.01$, $\alpha=16.0^\circ$

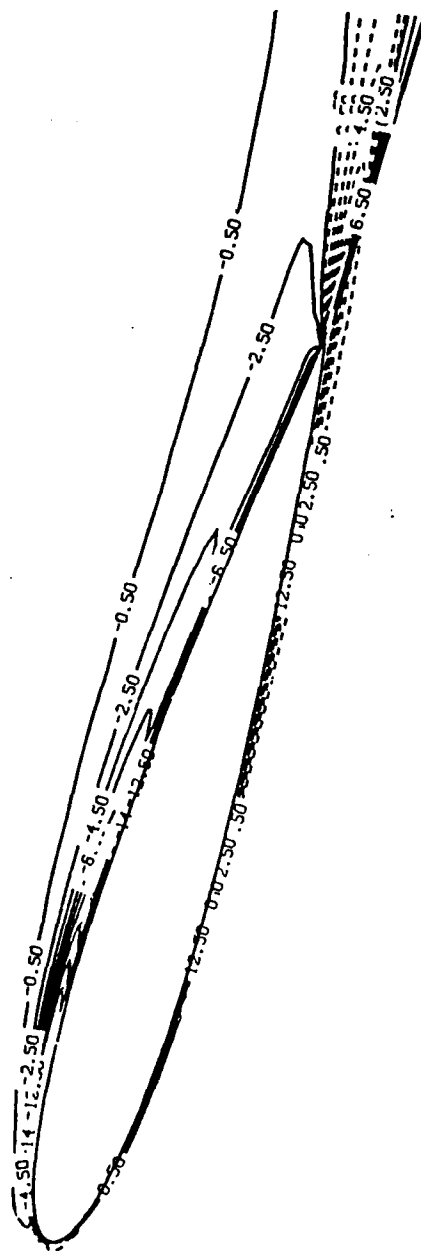


Figure 24. Vorticity Contours, NACA 0012-63, $M=0.4$, $k=0.01$, $\alpha=16.0^\circ$

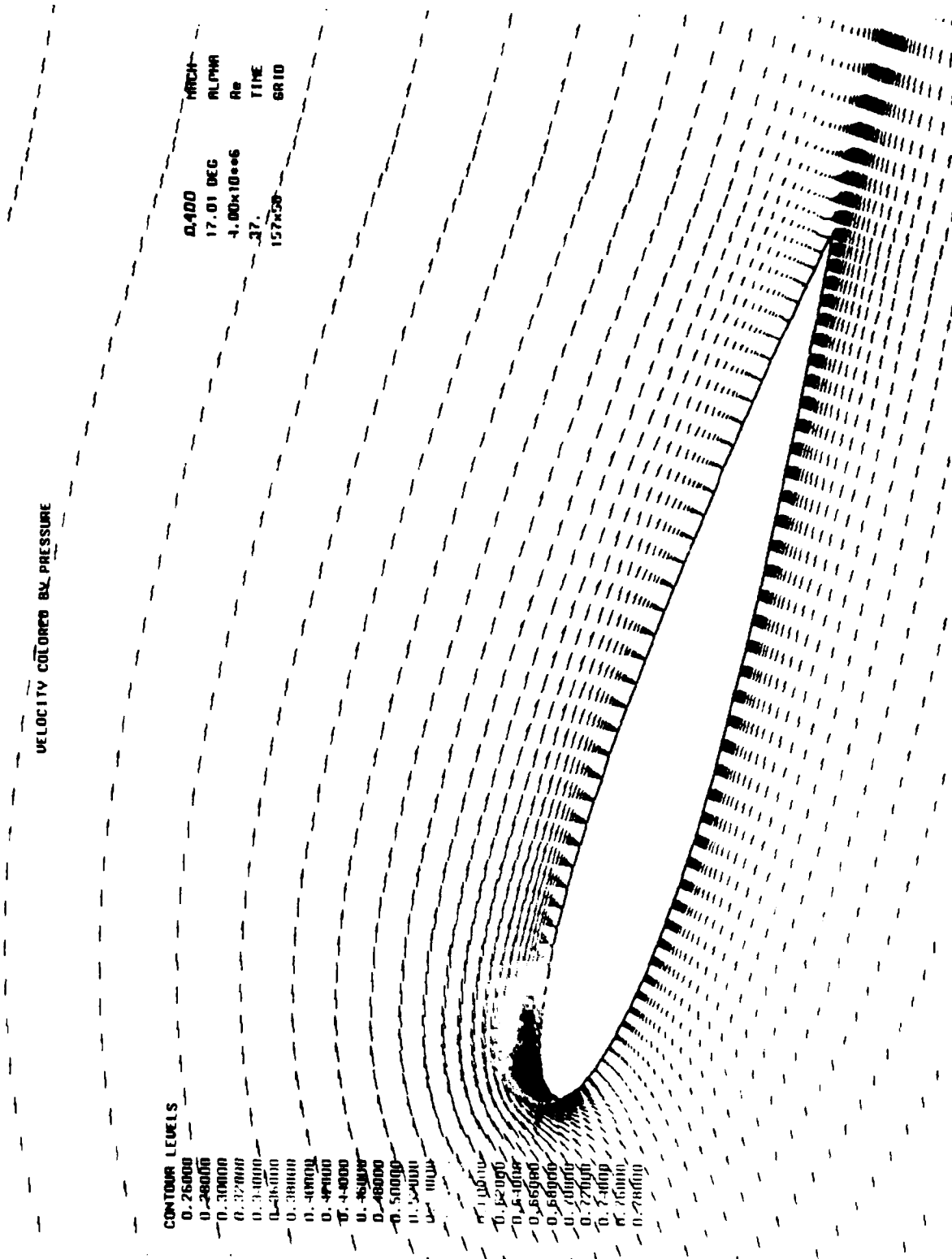


Figure 25. Velocity Field, NACA 0012-63, $M=0.4$, $k=0.01$, $\alpha=17.0^\circ$

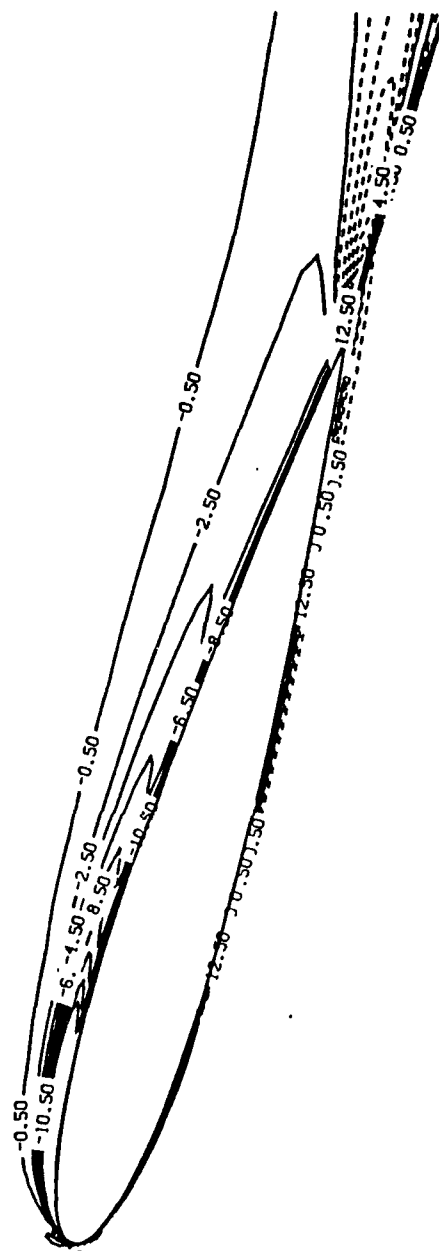


Figure 26. Vorticity Contours, NACA 0012-63, $M=0.3$, $k=0.01$, $\alpha=17.0^\circ$

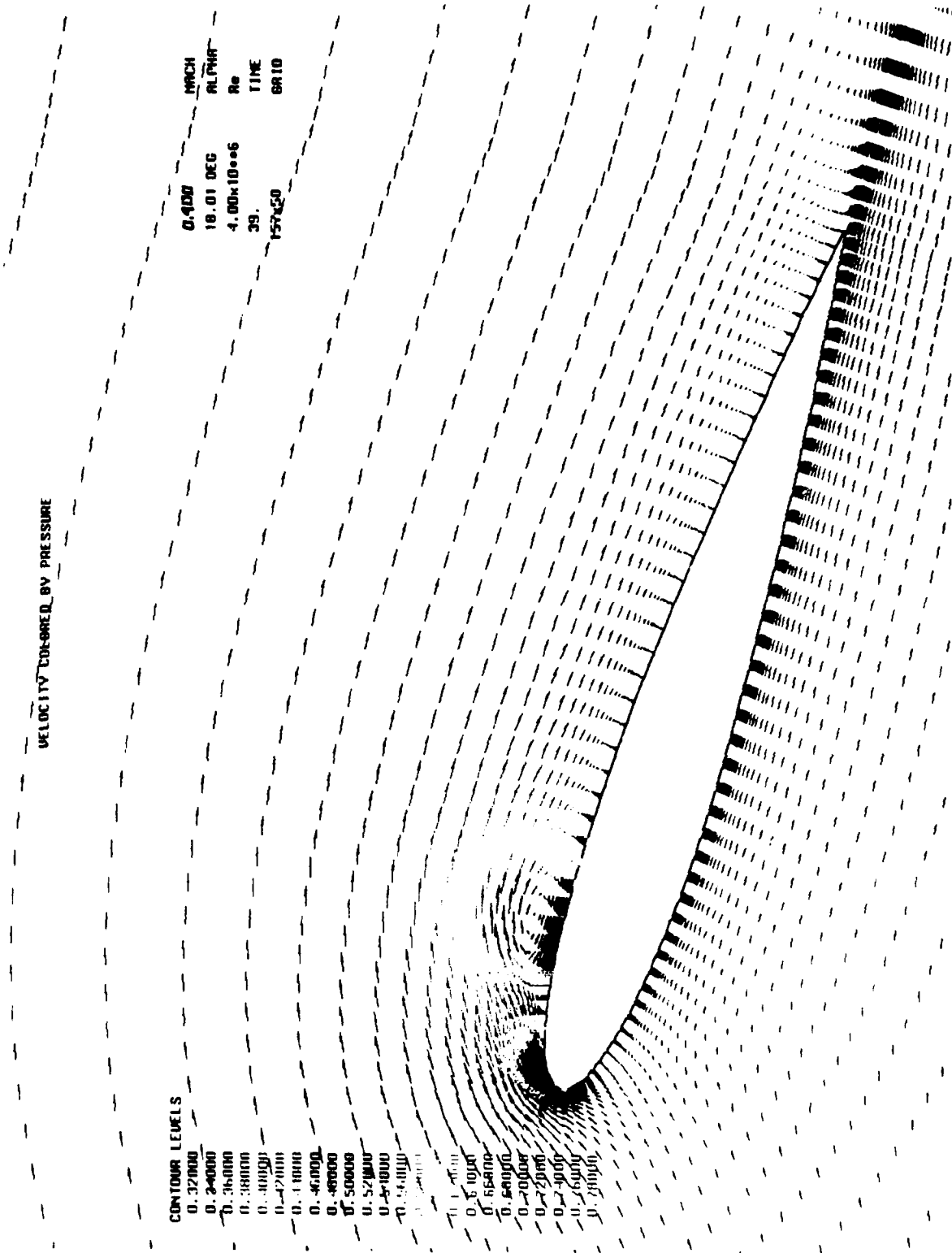


Figure 27. Velocity Field, NACA 0012-63, $M=0.4$, $k=0.01$, $\alpha=18.0^\circ$

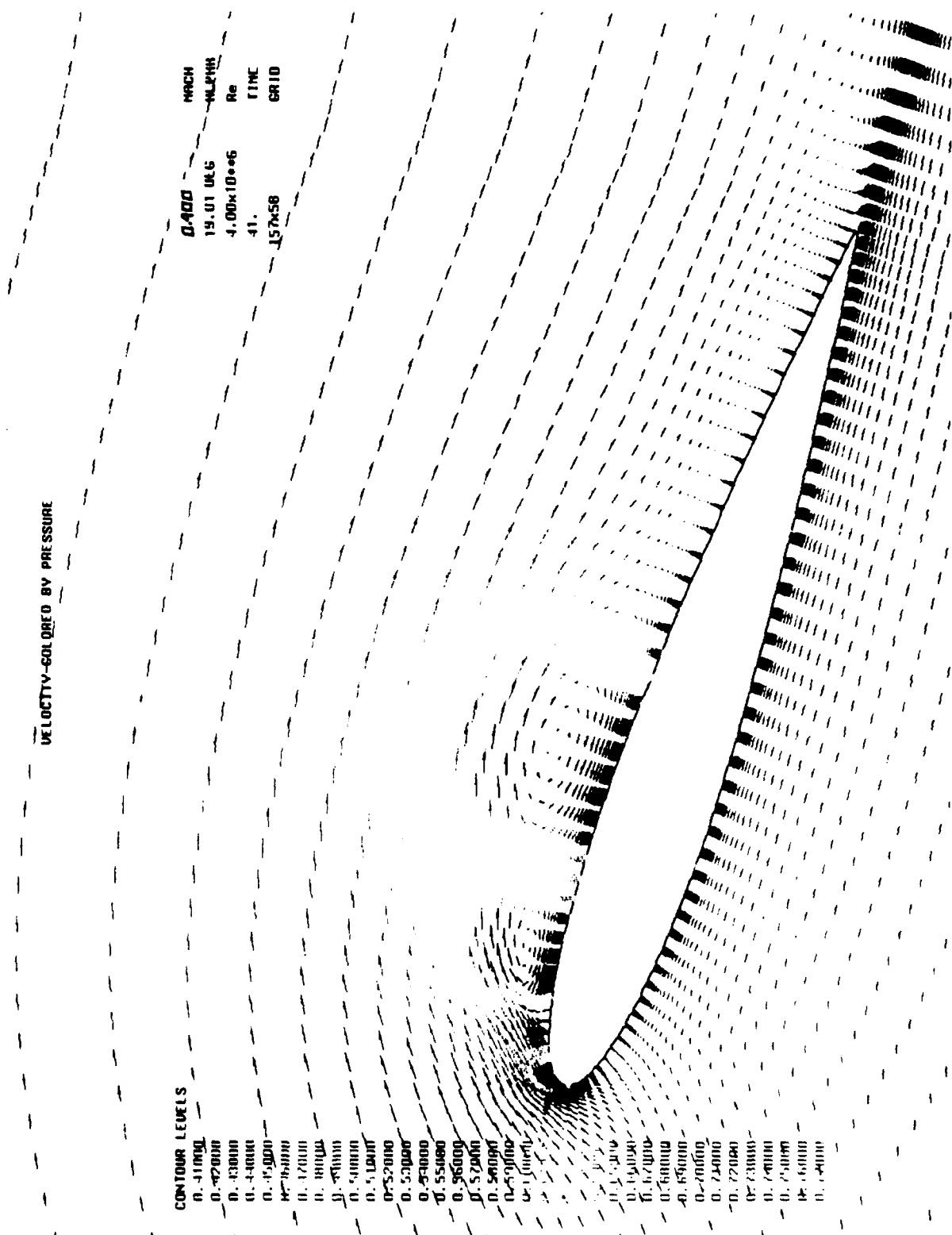


Figure 28. Velocity Field, NACA 0012-63, $M=0.4$, $k=0.01$, $\alpha=19.0^\circ$

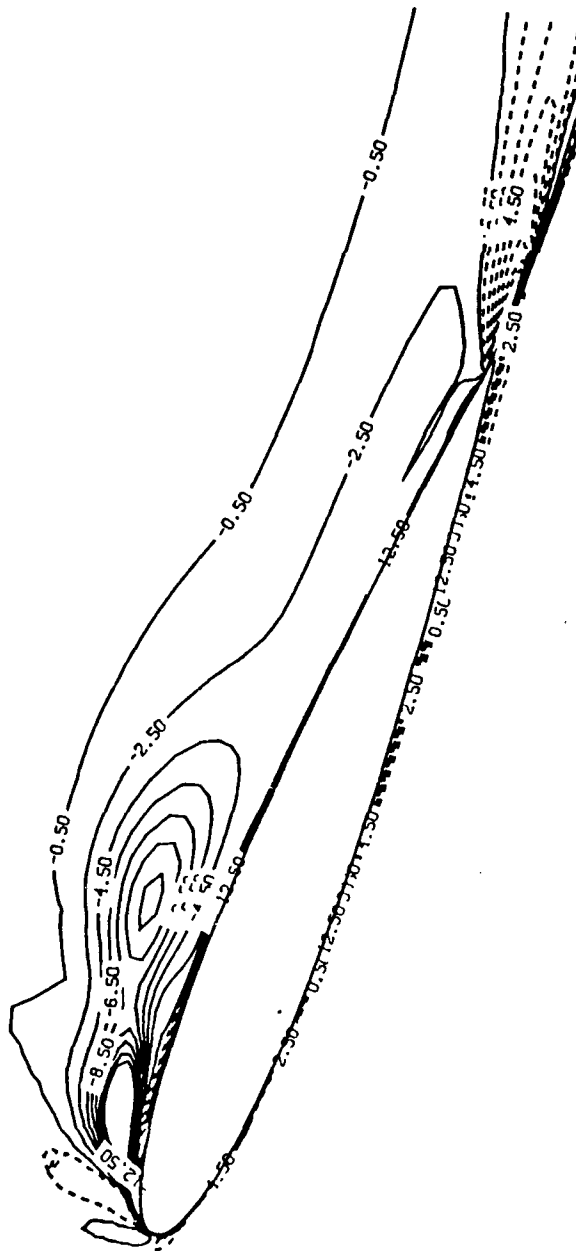


Figure 29. Vorticity Contours, NACA 0012-63, $M=0.4$, $k=0.01$, $\alpha=19.0^\circ$

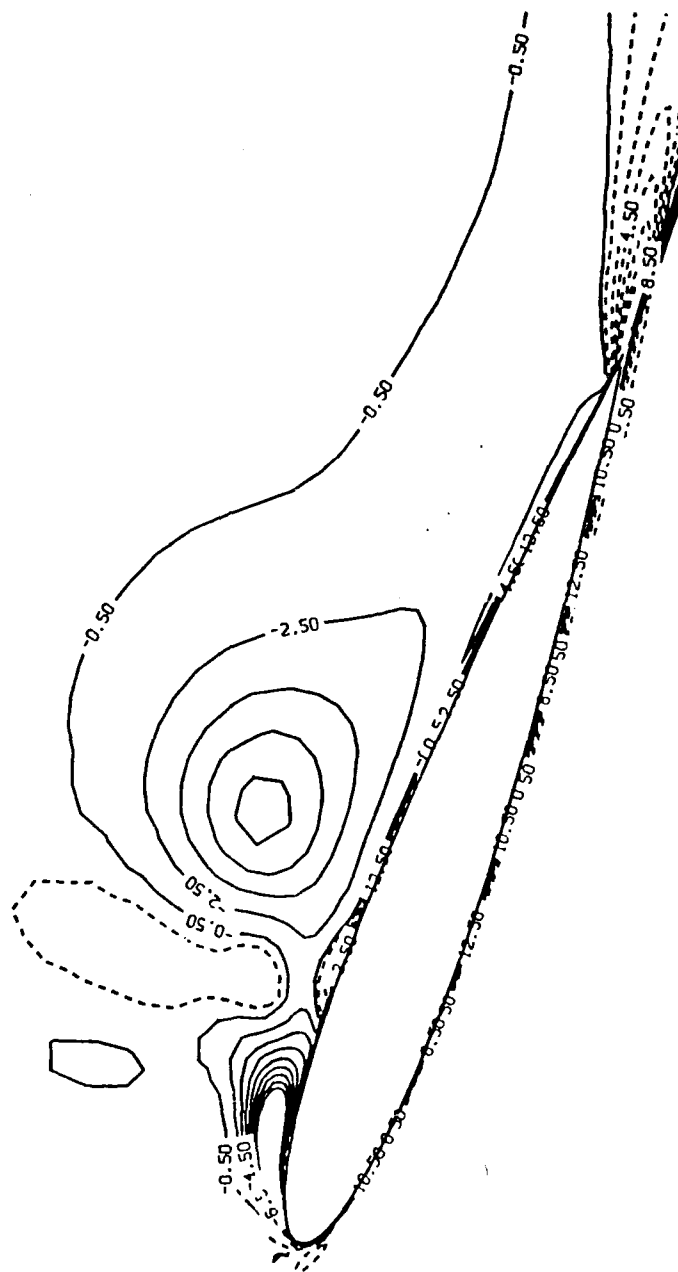


Figure 31. Vorticity Contours, NACA 0012-63, $M=0.3$, $k=0.01$, $\alpha=20.0^\circ$

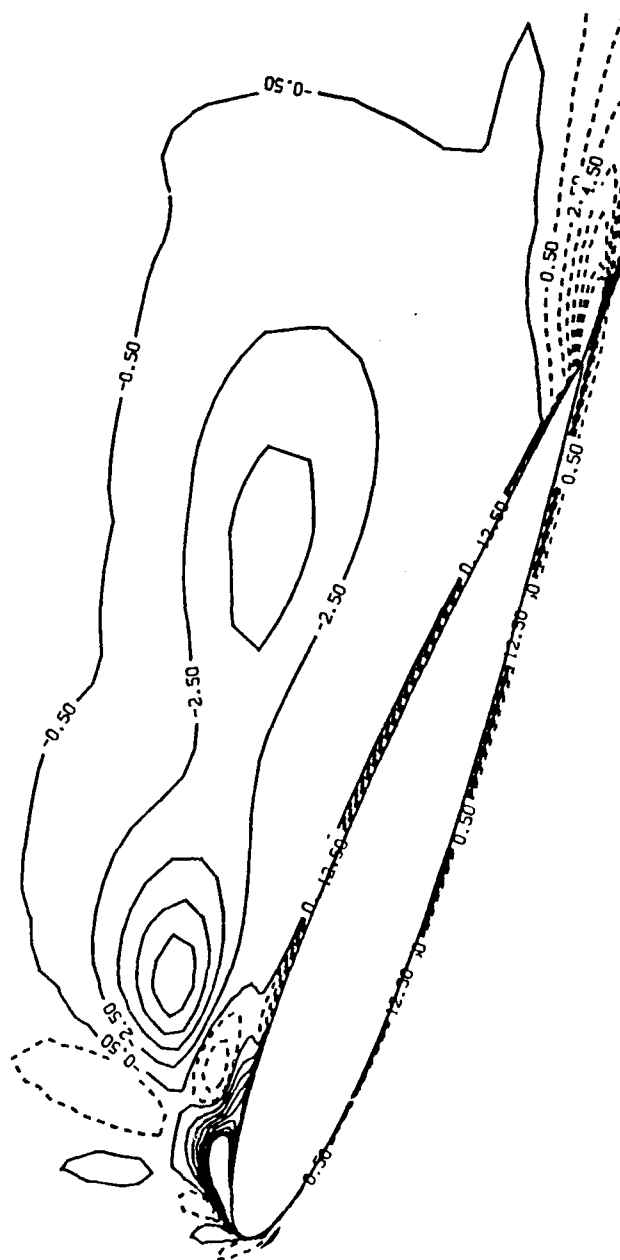


Figure 33. Vorticity Contours, NACA 0012-63, $M=0.4$, $k=0.01$, $\alpha=21.0^\circ$

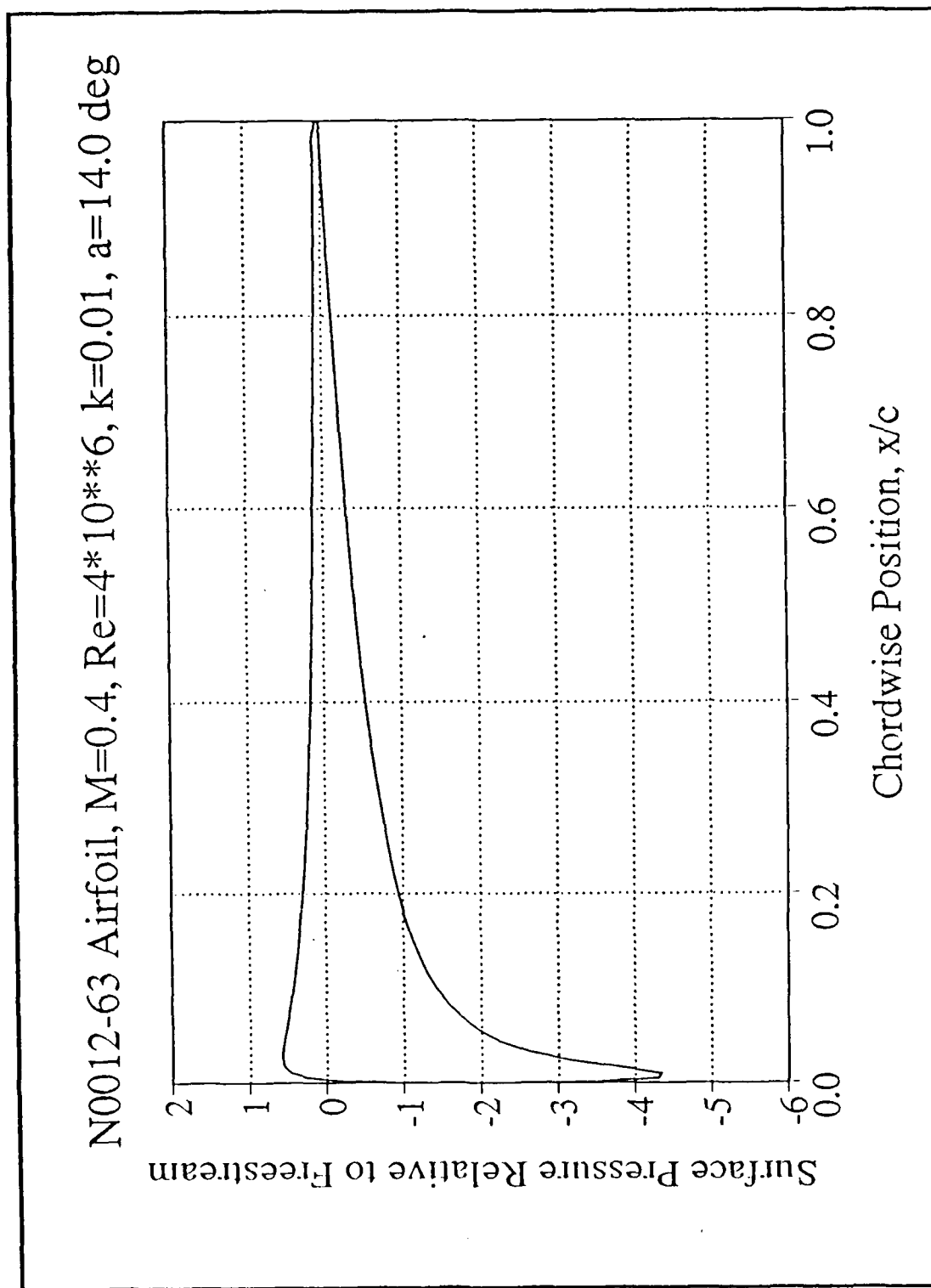


Figure 34. Surface Pressure, NACA 0012-63, $M=0.4$, $k=0.01$, $\alpha=14.0^\circ$

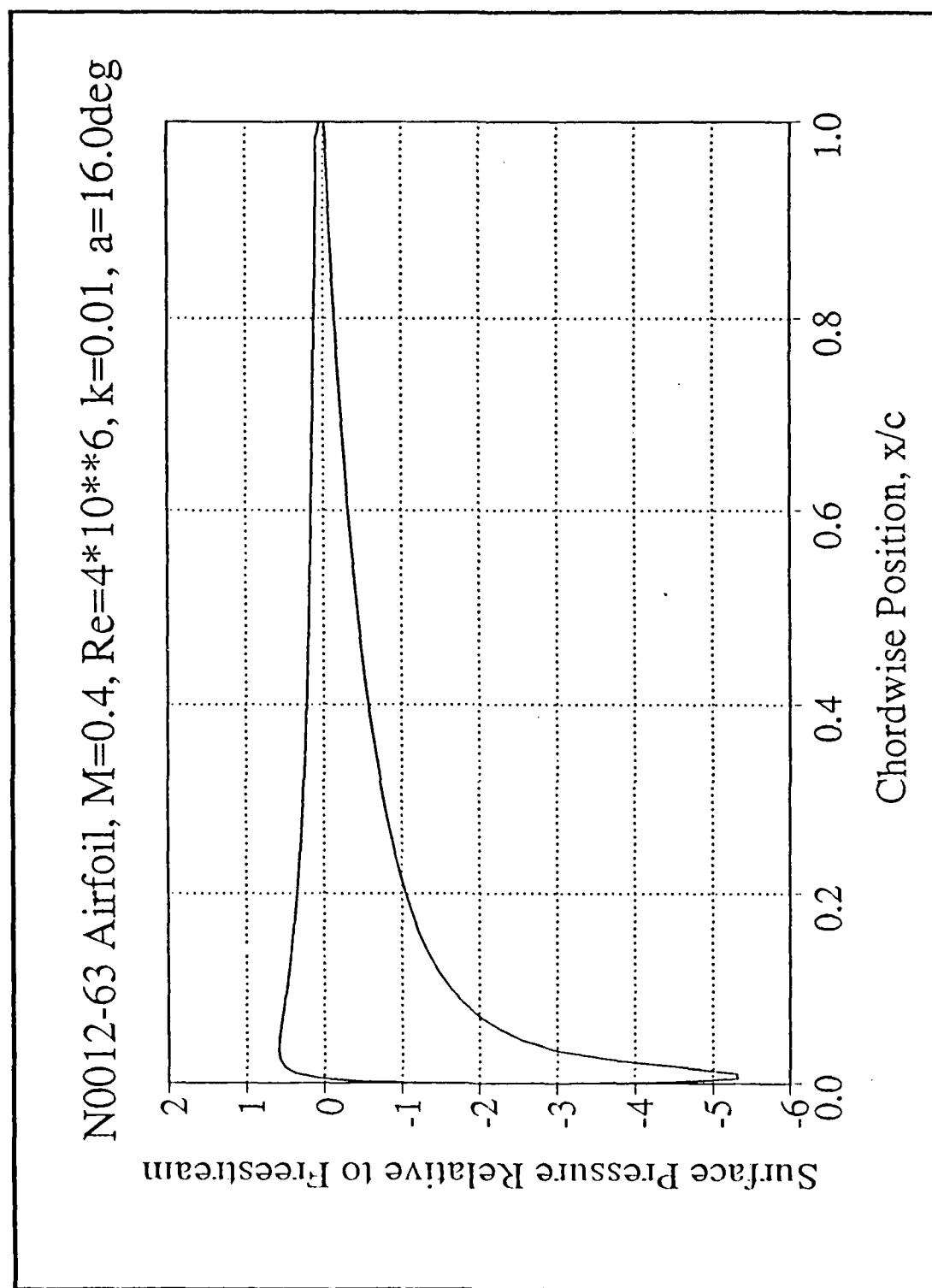


Figure 35. Surface Pressure, NACA 0012-63, $M=0.4$, $k=0.01$, $\alpha=16.0^\circ$

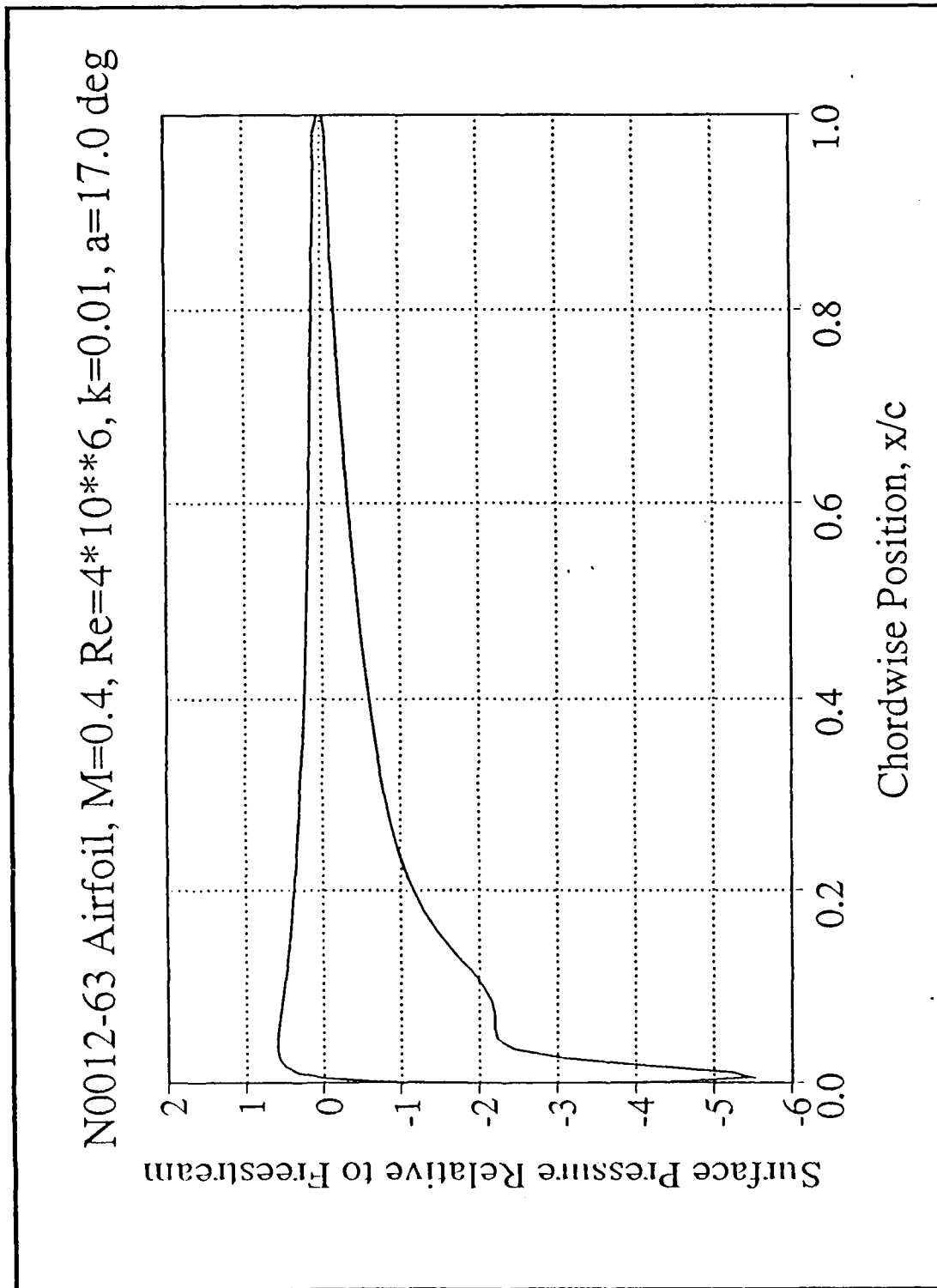


Figure 36. Surface Pressure, NACA 0012-63, $M=0.4$, $k=0.01$, $\alpha=17.0^\circ$

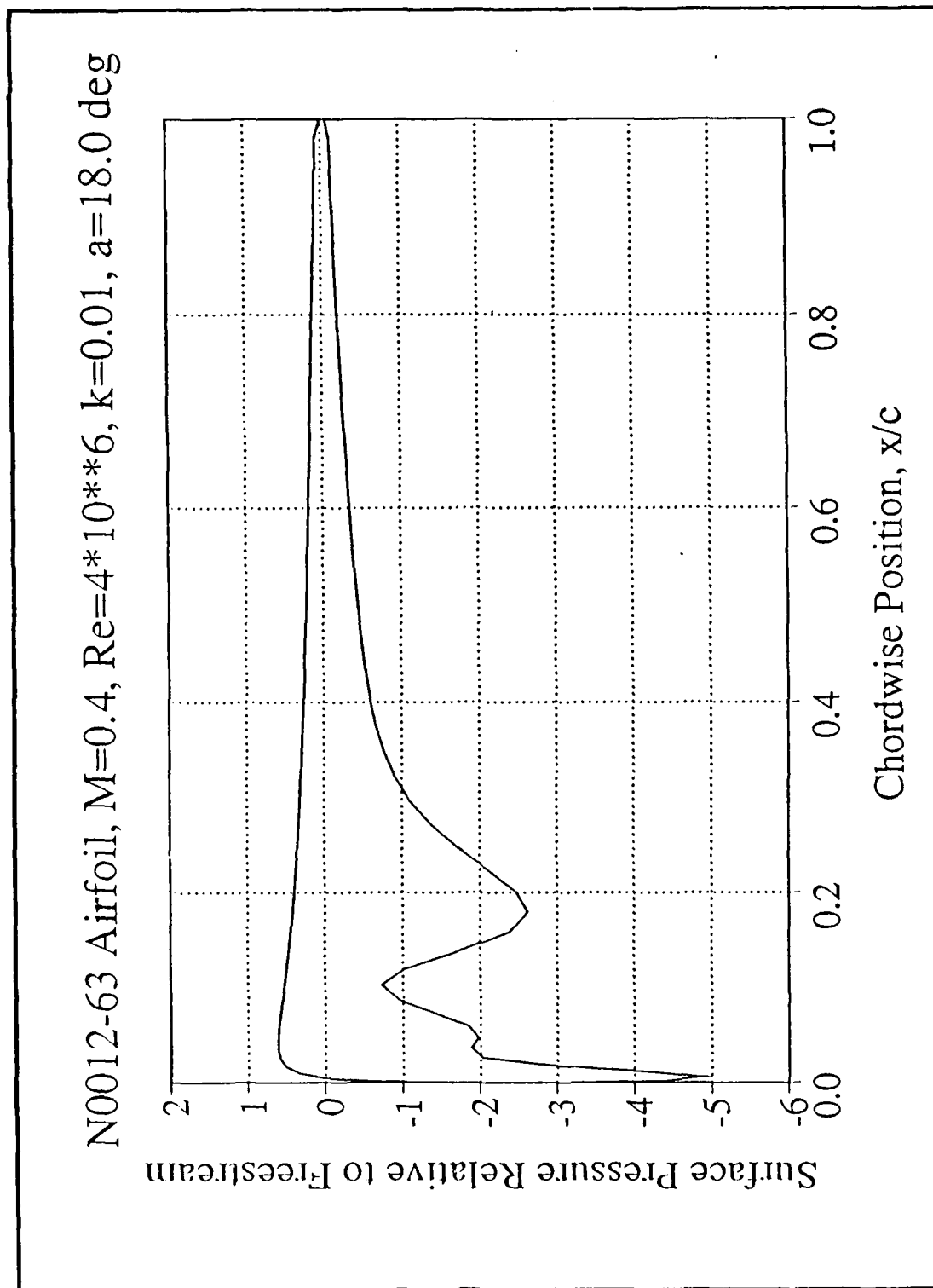


Figure 37. Surface Pressure, NACA 0012-63, $M=0.4$, $k=0.01$, $\alpha=18.0^\circ$

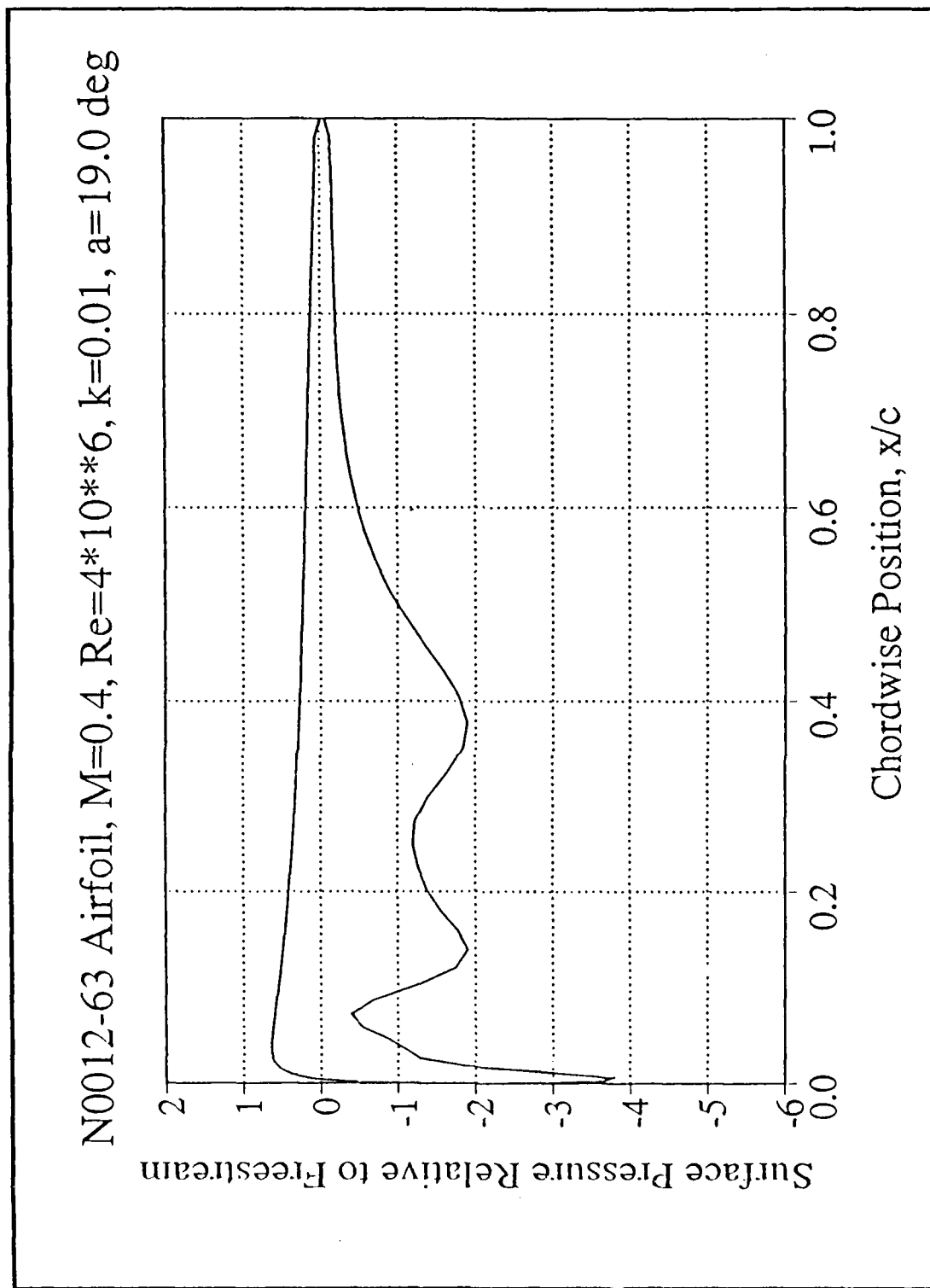


Figure 38. Surface Pressure, NACA 0012-63, $M=0.4$, $k=0.01$, $\alpha=19.0^\circ$

N0012-63 Airfoil, $M=0.4$, $Re=4 \times 10^6$, $k=0.01$, $\alpha=20.0^\circ$

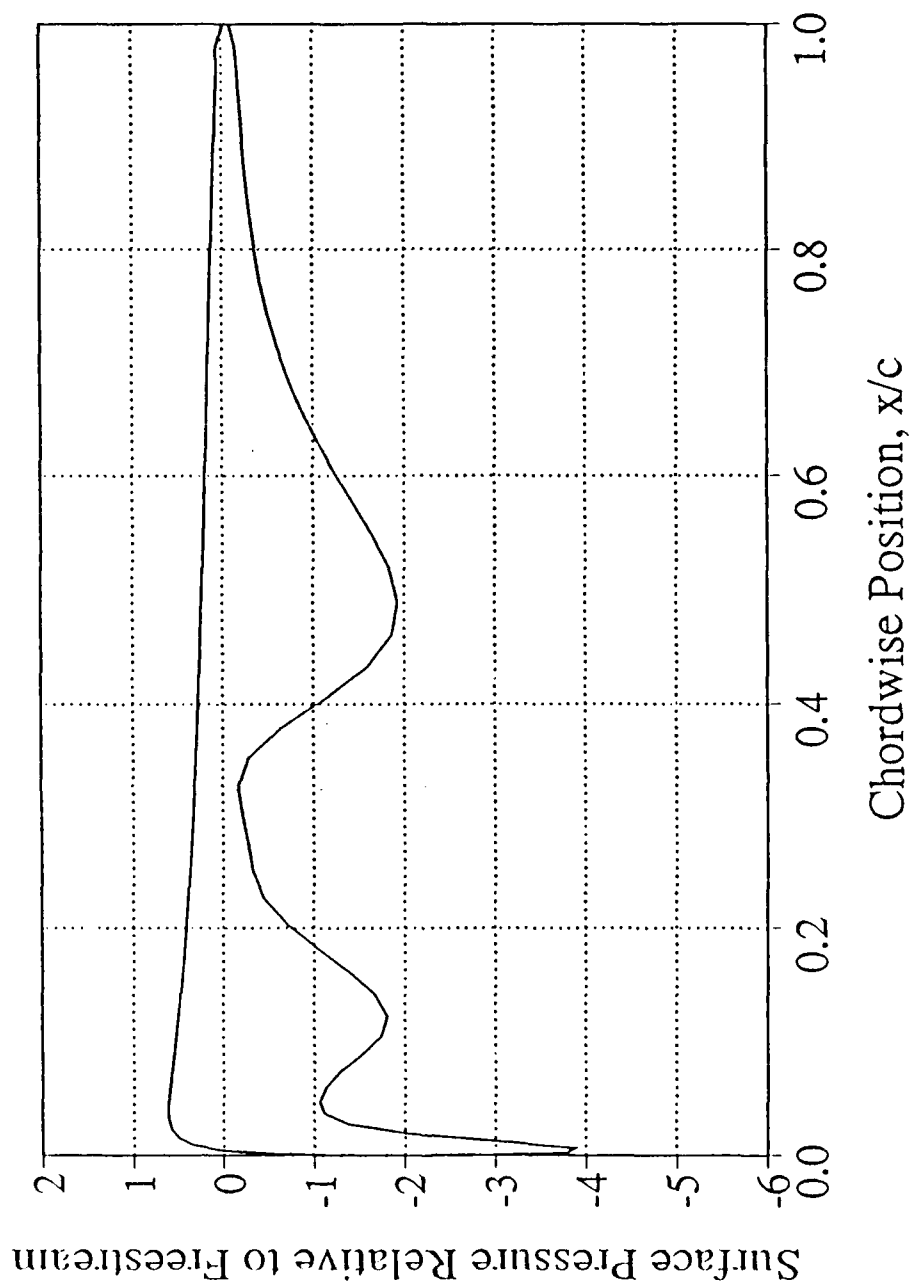


Figure 39. Surface Pressure, NACA 0012-63, $M=0.4$, $k=0.01$, $\alpha=20.0^\circ$

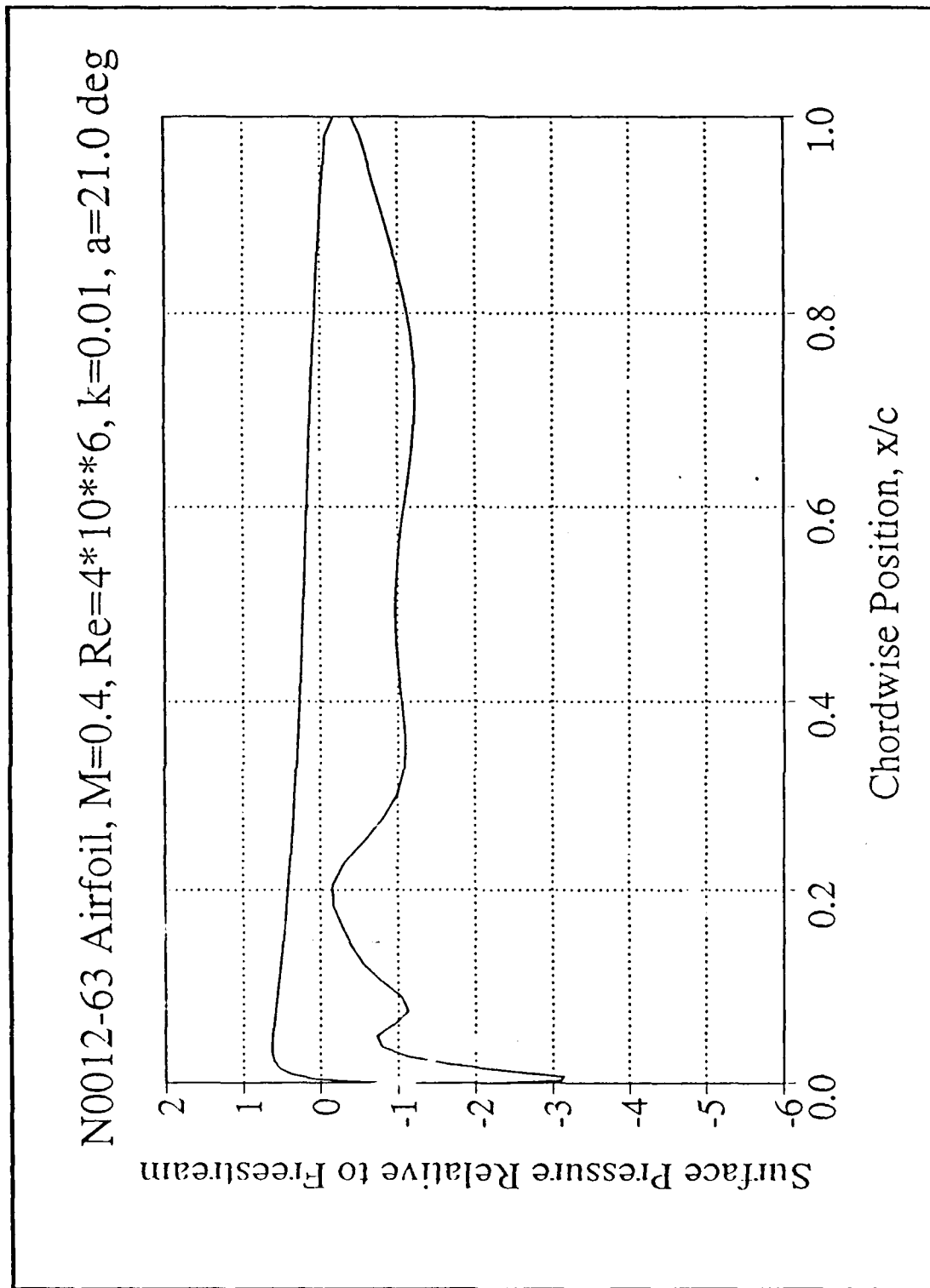


Figure 40. Surface Pressure, NACA 0012-63, $M=0.4$, $k=0.01$, $\alpha=21.0^\circ$

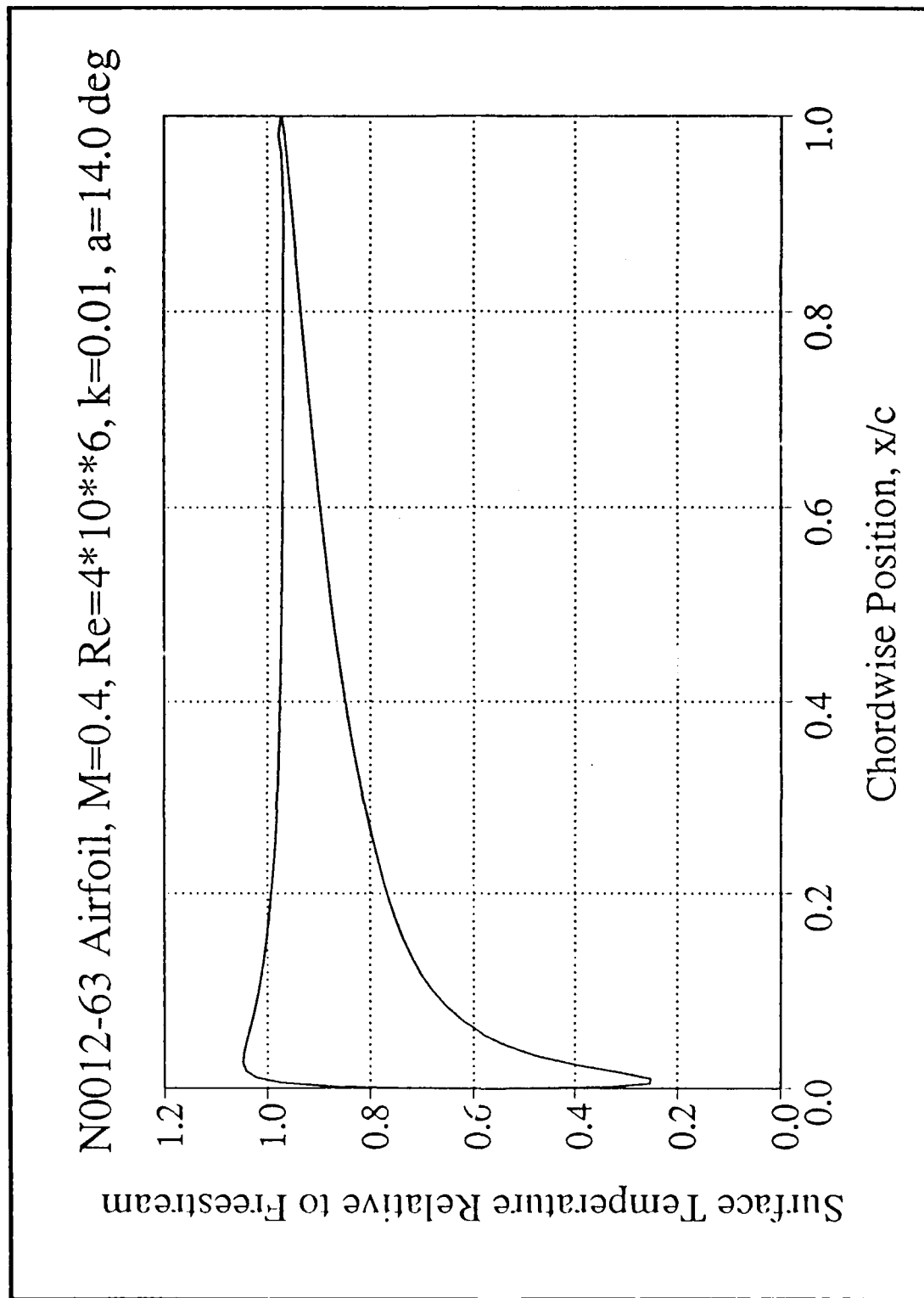


Figure 41. Surface Temperature, NACA 0012-63, $M=0.4$, $k=0.01$, $\alpha=14.0^\circ$

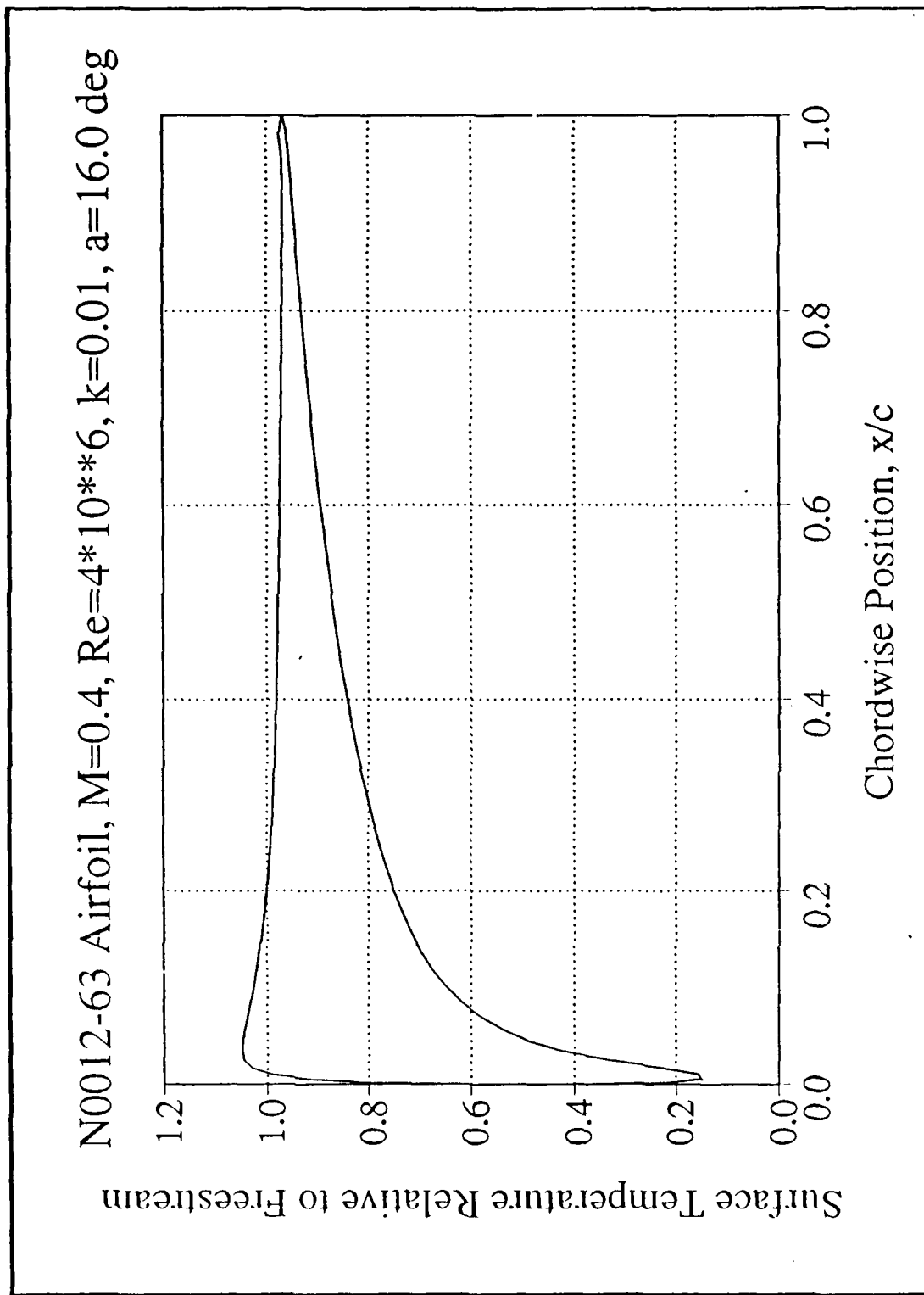


Figure 42. Surface Temperature, NACA 0012-63, $M=0.4$, $k=0.01$, $\alpha=16.0^\circ$

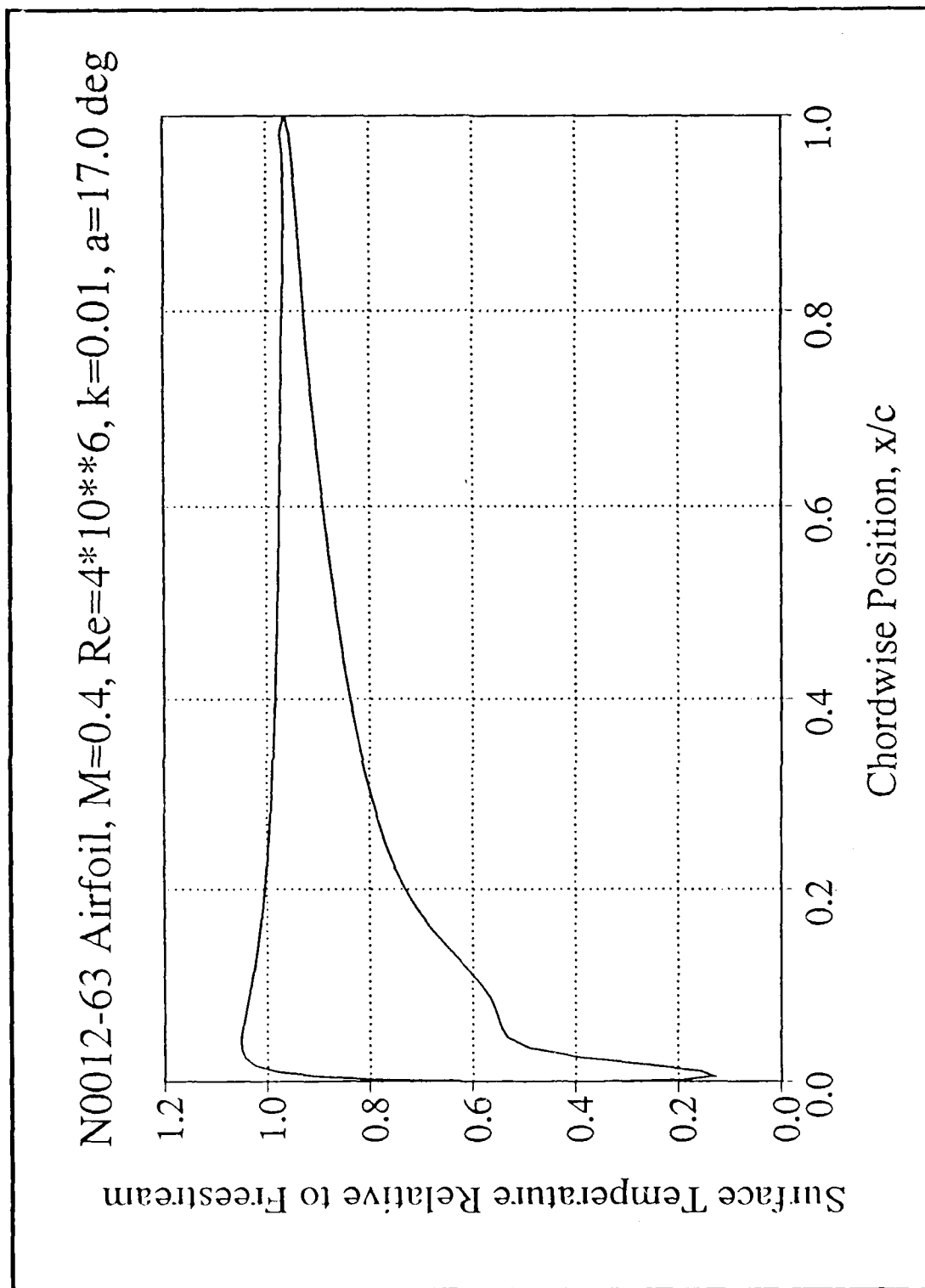


Figure 43. Surface Temperature, NACA 0012-63, $M=0.4$, $k=0.01$, $\alpha=17.0^\circ$

N0012-63 Airfoil, $M=0.4$, $Re=4 \times 10^6$, $k=0.01$, $\alpha=18.0^\circ$

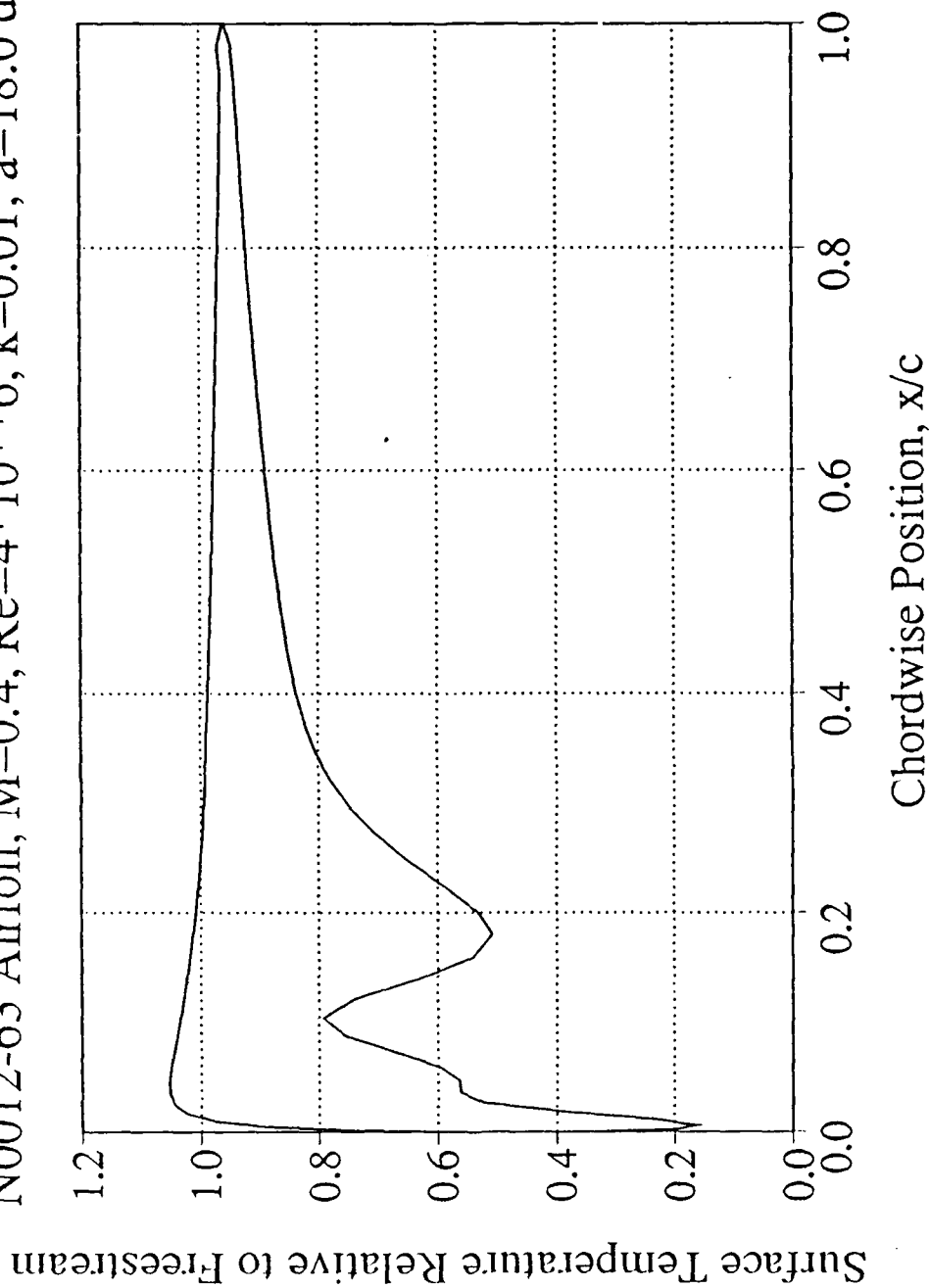


Figure 44. Surface Temperature, NACA 0012-63, $M=0.4$, $k=0.01$, $\alpha=18.0^\circ$

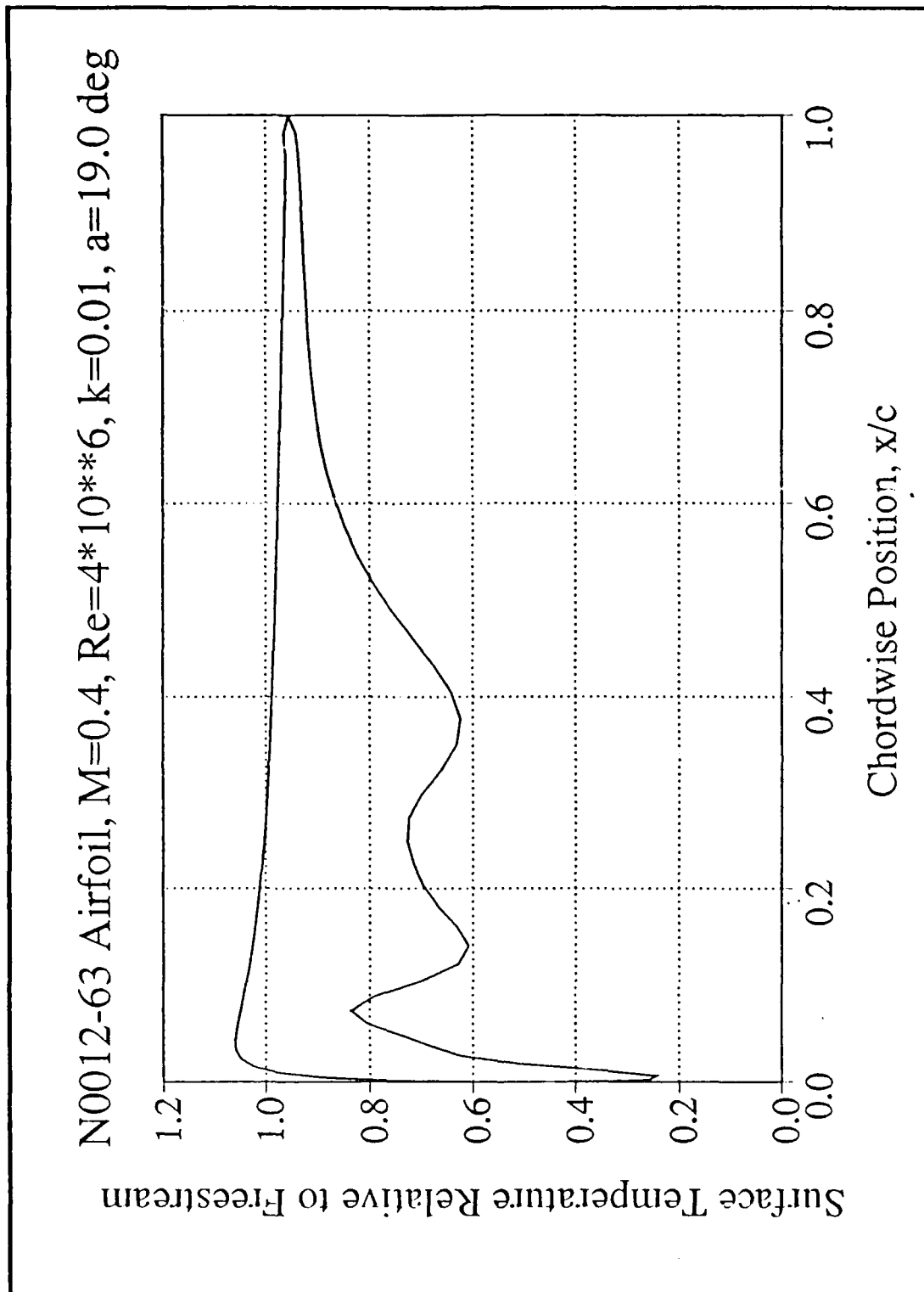


Figure 45. Surface Temperature, NACA 0012-63, $M=0.4$, $k=0.01$, $\alpha=19.0^\circ$

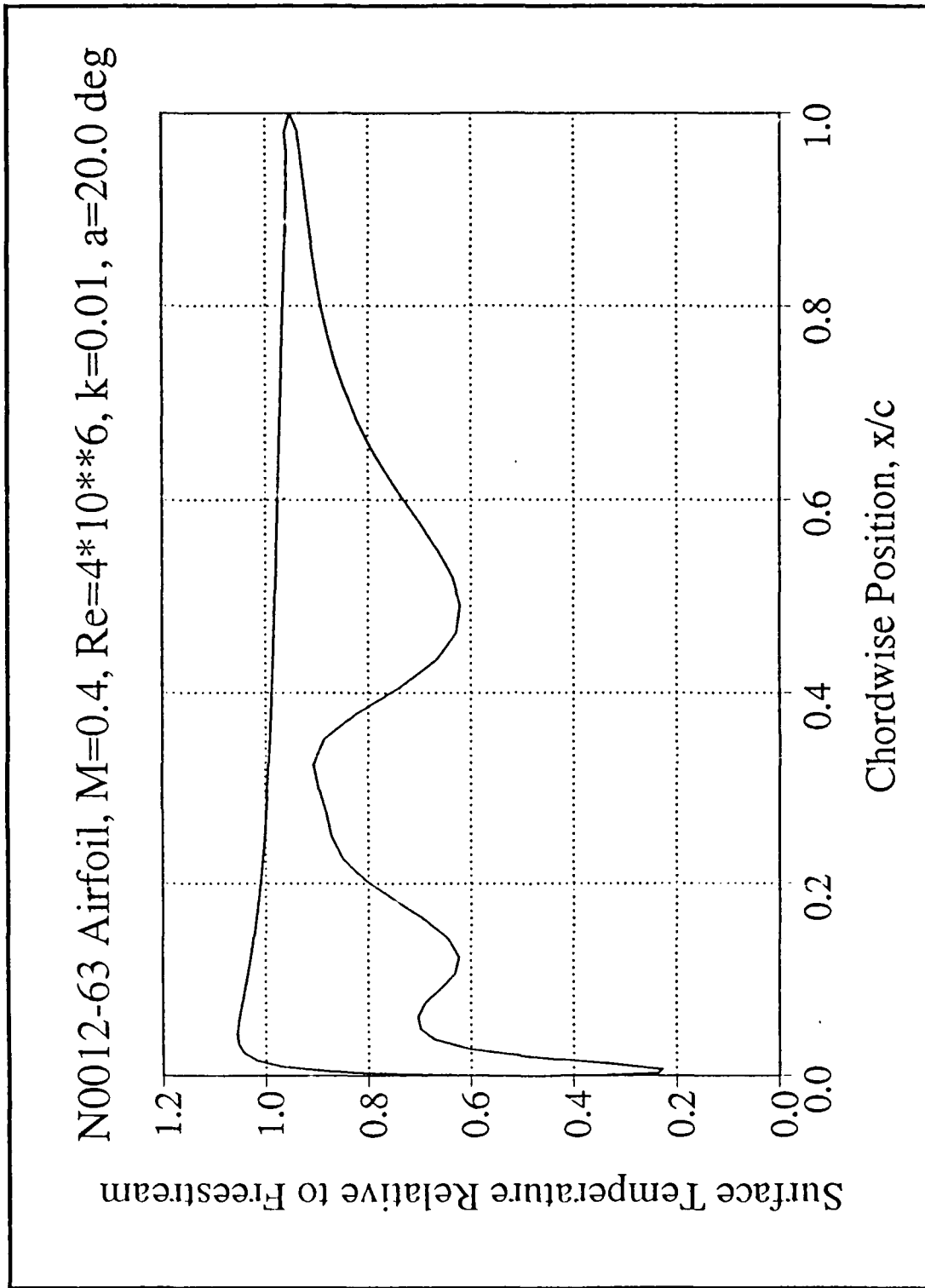


Figure 46. Surface Temperature, NACA 0012-63, $M=0.4$, $k=0.01$, $\alpha=20.0^\circ$

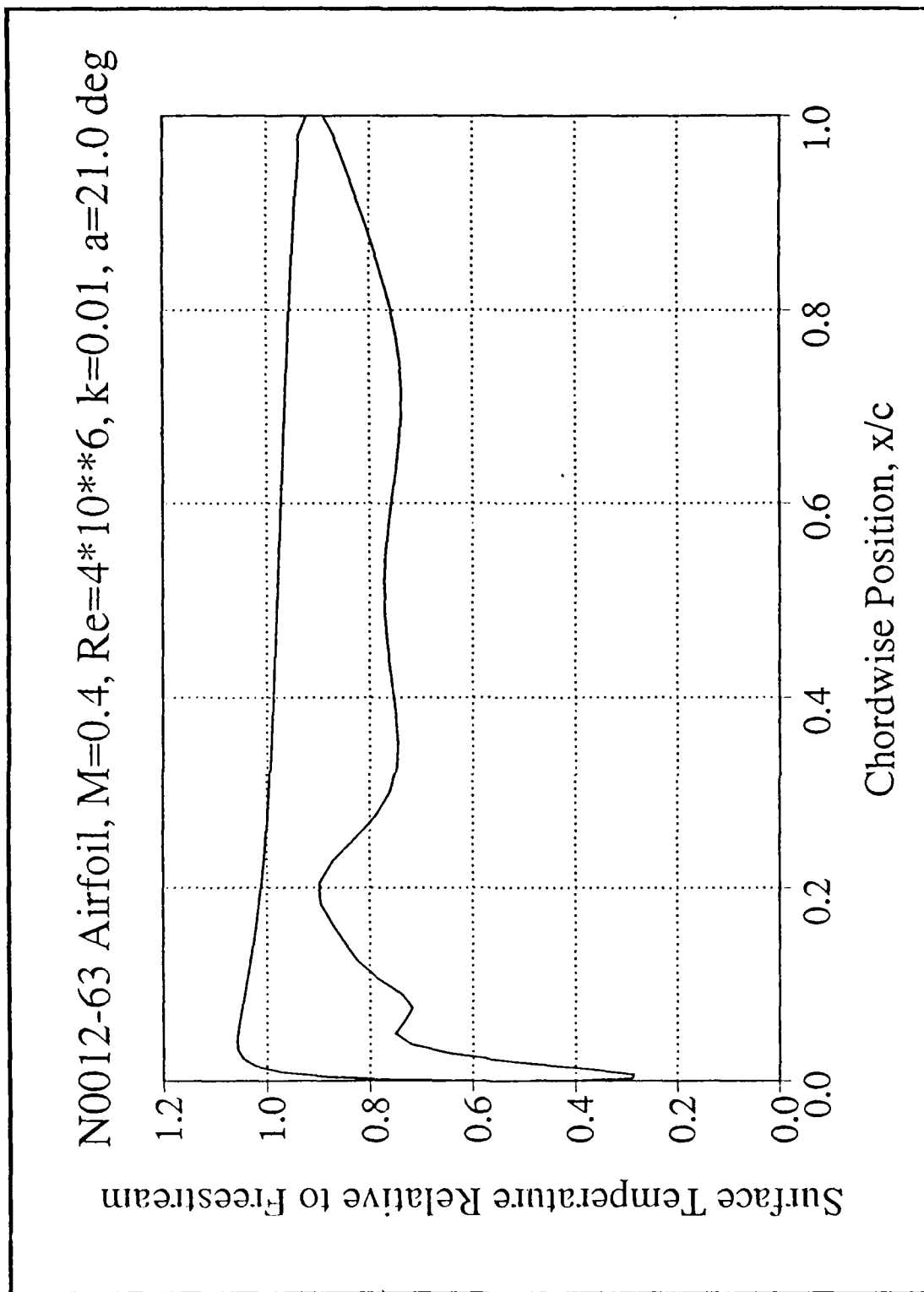


Figure 47. Surface Temperature, NACA 0012-63, $M=0.4$, $k=0.01$, $\alpha=21.0^\circ$

2. Harmonically Oscillating Airfoil

The process of vortical flow development at the leading edge during the upstroke is similar to that of a rapidly pitching airfoil examined in the previous section. Although the pitching rate is not constant in the case of the harmonically oscillating airfoil, boundary layer separation and vortex development and shedding also occur during the upstroke.

The flow reattachment process during the downstroke involves the shedding of the large primary vortex into the wake and the diminishing intensity of the trailing edge vortex. Prior to the downstroke, the combination of the large clockwise primary vortex and the counter-clockwise trailing edge vortex cause extensive reverse flow, even outside the boundary layer, over the airfoil upper surface aft of 30% chord (Figure 50). As the angle of attack decreases further, flow over the leading edge upper surface rapidly reattaches, while the primary vortex is centered above the trailing edge (Figure 51). With further reduction in angle of attack, the primary vortex moves downstream of the airfoil, and the trailing edge vortex diminishes (Figure 52). Reverse flow at this time exists only on aft portions of the airfoil. As the angle of attack approaches $10-11^\circ$, the primary vortex has been swept downstream, the trailing edge vortex has diminished, and smooth, attached flow is established over the upper surface (Figure 53).

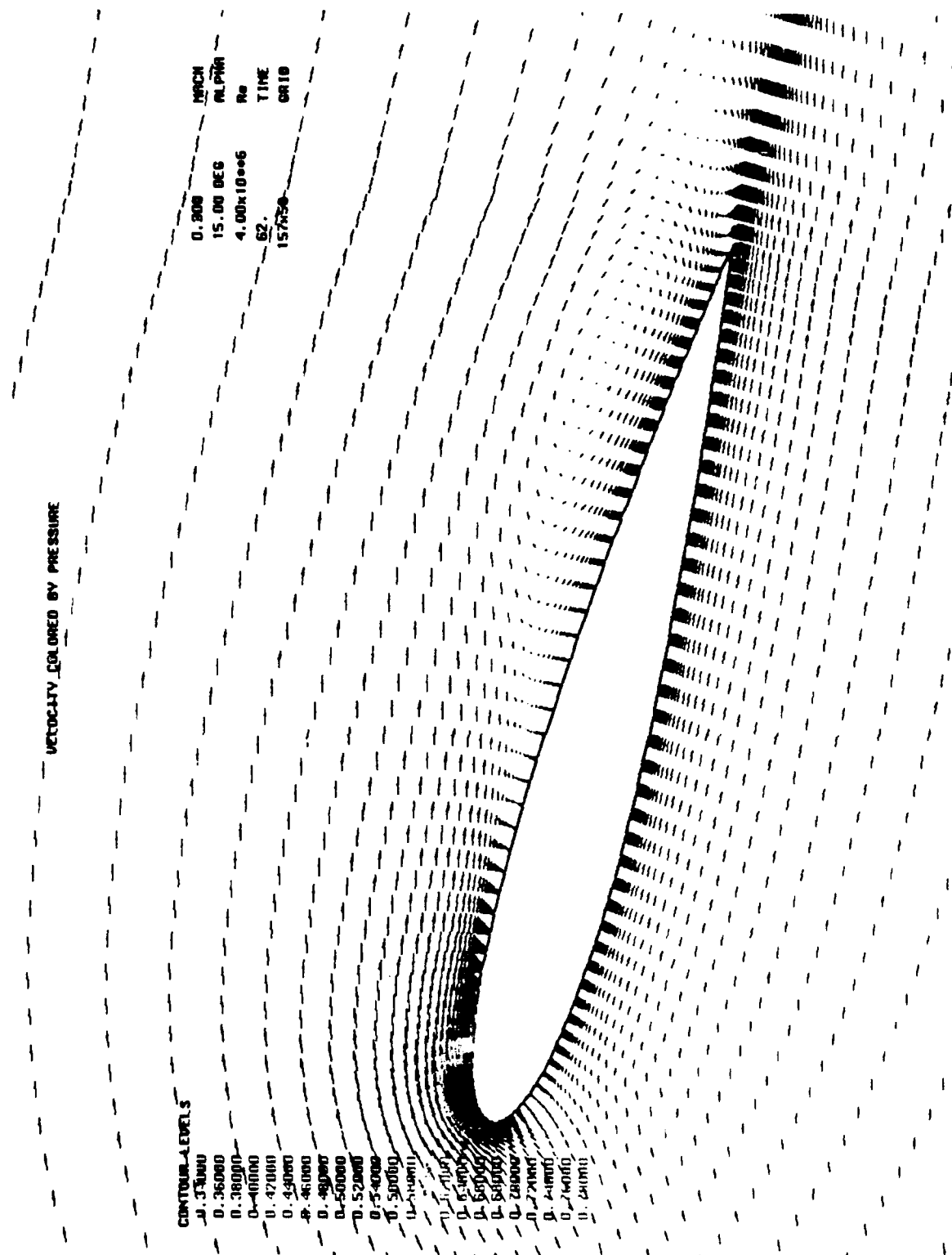
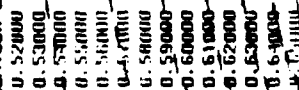


Figure 50. Velocity Field, NACA 0012, $M=0.3$, $k=0.1$, $\alpha=15.0^\circ$ downstroke



94

D. REDUCED FREQUENCY EFFECT

At a given Mach number the three airfoils exhibited higher peak lift coefficients at respectively higher angles of attack at a reduced frequency of $k=0.02$ when compared to that of $k=0.01$. Lift curve slopes for a given airfoil at the two reduced frequencies were nearly identical to the point of initial flow separation and subsequent dynamic stall at $k=0.01$. Lift coefficient at $k=0.02$ continued increasing, showing the increase in unsteady lift with higher pitching rate. The effect of increasing the reduced frequency at a freestream Mach number of 0.3 is shown in Figures 54 and 55 for the NACA 0012 and NACA 0012-33 airfoils, respectively. At the higher reduced frequency of 0.02, formation of the primary vortex occurred at angles of attack 0.7° to 1.6° higher than at a reduced frequency of 0.01 in all cases. As a result, the entire vortical flow development was delayed to progressively higher angles of attack. Dynamic stalling angle occurred 4.0° to 4.8° higher at the higher reduced frequency and the resulting peak lift coefficients were 15-20% higher compared to the $k=0.01$ cases (Table 3).

Experimental work by Chandrasekhara and Carr [Ref. 3] using the NACA 0012 airfoil demonstrated the same trends, wherein a higher reduced frequency resulted in retaining the vortex above the airfoil to higher angles of attack, thereby delaying dynamic stall.

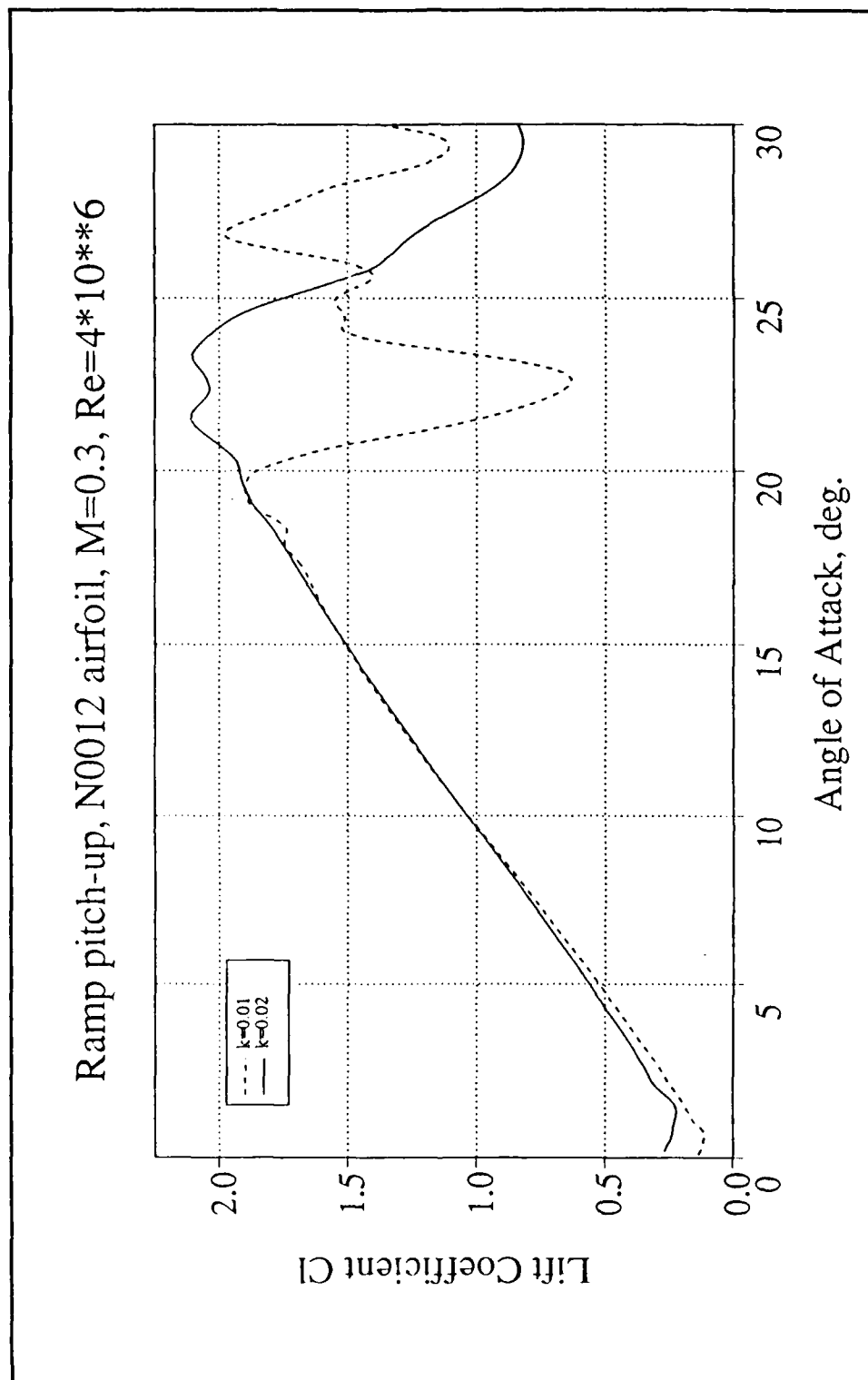


Figure 54. Reduced Frequency Effect, NACA 0012, $M=0.3$

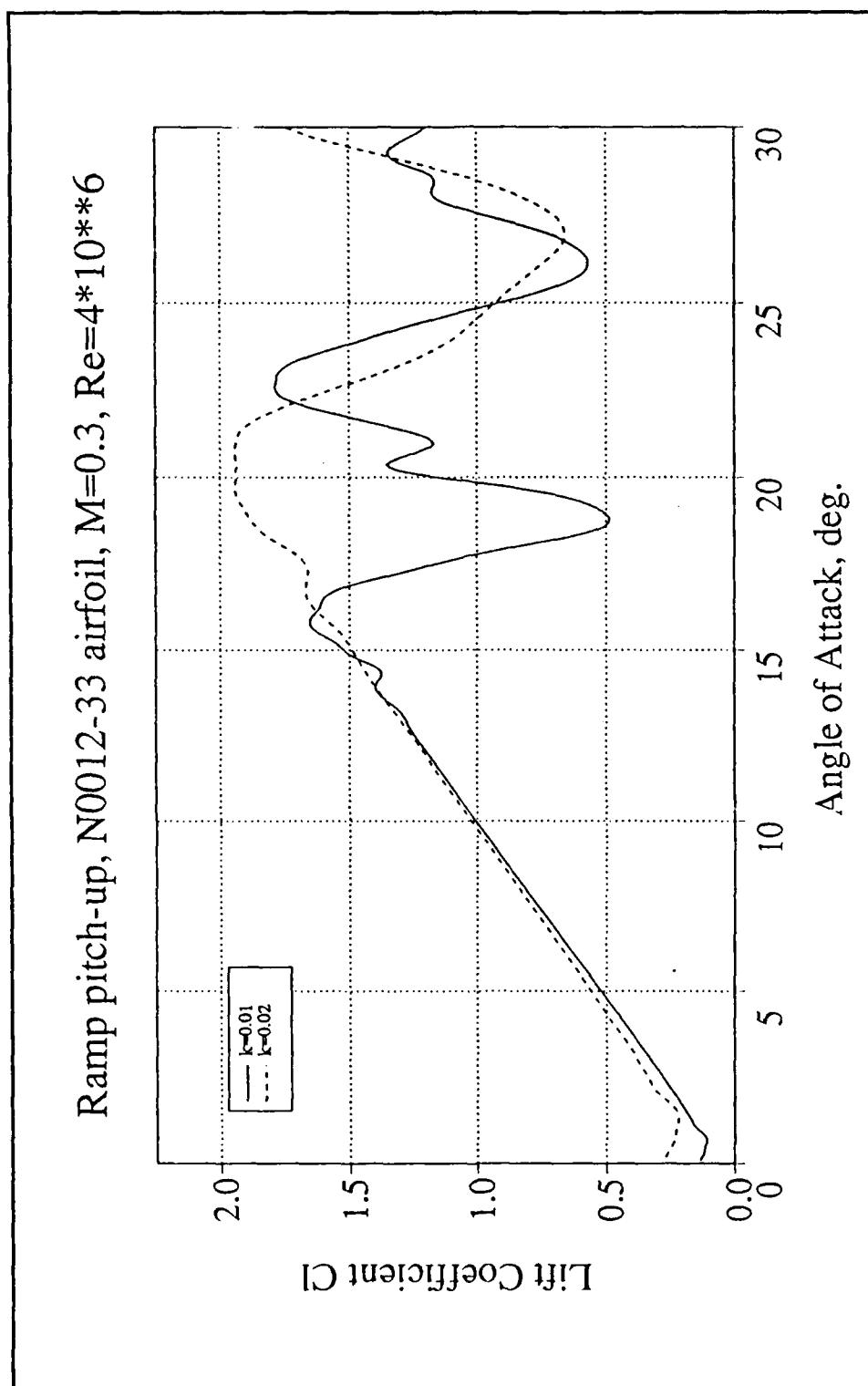


Figure 55. Reduced Frequency Effect, NACA 0012-33, $M=0.3$

The effect of the increased pitching rate in delaying the onset of dynamic stall and increasing the unsteady lift may prove to be of practical operational benefit as knowledge of the details of the flow development increases.

E. EFFECT OF FREESTREAM MACH NUMBER

The effect of increasing freestream Mach number from 0.3 to 0.4 resulted in slightly displacing the lift curve upward for the higher Mach number. The slope of the lift curve was unchanged. However, for a given angle of attack, a very slight increase in lift coefficient was observed at the higher Mach number before the onset of dynamic stall. Figures 56 and 57 show the effect of increasing Mach number for the NACA 0012 and 0012-33 airfoils at a reduced frequency of $k=0.02$. Flow at a Mach number of 0.4 resulted in slightly higher peak lift coefficients than at $M=0.3$. In addition, the peak lift coefficient at $M=0.4$ occurred $1-2^\circ$ higher angle of attack than at $M=0.3$.

The initial development of reverse flow regions and vorticity was largely independent of Mach number for a given airfoil in that the primary vortex originated at approximately the same angle of attack for the two Mach numbers. Subsequent growth of the primary vortex and development of the secondary, tertiary, and trailing edge vortices are delayed to slightly higher angles of attack at $M=0.4$ compared to the $M=0.3$ case. As a result, dynamic stall occurs at a higher angle of attack.

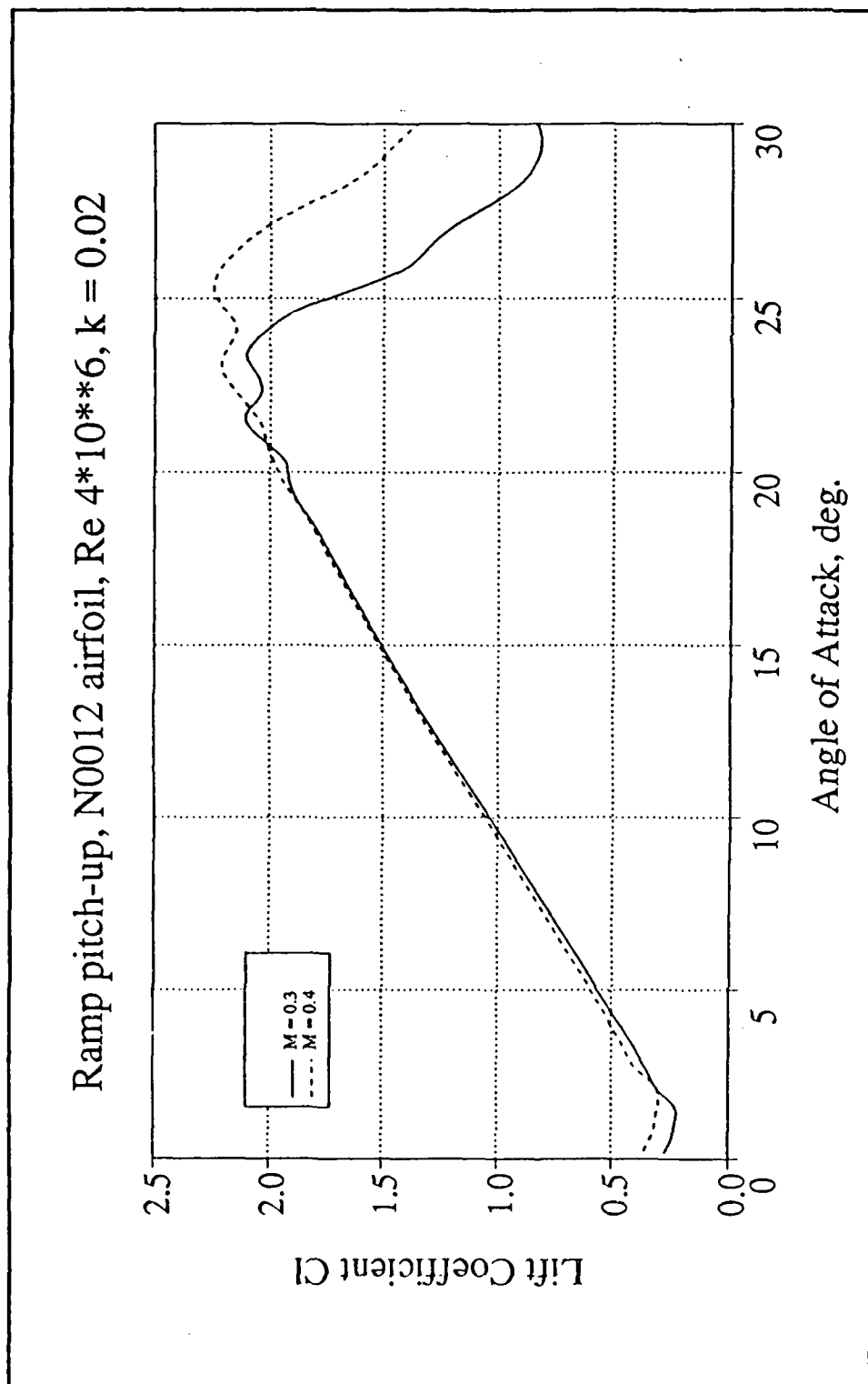


Figure 56. Freestream Speed Effect, NACA 0012, $k=0.02$

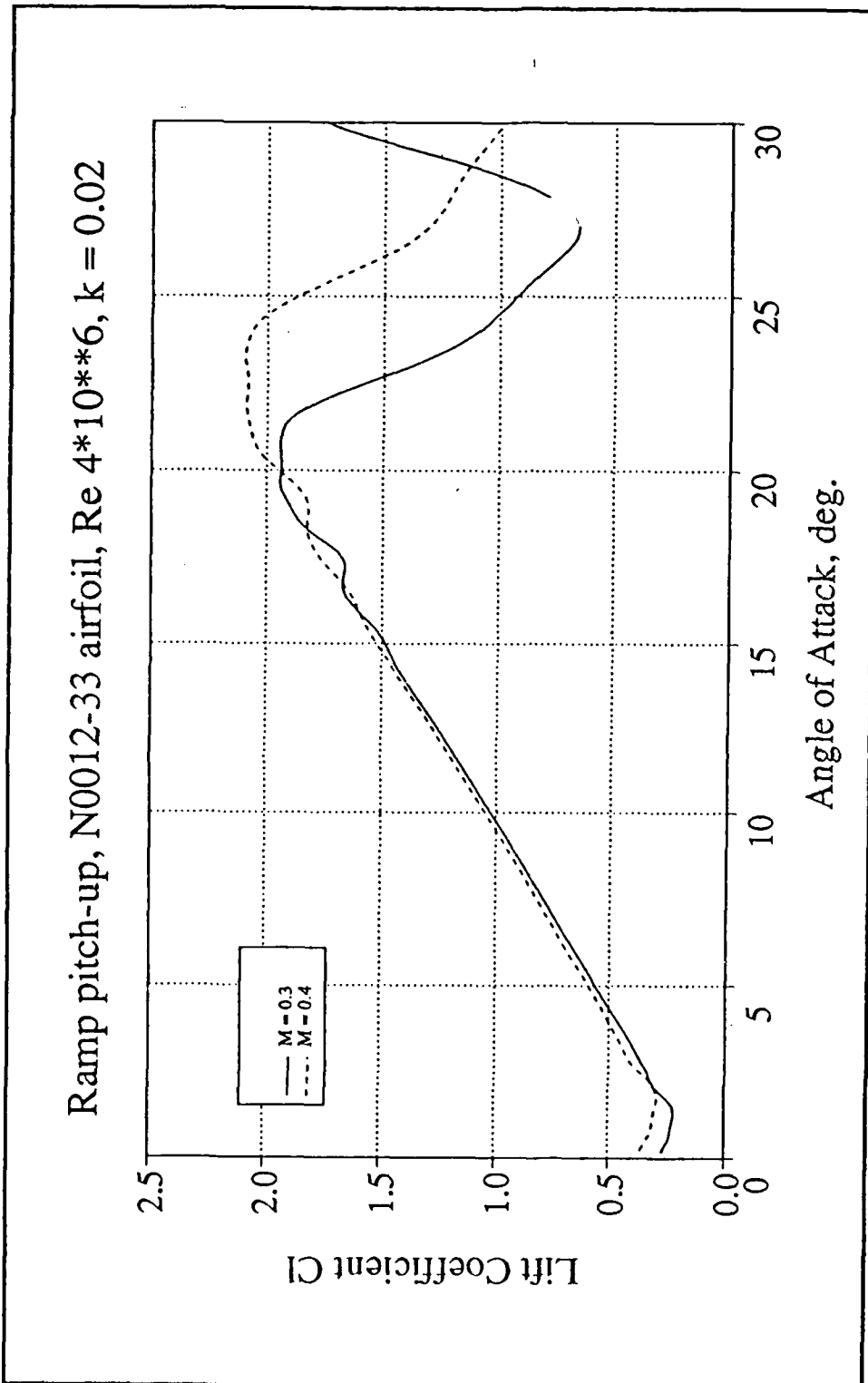


Figure 57. Freestream Speed Effect, NACA 0012-33, $k=0.02$

Ekaterinaris [Ref. 11] found that for the SSC-a90 airfoil with 9% thickness ratio, increasing Mach number from 0.2 to 0.4 resulted in decreasing both lift coefficient and dynamic stalling angle of attack at a reduced frequency of 0.01. The experimental work by Chandrasekhara and Carr [Ref. 3] using a harmonically oscillating NACA 0012 airfoil also showed that increasing Mach number reduces the angle of attack at which dynamic stall occurred. Further experimental and computational investigation is required at comparable pitching rates to ascertain the accuracy of the computational model used at compressible flow Mach numbers. Further investigation into the influence of airfoil thickness ratio on Mach number effects is needed.

F. PRESSURE GRADIENT AT FLOW SEPARATION

The peak pressure gradient observed at initial flow separation occurring aft of the leading edge was investigated for the three airfoils at the reduced frequencies and Mach numbers listed in Table 2. Figure 58 displays a plot of streamwise pressure gradient along the airfoil chord for the NACA 0012-63 airfoil at different freestream conditions. The figure shows that, for the same airfoil, the peak pressure gradient encountered by the flow at initial flow separation is independent of freestream speed or pitching rate. Similar results were obtained for the other airfoils. Figure 59 shows the streamwise pressure gradient for the NACA 0012-33 airfoil.

Figure 60 displays pressure gradients at initial flow separation angle of attack for the three airfoils at the freestream condition of 0.4 Mach and reduced frequency of $k=0.01$. The peak pressure gradient observed at the instant of flow reversal was higher for the NACA 0012-33 airfoil than for the airfoils with larger leading edge radius. Similar results were obtained at other freestream conditions. The streamwise location of the peak pressure gradient for the NACA 0012-33 airfoil was slightly upstream of that for the NACA 0012-63 airfoil as shown in Figure 61. The higher peak pressure gradient observed for the NACA 0012-33 airfoil is an indication that flow momentum near the surface is higher around the smaller leading edge radius. The higher flow momentum combined with the relatively upstream location of the peak pressure gradient and sharper flow turning angle combined to cause the magnitude of the peak pressure gradient for the NACA 0012-33 airfoil to be 33% greater than that of the NACA 0012-63 airfoil. Thus, the critical pressure gradient required for flow reversal is dependent on leading edge radius, in that a smaller leading edge radius increases the peak pressure gradient at flow reversal.

The streamwise location of flow separation is, in turn, dependent on the location of the peak pressure gradient. The actual location of flow reversal on the airfoil surface occurred 1.0-1.5% chord length downstream of the location of the peak pressure gradient as shown in Figure 61. This delay

is attributed to the time lag in the aerodynamic response to the rapid increase in pressure gradient. The more downstream location of the peak pressure gradient of the NACA 0012-63 airfoil caused a similar relative location of the position of initial flow reversal compared the NACA 0012-33 airfoil.

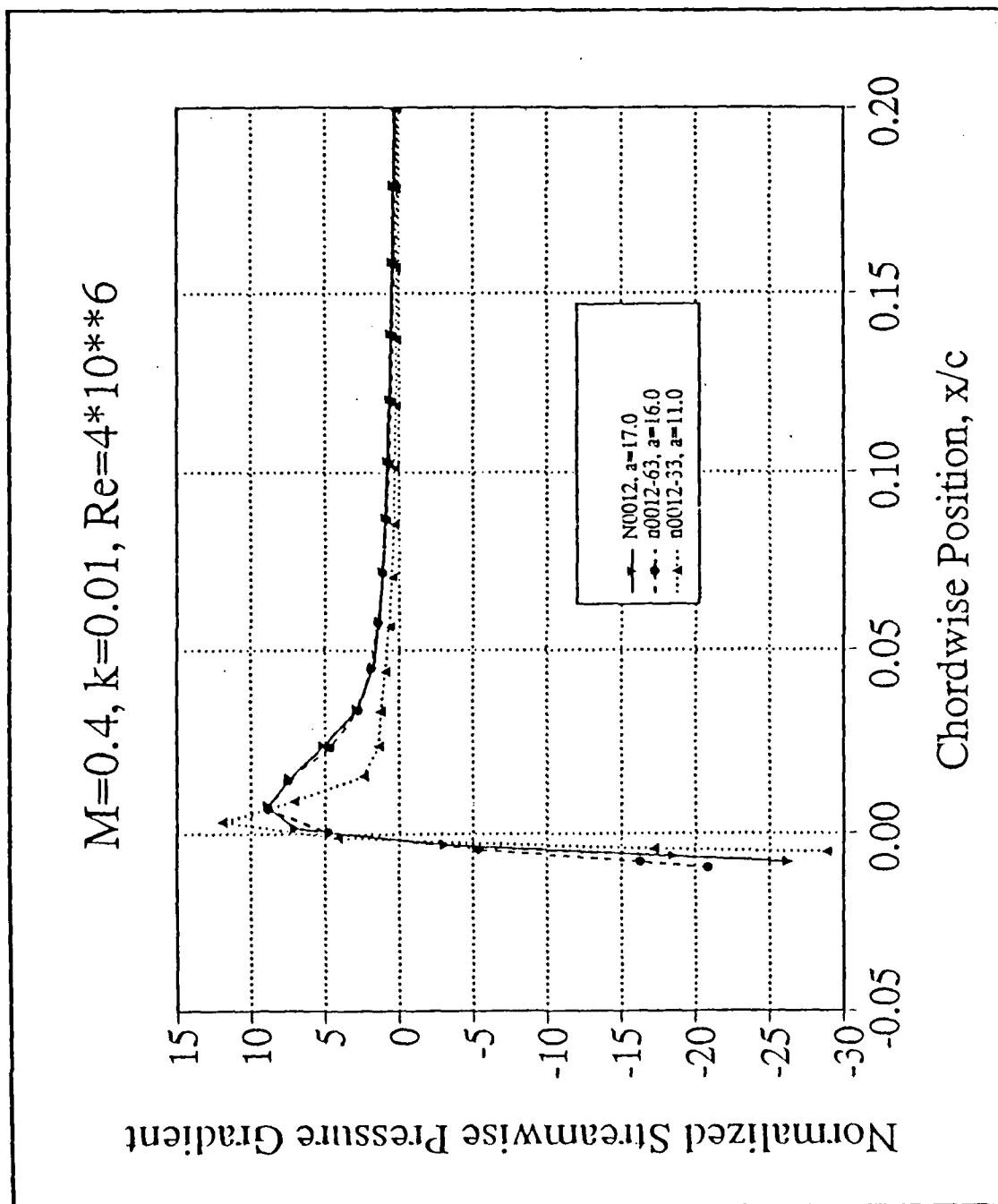


Figure 60. Pressure Gradient Comparison, $M=0.4, k=0.01$

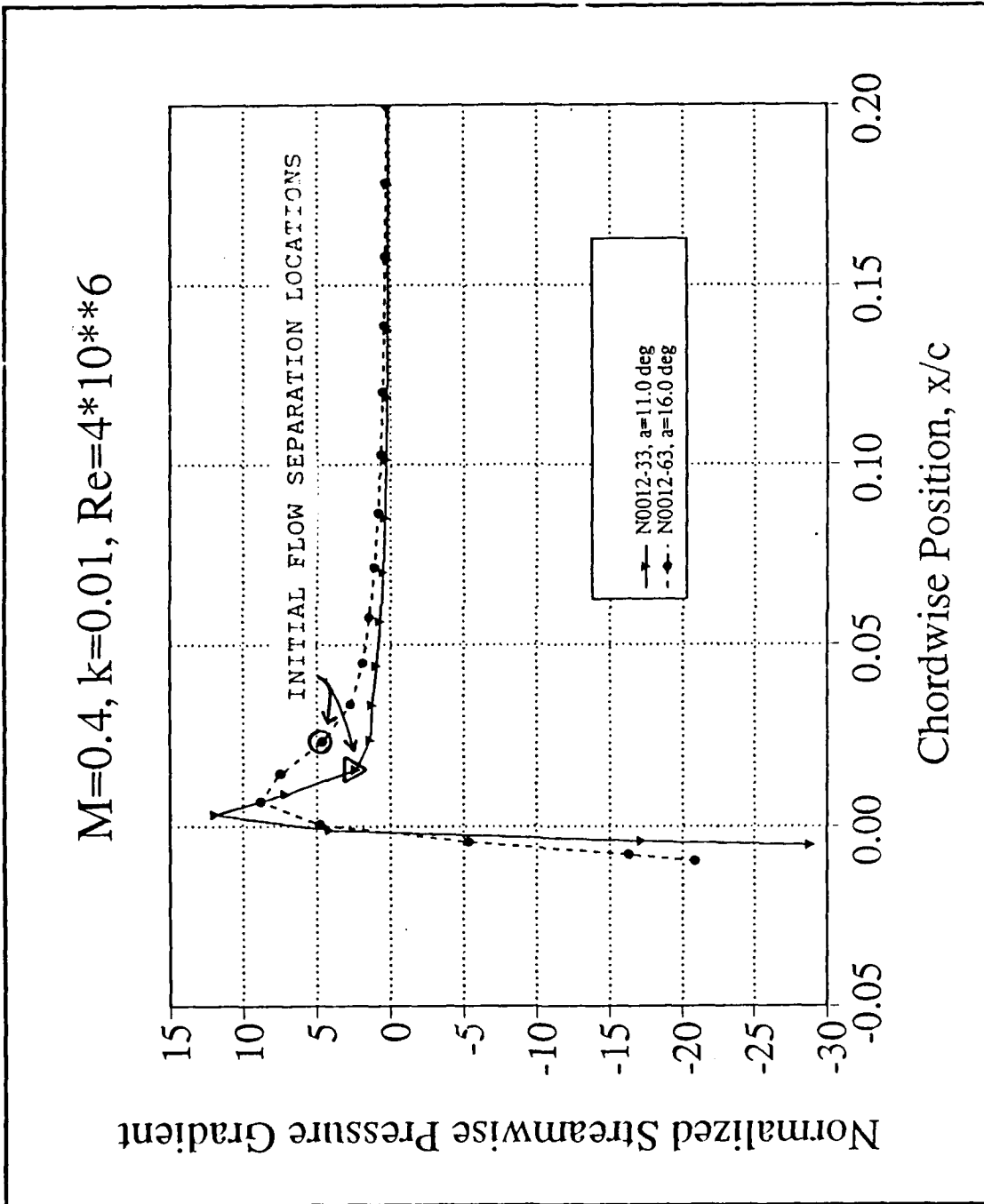


Figure 61. Flow Reversal Location, $M=0.4, k=0.01$

V. CONCLUSIONS AND RECOMMENDATIONS

A. CONCLUSIONS

1. The results of the unsteady flow solutions displayed good agreement with the experimental results for the harmonically oscillating airfoil at a reduced frequency of 0.1 and Mach number of 0.3. At a higher reduced frequency of 0.2, however, the agreement with experimental results was poor during the downstroke.
2. The leading edge geometry of an airfoil was found to have a significant effect on the development of the vortical flowfield and dynamic stall characteristics of the airfoil. Of primary importance is the size of the leading edge radius. A larger leading edge radius delays development of the adverse pressure gradient necessary for boundary layer separation and eventual vortex formation. Of secondary importance is the contouring of the airfoil aft of the leading edge. Thicker contouring forward of the location of maximum thickness contributes to delaying flow separation.
3. The effect of increasing the pitching rate of the airfoil is to enhance unsteady lift by delaying vortex formation to a higher angle of attack. The flow solutions presented in this study on the effects of reduced frequency are in good agreement with trends observed in experimental work.
4. The streamwise pressure gradient required for flow separation is a function of airfoil leading edge radius and is independent of reduced frequency or freestream speed.

B. RECOMMENDATIONS

1. Conduct further experimental and computational investigations to compare Mach number effects on flow development and dynamic stall. The investigations should be conducted at comparable Mach and Reynolds numbers.
2. Investigate the effect of airfoil thickness ratio on dynamic stall.

3. The understanding of harnessing the unsteady lift generated by rapidly pitching airfoils is only part of the knowledge required for practical implementation. Further investigations must include examining pitching moment development and how to minimize the adverse pitching moments produced.
4. Conduct further computational work at higher reduced frequencies and Mach number to check the validity of using this eddy-viscosity model at those flow conditions.

LIST OF REFERENCES

1. McCroskey, W. J., *The Phenomenon of Dynamic Stall*, National Aeronautics and Space Administration Technical Memorandum 81264, March 1981.
2. McCroskey, W. J., and Pucci, S. L., *Viscous-Inviscid Interaction on Oscillating Airfoils in Subsonic Flow*, American Institute of Aeronautics and Astronautics Paper 81-0051R, January 1981.
3. Chandrasekhara, M., and Carr, L., *Flow Visualization Studies of the Mach Number Effects on the Dynamic Stall of an Oscillating Airfoil*, American Institute of Aeronautics and Astronautics Paper 89-0023, January 1989.
4. Chandrasekhara, M. and Brydges, B., "Amplitude Effects on Dynamic Stall of an Oscillating Airfoil," paper presented at the Aerospace Sciences Meeting, 28th, Reno, NV, 9-12 January 1990.
5. Mehta, U. B., *Dynamic Stall of Oscillating Airfoils*, Advisory Group for Aerospace Research and Development Paper #23 CP-227, Unsteady Aerodynamics, September 1977.
6. Wu, J. C. and others, "Dynamic Stall of Oscillating Airfoils," paper presented at 42nd Annual Forum of American Helicopter Society, Washington, D.C., June 1986.
7. Beddoes, T. S., *Prediction Methods for Unsteady Separated Flows*, Advisory Group for Aerospace Research and Development Paper #15 CP-679, 1980.
8. Jang, H. M., Ekaterinaris, J. A., Platzler, M. F., and Cebeci, T., "Essential Ingredients for the Computation of Steady and Unsteady Blade Boundary Layers," ASME Paper 90-GT-160, June 1990.
9. Sankar, N. L., and Tang, W., *Numerical Solution of Unsteady Viscous Flow for Rotor Sections*, American Institute of Aeronautics and Astronautics Paper 85-0129, January 1985.
10. Visbal, M. R., *Effect of Compressibility on Dynamic Stall of a Pitching Airfoil*, American Institute of Aeronautics and Astronautics Paper 88-0132, January 1988.

11. Ekaterinaris, J. A. *Compressible Studies on Dynamic Stall*, American Institute of Aeronautics and Astronautics Paper 89-0024, January 1989.
12. Abbott, I. H. and Von Doenhoff, A. E., *Theory of Wing Sections*, Ch. 6, Dover Publications, Inc., 1959.
13. Schlichting, H., *Boundary Layer Theory*, McGraw-Hill Book Company, 1979.
14. Vivand, H., "Conservative Forms of Gas Dynamic Equations," *La Recherche Aerospatiale*, No. 1 pp. 65-68, January-February 1974.
15. Beam, R. M. and Warming, R. F., "An Implicit Factored Scheme for the Compressible Navier-Stokes Equations," *American Institute of Aeronautics and Astronautics Journal*, v. 16, no. 4, pp. 393-402, April 1978.
16. Baldwin, B. S. and Lomax, H., *Thin Layer Approximation and Algebraic Model for Separated Turbulent Flows*, American Institute of Aeronautics and Astronautics Paper 78-257, January 1978.
17. Cebeci, T., *Calculation of Compressible Turbulent Boundary Layers with Heat and Mass Transfer*, American Institute of Aeronautics and Astronautics Paper 70-741, June 1970.
18. Anderson, D. A., Tannehill, J. C., and Pletcher, R. H., *Computational Fluid Mechanics and Heat Transfer*, p. 490, Hemisphere Publishing Company, 1984.

APPENDIX A - USING THE PROGRAM

A. THE NAVIER-STOKES CODE FOR GENERATING FLOW SOLUTIONS

The main program *NSE2D* (listed in Appendix B for reference) reads input data as supplied by the input file *NSE.1d*, the grid files *fort.11* or *fort.21* as appropriate, and the flow file *fort.31*. The program forms the metrics and the Jacobian by calling the *METRIC* subroutine. After calling the *SLPS* subroutine to perform the computations, the main program outputs the rotated grid and the flow solution to the file *fort.20*, and outputs the data of lift, drag, moment and pressure coefficients, time, angle of attack, and rotational frequency to the loads file *fort.3*.

The subroutine *SLPS* is the primary subroutine, and it calls other subroutines to perform the steps in the ADI algorithm. The major subroutines that *SLPS* calls are:

<u>Subroutine</u>	<u>Function</u>
MATRIX1, MATRIX2	Form block tridiagonal matrices for the ξ and η directions
AMAT1, AMAT2	compute coefficient matrices $\partial F / \partial \xi$ and $\partial G / \partial \eta$
STRESS	supplies the viscous terms
DISSIP	adds fourth-order dissipation terms to the right-hand side of the Navier-Stokes Equations
EXPBC	applies boundary conditions

RES1	computes residuals from inviscid part of equations
EDDY	applies Baldwin-Lomax model

B. DIRECTIONS FOR EDITING INPUT FILES FOR THE PURPOSE OF GENERATING FLOW SOLUTIONS

1. Generating a Grid

Initially, a grid must be generated as described in Chapter III in order to compute the flow about the airfoil in question. For this, it is necessary to use the *AIRFGR.F* program. With the rectangular coordinates of the desired airfoil, edit the input file *AIRFGR.IN* using the "ex" or the "vi" editors. Ensure that enough points are defined in regions of high curvature such as the leading edge regions. Then ensure that no *fort.21* file exists by renaming or deleting it. At this time, run the grid program by typing

```
AIRFGR < AIRFGR.IN
```

After the program has run, ensure that the grid is satisfactory by running *PLOT3D*. It may be necessary to define more coordinate points to ensure leading edge radius definition, upper or lower surface curvature, or trailing edge closure. Accuracy of trailing edge closure will determine wake thickness. The *AIRFGR.F* program is listed in Appendix C for reference.

2. Rotating a Grid

The grid generated in part 1 is for a zero degree angle of attack. Often it is desired to compute a steady flow or to

start an unsteady flow at an AOA other than zero. In order to do this the *ROTGR.F* program must be used. It is necessary to edit the *ROTGR.F* program and set the desired rotated grid angle by changing the α_1 value in line 10. After the program has been edited, then:

1. Compile *ROTGR.F* by typing "cf77 rotgr.f".
2. Compiling *ROTGR.F* results in an output file named a.out. Move a.out to rotgr by typing "mv a.out rotgr".
3. Execute the program by typing "rotgr".
4. The output file produced by rotgr is fort.12. It contains the desired grid rotation. Copy fort.12 to fort.11 or fort.21 as necessary for future flow solutions.

The commands within the quotation marks should be typed, not the quotation marks themselves. Upper and lower case are not important.

3. Steady-State Solutions

Ensure that the grid is rotated to the desired angle of attack of the flow solution (part 2). The rotated grid should be copied to the file fort.21. The fort.21 file must have the grid rotated to the desired angle of attack for the steady-state solution!

Modify the *NSE.IN* file as follows:

line 2:

- set desired computational time interval (DT)
- set ALFA, ALFAI, ALFA1 to zero
- set REDFRE to desired reduced frequency
- set AMINF to desired Mach number

line 8:

- set number of time steps (ISTP); usually 3000 are necessary for convergence at AOA \neq 0. In order to run interac-

tively and not exceed time limit, set ISTEP=1000 and run three times.

line 10:

- ensure that XREF=0.25
- set TSHIFT=0.0
- set REYREF to desired Reynolds number

line 14:

- For initial run, set RESTART OSCIL RAMP as FALSE TRUE TRUE. To restart (2nd and 3rd runs), set TRUE TRUE FALSE

line 22:

- Set time to 0.0 for 1st run. Set to preceding run time for restart.

To run interactively and observe output as it develops, type:

```
NSE < NSE.IN
```

To run in the background, type:

```
NSE < NSE.IN > NSE.OUT
```

When the run is finished the last time step solution will consist of grid and flow solutions in file *fort.20*. It will be necessary to separate the grid and flow solution to restart the second run. The command "SPLIT20" will move the grid solution to *fort.11* and the flow solution to *fort.31*, and will display the final run non-dimensional time. When restarting the second run, modify NSE.IN line 14 to RESTART=TRUE. A restarted solution uses grid file *fort.11* and flow file *fort.31*. Set time in NSE.IN to time specified for the previous run when SPLIT20 was executed. Execute the next run by the desired method as before.

After convergence, save the grid and flow files (SPLIT20 to *fort.11* and *fort.31*).

4. Unsteady Solutions

Both oscillatory and ramp (constant pitch rate) solutions can be obtained by the *NSE.F* program. One must ensure that the desired steady state initial angle of attack grid and flow solutions are obtained. The input file *NSE.IN* is modified as follows:

line 2:

- set time interval, freestream Mach number and reduced frequency, where $k = \omega c / 2U_\infty$ for ramp solution and $k = \omega c / 2U_\infty$ for oscillatory solution.
- For ramp response: set ALFAI to steady-state initial conditions; ALFA, ALFA1 are unused.
- For oscillatory response of form $\alpha = \alpha_0 + \alpha_1 \sin(\omega t)$, set ALFA = α_0 , ALFA1 = α_1 , ALFAI = $(\alpha_0 - \alpha_1)$ since response will start at min α .

line 8:

- set ISTP 6000-12000 depending on length of response desired.

line 10:

- set REYREF to desired Reynolds number.
- set XREF=0.25
- set TSHIFT = -0.5 so that response starts at min α which is 1/4 cycle ($-\pi/2$ time shift as $\alpha = \alpha_0 + \alpha_1 \sin(\omega t - \pi/2)$) from mean α .

line 14:

- set RESTART to TRUE
- set OSCIL to TRUE for oscillatory response (else FALSE)
- set RAMP to TRUE for ramp response (else FALSE)

line 19:

- Program flow solution outputs can be selected for various angles of attack desired. Select desired AOA solutions by listing them multiplied by 100 (i.e. 11 degrees as 1100). The outputs are listed as files *fort.61* through *fort.72*.

line 22:

- Set time to 0.0 for initial run. For restart set time to the *fort.20* output from the last timestep of the last run.

Run the program by submitting it as a job to the queue by typing "qsub -lt 7200 subunst". The subunst file is a command file which will order the steps for the Cray when the job number comes up in the queue. With at least 1 1/2 hours in computation, go run 5 miles, eat lunch, or play with the kids. Upon returning, check on queue status by typing "mqgs". If no entries, the run is finished and you can split the output files and continue, if desired.

Any of the output files *fort.61* through *fort.72* and *fort.20* can be split into grid solutions and flow solutions for further analysis. *Fort.20* file must be split to continue the response at further angles of attack, and to use the run time as the next run *NSE.IN* input in line 22. For continuous ramp or oscillatory responses, it is not necessary to reset ALFA, ALFAI, ALFA1, or RESTART; it is only necessary to reset desired AOA solutions to be recorded (line 19) and the time.

5. Example

As an example, to run an oscillatory solution for $\alpha = 10 + 7 \sin(t)$, it is necessary to get a steady flow solution at $\alpha = 3^\circ$ ($3 = 10 - 7$). The grid developed for the airfoil must be rotated to 3° using the *ROTGR.F* program and input to *fort.21*. At this time a steady-state solution is obtained by modifying *NSE.IN* with the following inputs:

ALFA	0.0
ALFAI	0.0
ALFA1	0.0
REDFRE	as desired
AMINF	as desired
TIME	0.0
RESTART OSCIL RAMP	FALSE TRUE FALSE
XREF	0.25
TSHIFT	0.0

Run the program by typing " NSE < NSE.IN (>NSE.OUT) "

After 1000 timesteps, issue the command SPLIT20, so that the files *fort.11* and *fort.31* will be opened. Edit *NSE.IN* with the SPLIT20 time and set RESTART=TRUE. Run the program again, and then a third time, ensuring convergence (in lift coefficient, drag coefficient, etc.) Save the final *fort.11* and *fort.31* files.

Then, modify *NSE.IN* as follows

ALFA	10.0
ALFAI	3.0
ALFA1	7.0
ISTP	6000-12000
TIME	0.0
RESTART OSCIL RAMP	TRUE TRUE FALSE
XREF	0.25
TSHIFT	-0.5

ia1, ia2, ... ia12 as desired

Run the program by issuing the command "qsub -lt 7200 subunst". After completion, save the output files (*fort.61* through *fort.72*) and *fort.20*. Do a SPLIT20, note time and AOA, then input TIME into *NSE.IN* for further runs.

Graphs of the output files may be obtained by using the plot program *PLOT3D*. Observe output files (for example *fort.65*) and graph by typing the commands: "split" and then on

the next line "65". Outputs will be in files *fort.11* (grid) and *fort.31* (flow) which are read into the *PLOT3L* input.

A typical NSE.IN file for the unsteady solution of the example problem at $k=0.02$ and $M=0.4$ would be as follows.

```

IMAX  KMAX    DT      WW   ALFA  ALFA1  ALFAI  REDFRE  AMINF
 157   58  0.005   2.00  10.00   7.00   3.00   0.02   0.40
ISPEC (FLAG FOR CHOOSING DIFFERENT SPECTRAL RADIUS)
 3
WW2X, WW2Y, WW4X, WW4Y (EXPLICIT DISSIPATION COEF. FOR X AND Y)
 0.00      0.00      0.030   0.030
  ISTEP      NPER      NOUT      RES  STRUNST
 9000.    18000.    1000.    100.    0.
  REYREF      DMIN      XREF      TSHIFT
  4.00    0.00002      0.25      -0.5
TSTAR1
-1.0
RESTART,MULTIGRID OPTIONS SPECIFIED IN THE NEXT CARD
TRUE TRUE FALSE
CIRCOR ( CIRCULATION CORRECTION)
TRUE
 31   127
ITEL ITEU
0300 0400 0500 0600 0700 0800 0900 1000 1100 1200 1300 1400
 ia1  ia2  ia3  ia4  ia5  ia6  ia7  ia8  ia9 ia10 ia11 ia12
TIME
0.0

```

```

LINE # SOURCE TEXT
1 C*****
2 C*
3 C* MAIN PROGRAM
4 C*
5 C*****
6 PROGRAM NSFMAIN
7 PARAMETER (IX=180,KX=60)
8 COMMON/SURF/PSUR(IX)
9 COMMON/IX/OMEGA,BDOT
10 COMMON/MUTUR/CMU(IX,KX)
11 COMMON/SKINCF/CF(IX)
12 COMMON/GRID/X(IX,KX),Z(IX,KX)
13 COMMON/PAR/GAMMA,REYREF,ALFA,ALFAI,ALFAI,REDFRE,AMINF,ALFAI
14 COMMON/DEID/DT,IMAX,KMAX,ITEU,ITEU
15 COMMON/GRID/YACOB(IX,KX)
16 COMMON/DAMP/WW,WMI,WW2X,WW2Y,WW4X,WW4Y
17 COMMON/FLOW/Q1(IX,KX),Q2(IX,KX),Q3(IX,KX),Q4(IX,KX)
18 COMMON/MTRIX/ X12(IX,KX),X12(IX,KX),ZETAZ(IX,KX),ZETAZ(IX,KX)
19 1,XIT(IX,KX),ZETAT(IX,KX)
20 COMMON/PLOT/TITLE(10),NSTPT,RES(3000),RES,CLB(3000),CDPH(3000)
21 DIMENSION DRBO(IX,KX)
22 COMMON/INITI/UINF,VINF
23 COMMON/BCLOG/CIRCOR
24 COMMON/LOGIC/RSTRT,PITCH,RAMP
25 LOGICAL CIRCOR
26 LOGICAL RSTRT,PITCH,RAMP
27 CHARACTER ITITLE*80
28 COMMON/TITL/ITITLE
29 COMMON/L2NORM/ RESDL2(10000)
30 PI = 4. * ATAN(1.)
31 C
32 C*** PROGRAM SOLVES TWO-DIMENSIONAL VISCOUS FLOW PAST ARBITRARY
33 C*** GEOMETRIES USING ADI PROCEDURE.
34 C
35 TAPE5 = FILE CONTAINING INPUT DATA
36 TAPE6 = OUTPUT
37 TAPE8 = FILE THAT SAVES THE FLOW FIELD AT THE END OF A RUN
38 IF THE CURRENT RUN IS A RESTART OF A PREVIOUS RUN, THEN
39 TAPE7 IS USED TO READ THE FLOW FIELD INTO MEMORY
40 C
41 C*** READ INPUT DATA
42 C
43 READ *,ITITLE
44 READ (5,1) TITLE
45 READ(5,20(1))
46 READ (5,2) IMAX,KMAX,DT,WW,ALFA,ALFAI,ALFAI,REDFRE,AMINF
47 C
48 ISPEC = FLAG TO SPECIFY DIFFERENT SPECTRAL RADIUS FOR SCALING
49 WITH THE DISSIPATION
50 C
51 READ(5,20(1))
52 READ(5,2) ISPEC
53 READ(5,20(1))
54 READ(5,22(1)) WW2X,WW2Y,WW4X,WW4Y
55 C
56 NSTP = NO. OF TIME STEPS TO BE DONE ON THIS RUN
57 READ(5,20(1))
58 READ (5,2,21) FNSTP,FNPER, FNOUT,RES
59 NPER = FNPER
60 NSTP = FNSTP
61 FNOUT = FNOUT
62 C
63 REYREF= REYNOLDS NUMBER IN MILLIONS
64 DNMIN = DISTANCE OF FIRST POINT OFF THE WALL
65 FOR REYNOLDS NUMBERS UPTO 3 MILLION USE 0.00005
66 XREF = REFERENCE VALUE AT X-AXIS
67 C
68 READ (5,2(01))
69 READ (5,22(1)) REYREF,DNMIN,XREF,TSBIFT
70 TSBIFT = TSBIFT * PI
71 REREAL = REYREF * 1000000.
72 REYREF = REYREF * 1.E+06
73 C
74 TSTART = TIME THAT THE CALCULATIONS HAVE BEEN ADVANCED
75 UPTO THE PREVIOUS RUN. IF TSTART IS NEGATIVE THIS VALUE IS
76 OBTAINED FROM THE TAPE 3.
77 READ (5,20(1))
78 READ (5,22(1)) TSTART
79 2221 FORMAT(4F10.0)
80 READ (5,2(01))
81 2001 FORMAT(1X)
82 READ (5,20(00)) RSTRT,PITCH,RAMP
83 READ(5,20(1))
84 2000 FORMAT(31X)
85 read(5,*) ia1,ia2,ia3,ia4,ia5,ia6,ia7,ia8,ia9,ia10
86 @ ia11,ia12,ia13,ia14,ia15
87 ialfad = 100.*alfad
88 IF( PITCH ) DT = PI / (NPER*REDFRE*AMINF)
89 C
90 NEGATIVE REYREF MEANS INVISCID FLOW
91 C
92 C*** PRINT OUT THE INPUT DATA
93 C
94 WMI = 3. * WW
95 WRITE (6,4) TITLE
96 WRITE (6,3) IMAX,KMAX,DT,WW,WMI,ALFA,ALFAI,ALFAI,REDFRE,AMINF,XREF
97 WRITE (6,6) NPER, NSTP, FNOUT
98 66 FORMAT(/,2X,5ENPER=,I8,5X,5ENSTP=,I8,5X,5ENOUT=,I8,/)
99 IF(REYREF.GT.0.) WRITE (6,3700) REYREF
100 WRITE(6,67) WW2X, WW2Y, WW4X, WW4Y
101 67 FORMAT(/,2X,5BNW2X=,F8.4,5X,5BNW2Y=,F8.4,5X,5BNW4X=,F8.4,5X,
102 1 5BNW4Y=,F8.4,/)
103 GAMMA=1.4
104 ITEU = 31
105 ITEU = 133
106 ILE = ( ITEU - ITEU ) / 2 + ITEU
107 C
108 CALL A*RFOL(ITEU,ITEU,ILE)
109 IF(REYREF.GT.0.) CALL CLUSTR(DNMIN)
110 C
111 READ(21) IMAX,KMAX
112 read(21) (( X(I,K),I=1,IMAX),K=1,KMAX ),
113 @ (( Z(I,K),I=1,IMAX),K=1,KMAX )
114 C
115 C***C STARTING CONDITIONS.
116 C*** DENSITY NORMALISED WITH RESPECT TO ROINF
117 C*** VELOCITIES NORMALISED WITH RESPECT TO AINF
118 C*** TOTAL ENERGY NORMALISED WITH RESPECT TO (ROINF*AINF*AINF)
119 C
120 TOTEN=AMINF*AMINF*0.5-1./(GAMMA*(GAMMA-1.))
121 ALFA = ALFA * PI / 180.
122 ALFAI = ALFAI * PI / 180.

```

```

LINE # SOURCE TEXT
121 ALMEAN = ALFA
122 ALFA1 = ALFA1 * PI / 180.
123 ALFAMAX = ALFA1 + ALMEAN
124 ALFACR = ALFAMAX
125 C ALFA IS THE ANGLE OF AIRFOIL WITH RESPECT TO FREESTREAM AT STEADY-STATE
126 C OR INITIAL POSITION OF UNSTEADY MOTION.
127 C IT SHOULD BE SET ACCORDING TO THE TYPE OF MOTION
128 C ALFA = ALMEAN - ALFA1 * COS(0.)
129 C UINF = AMINF * COS(ALFA)
130 C VINP = AMINF * SIN(ALFA)
131 C uinf = aminf
132 C vinf = 0.0
133 C call rotgrid( imax,kmax,alfa )
134 DO 7 I=1,IMAX
135 DO 7 K=1,KMAX
136 Q1(I,K)=1.
137 Q2(I,K)=UINF
138 Q3(I,K)=VINP
139 Q4(I,K)=TOTEN
140 7 CONTINUE
141 IF(RSTRT) THEN
142 REWIND 11
143 READ (11) IMAX , KMAX
144 READ (11) ( ( X(I,K), I=1,IMAX ), K=1,KMAX ),
145 & ( ( Z(I,K), I=1,IMAX ), K=1,KMAX )
146 REWIND 31
147 READ (31) IMAX , KMAX
148 READ (31) FSMACH, ALFAD, RREAL, TIME
149 READ (31) ( ( Q1(I,K), I=1,IMAX ), K=1,KMAX ),
150 & ( ( Q2(I,K), I=1,IMAX ), K=1,KMAX ),
151 & ( ( Q3(I,K), I=1,IMAX ), K=1,KMAX ),
152 & ( ( Q4(I,K), I=1,IMAX ), K=1,KMAX )
153 ENDIF
154 C
155 if( time .gt. 500. ) time = 0.
156 if( alfad .eq. 0 ) time = 0.
157 TSTART = TIME
158 IF(TSTART GE.0.) TIME = TSTART
159 IF(.NOT.(RSTRT)) TIME = 0.
160 WRITE(6,62) TIME
161 62 FORMAT(/,40BTHE CALCULATIONS STARTED AT TIME T = ,F12.4,/)
162 ASTART = ALFA + ALFA1 * SIN( 2*REDFRE*AMINF * TIME + TSHIFT )
163 ASTART = ASTART * ( 180. / PI )
164 IDONE = TIME / DT
165 WRITE(6,661) ASTART, IDONE
166 661 FORMAT(2X,10HALFASTART=,F10.4,8X,15ITERATIONS DONE,5X,16,/)
167 CALL METRIC
168 IMIN = ( ITEU - ITEL ) / 2 + ITEL
169 ILOW = 2 * IMIN
170 CHD = X(ITEU,1) - X(IMIN,1)
171 NSTPT = NSTP + NSTPP
172 C
173 C-----> STARTING FROM A STEADY-SATE SOLUTION AT CERTAIN ANGLE <Ao>
174 C GIVE A TIME SHIFT <TSHIFT> TO START FROM Ao AND SET INITIALY
175 C TIME=0., KEEP TSHIFT THE SAME THROUGH THE ONST. CALCUL.
176 C
177 C
178 IF ( PITCH ) THEN
179 DTP = PI / (NPER*REDFRE*AMINF)
180 dt = dtp
181 endif
182 alfacr = pi / 9.
183 alfamax = almean + alfa1
184 IF( RAMP ) READ (5,*) TIME
185 DO 1000 ITN=1,NSTP
186 TIME = TIME + DT
187 C
188 C
189 C
190 C
191 IF (ALFA .GT. ALFACR ) THEN
192 DT = DTP * ( 1. - .5*(ALFA-ALFACR)/(ALFAMAX-ALFACR) )
193 ELSE
194 DT = DTP
195 END IF
196 C
197 OMEGA = 2.*REDFRE*AMINF * COS( REDFRE* 2.*TIME*AMINF +TSHIFT)
198 1 ALFA1 = ALFA1
199 ALOLD = ALMEAN + ALFA1 * SIN( 2. * REDFRE * AMINF *
200 1(TIME - DT) + TSHIFT )
201 ALFA = ALMEAN + ALFA1 * SIN( REDFRE * 2. * TIME * AMINF
202 1 + TSHIFT )
203 ALFAD = ALFA * 45. / ATAN(1.)
204 DALFA = ALFA - ALOLD
205 CALL ROTGRID(IMAX,KMAX,DALFA)
206 CALL METRIC
207 END IF
208 IF (RAMP) THEN
209 OMEGA = 2. * REDFRE * AMINF
210 ALOLD = OMEGA * ( TIME - DT )
211 ALFA = OMEGA * TIME
212 ALFAD = ALFA * 45. / ATAN(1.)
213 DALFA = ALFA - ALOLD
214 CALL ROTGRID(IMAX,KMAX,DALFA)
215 CALL METRIC
216 END IF
217 ALFAD = ALFA * 45. / ATAN(1.)
218 C
219 CALL SLP5(ITN,ISPEC)
220 C
221 C
222 C
223 C
224 CALL EXPBC(CL)
225 C
226 CALL LOAD(CL,CDP,CDF,CM,ALFAS,XREF)
227 C
228 C
229 PRINT OUT PRESSURE AT THE SURFACE
230 C
231 IF(ITN/50*50.EQ.ITN) THEN
232 WRITE (6,19)
233 WRITE (6,33) ITN, TIME , DT
234 IF(PITCH OR. RAMP) WRITE (6,3500) ALFAD,OMEGA
235 IF(ITN/50*500.EQ.ITN)CALL CPPLT(ITEU,ITEU,AMINF,X(1,1),Z(1,1))
236 IF(ITN/400*400.EQ.ITN) WRITE(6,12) [I,CF(I),I=1,IMAX]
237 WRITE (6,3000) CL , CDP , CDF , CM
238 END IF
239 TIMPI = TIME / AMINF
240 IF(ITN/50*50.EQ.ITN)WRITE(3,8000)TIME,ALFAD,OMEGA,CL,CDP,CDF,CM
241 IF(ITN/1000*1000.EQ.ITN) THEN
242 DO 100 ? = IMIN , ITEU

```

LINE # SOURCE TEXT

```

241 C      XOC = ( X(I,1) - X(IMIN,1) ) / CHD
242 C      WRITE(2,7000) XOC , PSUR(ILOW-1) , PSUR(I)
243 C      WRITE(9,7000) XOC , CF(ILOW-1) , CF(I)
244 C 100  CONTINUE
245 C
246 C      ENDIF
247 C      CMU TO CALCULATE THE AVERAGE VALUES OF CL, CD, CM
248 C      SCL = SCL + CL
249 C      SCDF = SCDF + CDF
250 C      SCDP = SCDP + CDP
251 C      SCM = SCM + CM
252 C      CMU TO NEXT CMU FOR USER SPECIFIED PLOTS
253 C      DO 984 K = 1 , KMAX
254 C      DO 984 I = 1 , IMAX
255 C 984 DRHO(I,K) = ABS( Q1(I,K) - DRHO(I,K) )
256 C      IRES = IFIX(RES)
257 C      IF(ITN/IRES*IRES.EQ.ITN) THEN
258 C      IPLOT = ( NSTPP + ITN ) / IRES
259 C      RESD(IPLOT) = 0.
260 C      CLH(IPLOT) = CL
261 C      CDPH(IPLOT) = CDP
262 C      DO 985 K = 1 , KMAX
263 C      DO 985 I = 1 , IMAX
264 C 985 RESD(IPLOT) = AMAX1(RESD(IPLOT),DRHO(I,K))
265 C 985 RESD(IPLOT) = RESD(I,ITN)
266 C      ENDIF
267 C
268 C      IF(ITN/NOU*NOU.EQ.ITN) THEN
269 C      IF( ITN .EQ. 1*NOU ) IOUT = 31
270 C      IF( ITN .EQ. 2*NOU ) IOUT = 32
271 C      IF( ITN .EQ. 3*NOU ) IOUT = 33
272 C      IF( ITN .EQ. 4*NOU ) IOUT = 34
273 C      IF( ITN .EQ. 5*NOU ) IOUT = 35
274 C      IF( ITN .EQ. 6*NOU ) IOUT = 36
275 C      IF( ITN .EQ. 7*NOU ) IOUT = 37
276 C      IF( ITN .EQ. 8*NOU ) IOUT = 38
277 C      IF( ITN .EQ. 9*NOU ) IOUT = 39
278 C      IF( ITN .EQ. 10*NOU ) IOUT = 40
279 C      IF( ITN .EQ. 11*NOU ) IOUT = 41
280 C      IF( ITN .EQ. 12*NOU ) IOUT = 42
281 C      IF( ITN .EQ. 13*NOU ) IOUT = 43
282 C      IF( ITN .EQ. 14*NOU ) IOUT = 44
283 C      IF( ITN .EQ. 15*NOU ) IOUT = 45
284 C      IF( ITN .EQ. 16*NOU ) IOUT = 46
285 C
286 C      IOUT = 20
287 C      REWIND IOUT
288 C      WRITE (IOUT) IMAX , KMAX
289 C      WRITE (IOUT) ( ( X(I,K), I=1,IMAX ), K=1,KMAX ),
290 C      ( ( Z(I,K), I=1,IMAX ), K=1,KMAX )
291 C      WRITE (IOUT) IMAX , KMAX
292 C      WRITE (IOUT) AMINF, ALFAD, REREAL, TIME
293 C      WRITE (IOUT) ( ( Q1(I,K), I=1,IMAX ), K=1,KMAX ),
294 C      ( ( Q2(I,K), I=1,IMAX ), K=1,KMAX ),
295 C      ( ( Q3(I,K), I=1,IMAX ), K=1,KMAX ),
296 C      ( ( Q4(I,K), I=1,IMAX ), K=1,KMAX )
297 C
298 C      REWIND IOUT
299 C
300 C      ENDIF
301 C
302 C      IALFAD = 100.*alfad
303 C      IAL1 = 100
304 C      IAL2 = 200
305 C      IAL3 = 300
306 C      IAL4 = 400
307 C      IAL5 = 500
308 C      IAL6 = 600
309 C      IAL7 = 700
310 C      IAL8 = 800
311 C      IAL9 = 900
312 C      IAL10 = 1000
313 C      IAL11 = 1050
314 C      IAL12 = 1100
315 C      IF( IALFAD .EQ. IAL1 .OR.
316 C      @ IALFAD .EQ. IAL2 .OR.
317 C      @ IALFAD .EQ. IAL3 .OR.
318 C      @ IALFAD .EQ. IAL4 .OR.
319 C      @ IALFAD .EQ. IAL5 .OR.
320 C      @ IALFAD .EQ. IAL6 .OR.
321 C      @ IALFAD .EQ. IAL7 .OR.
322 C      @ IALFAD .EQ. IAL8 .OR.
323 C      @ IALFAD .EQ. IAL9 .OR.
324 C      @ IALFAD .EQ. IAL10 .OR.
325 C      @ IALFAD .EQ. IAL11 .OR.
326 C      @ IALFAD .EQ. IAL12 ) THEN
327 C      IF( IALFAD .EQ. IAL1 ) IAOOUT = 61
328 C      IF( IALFAD .EQ. IAL2 ) IAOOUT = 62
329 C      IF( IALFAD .EQ. IAL3 ) IAOOUT = 63
330 C      IF( IALFAD .EQ. IAL4 ) IAOOUT = 64
331 C      IF( IALFAD .EQ. IAL5 ) IAOOUT = 65
332 C      IF( IALFAD .EQ. IAL6 ) IAOOUT = 66
333 C      IF( IALFAD .EQ. IAL7 ) IAOOUT = 67
334 C      IF( IALFAD .EQ. IAL8 ) IAOOUT = 68
335 C      IF( IALFAD .EQ. IAL9 ) IAOOUT = 69
336 C      IF( IALFAD .EQ. IAL10 ) IAOOUT = 70
337 C      IF( IALFAD .EQ. IAL11 ) IAOOUT = 71
338 C      IF( IALFAD .EQ. IAL12 ) IAOOUT = 72
339 C      REWIND IAOOUT
340 C      WRITE (IAOOUT) IMAX , KMAX
341 C      WRITE (IAOOUT) ( ( X(I,K), I=1,IMAX ), K=1,KMAX ),
342 C      ( ( Z(I,K), I=1,IMAX ), K=1,KMAX )
343 C      WRITE (IAOOUT) IMAX , KMAX
344 C      WRITE (IAOOUT) AMINF, ALFAD, REREAL, TIME
345 C      WRITE (IAOOUT) ( ( Q1(I,K), I=1,IMAX ), K=1,KMAX ),
346 C      ( ( Q2(I,K), I=1,IMAX ), K=1,KMAX ),
347 C      ( ( Q3(I,K), I=1,IMAX ), K=1,KMAX ),
348 C      ( ( Q4(I,K), I=1,IMAX ), K=1,KMAX )
349 C      REWIND IAOOUT
350 C      ENDIF
351 C
352 C      1000 CONTINUE
353 C
354 C      REWIND 20
355 C      WRITE (20) IMAX , KMAX
356 C      WRITE (20) ( ( X(I,K), I=1,IMAX ), K=1,KMAX ),
357 C      ( ( Z(I,K), I=1,IMAX ), K=1,KMAX )
358 C      WRITE (20) IMAX , KMAX
359 C      WRITE (20) AMINF, ALFAD, REREAL, TIME
360 C      WRITE (20) ( ( Q1(I,K), I=1,IMAX ), K=1,KMAX ),
361 C      ( ( Q2(I,K), I=1,IMAX ), K=1,KMAX ),
362 C      ( ( Q3(I,K), I=1,IMAX ), K=1,KMAX ),
363 C      ( ( Q4(I,K), I=1,IMAX ), K=1,KMAX )

```

LINE # SOURCE TEXT

```

361 C
362   alfaf = alfa * (180/pi)
363   write(6,667) alfaf, time
364 667 format(1'hANGLE OF ATTACK =,F15.10,5X,5HTIME=,F10.4,/)
365 C
366   PRINT OUT VELOCITY PROFILE
367 C
368   WRITE(6,668)
369 668 format(/,14X,2HUX,14X,2HUY,10X,8HDENSITY ,6X,8HPRESSURE,/)
370   CMUL = AMINF / REYREF
371   DO 4000 I = 70,130,2
372     S = 0.
373     DO 4000 K = 2 , 20
374       S = S + SQRT( (X(I,K)-X(I,K-1))**2 + (Z(I,K)-Z(I,K-1))**2 )
375       U = ( Q2(I,K)/Q1(I,K) )
376       V = ( Q3(I,K)/Q1(I,K) )
377       UTOT = U*U + V*V
378       P = (GAMMA-1.)*( Q4(I,K) - .5*Q1(I,K)*UTOT )
379       WRITE (6,2002) I,K, U,V , Q1(I,K) , P
380 4000 CONTINUE
381 C
382   CALL OUTRVC(RERFAL)
383   STOP
384 C
385 1  FORMAT(12A6)
386 1  FORMAT(12A8)
387 2  FORMAT(215,7F10.0)
388 11 FORMAT(7F10.0)
389 3  FORMAT(/,5X,5HIMAX=,I10,/,5X,5HIMAX=,I10,
390       1/,5X,5H DT=,F20.8,/,5X,5HMM =,F20.8,/,5X,5HMMI =,F20.8,
391       2/,5X,5HALFA=,F20.8,/,5X,6HALFAI=,F20.8,/,5X,6HALFAI=,F20.8,/,
392       +5X,7HREDFRE=,F18.8,/,5X,6HAMINF=,F20.8,/,5X,5HIREF=,F21.8)
393 4  FORMAT(1H1,5X,10A6)
394 12 FORMAT(8(14,F10.4))
395 19 FORMAT(/)
396 C
397 22 FORMAT(2F10.6,I5)
398 33 FORMAT(5X,5HISTP=,I5,5X,5HTIME=,F9.5,5X,3HDT=,F9.5)
399 2002 FORMAT(2I5,5E14.6)
400 3000 FORMAT(5X,3HCL=,F10.4,5X,4HCDP=,F10.4,5X,4HCDP=,F10.4,5X,3HCM=,
401       +F10.4)
402 3500 FORMAT(5X,5HALFA=,F10.4,5X,6HOMEGA=,F10.4,5X,2HB=,F10.4,5X,5HBDOT=
403       1,F10.4)
404 3700 FORMAT(5X,7HREYREF=,F20.4)
405 C5000 FORMAT(2F10.6)
406 6000 FORMAT(8F14.8)
407 7000 FORMAT(3H16.9)
408 8000 FORMAT(9I13.6)
409 8001 FORMAT(3,8HCL(AVG)=,F12.7,4X,9HCDP(AVG)=,F12.7,4X,9HCDP(AVG)=,
410       +F12.7,4X,8HCM(AVG)=,F12.7)
411   END

```

LINE # SOURCE TEXT

```

409 SUBROUTINE AMAT1(K,IMX1,XIX,XIZ,XIT)
410 C.....
411 C=
412 C=
413 C=
414 C=
415 C.....
416 PARAMETER (IX=180,KX=60)
417 COMMON/FLON/Q1(IX,KX),Q2(IX,KX),Q3(IX,KX),Q4(IX,KX)
418 COMMON/PERTR/DQ1(IX,KX),DQ2(IX,KX),DQ3(IX,KX),DQ4(IX,KX)
419 COMMON/AM A(4,4,IX)
420 COMMON/PA/GAMMA,REYREF,ALFA,ALFA1,REDFRE,AMINF,ALFAI
421 DIMENSION XIT(IX,KX),XIX(IX,KX),XIZ(IX,KX)
422 REAL K0,K1,K2
423 C
424 C*** AMAT1 COMPUTES THE COEFFICIENT MATRIX DE/DQ DURING XI SWEEP
425 C
426 GM1 = GAMMA - 1.
427 DO 1000 I = 2, IMX1
428 K0 = XIT(I,K)
429 K1 = XIX(I,K)
430 K2 = XIZ(I,K)
431 U = Q2(I,K) / Q1(I,K)
432 W = Q3(I,K) / Q1(I,K)
433 EBYR = Q4(I,K) / Q1(I,K)
434 PHI2 = 0.5 * GM1 * (U * U + W * W)
435 THETA = K1 * U + K2 * W
436 A(1,1,I) = K0
437 A(1,2,I) = K1
438 A(1,3,I) = K2
439 A(1,4,I) = 0
440 A(2,1,I) = K1 * PHI2 - U * THETA
441 A(2,2,I) = K0 + THETA - K1 * (GM1 - 1.) * U
442 A(2,3,I) = K2 * U - GM1 * K1 * W
443 A(2,4,I) = K1 * GM1
444 A(3,1,I) = K2 * PHI2 - W * THETA
445 A(3,2,I) = K1 * W - K2 * GM1 * U
446 A(3,3,I) = K0 + THETA - K2 * (GM1 - 1.) * W
447 A(3,4,I) = K2 * GM1
448 A(4,1,I) = THETA * (2. * PHI2 - GAMMA * EBYR)
449 A(4,2,I) = K1 * (GAMMA * EBYR - PHI2) - GM1 * U * THETA
450 A(4,3,I) = K2 * (GAMMA * EBYR - PHI2) - GM1 * W * THETA
451 A(4,4,I) = K0 + GAMMA * THETA
452 1000 CONTINUE
453 RETURN
454 END

```

LINE # SOURCE TEXT

```

454 SUBROUTINE AMAT2(I,KM1,ZETAX,ZETAZ,ZETAT)
455 C*****
456 C*
457 C* SUBROUTINE AMAT2
458 C*
459 C*****
460 PARAMETER (IX=180,KX=60)
461 COMMON/FLOW/Q1(I,K),Q2(I,K),Q3(I,K),Q4(I,K)
462 COMMON/PERTR/DQ1(I,K),DQ2(I,K),DQ3(I,K),DQ4(I,K)
463 COMMON/AM/A(4,4,I)
464 COMMON/PAR/GAMMA,REYRFF,ALFA,ALF1,REDFPE,AMINF,ALFAI
465 DIMENSION ZETAX(I,K),ZETAZ(I,K),ZETA7(I,K)
466 REAL K0,K1,K2
467 C
468 C*** AMAT2 COMPUTES THE COEFFICIENT MATRIX DE/DQ DURING ETA SWEEP
469 C
470 GM1 = GAMMA - 1.
471 DO 1000 K = 2, KM1
472 K0 = ZETAT(I,K)
473 K1 = ZETAX(I,K)
474 K2 = ZETAZ(I,K)
475 U = Q2(I,K) / Q1(I,K)
476 W = Q3(I,K) / Q1(I,K)
477 EBYR = Q4(I,K) / Q1(I,K)
478 PHI2 = 0.5 * GM1 * (U * U + W * W)
479 THETA = K1 * U + K2 * W
480 A(1,1,K) = K0
481 A(1,2,K) = K1
482 A(1,3,K) = K2
483 A(1,4,K) = 0
484 A(2,1,K) = K1 * PHI2 - U * THETA
485 A(2,2,K) = K0 + THETA - K1 * (GM1-1.) * U
486 A(2,3,K) = K2 * U - GM1 * K1 * W
487 A(2,4,K) = K1 * GM1
488 A(3,1,K) = K2 * PHI2 - W * THETA
489 A(3,2,K) = K1 * W - K2 * GM1 * U
490 A(3,3,K) = K0 + THETA - K2 * (GM1-1.) * W
491 A(3,4,K) = K2 * GM1
492 A(4,1,K) = THETA * (2 * PHI2 - GAMMA * EBYR)
493 A(4,2,K) = K1 * (GAMMA * EBYR - PHI2) - GM1 * U * THETA
494 A(4,3,K) = K2 * (GAMMA * EBYR - PHI2) - GM1 * W * THETA
495 A(4,4,K) = K0 + GAMMA * THETA
496 1000 CONTINUE
497 RETURN
498 END

```



```

LINE #          SOURCE TEXT
499      SUBROUTINE SLPS(ITN,ISPEC)
500      C*****
501      C*
502      C*          SUBROUTINE SLPS
503      C*
504      C*****
505      PARAMETER (IX=180,KX=60)
506      COMMON/FLUX/Q1(IX,KX),Q2(IX,KX),Q3(IX,KX),Q4(IX,KX)
507      COMMON/FIX/OMEGA,BDOT
508      COMMON/PETR/DQ1(IX,KX),DQ2(IX,KX),DQ3(IX,KX),DQ4(IX,KX)
509      COMMON/AM A(4,4,IX)
510      COMMON/TRID1/DD(4,4,IX,KX)
511      COMMON/TRID2/MM(4,4,IX,KX)
512      COMMON/TRID3/EE(4,4,IX,KX)
513      COMMON/TRID4/GG(4,4,IX,KX)
514      COMMON/PAR/GAMMA,REYREF,ALFA,ALFAL,REDFRE,AMINF,ALFAI
515      COMMON/DGRID/DT,IMAX,KMAX,ITEL,ITEU
516      COMMON/GRID/YACOB(IX,KX)
517      COMMON/DAMP/WW,WW1,WW2X,WW2Y,WW4X,WW4Y
518      COMMON/MTRIX/ XIX(IX,KX),XIZ(IX,KX),ZETAX(IX,KX),ZETAZ(IX,KX)
519      1,XIT(IX,KX),ZETAT(IX,KX)
520      COMMON/RADIUS/ SPECX(IX,KX),SPECY(IX,KX)
521      COMMON/L2NORM/ RESDL2(10000)
522      REAL MM,DELTAT(IX,KX)
523      C
524      C*** THE SUBROUTINE SLPS DOES THE BULK OF THE WORK FOR THE ADI ALGORITHM.
525      C*** IT CALLS FLUX AND COMPUTES RIGHT HAND SIDE DURING THE TWO SWEEPS,
526      C*** ASSEMBLES THE COEFFICIENT MATRICES, ADDS IMPLICIT AND EXPLICIT
527      C*** DISSIPATION AND CALLS THE TRIDIAGONAL SOLVER TO OBTAIN THE FINAL
528      C*** SOLUTION.
529      IM1 = IMAX - 1
530      IM2 = IMAX - 2
531      KM1 = KMAX - 1
532      KM2 = KMAX - 2
533      C
534      C*** THE DISSIPATION TERMS ARE CONSTRUCTED AND STORED IN THE ARRAYS DQ1,
535      C*** DQ2,DQ3 AND DQ4.
536      C
537      CALL SPECX(ISPEC)
538      CALL DISSIP
539      C
540      C*** ON TO DQ1,DQ2,DQ3 AND DQ4.
541      C*** THE RIGHT HAND SIDE AT KNOWN TIME LEVEL IS NOW COMPUTED AND ADDED
542      CALL RESI
543      C
544      DO 8999 K = 2 , KM1
545      DO 8999 I = 2 , IM1
546      8999 DELTAT(I,K) = .
547      IF((REDFRE.LT.0.001).AND.ITN.EQ.1) THEN
548      DO 1 K = 2 , KM1
549      DO 1 I = 2 , IM1
550      1 DELTAT(I,K) = 1.0 / ( 1. + SQRT(ABS(YACOB(I,K)) ) )
551      ENDDIF
552      C
553      C*** IF VISCOUS FLOW IS COMPUTED THE VISCOUS TERMS ARE ADDED TO DQ1 ETC. HERE.
554      C
555      IF(REYREF.EQ.0.) CALL STRESS(ITN)
556      I-SWEEP.
557      DTH = DT * 0.5
558      DTW = DT * WW1
559      DO 3 K = 2 , KM1
560      CALL AMAT1(K,IMAX-1,XIX,XIZ,XIT)
561      DO 4 I1 = 1 , 4
562      DO 4 I2 = 1 , 4
563      DO 5 I = 2 , IM1
564      EE(I1,I2,I-1,K) = A(I1,I2,I+1) * DTH * DELTAT(I,K)
565      DD(I1,I2,I-1,K) = - A(I1,I2,I-1) * DTH * DELTAT(I,K)
566      5 CONTINUE
567      4 CONTINUE
568      C
569      C*** IMPLICIT DAMPING ADDED HERE.
570      C
571      DO 6 I = 2 , IM1
572      DT1 = SPECX(I,K) * DTW * DELTAT(I,K)
573      DTW1 = 2. * SPECX(I,K) * YACOB(I,K) * DTW*DELTAT(I,K)
574      DD(1,1,I-1,K) = DD(1,1,I-1,K) - DT1 * YACOB(I-1,K)
575      DD(2,2,I-1,K) = DD(2,2,I-1,K) - DT1 * YACOB(I-1,K)
576      DD(3,3,I-1,K) = DD(3,3,I-1,K) - DT1 * YACOB(I-1,K)
577      DD(4,4,I-1,K) = DD(4,4,I-1,K) - DT1 * YACOB(I-1,K)
578      EE(1,1,I-1,K) = EE(1,1,I-1,K) - DT1 * YACOB(I+1,K)
579      EE(2,2,I-1,K) = EE(2,2,I-1,K) - DT1 * YACOB(I+1,K)
580      EE(3,3,I-1,K) = EE(3,3,I-1,K) - DT1 * YACOB(I+1,K)
581      EE(4,4,I-1,K) = EE(4,4,I-1,K) - DT1 * YACOB(I+1,K)
582      MM(1,1,I-1,K) = 1. + DTW1
583      MM(2,2,I-1,K) = 1. + DTW1
584      MM(3,3,I-1,K) = 1. + DTW1
585      MM(4,4,I-1,K) = 1. + DTW1
586      6 CONTINUE
587      3 CONTINUE
588      DO 890 K = 2 , KM1
589      DO 890 I = 2 , IM1
590      GG(1,I-1,K) = DQ1(I,K) * DELTAT(I,K)
591      GG(2,I-1,K) = DQ2(I,K) * DELTAT(I,K)
592      GG(3,I-1,K) = DQ3(I,K) * DELTAT(I,K)
593      GG(4,I-1,K) = DQ4(I,K) * DELTAT(I,K)
594      890 CONTINUE
595      C
596      C*
597      C*          PERFORM BLOCK TRIDIAGONAL MATRIX INVERSION FOR THE ENTIRE PLANE
598      C*
599      CALL MATRX1(IMAX,KMAX)
600      DO 991 K = 2 , KM1
601      DO 991 I = 2 , IM1
602      DQ1(I,K) = GG(1,I-1,K)
603      DQ2(I,K) = GG(2,I-1,K)
604      DQ3(I,K) = GG(3,I-1,K)
605      DQ4(I,K) = GG(4,I-1,K)
606      991 CONTINUE
607      C
608      C*
609      C*          K-SWEEP BEGINS HERE.
610      C*
611      DO 13 I = 2 , IM1
612      CALL AMAT2(I,KMAX-1,ZETAX,ZETAZ,ZETAT)
613      DO 15 I1 = 1 , 4
614      DO 15 I2 = 1 , 4
615      DO 15 K = 2 , KM1
616      EE(I1,I2,I,K-1) = A(I1,I2,K+1)*DTH * DELTAT(I,K)
617      DD(I1,I2,I,K-1) = -A(I1,I2,K-1)*DTH * DELTAT(I,K)
618      15 CONTINUE
619      C
620      C*** SECOND ORDER DAMPING ADDED HERE.

```

```

LINE # SOURCE TEXT
619 C
620 DO 16 K = 2, KM1
621 DT1 = SPECY(I,K) * DTW * DELTAT(I,K)
622 DTW1 = 2. * SPECY(I,K) * YACOB(I,K) * DTW * DELTAT(I,K)
623 DD(1,1,I,K-1) = DD(1,1,I,K-1) - DT1 * YACOB(I,K-1)
624 DD(2,2,I,K-1) = DD(2,2,I,K-1) - DT1 * YACOB(I,K-1)
625 DD(3,3,I,K-1) = DD(3,3,I,K-1) - DT1 * YACOB(I,K-1)
626 DD(4,4,I,K-1) = DD(4,4,I,K-1) - DT1 * YACOB(I,K-1)
627 EE(1,1,I,K-1) = EE(1,1,I,K-1) - DT1 * YACOB(I,K+1)
628 EE(2,2,I,K-1) = EE(2,2,I,K-1) - DT1 * YACOB(I,K+1)
629 EE(3,3,I,K-1) = EE(3,3,I,K-1) - DT1 * YACOB(I,K+1)
630 EE(4,4,I,K-1) = EE(4,4,I,K-1) - DT1 * YACOB(I,K+1)
631 MM(1,1,I,K-1) = 1. + DTW1
632 MM(2,2,I,K-1) = 1. + DTW1
633 MM(3,3,I,K-1) = 1. + DTW1
634 MM(4,4,I,K-1) = 1. + DTW1
635 16 CONTINUE
636 DO 17 K = 2, KM1
637 DO 17 I = 2, IM1
638 GG(1,I,K-1) = DQ1(I,K)
639 GG(2,I,K-1) = DQ2(I,K)
640 GG(3,I,K-1) = DQ3(I,K)
641 GG(4,I,K-1) = DQ4(I,K)
642 17 CONTINUE
643 C
644 C PERFORM BLOCK TRIDIAGONAL MATRIX INVERSION FOR THE ENTIRE PLANE
645 C
646 CALL MATRI2(IMAX,KMAX)
647 DO 18 K = 2, KM1
648 DO 18 I = 2, IM1
649 DQ1(I,K) = GG(1,I,K-1)
650 DQ2(I,K) = GG(2,I,K-1)
651 DQ3(I,K) = GG(3,I,K-1)
652 DQ4(I,K) = GG(4,I,K-1)
653 18 CONTINUE
654 C
655 C*** UPDATE FLOW VARIABLES AT INTERIOR POINTS.
656 967 CONTINUE
657 RMAX = 0.
658 RUMAX = 0.
659 RVMAX = 0.
660 EMAX = 0.
661 DO 995 K = 2, KM1
662 DO 19 I = 2, IM1
663 Q1(I,K) = Q1(I,K) + DQ1(I,K) * YACOB(I,K)
664 Q2(I,K) = Q2(I,K) + DQ2(I,K) * YACOB(I,K)
665 Q3(I,K) = Q3(I,K) + DQ3(I,K) * YACOB(I,K)
666 Q4(I,K) = Q4(I,K) + DQ4(I,K) * YACOB(I,K)
667 19 CONTINUE
668 DO 995 I = 2, IM1
669 IF (RMAX.LT.ABS(DQ1(I,K)*YACOB(I,K))) THEN
670 IR = I
671 KR = K
672 END IF
673 RMAX = AMAX1(RMAX,ABS(DQ1(I,K) * YACOB(I,K)))
674 RUMAX = AMAX1(RUMAX,ABS(DQ2(I,K) * YACOB(I,K)))
675 RVMAX = AMAX1(RVMAX,ABS(DQ3(I,K) * YACOB(I,K)))
676 EMAX = AMAX1(EMAX,ABS(DQ4(I,K) * YACOB(I,K)))
677 995 CONTINUE
678 C
679 C COMPUTE L2 NORM OF Q1, Q2, Q3, AND Q4 RESIDUAL
680 C
681 RL2 = 0.
682 RUL2 = 0.
683 RVL2 = 0.
684 EL2 = 0.
685 DO 996 K = 2, KM1
686 DO 996 I = 2, IM1
687 RL2 = RL2 + DQ1(I,K)**2
688 RUL2 = RUL2 + DQ2(I,K)**2
689 RVL2 = RVL2 + DQ3(I,K)**2
690 EL2 = EL2 + DQ4(I,K)**2
691 996 CONTINUE
692 RL2 = RL2 / ( IM2*KM2 )
693 RUL2 = RUL2 / ( IM2*KM2 )
694 RVL2 = RVL2 / ( IM2*KM2 )
695 EL2 = EL2 / ( IM2*KM2 )
696 RL2 = SQRT(RL2)
697 RUL2 = SQRT(RUL2)
698 RVL2 = SQRT(RVL2)
699 EL2 = SQRT(EL2)
700 RESDL2(ITN) = RL2
701 IF((ITN-1)/500*500.EQ.(ITN-1)) WRITE (6,3002)
702 IF(ITN/50*50.EQ.ITN) WRITE (6,3001) RMAX,RUMAX,RVMAX,EMAX,IR,KR
703 IF(ITN/50*50.EQ.ITN) WRITE (6,6004) RL2 ,RUL2 ,RVL2 ,EL2
704 RETURN
705 3002 FORMAT(/,5X,'DRMAX',11X,'DUMAX',11X,'DVMAX',11X,'DEMAX',9X,
706 1'IR',3X,'KR')
707 3001 FORMAT(4(E14.8,2X),2I5)
708 6004 FORMAT(4(E14.8,2X) )
709 END

```

```

LINE # SOURCE TEXT
710 SUBROUTINE MATRX1(IMAX,KMAX)
711 C.....
712 C
713 C
714 C SUBROUTINE MATRX1
715 C.....
716 PARAMETER (IX=180,KX=60)
717 COMMON/TRID1/DD(4,4,IX,KX)
718 COMMON/TRID2/MM(4,4,IX,KX)
719 COMMON/TRID3/EE(4,4,IX,KX)
720 COMMON/TRID4/GG(4,IX,KX)
721 COMMON/TRID5/A(4,IX,IX),HH(4,IX,KX),C(4,5,IX)
722 REAL MM
723 REAL L11,L21,L31,L41,L22,L32,L42,L33,L43,L44
724 2,L11,L21,L31,L41
725 C
726 THIS SUBROUTINE PERFORMS THE BLOCK TRIDIAGONAL MATRIX INVERSION FOR
727 AN ENTIRE PLANE DURING THE XI- SWEEP
728 C
729 KM1 = KMAX - 1
730 DO 1 I1 = 1, 4
731 DO 1 K = 2, KM1
732 AI = 1. / MM(1,1,1,K)
733 GG(11,1,K) = GG(11,1,K) * AI
734 HH(11,1,1,K) = EE(11,1,1,K) * AI
735 HH(11,2,1,K) = EE(11,2,1,K) * AI
736 HH(11,3,1,K) = EE(11,3,1,K) * AI
737 HH(11,4,1,K) = EE(11,4,1,K) * AI
738 1 CONTINUE
739 C
740 DO 1000 I = 2, IMAX - 2
741 DO 5 I1 = 1, 4
742 DO 2 K = 2, KM1
743 C(11,1,K) = GG(11,1,K) - DD(11,1,I,K) * GG(1,I-1,K)
744 1 - DD(11,2,I,K) * GG(2,I-1,K)
745 2 - DD(11,3,I,K) * GG(3,I-1,K)
746 3 - DD(11,4,I,K) * GG(4,I-1,K)
747 2 CONTINUE
748 DO 5 I2 = 1, 4
749 DO 5 K = 2, KM1
750 A(11,12,K) = MM(11,12,I,K) - DD(11,1,I,K) * HH(1,12,I-1,K)
751 1 - DD(11,2,I,K) * HH(2,12,I-1,K)
752 2 - DD(11,3,I,K) * HH(3,12,I-1,K)
753 3 - DD(11,4,I,K) * HH(4,12,I-1,K)
754 C(11,12+1,K) = EE(11,12+1,K)
755 5 CONTINUE
756 DO 3 K = 2, KM1
757 L11 = A(1,1,K)
758 L11 = 1. / L11
759 U12 = A(1,2,K) * L11
760 U13 = A(1,3,K) * L11
761 U14 = A(1,4,K) * L11
762 L21 = A(2,1,K)
763 L31 = A(3,1,K)
764 L41 = A(4,1,K)
765 L22 = A(2,2,K) - L21 * U12
766 L21 = 1. / L22
767 U23 = (A(2,3,K) - L21 * U13) * L21
768 U24 = (A(2,4,K) - L21 * U14) * L21
769 L32 = A(3,2,K) - L31 * U12
770 L42 = A(4,2,K) - L41 * U12
771 L33 = A(3,3,K) - L31 * U13 - L32 * U23
772 L31 = 1. / L33
773 U34 = (A(3,4,K) - L31 * U14 - L32 * U24) * L31
774 L43 = A(4,3,K) - L41 * U13 - L42 * U23
775 L44 = A(4,4,K) - L41 * U14 - L42 * U24 - L43 * U34
776 L41 = 1. / L44
777 C(1,1,K) = C(1,1,K) * L11
778 C(2,1,K) = (C(2,1,K) - L21 * C(1,1,K)) * L21
779 C(3,1,K) = (C(3,1,K) - L31 * C(1,1,K)
780 1 - L32 * C(2,1,K)) * L31
781 C(4,1,K) = (C(4,1,K) - L41 * C(1,1,K) - L42 * C(2,1,K)
782 1 - L43 * C(3,1,K)) * L41
783 C(1,2,K) = C(1,2,K) * L11
784 C(2,2,K) = (C(2,2,K) - L21 * C(1,2,K)) * L21
785 C(3,2,K) = (C(3,2,K) - L31 * C(1,2,K)
786 1 - L32 * C(2,2,K)) * L31
787 C(4,2,K) = (C(4,2,K) - L41 * C(1,2,K) - L42 * C(2,2,K)
788 1 - L43 * C(3,2,K)) * L41
789 C(1,3,K) = C(1,3,K) * L11
790 C(2,3,K) = (C(2,3,K) - L21 * C(1,3,K)) * L21
791 C(3,3,K) = (C(3,3,K) - L31 * C(1,3,K)
792 1 - L32 * C(2,3,K)) * L31
793 C(4,3,K) = (C(4,3,K) - L41 * C(1,3,K) - L42 * C(2,3,K)
794 1 - L43 * C(3,3,K)) * L41
795 C(1,4,K) = C(1,4,K) * L11
796 C(2,4,K) = (C(2,4,K) - L21 * C(1,4,K)) * L21
797 C(3,4,K) = (C(3,4,K) - L31 * C(1,4,K)
798 1 - L32 * C(2,4,K)) * L31
799 C(4,4,K) = (C(4,4,K) - L41 * C(1,4,K) - L42 * C(2,4,K)
800 1 - L43 * C(3,4,K)) * L41
801 C(1,5,K) = C(1,5,K) * L11
802 C(2,5,K) = (C(2,5,K) - L21 * C(1,5,K)) * L21
803 C(3,5,K) = (C(3,5,K) - L31 * C(1,5,K)
804 1 - L32 * C(2,5,K)) * L31
805 C(4,5,K) = (C(4,5,K) - L41 * C(1,5,K) - L42 * C(2,5,K)
806 1 - L43 * C(3,5,K)) * L41
807 C(3,1,K) = C(3,1,K) - U34 * C(4,1,K)
808 C(2,1,K) = C(2,1,K) - U24 * C(4,1,K)
809 1 - U23 * C(3,1,K)
810 C(1,1,K) = C(1,1,K) - U14 * C(4,1,K)
811 1 - U13 * C(3,1,K) - U12 * C(2,1,K)
812 C(3,2,K) = C(3,2,K) - U34 * C(4,2,K)
813 C(2,2,K) = C(2,2,K) - U24 * C(4,2,K)
814 1 - U23 * C(3,2,K)
815 C(1,2,K) = C(1,2,K) - U14 * C(4,2,K)
816 1 - U13 * C(3,2,K) - U12 * C(2,2,K)
817 C(3,3,K) = C(3,3,K) - U34 * C(4,3,K)
818 C(2,3,K) = C(2,3,K) - U24 * C(4,3,K)
819 1 - U23 * C(3,3,K)
820 C(1,3,K) = C(1,3,K) - U14 * C(4,3,K)
821 1 - U13 * C(3,3,K) - U12 * C(2,3,K)
822 C(3,4,K) = C(3,4,K) - U34 * C(4,4,K)
823 C(2,4,K) = C(2,4,K) - U24 * C(4,4,K)
824 1 - U23 * C(3,4,K)
825 C(1,4,K) = C(1,4,K) - U14 * C(4,4,K)
826 1 - U13 * C(3,4,K) - U12 * C(2,4,K)
827 C(3,5,K) = C(3,5,K) - U34 * C(4,5,K)
828 C(2,5,K) = C(2,5,K) - U24 * C(4,5,K)
829 1 - U23 * C(3,5,K)

```

LINE # SOURCE TEXT

```

830 C(1,5,K) = C(1,5,K) - U14 * C(4,5,K)
831 1 - U13 * C(3,5,K) - U12 * C(2,5,K)
832 3 CONTINUE
833 C
834 DO 6 I1 = 1, 4
835 DO 9 K = 2, KM1
836 9 GG(I1,I,K) = C(I1,I,K)
837 DO 6 I2 = 1, 4
838 DO 6 K = 2, KM1
839 HH(I1,I2,I,K) = C(I1,I2+1,K)
840 6 CONTINUE
841 1000 CONTINUE
842 C
843 C C C C
844 C BACKWARD SUBSTITUTION
845 DO 7 I = IMAX - 3, 1, - 1
846 DO 7 I1 = 1, 4
847 DO 7 K = 2, KM1
848 GG(I1,I,K) = GG(I1,I,K) - HH(I1,1,I,K) * GG(1,I+1,K)
849 1 - HH(I1,2,I,K) * GG(2,I+1,K)
850 2 - HH(I1,3,I,K) * GG(3,I+1,K)
851 3 - HH(I1,4,I,K) * GG(4,I+1,K)
852 7 CONTINUE
853 RETURN
854 END

```

```

LINE #          SOURCE TEXT
855      SUBROUTINE MATRI2(IMAX,KMAX)
856      C*****
857      C*
858      C*          SUBROUTINE MATRI2
859      C*
860      C*****
861      PARAMETER (IX=180,KX=60)
862      COMMON/TRID1/DD(4,4,IX,KX)
863      COMMON/TRID2/MM(4,4,IX,KX)
864      COMMON/TRID3/EE(4,4,IX,KX)
865      COMMON/TRID4/GG(4,4,IX,KX)
866      COMMON/SCRAT/A(4,4,IX),BH(4,4,IX,KX),C(4,5,IX)
867      REAL MM
868      REAL L11,L21,L31,L41,L22,L32,L42,L33,L43,L44
869      2,L11,L21,L31,L41
870      C
871      C      THIS SUBROUTINE PERFORMS THE BLOCK TRIDIAGONAL MATRIX INVERSION FOR
872      C      AN ENTIRE J=CONSTANT PLANE DURING THE ETA- SWEEP
873      C
874      KMI = KMAX - 1
875      IMI = IMAX - 1
876      DO 1 I1 = 1, 4
877      DO 1 I = 2, IMI
878      AI = 1. / MM(1,1,I,1)
879      GG(1,1,I) = GG(1,1,I) * AI
880      BH(1,1,1,1) = EE(1,1,1,1) * AI
881      BH(1,2,1,1) = EE(1,2,1,1) * AI
882      BH(1,3,1,1) = EE(1,3,1,1) * AI
883      BH(1,4,1,1) = EE(1,4,1,1) * AI
884      1 CONTINUE
885      C
886      DO 1000 F = 2, KMAX - 2
887      DO 5 I1 = 1, 4
888      DO 2 I = 2, IMI
889      C(1,1,I) = GG(1,1,I,K) - DD(1,1,I,K) * GG(1,I,K-1)
890      1 - DD(1,2,I,K) * GG(2,I,K-1)
891      2 - DD(1,3,I,K) * GG(3,I,K-1)
892      3 - DD(1,4,I,K) * GG(4,I,K-1)
893      2 CONTINUE
894      DO 5 I2 = 1, 4
895      DO 5 I = 2, IMI
896      A(1,1,2,I) = MM(1,1,2,I,K) - DD(1,1,1,I,K) * BH(1,1,2,I,K-1)
897      1 - DD(1,2,1,I,K) * BH(2,1,2,I,K-1)
898      2 - DD(1,3,1,I,K) * BH(3,1,2,I,K-1)
899      3 - DD(1,4,1,I,K) * BH(4,1,2,I,K-1)
900      C(1,1,2,I) = EE(1,1,2,I,K)
901      5 CONTINUE
902      DO 3 I = 2, IMI
903      L11 = A(1,1,1,I)
904      L11 = 1. / L11
905      U12 = A(1,2,1,I) * L11
906      U13 = A(1,3,1,I) * L11
907      U14 = A(1,4,1,I) * L11
908      L21 = A(2,1,1,I)
909      L31 = A(3,1,1,I)
910      L41 = A(4,1,1,I)
911      L22 = A(2,2,1,I) - L21 * U12
912      L21 = 1. / L22
913      U23 = (A(2,3,1,I) - L21 * U13) * L21
914      U24 = (A(2,4,1,I) - L21 * U14) * L21
915      L32 = A(3,2,1,I) - L31 * U12
916      L42 = A(4,2,1,I) - L41 * U12
917      L33 = A(3,3,1,I) - L31 * U13 - L32 * U23
918      L31 = 1. / L33
919      U34 = (A(3,4,1,I) - L31 * U14 - L32 * U24) * L31
920      L43 = A(4,3,1,I) - L41 * U13 - L42 * U23
921      L44 = A(4,4,1,I) - L41 * U14 - L42 * U24 - L43 * U34
922      L41 = 1. / L44
923      C(1,1,1,I) = C(1,1,1,I) * L11
924      C(2,1,1,I) = (C(2,1,1,I) - L21 * C(1,1,1,I)) * L21
925      C(3,1,1,I) = (C(3,1,1,I) - L31 * C(1,1,1,I)
926      1 - L32 * C(2,1,1,I)) * L31
927      C(4,1,1,I) = (C(4,1,1,I) - L41 * C(1,1,1,I) - L42 * C(2,1,1,I)
928      1 - L43 * C(3,1,1,I)) * L41
929      C(1,2,1,I) = C(1,2,1,I) * L11
930      C(2,2,1,I) = (C(2,2,1,I) - L21 * C(1,2,1,I)) * L21
931      C(3,2,1,I) = (C(3,2,1,I) - L31 * C(1,2,1,I)
932      1 - L32 * C(2,2,1,I)) * L31
933      C(4,2,1,I) = (C(4,2,1,I) - L41 * C(1,2,1,I) - L42 * C(2,2,1,I)
934      1 - L43 * C(3,2,1,I)) * L41
935      C(1,3,1,I) = C(1,3,1,I) * L11
936      C(2,3,1,I) = (C(2,3,1,I) - L21 * C(1,3,1,I)) * L21
937      C(3,3,1,I) = (C(3,3,1,I) - L31 * C(1,3,1,I)
938      1 - L32 * C(2,3,1,I)) * L31
939      C(4,3,1,I) = (C(4,3,1,I) - L41 * C(1,3,1,I) - L42 * C(2,3,1,I)
940      1 - L43 * C(3,3,1,I)) * L41
941      C(1,4,1,I) = C(1,4,1,I) * L11
942      C(2,4,1,I) = (C(2,4,1,I) - L21 * C(1,4,1,I)) * L21
943      C(3,4,1,I) = (C(3,4,1,I) - L31 * C(1,4,1,I)
944      1 - L32 * C(2,4,1,I)) * L31
945      C(4,4,1,I) = (C(4,4,1,I) - L41 * C(1,4,1,I) - L42 * C(2,4,1,I)
946      1 - L43 * C(3,4,1,I)) * L41
947      C(1,5,1,I) = C(1,5,1,I) * L11
948      C(2,5,1,I) = (C(2,5,1,I) - L21 * C(1,5,1,I)) * L21
949      C(3,5,1,I) = (C(3,5,1,I) - L31 * C(1,5,1,I)
950      1 - L32 * C(2,5,1,I)) * L31
951      C(4,5,1,I) = (C(4,5,1,I) - L41 * C(1,5,1,I) - L42 * C(2,5,1,I)
952      1 - L43 * C(3,5,1,I)) * L41
953      C(3,1,1,I) = C(3,1,1,I) - U34 * C(4,1,1,I)
954      C(2,1,1,I) = C(2,1,1,I) - U24 * C(4,1,1,I)
955      1 - U23 * C(3,1,1,I)
956      C(1,1,1,I) = C(1,1,1,I) - U14 * C(4,1,1,I)
957      1 - U13 * C(3,1,1,I) - U12 * C(2,1,1,I)
958      C(3,2,1,I) = C(3,2,1,I) - U34 * C(4,2,1,I)
959      C(2,2,1,I) = C(2,2,1,I) - U24 * C(4,2,1,I)
960      1 - U23 * C(3,2,1,I)
961      C(1,2,1,I) = C(1,2,1,I) - U14 * C(4,2,1,I)
962      1 - U13 * C(3,2,1,I) - U12 * C(2,2,1,I)
963      C(3,3,1,I) = C(3,3,1,I) - U34 * C(4,3,1,I)
964      C(2,3,1,I) = C(2,3,1,I) - U24 * C(4,3,1,I)
965      1 - U23 * C(3,3,1,I)
966      C(1,3,1,I) = C(1,3,1,I) - U14 * C(4,3,1,I)
967      1 - U13 * C(3,3,1,I) - U12 * C(2,3,1,I)
968      C(3,4,1,I) = C(3,4,1,I) - U34 * C(4,4,1,I)
969      C(2,4,1,I) = C(2,4,1,I) - U24 * C(4,4,1,I)
970      1 - U23 * C(3,4,1,I)
971      C(1,4,1,I) = C(1,4,1,I) - U14 * C(4,4,1,I)
972      1 - U13 * C(3,4,1,I) - U12 * C(2,4,1,I)
973      C(3,5,1,I) = C(3,5,1,I) - U34 * C(4,5,1,I)
974      C(2,5,1,I) = C(2,5,1,I) - U24 * C(4,5,1,I)

```

LINE #	SOURCE TEXT
975	1
976	1 C(1,5,I) = C(1,5,I) - U23 * C(3,5,I)
977	1 C(1,5,I) = C(1,5,I) - U14 * C(4,5,I)
978	1 - U13 * C(3,5,I) - U12 * C(2,5,I)
979	3 CONTINUE
980	C
981	DO 6 I1 = 1, 4
982	DO 9 I = 2, IM1
983	9 GG(I1,I,K) = C(I1,1,I)
984	DO 6 I2 = 1, 4
985	DO 6 I = 2, IM1
986	HH(I1,I2,I,K) = C(I1,I2+1,I)
987	6 CONTINUE
988	1000 CONTINUE
989	C
990	C BACKWARD SUBSTITUTION
991	DO 7 K = KMAX - 3, 1, - 1
992	DO 7 I1 = 1, 4
993	DO 7 I = 2, IM1
994	GG(I1,1,K) = GG(I1,I,K) - HH(I1,1,I,K) * GG(1,I,K+1)
995	1 - HH(I1,2,I,K) * GG(2,I,K+1)
996	2 - HH(I1,3,I,K) * GG(3,I,K+1)
997	3 - HH(I1,4,I,K) * GG(4,I,K+1)
998	7 CONTINUE
999	RETURN
1000	END

```

LINE #          SOURCE TEXT
1001  SUBROUTINE METRIC
1002  C.....
1003  C*
1004  SUBROUTINE METRIC
1005  C*
1006  C.....
1007  PARAMETER (IX=180,KX=60)
1008  COMMON/FIX/OMEGA,HDOT
1009  COMMON/DGRID/DT,IMAX,KMAX,ITEL,ITEU
1010  COMMON/GRID1/X(IX,KX),Z(IX,KX)
1011  COMMON/GRID/YACOB(IX,KX)
1012  COMMON/MTRIX/XIX(IX,KX),XIZ(IX,KX),ZETAX(IX,KX),ZETAZ(IX,KX),
1013  XIT(IX,KX),ZETAT(IX,KX)
1014  C
1015  C*** THE SUBROUTINE METRIC COMPUTES THE METRICS IN ALL THE TWO DIRECTIONS AND
1016  THE UNSTEADY COEFFICIENTS ETAT ETC.
1017  C
1018  DO 1000 K = 1, KMAX
1019  DO 1000 I = 1, IMAX
1020  XTAU = OMEGA * Z(I,K)
1021  YTAU = OMEGA * (-X(I,K)) - HDOT
1022  C*** PRESENT SET UP IS FOR FLOW PAST AN AIRFOIL.
1023  C
1024  IF(I.EQ.1.OR.I.EQ.IMAX) GO TO 10
1025  XXI = .5 * (X(I+1,K)-X(I-1,K))
1026  XZI = .5 * (Z(I+1,K)-Z(I-1,K))
1027  GO TO 15
1028  10 IF(I.EQ.IMAX) GO TO 16
1029  XXI = 1.0 * (X(2,K) - X(1,K))
1030  XZI = 1.0 * (Z(2,K) - Z(1,K))
1031  GO TO 15
1032  16 XXI = 1.0 * (X(IMAX,K) - X(IMAX-1,K))
1033  XZI = 1.0 * (Z(IMAX,K) - Z(IMAX-1,K))
1034  15 CONTINUE
1035  IF(K.EQ.1.OR.K.EQ.KMAX) GO TO 17
1036  XZET = .5 * (X(I,K+1)-X(I,K-1))
1037  ZZET = .5 * (Z(I,K+1)-Z(I,K-1))
1038  GO TO 20
1039  17 IF(K.EQ.KMAX) GO TO 18
1040  XZET = 2. * X(I,2)-1.5 * X(I,1) - .5 * X(I,3)
1041  ZZET = 2. * Z(I,2) - 1.5 * Z(I,1) - .5 * Z(I,3)
1042  GO TO 20
1043  18 XZET = 1.5 * X(I,KMAX)-2. * X(I,KMAX-1)+.5 * X(I,KMAX-2)
1044  ZZET = 1.5 * Z(I,KMAX)-2. * Z(I,KMAX-1)+.5 * Z(I,KMAX-2)
1045  20 CONTINUE
1046  YACOBI = XXI * ZZET - XZET * XZI
1047  YACOB(I,K) = 1. / YACOBI
1048  XIX(I,K) = ZZET * YACOB(I,K)
1049  XIZ(I,K) = -XZET * YACOB(I,K)
1050  XTAU = OMEGA * Z(I,K)
1051  YTAU = - OMEGA * X(I,K) - HDOT
1052  XIT(I,K) = - XIX(I,K) * XTAU - XIZ(I,K) * YTAU
1053  ZETAX(I,K) = -XZI * YACOB(I,K)
1054  ZETAZ(I,K) = XXI * YACOB(I,K)
1055  ZETAT(I,K) = - ZETAX(I,K) * XTAU - ZETAZ(I,K) * YTAU
1056  1000 CONTINUE
1057  RETURN
1058  END

```

Program

```

LINE #      SOURCE TEXT
1059      SUBROUTINE DISSIP
1060      C*****
1061      C*
1062      C*      SUBROUTINE DISSIP
1063      C*
1064      C*****
1065      PARAMETER (IX=180,KX=60)
1066      COMMON/FLOW/Q1(IX,KX),Q2(IX,KX),Q3(IX,KX),Q4(IX,KX)
1067      COMMON/MTRIX/X1X(IX,KX),X1Z(IX,KX),ZETA1(IX,KX),ZETA2(IX,KX),
1068      1XIT(IX,KX),ZETAT(IX,KX)
1069      COMMON/PERTR/DQ1(IX,KX),DQ2(IX,KX),DQ3(IX,KX),DQ4(IX,KX)
1070      COMMON/DGRID/DT,IMAX,KMAX,ITEL,ITEU
1071      COMMON/PAR/GAMMA,REYREF,ALFA,ALFAL,REDFRE,AMINF,ALFAI
1072      COMMON/GRID/YACOB(IX,KX)
1073      COMMON/DAMP/WW,WM1,WN2X,WN2Y,WM4X,WM4Y
1074      COMMON/RADIUS/ SPECX(IX,KX),SPECY(IX,KX)
1075      COMMON/SPEED/ U(IX,KX),V(IX,KX),AA(IX,KX)
1076      DIMENSION P(IX),EPS(IX),DIS1(IX,4),DIS2(IX,4),DIS3(IX,4)
1077      DIMENSION QQ(4)
1078      C
1079      C      THIS SUBROUTINE ADDS THE FOURTH ORDER DISSIPATION TERMS TO THE
1080      C      RIGHT HAND SIDE
1081      C
1082      C
1083      IM1 = IMAX - 1
1084      IM2 = IMAX - 2
1085      KM1 = KMAX - 1
1086      KM2 = KMAX - 2
1087      WDT = WM*DT
1088      GM1 = GAMMA - 1.
1089      DO 20 K = 2, KM1
1090      C
1091      C      COMPUTE SWITCHING FUNCTION BASED ON SECOND DERIVATIVE OF PRESSURE
1092      C
1093      DO 1 I = 1, IMAX
1094      1 P(I) = GM1 * (Q4(I,K) - 0.5*Q1(I,K)*(U(I,K)**2 + V(I,K)**2))
1095      DO 3 I = 2, IM1
1096      PS1 = P(I+1) - 2.*P(I) + P(I-1)
1097      PS2 = P(I+1) + 2.*P(I) + P(I-1)
1098      EPS(I) = ABS(PS1/PS2)
1099      3 CONTINUE
1100      EPS(1) = EPS(2)
1101      EPS(IMAX) = EPS(IM1)
1102      C
1103      C      SMOOTH OUT PRESSURE COEFFICIENT
1104      C
1105      DO 4 I = 2, IM1
1106      P(I) = AMAX1( EPS(I+1),EPS(I),EPS(I-1) )
1107      4 CONTINUE
1108      P(1) = P(2)
1109      P(IMAX) = P(IM1)
1110      C
1111      DO 10 I = 2, IM1
1112      C2 = WN2X * P(I)
1113      C4 = WM4X - AMIN1(WM4X,C2)
1114      C22 = C2*WDT + ( SPECX(I,K) + SPECX(I+1,K) )
1115      C44 = -C4*WDT* SPECX(I,K)
1116      HPM = Q4(I-1,K) + P(I-1)
1117      HP = Q4(I,K) + P(I)
1118      HPP = Q4(I+1,K) + P(I+1)
1119      DIS1(1,1) = C22* ( Q1(I+1,K) - Q1(I,K) )
1120      DIS1(1,2) = C22* ( Q2(I+1,K) - Q2(I,K) )
1121      DIS1(1,3) = C22* ( Q3(I+1,K) - Q3(I,K) )
1122      DIS1(1,4) = C22* ( Q4(I+1,K) - Q4(I,K) )
1123      C
1124      DIS1(1,4) = C22* ( HPP - HP )
1125      DIS2(1,1) = C44 * ( Q1(I+1,K) - 2.*Q1(I,K) + Q1(I-1,K) )
1126      DIS2(1,2) = C44 * ( Q2(I+1,K) - 2.*Q2(I,K) + Q2(I-1,K) )
1127      DIS2(1,3) = C44 * ( Q3(I+1,K) - 2.*Q3(I,K) + Q3(I-1,K) )
1128      DIS2(1,4) = C44 * ( Q4(I+1,K) - 2.*Q4(I,K) + Q4(I-1,K) )
1129      C
1130      DIS2(1,4) = C44 * ( HPP - 2.*HP + HPM )
1131      10 CONTINUE
1132      C
1133      C      B.C. TREATMENT
1134      QQ(1) = Q1(2,K) - Q1(1,K)
1135      QQ(2) = Q2(2,K) - Q2(1,K)
1136      QQ(3) = Q3(2,K) - Q3(1,K)
1137      QQ(4) = Q4(2,K) - Q4(1,K)
1138      C
1139      QQ(4) = Q4(2,K) + P(2) - Q4(1,K) - P(1)
1140      DO 15 N4 = 1, 4
1141      C2 = WN2X*P(1)
1142      C22 = C2 * WDT * ( SPECX(1,K) + SPECX(2,K) )
1143      DIS1(1,N4) = C22 * QQ(N4)
1144      DIS2(1,N4) = 0.
1145      15 DIS2(IMAX,N4) = 0.
1146      C
1147      DO 16 I = 1, IM1
1148      DIS3(1,1) = DIS1(I,1) + DIS2(I+1,1) - DIS2(I,1)
1149      DIS3(1,2) = DIS1(I,2) + DIS2(I+1,2) - DIS2(I,2)
1150      DIS3(1,3) = DIS1(I,3) + DIS2(I+1,3) - DIS2(I,3)
1151      DIS3(1,4) = DIS1(I,4) + DIS2(I+1,4) - DIS2(I,4)
1152      16 CONTINUE
1153      C
1154      C      FILL IN DISSIPATION TERMS
1155      C
1156      DO 18 I = 2, IM1
1157      DQ1(I,K) = DIS3(I,1) - DIS3(I-1,1)
1158      DQ2(I,K) = DIS3(I,2) - DIS3(I-1,2)
1159      DQ3(I,K) = DIS3(I,3) - DIS3(I-1,3)
1160      DQ4(I,K) = DIS3(I,4) - DIS3(I-1,4)
1161      18 CONTINUE
1162      20 CONTINUE
1163      C
1164      C      K DIRECTION
1165      C
1166      DO 100 I = 2, IM1
1167      C
1168      C      COMPUTE SWITCHING FUNCTION BASED ON SECOND DERIVATIVE OF PRESSURE
1169      C
1170      DO 31 K = 2, KMAX
1171      31 P(K) = GM1 * (Q4(I,K) - 0.5*Q1(I,K) * (U(I,K)**2 + V(I,K)**2))
1172      P(1) = ( 4.*P(2) - P(3) ) / 3.
1173      DO 33 K = 2, KM1
1174      PS1 = P(K+1) - 2.*P(K) + P(K-1)
1175      PS2 = P(K+1) + 2.*P(K) + P(K-1)
1176      EPS(K) = ABS(PS1/PS2)
1177      33 CONTINUE
1178      EPS(1) = EPS(2)
1179      EPS(KMAX) = EPS(KM1)
1180      C
1181      C      SMOOTH OUT PRESSURE COEFFICIENT
1182      C

```


LINE # SOURCE TEXT

```

1179 DO 34 K = 2 , KM1
1180 P(K) = AMAX1( EPS(K+1),EPS(K),EPS(K-1) )
1181 34 CONTINUE
1182 P(1) = P(2)
1183 P(KMAX) = P(KM1)
1184 C
1185 DO 52 K = 2 , KM1
1186 C2 = WN2Y * P(K)
1187 C4 = WN4Y - AMIN1(WN4Y,C2)
1188 C22 = C2 * WDT * ( SPECY(I,K) + SPECY(I,K+1) )
1189 C44 = -C4*WDT* SPECY(I,K)
1190 C HPM = Q4(I,K-1) + P(K-1)
1191 C HP = Q4(I,K) + P(K)
1192 C HPP = Q4(I,K+1) + P(K+1)
1193 DIS1(K,1) = C22 * ( Q1(I,K+1) - Q1(I,K) )
1194 DIS1(K,2) = C22 * ( Q2(I,K+1) - Q2(I,K) )
1195 DIS1(K,3) = C22 * ( Q3(I,K+1) - Q3(I,K) )
1196 DIS1(K,4) = C22 * ( Q4(I,K+1) - Q4(I,K) )
1197 C DIS1(K,4) = C22 * ( HPP - HP )
1198 DIS2(K,1) = C44 * ( Q1(I,K+1) - 2.*Q1(I,K) + Q1(I,K-1) )
1199 DIS2(K,2) = C44 * ( Q2(I,K+1) - 2.*Q2(I,K) + Q2(I,K-1) )
1200 DIS2(K,3) = C44 * ( Q3(I,K+1) - 2.*Q3(I,K) + Q3(I,K-1) )
1201 DIS2(K,4) = C44 * ( Q4(I,K+1) - 2.*Q4(I,K) + Q4(I,K-1) )
1202 C DIS2(K,4) = C44 * ( HPP - 2.*HP + HPM )
1203 52 CONTINUE
1204 C B.C. TREATMENT
1205 QQ(1) = Q1(I,2) - Q1(I,1)
1206 QQ(2) = Q2(I,2) - Q2(I,1)
1207 QQ(3) = Q3(I,2) - Q3(I,1)
1208 QQ(4) = Q4(I,2) - Q4(I,1)
1209 C QQ(4) = Q4(I,2) + P(2) - Q4(I,1) - P(1)
1210 DO 59 N4 = 1 , 4
1211 C2 = WN2Y * P(1)
1212 C22 = C2 * WDT * ( SPECY(I,1) + SPECY(I,2) )
1213 DIS1(1,N4) = C22 * QQ(N4)
1214 DIS2(1,N4) = 0.
1215 59 DIS2(KMAX,N4) = 0.
1216 C
1217 DO 60 K = 1 , KM1
1218 DIS3(K,1) = DIS1(K,1) + DIS2(K+1,1) - DIS2(K,1)
1219 DIS3(K,2) = DIS1(K,2) + DIS2(K+1,2) - DIS2(K,2)
1220 DIS3(K,3) = DIS1(K,3) + DIS2(K+1,3) - DIS2(K,3)
1221 DIS3(K,4) = DIS1(K,4) + DIS2(K+1,4) - DIS2(K,4)
1222 60 CONTINUE
1223 C
1224 C FILL IN DISSIPATION TERMS
1225 C
1226 DO 65 K = 2 , KM1
1227 DQ1(I,K) = DQ1(I,K) + DIS3(K,1) - DIS3(K-1,1)
1228 DQ2(I,K) = DQ2(I,K) + DIS3(K,2) - DIS3(K-1,2)
1229 DQ3(I,K) = DQ3(I,K) + DIS3(K,3) - DIS3(K-1,3)
1230 DQ4(I,K) = DQ4(I,K) + DIS3(K,4) - DIS3(K-1,4)
1231 65 CONTINUE
1232 100 CONTINUE
1233 RETURN
1234 END

```

Program

SOURCE TEXT

```

1235 SUBROUTINE SPECR(ISPEC)
1236 C*****
1237 C*
1238 C* SUBROUTINE SPECR
1239 C*
1240 C*****
1241 PARAMETER (IX=180,KX=60)
1242 COMMON/PAR/GAMMA,REYREF,ALFA,ALFA1,REDFRE,AMINF,ALFAI
1243 COMMON/DGR:ID,DT,IMAX,KMAX,ITEL,ITEU
1244 COMMON/MTRIX/ XIX(I,K),XIZ(I,K),ZETAX(I,K),ZETAZ(I,K)
1245 1,XIT(I,K),ZETAT(I,K)
1246 COMMON/FLOW/Q1(I,K),Q2(I,K),Q3(I,K),Q4(I,K)
1247 COMMON/RADIUS/ SPECX(I,K),SPECY(I,K)
1248 COMMON/SPEED/ U(I,K),V(I,K),AA(I,K)
1249 COMMON/GRID/YACOB(I,K)
1250 C
1251 C THIS SUBROUTINE COMPUTE THE SPECTRAL RADIUS FOR SCALING THE
1252 C EXPLICIT AND IMPLICIT DISSIPATIONS
1253 C
1254 IM1 = IMAX - 1
1255 IMI = KMAX - 1
1256 GAM = GAMMA * ( GAMMA - 1. )
1257 DO 5 K = 1, KMAX
1258 DO 5 I = 1, IMAX
1259 U(I,K) = Q2(I,K) / Q1(I,K)
1260 V(I,K) = Q3(I,K) / Q1(I,K)
1261 AA(I,K) = GAM * ( Q4(I,K)/Q1(I,K) - 0.5*(U(I,K)**2 + V(I,K)**2) )
1262 IF(AA(I,K).LT.0.) PRINT*, 'NEGATIVE A*A = ',AA(I,K), ' AT ',I,K
1263 5 CONTINUE
1264 C
1265 C COMPUTE IMPLICIT DISSIPATION SCALING
1266 C SPECX = SPECTRAL RADIUS FOR XI-DIRECTION
1267 C SPECY = SPECTRAL RADIUS FOR ZETA-DIRECTION
1268 C
1269 C
1270 IF(ISPEC.EQ.1) THEN
1271 DO 20 K = 1, KMAX
1272 DO 20 I = 1, IMAX
1273 SPECX(I,K) = 1. / YACOB(I,K)
1274 SPECY(I,K) = 1. / YACOB(I,K)
1275 20 CONTINUE
1276 ELSEIF(ISPEC.EQ.2) THEN
1277 DO 30 K = 1, KMAX
1278 DO 30 I = 1, IMAX
1279 UCON = U(I,K)*XIX(I,K) + V(I,K)*XIZ(I,K) + XIT(I,K)
1280 VCON = U(I,K)*ZETAX(I,K) + V(I,K)*ZETAZ(I,K) + ZETAT(I,K)
1281 SPECX(I,K) = ABS(UCON) / YACOB(I,K)
1282 SPECY(I,K) = ABS(VCON) / YACOB(I,K)
1283 30 CONTINUE
1284 ELSEIF(ISPEC.EQ.3) THEN
1285 DO 40 K = 1, KMAX
1286 DO 40 I = 1, IMAX
1287 UCON = U(I,K)*XIX(I,K) + V(I,K)*XIZ(I,K) + XIT(I,K)
1288 VCON = U(I,K)*ZETAX(I,K) + V(I,K)*ZETAZ(I,K) + ZETAT(I,K)
1289 XI2 = XIX(I,K)**2 + XIZ(I,K)**2
1290 ZETA2 = ZETAX(I,K)**2 + ZETAZ(I,K)**2
1291 SPECX(I,K) = (ABS(UCON) + SQRT(AA(I,K)*XI2) ) / YACOB(I,K)
1292 SPECY(I,K) = (ABS(VCON) + SQRT(AA(I,K)*ZETA2) ) / YACOB(I,K)
1293 40 CONTINUE
1294 ENDIF
1295 RETURN
1296 END

```

```

LINE #          SOURCE TEXT
1297  SUBROUTINE EXPEC(CI)
1298  C*****
1299  C*
1300  C*          SUBROUTINE EXPEC
1301  C*
1302  C*****
1303  PARAMETER (IX=180,KX=60)
1304  COMMON/SURF/PSUR(IX)
1305  COMMON/GRID1/X(IX,KX),Z(IX,KX)
1306  COMMON/PAR/GAMMA,REYREF,ALFA,ALFAL,REDFRE,AMINF
1307  COMMON/DGRID/DT,IMAX,KMAX,ITEL,ITEU
1308  COMMON/GRID/YACOB(IX,KX)
1309  COMMON/DAMP/WW,WW1,WW2X,WW2Y,WW4X,WW4Y
1310  COMMON/MTRIX/XIX(IX,KX),XIZ(IX,KX),ZETAX(IX,KX),ZETAZ(IX,KX),
1311  XIT(IX,KX),ZETAT(IX,KX)
1312  COMMON/FLOW/Q1(IX,KX),Q2(IX,KX),Q3(IX,KX),Q4(IX,KX)
1313  COMMON/SPEED/ U(IX,KX),V(IX,KX),AA(IX,KX)
1314  COMMON/INITI/UINF,VINF
1315  COMMON/BCLOG/CIRCOR
1316  COMMON/LOGIC/RSTRT,PITCH,RAMP
1317  LOGICAL RSTRT,PITCH,RAMP
1318  LOGICAL CIRCOR
1319  DIMENSION CI(4)
1320  DIMENSION A(2,2),RHS(2)
1321  DATA PI/3.1415927/
1322  DATA CHORD/1./
1323  C
1324  GAM1 = 1. / GAMMA
1325  GAMM = GAMMA - 1.
1326  GAMMI = 1. / GAMM
1327  C
1328  C          INVISCID AND VISCOUS B.C. ON SOLID WALL
1329  C
1330  DO 1 I= ITEL , ITEU
1331  K = 3
1332  C1(1) = XIT(I,K)
1333  C1(2) = XIX(I,K)
1334  C1(3) = XIZ(I,K)
1335  UCON3 = (Q2(I,K)*C1(2)+Q3(I,K)*C1(3))
1336  1/Q1(I,K)
1337  K = 2
1338  C1(1) = XIT(I,K)
1339  C1(2) = XIX(I,K)
1340  C1(3) = XIZ(I,K)
1341  UCON2 = (Q2(I,K)*C1(2)+Q3(I,K)*C1(3))
1342  1/Q1(I,K)
1343  RHS(1) = 2. * UCON2 - UCON3 - XIT(I,1)
1344  C          FOR VISCOUS FLOWS SET UCON TO ZERO ALSO
1345  IF(REYREF GT.0.) RHS(1) = - XIT(I,1)
1346  A(1,1) = XIX(I,1)
1347  A(1,2) = XIZ(I,1)
1348  A(2,1) = ZETAX(I,1)
1349  A(2,2) = ZETAZ(I,1)
1350  RHS(2) = - ZETAT(I,1)
1351  TEMP1 = A(1,1)
1352  TEMP2 = A(1,2)
1353  TEMP3 = A(2,1)
1354  TEMP4 = A(2,2)
1355  DEN = 1. / (TEMP1 * TEMP4 - TEMP2 * TEMP3)
1356  A(1,1) = A(2,2) * DEN
1357  A(1,2) = - TEMP2 * DEN
1358  A(2,1) = - TEMP3 * DEN
1359  A(2,2) = TEMP1 * DEN
1360  Q1(I,1) = 2. * Q1(I,2) - Q1(I,3)
1361  Q2(I,1) = Q1(I,1)*A(1,1)*RHS(1)+A(1,2)*RHS(2)
1362  Q3(I,1) = Q1(I,1) * (A(2,1)*RHS(1)+A(2,2)*RHS(2))
1363  1 CONTINUE
1364  DO 10 I=ITEL ,ITEU
1365  P2=GAMM*(Q4(I,2)-0.5*Q1(I,2)*(U(I,2)**2+V(I,2)**2))
1366  P3=GAMM*(Q4(I,3)-0.5*Q1(I,3)*(U(I,3)**2+V(I,3)**2))
1367  P1=(4.*P2-P3)/3.
1368  PSUR(I)=(GAMMA*P1-1.)/(1.7*AMINF**2)
1369  10 Q4(I,1)=P1/GAMM+0.5*Q1(I,1)*(U(I,1)**2+V(I,1)**2)
1370  C
1371  C          FAR FIELD BOUNDARY CONDITION ONLY FOR STEADY FLOW
1372  C
1373  CIRC = 0
1374  IF(PITCH.OR.RAMP) GO TO 999
1375  IF(AMINF.GT.1.) GO TO 65
1376  C
1377  C          CIRCULATION CORRECTION AT THE FAR FIELD IS BASED ON POTENTIAL
1378  C          VORTEX
1379  C
1380  BETA = SORT( 1. - AMINF**2 )
1381  IF(CIRCOR) CIRC = 0.25 * CHORD * CL * BETA * AMINF / PI
1382  C
1383  COSAL = COS(ALFA)
1384  SINAL = SIN(ALFA)
1385  AINF = 1.
1386  BINF = GAMMI + 0.5 * AMINF**2
1387  C
1388  CIRCQ = CIRCULATION CORRECTION QUANTITY
1389  C
1390  K = KMAX
1391  DO 60 I = 2 , IMAX-1
1392  XLOC = X(I,K) - XREF
1393  ZLOC = Z(I,K)
1394  RADIUS = SQRT( XLOC**2 + ZLOC**2 )
1395  ANGLE = ATAN2(ZLOC,XLOC)
1396  CIRCQ = CIRC / ( RADIUS * ( 1. - (AMINF*SIN(ANGLE-ALFA))**2 ) )
1397  UF = UINF + CIRCQ * SIN(ANGLE)
1398  VF = VINF - CIRCQ * COS(ANGLE)
1399  AFSQ = GAMM * ( BINF - 0.5*( UF**2 + VF**2 ) )
1400  AF = SQRT(AFSQ)
1401  C
1402  C          NONREFLECTING B.C. BASE ON 1-D RIEMANN INVARIANTS
1403  ZETXN, ZETZN = NORMALIZED NORMAL VECTOR
1404  C
1405  ANOR = 1. / SQRT( ZETAX(I,K)**2 + ZETAZ(I,K)**2 )
1406  ZETXN = ZETAX(I,K) * ANOR
1407  ZETZN = ZETAZ(I,K) * ANOR
1408  C
1409  C          CHECK FOR INFLOW OR OUTFLOW
1410  FOR INFLOW: R1, VET, ENTROY ARE SPECIFIED AS FREE STREAM VALUES
1411  R2 IS EXTRAPOLATED
1412  FOR OUTFLOW: R1 IS SPECIFIED AS FREE STREAM VALUE
1413  R2, VET, ENTROPY ARE EXTRAPOLATED
1414  C
1415  RBOEXT = Q1(I,K-1)
1416  RBOI = 1. - Q1(I,K-1)

```

LINE # SOURCE TEXT

```

1417 UEXT = Q1(I,K-1) * RHO1
1418 VEXT = Q3(I,K-1) * RHO1
1419 EEXT = Q4(I,K-1)
1420 PEXT = GAMM * ( EEXT - 0.5*RHOEXT*( UEXT**2 + VEXT**2 ) )
1421
1422 SET RIEMANN INVARIANTS R1, AND R2
1423 VELN = NORMAL VELOCITY, VELT = TANGENTIAL VELOCITY
1424
1425 R1 = ZETXN * UF + ZETZN * VF - 2. * AF * GAMM1
1426 R2 = ZETXN * UEXT + ZETZN * VEXT + 2. * SQRT( GAMMA * PEXT /
1427 1 RHOEXT ) * GAMM1
1428
1429 VELN = ( R1 + R2 ) * 0.5
1430 SPSQ = ( R2 - R1 ) * GAMM * 0.25
1431 A2 = SPSQ**2
1432
1433 SET OTHER FIXED OR EXTRAPOLATED VARIABLES
1434
1435 IF(VELN.LE.0.) THEN
1436 VELT = ZETZN * UF - ZETXN * VF
1437 ENTRO = GAMMA
1438 ELSE
1439 VELT = ZETZN * UEXT - ZETXN * VEXT
1440 ENTRO = RHOEXT**GAMMA / PEXT
1441 ENDIF
1442
1443 NOW COMPUTE FLOW VARIABLES
1444
1445 U(I,K) = ZETXN * VELN + ZETZN * VELT
1446 V(I,K) = ZETZN * VFLN - ZETXN * VELT
1447 Q1(I,K) = ( A2 * ENTRO * GAM1 ) ** GAMM1
1448 PRESS = A2 * Q1(I,K) * GAM1
1449 Q2(I,K) = Q1(I,K) * U(I,K)
1450 Q3(I,K) = Q1(I,K) * V(I,K)
1451 Q4(I,K) = PRESS * GAMM1 + 0.5 * Q1(I,K) * ( U(I,K)**2 + V(I,K)**2 )
1452 60 CONTINUE
1453 GO TO 67
1454 65 CONTINUE
1455
1456 B.C. FOR SUPERSONIC FLOW
1457
1458 K = KMAX
1459 DO 66 I = 2 , IMAX-1
1460 RHO1 = 1. / Q1(I,K)
1461 U(I,K) = Q2(I,K) * RHO1
1462 V(I,K) = Q3(I,K) * RHO1
1463 ANOR = 1. / SQRT( ZETAX(I,K)**2 + ZETAZ(I,K)**2 )
1464 ZETXN = ZETAX(I,K) * ANOR
1465 ZETZN = ZETAZ(I,K) * ANOR
1466 VELN = ZETXN * U(I,K) + ZETZN * V(I,K)
1467 IF(VELN.GE.0.) THEN
1468 Q1(I,K) = Q1(I,K-1)
1469 Q2(I,K) = Q2(I,K-1)
1470 Q3(I,K) = Q3(I,K-1)
1471 Q4(I,K) = Q4(I,K-1)
1472 ENDIF
1473 66 CONTINUE
1474
1475 67 CONTINUE
1476
1477 OUTFLOW B.C. AT THE DOWNSTREAM OF C-GRID ONLY FOR INVISCID FLOW
1478
1479 IF(REYREF.LT.0.) THEN
1480 I = 1
1481 IP1 = 1
1482 SIGN = -1.
1483
1484 CHECK FOR SUPERSONIC FLOW
1485
1486 IF(AMINF.GT.1.) GO TO 75
1487
1488 72 CONTINUE
1489 DO 74 K = 1 , KMAX
1490
1491 CORRECT FREE STREAM VALUES WITH CIRCULATION CORRECTION
1492
1493 XLOC = X(I,K) - XREF
1494 ZLOC = Z(I,K)
1495 RADIUS = SQRT( XLOC**2 + ZLOC**2 )
1496 ANGLE = ATAN2(ZLOC,XLOC)
1497 CIRCQ = CIRC / ( RADIUS * ( 1. - (AMINF*SIN(ANGLE-ALFA))**2 ) )
1498 UF = UINF + CIRCQ * SIN(ANGLE)
1499 VF = VINF - CIRCQ * COS(ANGLE)
1500 AFSQ = GAMM * ( BINF - 0.5*( UF**2 + VF**2 ) )
1501 AF = SQRT(AFSQ)
1502
1503 XIHX, XIZH = NORMALIZED HORIZONTAL VECTOR
1504
1505 ANOR = 1. / SQRT( XIHX(I,K)**2 + XIZ(I,K)**2 )
1506 XIHX = XIHX(I,K) * ANOR
1507 XIZH = XIZ(I,K) * ANOR
1508
1509 RHOEXT = Q1(I+IP1,K)
1510 RHO1 = 1. / Q1(I+IP1,K)
1511 UEXT = Q2(I+IP1,K)
1512 VEXT = Q3(I+IP1,K)
1513 EEXT = Q4(I+IP1,K)
1514 PEXT = GAMM * ( EEXT - 0.5*RHOEXT*( UEXT**2 + VEXT**2 ) )
1515
1516 SET RIEMANN INVARIANTS R1, AND R2
1517
1518 R1 = XIHX * UF + XIZH * VF - SIGN * 2. * AF * GAMM1
1519 R2 = XIHX * UEXT + XIZH * VEXT + SIGN * 2. * SQRT( GAMMA * PEXT /
1520 1 RHOEXT ) * GAMM1
1521
1522 VELN = ( R1 + R2 ) * 0.5
1523 SPSQ = SIGN * ( R2 - R1 ) * GAMM * 0.25
1524 A2 = SPSQ**2
1525
1526 SET OTHER FIXED OR EXTRAPOLATED VARIABLES
1527
1528 IF(SIGN*VELN.LE.0.) THEN
1529 VELT = -XIZH * UF + XIHX * VF
1530 ENTRO = GAMMA
1531 ELSE
1532 VELT = -XIZH * UEXT + XIHX * VEXT
1533 ENTRO = RHOEXT**GAMMA / PEXT
1534 ENDIF
1535
1536 COMPUTE FLOW VARIABLES

```

```

LINE #          SOURCE TEXT
1537 C
1538 U(I,K) = XIXH * VELN - XIZH * VELT
1539 V(I,K) = XIZH * VELN + XIXH * VELT
1540 Q1(I,K) = ( A2 * ENTRO * GAMI ) ** GAMMI
1541 PRESS = A2 * Q1(I,K) * GAMI
1542 Q2(I,K) = Q1(I,K) * U(I,K)
1543 Q3(I,K) = Q1(I,K) * V(I,K)
1544 Q4(I,K) = PRESS * GAMMI + 0.5 * Q1(I,K) * ( U(I,K)**2 + V(I,K)**2 )
1545 74 CONTINUE
1546 IF(I.EQ.IMAX) GO TO 79
1547 I = IMAX
1548 IP1 = -1
1549 SIGN = 1.
1550 GO TO 72
1551 79 CONTINUE
1552 GO TO 89
1553 C
1554 C      B.C. FOR SUPERSONIC FLOW
1555 C
1556 75 CONTINUE
1557 DO 84 K = 1 , KMAX
1558 C
1559 RBOI = 1. / Q1(I,K)
1560 U(I,K) = Q2(I,K) * RBOI
1561 V(I,K) = Q3(I,K) * RBOI
1562 ANOR = 1. / SQRT( XIX(I,K)**2 + XIZ(I,K)**2 )
1563 XIXH = XIX(I,K) * ANOR
1564 XIZH = XIZ(I,K) * ANOR
1565 VELN = SIGN * ( XIXH * U(I,K) + XIZH * V(I,K) )
1566 C
1567 IF(VELN.GE.0.) THEN
1568 Q1(I,K) = Q1(I+IP1,K)
1569 Q2(I,K) = Q2(I+IP1,K)
1570 Q3(I,K) = Q3(I+IP1,K)
1571 Q4(I,K) = Q4(I+IP1,K)
1572 ENDIF
1573 84 CONTINUE
1574 IF(I.EQ.IMAX) GO TO 89
1575 I = IMAX
1576 IP1 = -1.
1577 SIGN = 1.
1578 GO TO 75
1579 89 CONTINUE
1580 C
1581 C      DOWNSTREAM B.C. FOR VISCOUS FLOW
1582 C
1583 ELSEIF(REYREF.GT.0.) THEN
1584 C
1585 C      OUTFLOW B.C. FOR VISCOUS FLOW
1586 C      RBO, U AND V ARE SET TO THE VALUES OF THE NEXT INTERIOR POINTS
1587 C      PRESSURE IS EXTRAPOLATED AND THEN COMPUTE ENERGY (Q4)
1588 C
1589 DO 100 K = 1 , KMAX
1590 I = 1
1591 Q1(I,K) = Q1(I+1,K)
1592 Q2(I,K) = Q2(I+1,K)
1593 Q3(I,K) = Q3(I+1,K)
1594 PEXT = GAMM * ( Q4(I+1,K) - 0.5 * ( Q2(I+1,K)**2 + Q3(I+1,K)**2 )
1595 1 / Q1(I+1,K) )
1596 Q4(I,K) = PEXT / GAMM + 0.5 * ( Q2(I,K)**2 + Q3(I,K)**2 ) / Q1(I,K)
1597 I = IMAX
1598 Q1(I,K) = Q1(I-1,K)
1599 Q2(I,K) = Q2(I-1,K)
1600 Q3(I,K) = Q3(I-1,K)
1601 PEXT = GAMM * ( Q4(I-1,K) - 0.5 * ( Q2(I-1,K)**2 + Q3(I-1,K)**2 )
1602 1 / Q1(I-1,K) )
1603 Q4(I,K) = PEXT / GAMM + 0.5 * ( Q2(I,K)**2 + Q3(I,K)**2 ) / Q1(I,K)
1604 100 CONTINUE
1605 C
1606 C      ENDIF
1607 C
1608 C      AVERAGE FLOW VARIABLES ACROSS WAKE CUT (FOR C-GRID)
1609 C
1610 999 CONTINUE
1611 DO 120 J = 1 , ITEL - 1
1612 IU = IMAX + 1 - I
1613 Q1AVG = 0.5 * ( Q1(I,2) + Q1(IU,2) )
1614 Q2AVG = 0.5 * ( Q2(I,2) + Q2(IU,2) )
1615 Q3AVG = 0.5 * ( Q3(I,2) + Q3(IU,2) )
1616 Q1(I,1) = Q1AVG
1617 Q1(IU,1) = Q1AVG
1618 Q2(I,1) = Q2AVG
1619 Q2(IU,1) = Q2AVG
1620 Q3(I,1) = Q3AVG
1621 Q3(IU,1) = Q3AVG
1622 PSLOW = GAMM * ( Q4(I,2) - 0.5 * ( Q2(I,2)**2 + Q3(I,2)**2 ) /
1623 1 Q1(I,2) )
1624 PSUPP = GAMM * ( Q4(IU,2) - 0.5 * ( Q2(IU,2)**2 + Q3(IU,2)**2 ) /
1625 1 Q1(IU,2) )
1626 PSAVG = 0.5 * ( PSLOW + PSUPP )
1627 Q4AVG = PSAVG / GAMM + 0.5 * ( Q2(I,1)**2 + Q3(I,1)**2 ) /
1628 1 Q1(I,1)
1629 Q4(I,1) = Q4AVG
1630 Q4(IU,1) = Q4AVG
1631 120 CONTINUE
1632 RETURN
1633 END

```

```

LINE #          SOURCE TEXT
1634 SUBROUTINE STRESS(ITN)
1635 C.....
1636 C*
1637 C*          SUBROUTINE STRESS
1638 C*
1639 C*.....
1640 PARAMETER (IX=10,KX=60)
1641 COMMON/FLW/Q1(IX,KX),Q2(IX,KX),Q3(IX,KX),Q4(IX,KX)
1642 COMMON/DGRID/DT,IMAX,KMAX,ITEL,ITEU
1643 COMMON/GRD1/X(IX,KX),Z(IX,KX)
1644 COMMON/PAR/GAMMA,REYREF,ALFA,ALFA1,REDFRE,AMINF,ALFAI
1645 COMMON/SPEED/ U(IX,KX),V(IX,KX),AA(IX,KX)
1646 COMMON/PERTR/DQ1(IX,KX),DQ2(IX,KX),DQ3(IX,KX),DQ4(IX,KX)
1647 COMMON/MUTUR/CMU(IX,KX)
1648 DIMENSION RB1(IX),RB2(IX),RB3(IX),RB4(IX)
1649 COMMON/LOGIC/RSTRT,PITCH,RAMP
1650 LOGICAL RSTRT,PITCH,RAMP
1651 C THIS SUBROUTINE ADDS VISCOUS TERMS TO THE RIGHT HAND SIDE
1652 C
1653 C CMUL = LAMINAR OR MOLECULAR VISCOSITY
1654 C
1655 CMUL = AMI. / REYREF
1656 C CALL EDDY(CMUL)
1657 KMAXM1 = KMAX - 1
1658 IMAXM1 = IMAX - 1
1659 PR = 1.
1660 C
1661 C COMPUTE TXX,TTY AND VISCOUS DISSIPATION AT I - 1 / 2
1662 C
1663 DO 30 K = 2, KMAXM1
1664 DO 20 I = 2, IMAXM1
1665 UX1 = U(I,K) - U(I-1,K)
1666 VX1 = V(I,K) - V(I-1,K)
1667 AX1 = AA(I,K) - AA(I-1,K)
1668 UZET = .25 * (U(I,K+1) - U(I,K) + U(I-1,K+1) - U(I-1,K-1))
1669 VZET = .25 * (V(I,K+1) - V(I,K) + V(I-1,K+1) - V(I-1,K-1))
1670 AZET = .25 * (AA(I,K+1) - AA(I,K) + AA(I-1,K+1) - AA(I-1,K-1))
1671 XX1 = X(I,K) - X(I-1,K)
1672 ZX1 = Z(I,K) - Z(I-1,K)
1673 XZET = .25 * (X(I,K+1) - X(I,K) + X(I-1,K+1) - X(I-1,K-1))
1674 ZZET = .25 * (Z(I,K+1) - Z(I,K) + Z(I-1,K+1) - Z(I-1,K-1))
1675 YAC = XX1 * ZZET - ZX1 * XZET
1676 YAC = 1. / YAC
1677 XIX = ZZET * YAC
1678 ZETAX = - XX1 * YAC
1679 XII = -XZET * YAC
1680 ZETAZ = XI1 * YAC
1681 CNM = (.5 * (CMU(I,K) + CMU(I-1,K)) + CMUL) * DT
1682 UX = UX1 * XIX - UZET * ZETAX
1683 VX = VX1 * XIX - VZET * ZETAX
1684 AX = AX1 * XIX + AZET * ZETAX
1685 UZ = UX1 * XII + UZET * ZETAZ
1686 VZ = VX1 * XII - ET * ZETAZ
1687 AZ = AX1 * XII - AZET * ZETAZ
1688 TXX = (-4. * UX + 2. * VZ) * CNM / 3.
1689 TXY = CNM * (UZ + VX)
1690 TTY = -CNM / 3. * (-4. * VZ + 2. * UX)
1691 C R4 = ((U(I,K)+U(I-1,K))*TXX+(V(I,K)+V(I-1,K))*TXY)*0.5
1692 C 1 + CNM / PR / (GAMMA - 1.) * AX
1693 C S4 = ((V(I,K)+U(I-1,K))*TXY+(V(I,K)+V(I-1,K))*TTY)*0.5
1694 C 1 + CNM / PR / (GAMMA - 1.) * AZ
1695 C
1696 C DEBUG
1697 C TURN OFF ENRGY DISSIPATION AND DIFFUSION
1698 R4 = 0.
1699 S4 = 0.
1700 RB1(I) = 0.
1701 RB2(I) = (XIX * TXX + XII * TXY) / YAC
1702 RB3(I) = (XIX * TXY + XII * TTY) / YAC
1703 20 RB4(I) = (XIX * R4 + XII * S4) / YAC
1704 DO 30 I = 2, IMAXM1
1705 DQ1(I,K) = DQ1(I,K) + RB1(I-1) - RB1(I)
1706 DQ2(I,K) = DQ2(I,K) + RB2(I-1) - RB2(I)
1707 DQ3(I,K) = DQ3(I,K) + RB3(I-1) - RB3(I)
1708 DQ4(I,K) = DQ4(I,K) + RB4(I-1) - RB4(I)
1709 30 CONTINUE
1710 C
1711 C IN THE Z DIRECTION
1712 DO 70 I = 2, IMAXM1
1713 DO 60 K = 2, KMAX
1714 UX1 = .25 * (U(I+1,K) - U(I-1,K) + U(I+1,K-1) - U(I-1,K-1))
1715 VX1 = .25 * (V(I+1,K) - V(I-1,K) + V(I+1,K-1) - V(I-1,K-1))
1716 AX1 = .25 * (AA(I+1,K) - AA(I-1,K) + AA(I+1,K-1) - AA(I-1,K-1))
1717 XX1 = .25 * (X(I+1,K) - X(I-1,K) + X(I+1,K-1) - X(I-1,K-1))
1718 ZX1 = .25 * (Z(I+1,K) - Z(I-1,K) + Z(I+1,K-1) - Z(I-1,K-1))
1719 UZET = U(I,K) - U(I,K-1)
1720 VZET = V(I,K) - V(I,K-1)
1721 AZET = AA(I,K) - AA(I,K-1)
1722 XZET = X(I,K) - X(I,K-1)
1723 ZZET = Z(I,K) - Z(I,K-1)
1724 YAC = XX1 * ZZET - ZX1 * XZET
1725 YAC = 1. / YAC
1726 XIX = ZZET * YAC
1727 ZETAX = - ZX1 * YAC
1728 XII = -XZET * YAC
1729 ZETAZ = XI1 * YAC
1730 CNM = (.5 * (CMU(I,K) + CMU(I,K-1)) + CMUL) * DT
1731 UX = UX1 * XIX + UZET * ZETAX
1732 VX = VX1 * XIX + VZET * ZETAX
1733 AX = AX1 * XIX + AZET * ZETAX
1734 UZ = UX1 * XII + UZET * ZETAZ
1735 VZ = VX1 * XII + VZET * ZETAZ
1736 AZ = AX1 * XII + AZET * ZETAZ
1737 TXX = (-4. * UX + 2. * VZ) * CNM / 3.
1738 TXY = CNM * (UZ + VX)
1739 TTY = -CNM / 3. * (-4. * VZ + 2. * UX)
1740 C R4 = ((U(I,K)+U(I,K-1))*TXX+(V(I,K)+V(I,K-1))*TXY)*0.5
1741 C 1 + CNM / PR / (GAMMA - 1.) * AX
1742 C S4 = ((V(I,K)+U(I,K-1))*TXY+(V(I,K)+V(I,K-1))*TTY)*0.5
1743 C 1 + CNM / PR / (GAMMA - 1.) * AZ
1744 R4 = 0.
1745 S4 = 0.
1746 RB1(K) = 0.
1747 RB2(K) = (ZETAX * TXX + ZETAZ * TXY) / YAC
1748 RB3(K) = (ZETAX * TXY + ZETAZ * TTY) / YAC
1749 60 RB4(K) = (ZETAX * R4 + ZETAZ * S4) / YAC
1750 DO 70 K = 2, KMAXM1
1751 DQ1(I,K) = DQ1(I,K) + RB1(K+1) - RB1(K)
1752 DQ2(I,K) = DQ2(I,K) + RB2(K+1) - RB2(K)
1753 DQ3(I,K) = DQ3(I,K) + RB3(K+1) - RB3(K)
1754 DQ4(I,K) = DQ4(I,K) + RB4(K+1) - RB4(K)
1755 70 CONTINUE

```


LINE #	SOURCE TEXT
1757	SUBROUTINE LOAD(CL,CDP,CD,CM,ALFAS,XREF)
1758	C.....
1759	C*
1760	C* SUBROUTINE LOAD
1761	C*
1762	C.....
1763	PARAMETER (IX=180,KX=60)
1764	COMMON/GRID1/X(IX,KX),Y(IX,KX)
1765	COMMON/SKINCF/CF(IK)
1766	COMMON/DGRID/DT,IMAX,KMAX,ITEL,ITEU
1767	COMMON/SURF/PSUR(IK)
1768	C
1769	THIS SUBROUTINE COMPUTES THE INVISCID CONTRIBUTIONS
1770	TO LOADS ON THE AIRFOIL SURFACE
1771	C
1772	CL = 0.
1773	CD = 0.
1774	CDP = 0.
1775	CM = 0.
1776	DO 300 I = ITEL, ITEU - 1
1777	DX = X(I+1,1) - X(I,1)
1778	300 CDP = CDP + (CF(I) + CF(I+1)) * 0.5 * DX
1779	DO 400 I = ITEL, ITEU - 1
1780	XL = .5 * (X(I,1)+X(I+1,1))
1781	YL = .5 * (Y(I,1)+Y(I+1,1))
1782	DX = X(I+1,1) - X(I,1)
1783	DY = Y(I+1,1) - Y(I,1)
1784	CPA = PSUR(I+1) * .5 + PSUR(I) * .5
1785	DCL = CPA * (-DX)
1786	DCD = CPA * DY
1787	CL = CL + DCL
1788	CD = CD + DCD
1789	400 CM = CM + DCD * YL - DCL * (XL - XREF)
1790	C
1791	DCL = CL * COS(ALFAS) - CD * SIN(ALFAS)
1792	CDP = CL * SIN(ALFAS) + CD * COS(ALFAS)
1793	CL = DCL
1794	RETURN
1795	END

LINE #	SOURCE TEXT
1796	SUBROUTINE WRAP(II,JJ,XSING,YSING,XP,YP,S0,A0,Y0)
1797	C.....
1798	C.....
1799	C.....
1800	C.....
1801	C.....
1802	PARAMETER (IX=180,KX=60)
1803	DIMENSION S0(IX,4),Y0(60,4),A0(IX,4),XP(1),YP(1)
1804	C
1805	C THIS SUBROUTINE UNWRAPS THE AIRFOIL AND STORES THE UNWRAPPED
1806	C SURFACE IN ARRAYS A0 AND S0. IT ALSO DETERMINES THE STRETCHING
1807	C IN THE ETA DIRECTION.
1808	C
1809	IMID = (II + 1) / 2
1810	DY = .8 / (JJ - 2)
1811	DO 1 J = 2, JJ
1812	Y = FLOAT(J-2) * DY
1813	1 Y0(J,1) = 1.25 * Y / (1. - Y * Y)
1814	Y0(1,1) = - Y0(3,1)
1815	PI = 4. * ATAN (1.)
1816	ANGL = PI * PI
1817	U = XP(1) - XSING
1818	V = YP(1) - YSING
1819	U = 1.
1820	V = 0.
1821	IIM1 = II - 1
1822	DO 2 I = 1, IIM1
1823	X11 = XP(I) - XSING
1824	Y11 = YP(I) - YSING
1825	ANGL = ANGL + ATAN2((U*Y11-V*X11),(U*X11+V*Y11))
1826	R = SQRT(X11**2 + Y11**2)
1827	U = X11
1828	V = Y11
1829	R = SQRT(R)
1830	A0(I,1) = R * COS(.5 * ANGL)
1831	2 S0(I,1) = R * SIN(.5 * ANGL)
1832	C WRITE (6,1000)
1833	C WRITE (6,2000) (I,A0(I,1),S0(I,1),I = 1, IIM1)
1834	RETURN
1835	1000 FORMAT(1X,'UNWRAPPED COORDINATES IN THE TRANSFORMED PLANE')
1836	2000 FORMAT(15, 2F20.8)
1837	END

```

1838 SUBROUTINE TABINT(XP,YP,XSING,YSING,N)
1839 C-----
1840 C*
1841 C* SUBROUTINE TABINT
1842 C*
1843 C-----
1844 C
1845 PARAMETER (IX=180,KX=60)
1846 DIMENSION XP(IX),YP(IX),SO(IX),AO(IX)
1847 U = XP(1) - XSING
1848 V = YP(1) - YSING
1849 U = 1.
1850 V = 0.
1851 ANGL = 8. * ATAN(1.)
1852 DO 1 I = 1,N
1853 X11 = XP(I) - XSING
1854 Y11 = YP(I) - YSING
1855 ANGL = ANGL + ATAN2((U*Y11-V*X11),(U*X11+V*Y11))
1856 R = SQRT(X11**2 + Y11 ** 2)
1857 U = X11
1858 V = Y11
1859 R = SQRT(R)
1860 AO(I) = R * COS(ANGL * .5)
1861 SO(I) = R * SIN(ANGL * .5)
1862 DX = (AO(N)-AO(1))/96.
1863 AOST = AO(1)
1864 DO 3 I = 1 , 97
1865 XX = FLOAT(I-1) * DX + AOST
1866 CALL TAINI(AO,SO,XX,YY,N,3,NER,MON)
1867 XP(I) = XX * XX - YY * YY + XSING
1868 YP(I) = 2. * XX * YY + YSING
1869 RETURN
1870 END

```

LINE #	SOURCE TEXT
1870	SUBROUTINE TAIN(TAB,FTAB,X,FX,N,K,NER,MON)
1871	C.....
1872	C*
1873	C* SUBROUTINE TAIN
1874	C*
1875	C.....
1876	PARAMETER (IX=180,KX=50)
1877	DIMENSION TAB(1),FTAB(1),T(10),C(10)
1878	C
1879	C NASA - ANES SUBROUTINE FOR POLYNOMIAL INTERPOLATION
1880	C OF A TABULATED FUNCTION
1881	C
1882	IF(N-K) 1, 1, 2
1883	1 NER = 2
1884	RETURN
1885	2 IF(K-9) 3,3,1
1886	3 IF(MON) 4,4,5
1887	5 IF(MON-2) 6,7,4
1888	4 J = 0
1889	NM1 = N - 1
1890	DO 8 I = 1, NM1
1891	IF(TAB(I) - TAB(I+1)) 9,11,10
1892	11 NER = 3
1893	RETURN
1894	9 J = J-1
1895	GO TO 8
1896	10 J = J+1
1897	8 CONTINUE
1898	MON = 1
1899	IF(J) 12, 6, 6
1900	12 MON = 2
1901	7 DO 13 I = 1, N
1902	IF(X - TAB(I)) 14,14,13
1903	14 J = I
1904	GO TO 18
1905	13 CONTINUE
1906	GO TO 15
1907	6 DO 16 I = 1, N
1908	IF(X-TAB(I)) 16,17,17
1909	17 J = I
1910	GO TO 18
1911	16 CONTINUE
1912	15 J = N
1913	18 J = J - (K+1) / 2
1914	IF(J) 19,19,20
1915	19 J = 1
1916	20 M = J + K
1917	IF(M - N) 21,21,22
1918	22 J = J - 1
1919	GO TO 20
1920	21 KP1 = K + 1
1921	JSAVE = J
1922	26 DO 23 L = 1, KP1
1923	C(L) = X - TAB(J)
1924	T(L) = FTAB(J)
1925	23 J = J+1
1926	DO 24 J = 1,K
1927	I = J+1
1928	25 T(I) = (C(J)*T(I)-C(I)*T(J))/(C(J)-C(I))
1929	I = I+1
1930	IF(I-KP1) 25,25,24
1931	24 CONTINUE
1932	FX = T(KP1)
1933	NER = 1
1934	RETURN
1935	END

LINE #	SOURCE TEXT
936	SUBROUTINE SING(N2,N,X,Z,XLE,YLE,TEA,TES,XSING,YSING,CHD)
937	C*****
938	C
939	C SUBROUTINE SING
940	C
941	C*****
942	PARAMETER (IX=180,kx=60)
943	C
944	C
945	C THIS SUBROUTINE COMPUTES SINGULAR POINT LOCATIONS.
946	C
947	DIMENSION X(2) , Z(2)
948	NU = N2
949	N1 = N2 + 1
950	N3 = N2 - 1
951	X1 = X(N1)
952	Z1 = Z(N1)
953	X2 = X(N2)
954	Z2 = Z(N2)
955	X3 = X(N3)
956	Z3 = Z(N3)
957	D1 = X2 ** 2 - X1 ** 2
958	D2 = Z2 ** 2 - Z1 ** 2
959	D3 = X2 - X1
960	D4 = Z2 - Z1
961	D5 = X3 ** 2 - X1 ** 2
962	D6 = Z3 ** 2 - Z1 ** 2
963	D7 = X3 - X1
964	D8 = Z3 - Z1
965	B = (D7 * (D1 + D2) - D3*(D5+D6))/(2.*(D7*D4-D3*D8))
966	IF(ABS(D3).LT.ABS(D7)) GO TO 10
967	A = (D1 + D2 - 2. * B * D4) / (2. * D3)
968	GO TO 20
969	10 A = (D5 + D6 - 2. * B * D8) / (2. * D7)
970	20 CONTINUE
971	R = SQRT((X2-A)** 2 + (Z2-B)**2)
972	XLE = X(N1)
973	YLE = Z(N1)
974	CHD = X(1) - X(NU)
975	A2 = (Z(2)-Z(1))/(X(2) - X(1))
976	A1 = (Z(N)-Z(N-1))/(X(N)-X(N-1))
977	TES = .5 * (A1 + A2)
978	TEA = A2 - A1
979	TEA = TEA + 57.29578
980	XSING = (X-XLE) / 2.
981	YSING = (B-YLE) / 2.
982	RETURN
983	END

LINE # SOURCE TEXT

```
1984 SUBROUTINE AIRPOL(IT,IE,ILE)
1985 C*****
1986 C* SUBROUTINE AIRPOL
1987 C*****
1988 PARAMETER (IX=180,KX=60)
1989 COMMON/GRID1/X(IX,KX),Z(IX,KX)
1990 COMMON/DGRID/DT,IMAX,KMAX,ITEL,ITEU
1991 COMMON/YSYM/ISYM
1992 DIMENSION SO(IX,4),AO(IX,4),Y0(60,4),XP(IX),YP(IX),
1993 1E(IX),F(IX),BO(49)
1994 DIMENSION XL(IX),XU(IX),YL(IX),YU(IX),
1995 2 XX(IX),YY(IX)
1996 C
1997 DATA (BO(I),I=1,32)/1.,1.0414,1.0836,1.1270,1.1715,1.2175,1.2651,
1998 11.3145,1.3659,1.4199,1.4755,1.5349,1.5973,1.6636,1.7342,1.8099,
1999 21.8914,1.9799,2.0764,2.1829,2.3012,2.4341,2.5653,2.7597,2.9646,
2000 33.2106,3.5141,3.9019,4.4219,5.1687,6.3632,8.6809/
2001 C
2002 READ(5,*) IBMAX,ISYM
2003 IF( ISYM .EQ. 0 ) THEN
2004 DO 101 I=1,IBMAX
2005 READ(5,*) XU(I),YU(I),YL(I)
2006 101 CONTINUE
2007 ELSE
2008 DO 102 I=1,IBMAX
2009 102 READ(5,*) XU(I),YU(I)
2010 DO 103 I=1,IBMAX
2011 103 YL(I)=-YU(I)
2012 ENDIF
2013 C
2014 DO 1000 I=1,IBMAX
2015 IU=I+IBMAX
2016 XX(IU)=XU(I)
2017 YY(IU)=YU(I)
2018 II=IBMAX-I+1
2019 XX(II)=XU(II)
2020 YY(II)=YL(II)
2021 1000 CONTINUE
2022 C
2023 IBMAX2=2*IBMAX
2024 DO 1010 I=1,IBMAX2
2025 XP(I)=XX(I)
2026 YP(I)=YI(I)
2027 1010 CONTINUE
2028 FNU=IBMAX
2029 FNL=IBMAX
2030 C
2031 THIS SUBROUTINE GENERATES SHEAR PARABOLIC C-GRID
2032 THE FOLLOWING SUBROUTINES ARE RELATED TO THE GRID GENERATION
2033 WRAP SING
2034 TABINT CLUSTR
2035 TAINI STRTC
2036 C
2037 DO 8 I=1,32
2038 8 AO(I,1)=BO(I)
2039 II=IMAX
2040 JJ=KMAX-1
2041 IT=31
2042 IE=127
2043 IIP1=II+1
2044 IIM1=II-1
2045 IIJJ=II*JJ
2046 IIJJ2=II*(JJ-2)
2047 ILE=(IT+IE)/2
2048 PI=4.*ATAN(1.)
2049 NU=FNU
2050 NL=FNL
2051 N=NU+NL
2052 SCALE=1./((XP(1)-XP(NL)))
2053 DO 3333 I=1,N
2054 XP(I)=XP(I)*SCALE
2055 YP(I)=YP(I)*SCALE
2056 3333 CONTINUE
2057 CALL SING(NU,N,XP,YP,XLE,ZLE,TEA,TES,XSING,YSING,CBD)
2058 CALL TABINT(XP,YP,XSING,YSING,N)
2059 NBODY=IE+1-IT
2060 DO 6791 I=1,NBODY
2061 L=I-1
2062 E(IT+L)=XP(I)
2063 6791 F(IT+L)=YP(I)
2064 IEP1=IE+1
2065 SLOPT=TES*.75
2066 DO 438 I=IEP1,II
2067 II=I+1-IE
2068 E(I)=AO(II,1)
2069 DII=1./48.
2070 D=4./3.*(E(I)-.25)
2071 F(I)=F(IE)+SLOPT*ALOG(D)/D
2072 L=IIP1-I
2073 E(L)=E(I)
2074 438 F(L)=F(IT)+SLOPT*ALOG(D)/D
2075 C
2076 C439 WRITE(6,439)
2077 C439 FORMAT(2X,3H 1,19X,1EX,19X,1HY)
2078 WRITE(6,37)(I,E(I),F(I),I=1,II)
2079 CALL WRAP(II,JJ,XSING,YSING,E,F,SO,AO,YO)
2080 DO 10 J=2,JJ
2081 DO 10 I=1,II
2082 X(I,J-1)=AO(I,1)**2-(SO(I,1)+YO(J,1))**2
2083 10 Z(I,J-1)=2.*AO(I,1)*(SO(I,1)+YO(J,1))
2084 RETURN
2085 37 FORMAT(15,2F20.8)
2086 END
```

LINE #	SOURCE TEXT
--------	-------------

2086	SUBROUTINE CLUSTR(DS)
2087	C.....
2088	C*
2089	C* SUBROUTINE CLUSTR
2090	C*
2091	C.....
2092	PARAMETER (IX=180,KX=60)
2093	COMMON/GRID1/X(IX,KX),Z(IX,KX)
2094	COMMON/DGRID/DT,IMAX,KMAX,ITEL,ITEU
2095	DIMENSION S(60),XP(60),YP(60),R(60)
2096	C
2097	C THIS SUBROUTINE CLUSTERS A GIVEN X,Z GRID SUCH THAT THE FIRST POINT IS AT
2098	C
2099	DO 100 I = 1 , IMAX
2100	S(I) = 0.
2101	XP(I) = X(I,1)
2102	YP(I) = Z(I,1)
2103	DO 10 K = 2 , KMAX
2104	XP(K) = X(I,K)
2105	YP(K) = Z(I,K)
2106	10 S(K) = SORT((XP(K)-XP(K-1))**2+(YP(K)-YP(K-1))**2)
2107	1+S(K-1)
2108	SUMDX = S(KMAX)
2109	CALL STRICH(SUMDX,DS,F1,KMAX,FACTOR)
2110	C WRITE (6,200) I,FACTOR
2111	R(I) = 0.
2112	DR = DS
2113	DO 20 K = 2 , KMAX
2114	R(K) = R(K-1) + DR
2115	DR = DR * FACTOR
2116	20 CONTINUE
2117	RLAST = 1. / R(KMAX)
2118	DO 30 K = 2 , KMAX
2119	R1 = R(K) * RLAST * S(KMAX)
2120	CALL TAINI(S,XP,R1,XP1,KMAX,3,NER,MON)
2121	X(I,K) = XP1
2122	CALL TAINI(S,YP,R1,YP1,KMAX,3,NER,MON)
2123	Z(I,K) = YP1
2124	30 CONTINUE
2125	100 CONTINUE
2126	C WRITE (6,115)
2127	DO 110 I = 1 , IMAX
2128	DX = X(I,2) - X(I,1)
2129	DY = Z(I,2) - Z(I,1)
2130	DN = SORT(DX*DX+DY*DY)
2131	C WRITE(6,120) I , DX , DY , DN
2132	110 CONTINUE
2133	RETURN
2134	115 FORMAT(5X,6HNORMAL,1X,8HDISTANCE,3H AT,4H THE,5H WALL,/ 1,5H 1,8X,2HDX,8X,2HDY,8X,2HDN,///)
2135	120 FORMAT(15,3F10.5)
2136	200 FORMAT(15,F10.5)
2137	END
2138	

LINE #	SOURCE TEXT
2139	SUBROUTINE STATCH(SUMDX,DX1,F1,N1,R)
2140	C.....
2141	C.....
2142	C.....
2143	C.....
2144	C.....
2145	PARAMETER (IX=180,kx=60)
2146	C
2147	C THIS SUBROUTINE DETERMINES A GEOMETRIC
2148	C PROGRESSION OF GRID SPACING BETWEEN 1 AND N1 SUCH THAT
2149	C SUMDX) EQUALS SUMDX. THE RATIO BETWEEN SUCCESSIVE
2150	C SPACINGS IS R.
2151	N = N1 - 1
2152	R = 1.5
2153	E1 = 1.E-04
2154	E2 = 1.E-04
2155	DO 10 L = 1, 50
2156	F = (R-1) * SUMDX - DX1*(R**N-1)
2157	FP = SUMDX - DX1 * FLOAT(N) * R ** (N-1)
2158	RITER = F - F / FP
2159	C IF(1.E-02.LT.RITER.AND.RITER.LT.1.) RITER = 1.
2160	C IF(1..LT.RITER.AND.RITER.LT.100.) RITER=.01
2161	IF(ABS(R-RITER).LT.R*E1) GO TO 1
2162	R = RITER
2163	10 CONTINUE
2164	R = 1.0001
2165	C DX1 = DETOT/FLOAT(N1-1)
2166	RETURN
2167	1 R= RITER
2168	RETURN
2169	END

```
LINE # SOURCE TEXT
2170 SUBROUTINE EDDY(CMU)
2171 C*****
2172 C*
2173 C* SUBROUTINE EDDY
2174 C*
2175 C*****
2176 PARAMETER (IX=180,KX=60)
2177 COMMON/FLON/Q1(IX,KX),Q2(IX,KX),Q3(IX,KX),Q4(IX,KX)
2178 COMMON/MUTUR/CMU(IX,KX)
2179 COMMON/SKINCF/CF(IX)
2180 COMMON/DGRID/DT,IMAX,KMAX,ITEU,ITEU
2181 COMMON/PAR/GAMMA,REYREF,ALFA,ALFAI,REDPRE,AMINF,ALFAI
2182 COMMON/GRID1/I(IX,KX),Z(IX,KX)
2183 COMMON/SPEED/ U(IX,KX),V(IX,KX),AA(IX,KX)
2184 DIMENSION TIN(KX),TOUT(KX),Y(KX),TRANS(IX),S(IX),UU(KX),VE(IX)
2185 C
2186 CMUPP = 1000. * CMU
2187 KEDGE = KMAX
2188 ILE = ( ITEU + ITEU ) / 2
2189 CHORD = X(ITEU,1) - X(ILE,1)
2190 DO 100 I = 2, IMAX - 1
2191 C IF( ABS(X(I,1)).LT.( ABS(X(ILE,1)) + 0.05 * CHORD ) ) GO TO 100
2192 UDIF = 0.
2193 UMAX = 0.
2194 UMIN = 9999.
2195 FMAX = 0.1E-06
2196 YMAX = .1E-06
2197 FYMAX = 0.1E-06
2198 Y(1) = 0.
2199 C COMPUTE TAU AT THE WALL
2200 UET = U(I,2) - U(I,1)
2201 VET = V(I,2) - V(I,1)
2202 XXI = X(I-1,1) - X(I-1,1)
2203 ZXI = Z(I-1,1) - Z(I-1,1)
2204 XET = 4. * X(I,2) - 3. * X(I,1) - X(I,3)
2205 ZET = 4. * Z(I,2) - 3. * Z(I,1) - Z(I,3)
2206 XXI = .5 * XXI
2207 ZXI = .5 * ZXI
2208 XET = .5 * XET
2209 ZET = .5 * ZET
2210 YAC = 1. / (XXI * ZET - ZXI * XET)
2211 OMEGA = (UET * XXI + VET * ZXI) * YAC
2212 TWALL = AMINF * OMEGA / REYREF
2213 CF(I) = 2. * TWALL / (AMINF**2)
2214 FACT = SQRT(Q1(I,1) * ABS(TWALL)) * REYREF / (26. * AMINF)
2215 DO 10 K = 2, KEDGE-1
2216 UXI = U(I-1,K) - U(I-1,K)
2217 VXI = V(I-1,K) - V(I-1,K)
2218 UET = U(I,K-1) - U(I,K-1)
2219 VET = V(I,K-1) - V(I,K-1)
2220 XXI = X(I-1,K) - X(I-1,K)
2221 ZXI = Z(I-1,K) - Z(I-1,K)
2222 XET = X(I,K-1) - X(I,K-1)
2223 ZET = Z(I,K-1) - Z(I,K-1)
2224 YAC = 1. / (XXI * ZET - ZXI * XET)
2225 OMEGA = ABS(UET*XXI-VET*ZXI-UXI*XET-VXI*ZET) * YAC
2226 UTOT = SQRT(U(I,K)**2 + V(I,K)**2)
2227 UMAX = AMAX1(UTOT,UMAX)
2228 UMIN = AMIN1(UTOT,UMIN)
2229 Y(K) = SQRT((X(I,K)-X(I,K-1))**2+(Z(I,K)-Z(I,K-1))**2)*Y(K-1)
2230 F = Y(K) * OMEGA
2231 IF((Y(K)*FACT).GT.20.) GO TO 31
2232 IF(1.GT.ITEU.AND.1.LT.ITEU) F = F * (1. - EXP(-Y(K)*FACT))
2233 31 CONTINUE
2234 C
2235 IF(F.GT.FYMAX) THEN
2236 FMAX = F
2237 YMAX = Y(K)
2238 ENDIF
2239 FCT = Y(K) * FACT
2240 IF(FCT.GT.20.) FCT = 20.
2241 FCT = ABS(FCT)
2242 EL = .4 * Y(K) * (1. - EXP(-FCT))
2243 TIN(K) = Q1(I,K) * EL * EL * OMEGA
2244 TIN(K) = ABS(TIN(K))
2245 10 CONTINUE
2246 UDIF = ABS(UMAX-UMIN)
2247 KSWTCH = 0
2248 FFAKE = YMAX * FMAX
2249 F1 = 0.25 * YMAX * UDIF **2 / FMAX
2250 IF(F1.LT.FFAKE) FFAKE = F1
2251 DO 20 K = 2, KEDGE - 1
2252 FKLEB = 0
2253 IF(ABS(Y(K)/YMAX).LT.1.E+04) THEN
2254 FKLEB = 1. / (1. + 5.5 * (0.3 * Y(K)/YMAX) ** 6)
2255 END IF
2256 TOUT(K) = .0168 * 1.6 * Q1(I,K) * FFAKE * FKLEB
2257 TOUT(K) = ABS(TOUT(K))
2258 IF(KSWTCH.NE.0) GO TO 20
2259 IF(TIN(K).GT.TOUT(K)) KSWTCH = K - 1
2260 20 CONTINUE
2261 DO 30 K = 2, KEDGE - 1
2262 IF(K.LE.KSWTCH) THEN
2263 CMU(I,K) = ABS(TIN(K))
2264 ELSE
2265 CMU(I,K) = ABS(TOUT(K))
2266 END IF
2267 30 CONTINUE
2268 C
2269 C PROZE THE VALUE OF EDDY VISCOSITY TO AN UPPER LIMIT
2270 C
2271 C
2272 R = 1
2273 C 734 R = R + 1
2274 C IF(R.GT.KEDGE) GO TO 736
2275 C 735 IF(CMU(I,K).LE.CMUPP) GO TO 734
2276 C CMU(I,K) = CMUPP
2277 C R = R + 1
2278 C IF(R.LE.KEDGE) GO TO 735
2279 C 736 CONTINUE
2280 100 CONTINUE
2281 RETURN
2282 END
```



```

LINE #          SOURCE TEXT
2282          SUBROUTINE RESI
2283          C*****
2284          C C C C C
2285          C          SUBROUTINE RESI
2286          C C C C C
2287          C*****
2288          PARAMETER (IX=180,KX=60)
2289          COMMON/FIX/OMEGA,HDOT
2290          COMMON/PERTR/DQ1(IX,KX),DQ2(IX,KX),DQ3(IX,KX),DQ4(IX,KX)
2291          COMMON/GRID1/X(IX,KX),Z(IX,KX)
2292          COMMON/DGRID/DT,IMAX,KMAX,ITEL,ITEU
2293          COMMON/FLOW/Q1(IX,KX),Q2(IX,KX),Q3(IX,KX),Q4(IX,KX)
2294          COMMON/SPEED/ U(IX,KX),V(IX,KX),AA(IX,KX)
2295          COMMON/PAR/GAMMA,REYREF,ALFA,ALFAI,REDFRE,AMINF,ALFAI
2296          COMMON/COMRRS/ RRS(IX,4)
2297          XTAU(I,K) = OMEGA * Z(I,K)
2298          YTAU(I,K) = - OMEGA * X(I,K) - HDOT
2299          C THIS SUBROUTINE COMPUTES THE RESIDUAL ON THE RIGHT HAND
2300          C SIDE ARISING FROM THE EULER- PART OF THE GOVERNING EQUATIONS
2301          C C C C C
2302          C FLUX TERMS WITHIN THE XI- DERIVATIVE
2303          DO 100 K = 2 , KMAX - 1
2304          DO 10 I = 1 , IMAX
2305          UCON = U(I,K) * (Z(I,K+1)-Z(I,K-1))
2306          VCON = V(I,K) * (X(I,K+1)-X(I,K-1))
2307          UCON = 0.25 * DT * UCON
2308          XIT = - XTAU(I,K) * (Z(I,K+1)-Z(I,K-1))
2309          YIT = YTAU(I,K) * (X(I,K+1) - X(I,K-1))
2310          XIT = XIT * DT * 0.25
2311          UCON = UCON + XIT
2312          RRS(I,1) = UCON * Q1(I,K)
2313          P = (GAMMA-1.) * (Q4(I,K) - .5*Q1(I,K)*(U(I,K)**2 + V(I,K)**2) )
2314          RRS(I,2) = Q2(I,K) * UCON + P * DT * 0.25 * (Z(I,K+1) - Z(I,K-1))
2315          RRS(I,3) = Q3(I,K) * UCON - P * DT * 0.25 * (X(I,K+1)-X(I,K-1))
2316          RRS(I,4) = UCON * (Q4(I,K)+P) - XIT * P
2317          10 CONTINUE
2318          DO 11 I = 2 , IMAX - 1
2319          DQ1(I,K) = DQ1(I,K) - RRS(I+1,1) + RRS(I-1,1)
2320          DQ2(I,K) = DQ2(I,K) - RRS(I+1,2) + RRS(I-1,2)
2321          DQ3(I,K) = DQ3(I,K) - RRS(I+1,3) + RRS(I-1,3)
2322          11 DQ4(I,K) = DQ4(I,K) - RRS(I+1,4) + RRS(I-1,4)
2323          100 CONTINUE
2324          C C C C C
2325          C FLUX TERMS WITHIN THE ETA- DERIVATIVE
2326          C C C C C
2327          DO 200 I = 2 , IMAX - 1
2328          DO 20 K = 1 , KMAX
2329          VCON = U(I,K) * (Z(I-1,K)-Z(I+1,K))
2330          UCON = V(I,K) * (X(I+1,K)-X(I-1,K))
2331          VCON = VCON * 0.25 * DT
2332          ETAT = -XTAU(I,K) * (Z(I-1,K)-Z(I+1,K)) - YTAU(I,K)*
2333          (X(I+1,K)-X(I-1,K))
2334          ETAT = ETAT * 0.25 * DT
2335          VCON = VCON + ETAT
2336          RRS(K,1) = VCON * Q1(I,K)
2337          P = (GAMMA-1.) * (Q4(I,K) - 0.5 * Q1(I,K)*(U(I,K)**2 + V(I,K)**2) )
2338          RRS(K,2) = VCON * Q2(I,K) + P * DT * .25 * (Z(I-1,K)-Z(I+1,K))
2339          RRS(K,3) = VCON * Q3(I,K) + P * DT * .25 * (X(I+1,K) - X(I-1,K))
2340          RRS(K,4) = VCON * (Q4(I,K)+P) - ETAT * P
2341          20 CONTINUE
2342          DO 21 K = 2 , KMAX - 1
2343          DQ1(I,K) = DQ1(I,K) - RRS(K+1,1) + RRS(K-1,1)
2344          DQ2(I,K) = DQ2(I,K) - RRS(K+1,2) + RRS(K-1,2)
2345          DQ3(I,K) = DQ3(I,K) - RRS(K+1,3) + RRS(K-1,3)
2346          21 DQ4(I,K) = DQ4(I,K) - RRS(K+1,4) + RRS(K-1,4)
2347          200 CONTINUE
2348          C 300 FORMAT(216,4E14.6)
2349          RETURN
2350          END

```

Program

LINE #	SOURCE TEXT
2351	SUBROUTINE ROTGRID(IMAX,KMAX,DALFA)
2352	C.....
2353	C.....
2354	C.....
2355	C.....
2356	C.....
2357	PARAMETER (IX=180,KX=60)
2358	ROTATE GRID IN THE CLOCKWISE DIRECTION BY AN AMOUNT DALFA
2359	C.....
2360	COMMON/GRID1/X(IX,KI),Z(IX,KX)
2361	CA = COS(DALFA)
2362	SA = - SIN(DALFA)
2363	DO 20 K = 1 , KMAX
2364	DO 20 I = 1 , IMAX
2365	XI = X(I,K)
2366	ZI = Z(I,K)
2367	X(I,K) = XI * CA - ZI * SA
2368	Z(I,K) = ZI * CA + XI * SA
2369	20 RETURN
2370	END

LINE #	SOURCE TEXT
2370	SUBROUTINE CPPLLOT(I1,I2,FMACH,X,Y)
2371
2372	C.....
2373	C.....
2374	C.....
2375	C.....
2376	PARAMETER (IX=180,KX=60)
2377	C
2378	C
2379	C
2380	THIS SUBROUTINE PLOTS CP AT EQUAL INTERVALS IN THE MAPPED PLANE
2381	COMMON/SURF/PSUR(IX)
2382	DIMENSION KODE(4),LINE(90),X(IX),Y(IX)
2383	DATA KODE/1H,1H*,1H*,1H*,1H*/
2384	WRITE (6,2)
2385	2 FORMAT(50HOPLOT OF CP AT EQUAL INTERVALS IN THE MAPPED PLANE/
2386	1 10H0 X,10H X/C,10H CPL,10H CPL)
2387	CP0 = (1. + .2 * FMACH **2) ** 3.5 - 1.
2388	CP0 = CP0 / (.7 * FMACH **2)
2389	K0 = 30. * CP0 + 4.5
2390	IMIN = (I2-I1)/2 + I1
2391	ILOW = 2 * IMIN
2392	CHD=X(I1) - X(IMIN)
2393	DO 12 I = 1, 90
2394	12 LINE(I) = KODE(1)
2395	DO 34 I = IMIN, I2
2396	K = 30. * (CP0 - PSUR(I)) + 4.5
2397	K1 = 30. * (CP0 - PSUR(ILOW-I)) + 4.5
2398	IF(K.LT.1) K = 1
2399	IF(K.GT.90) K = 90
2400	IF(K1.GT.90) K1 = 90
2401	LINE(K0) = KODE(3)
2402	LINE(K) = KODE(2)
2403	LINE(K1) = KODE(4)
2404	XOC = (X(I) - X(IMIN)) / CHD
2405	WRITE (6,610) X(I),XOC,PSUR(ILOW-I),PSUR(I),LINE
2406	LINE(K1) = KODE(1)
2407	34 LINE(I) = KODE(1)
2408	RETURN
2409	600 FORMAT(4F10.4)
2410	610 FORMAT(4F10.4,90A1)
2411	END

LINE #	SOURCE TEXT
2412	SUBROUTINE OUTRVC(RREAL)
2413	C*****
2414	C*
2415	C* SUBROUTINE OUTRVC
2416	C*
2417	C*****
2418	PARAMETER (IX=180,KX=60)
2419	COMMON/PILOT/TITLE(10),NSTPT,RESD(3000),RES,CLB(3000),CDPH(3000)
2420	COMMON/DGRID/DT,IMAX,KMAX,ITEL,ITEU
2421	COMMON/FLOW/Q1(IX,KX),Q2(IX,KX),Q3(IX,KX),Q4(IX,KX)
2422	COMMON/PAR/GAMMA,REYREF,ALFA,ALFAI,REDFRE,AMINF,ALFAI
2423	COMMON/SURF/PSUR(IX)
2424	COMMON/SKINCF/CF(IX)
2425	COMMON/MUTUR/CMU(IX,KX)
2426	COMMON/TITL/ITITLE
2427	CHARACTER ITITLE*80
2428	DIMENSION ON FY(IX,KX)
2429	DUM = 0.
2430	CODE = 0.
2431	IRIS = IFIX(RES)
2432	ALFAD = ALFA * 45. / ATAN(1.)
2433	CMUL = AMINF / REYREF
2434	DO 10 K = 1 , KMAX
2435	DO 10 I = 1 , IMAX
2436	FY(I,K) = 0.
2437	10 CMU(I,K) = CMU(I,K) / CMUL
2438	WRITE(4) ITITLE
2439	WRITE(4) IMAX,KMAX,ITEL,ITEU,AMINF,ALFAD,RREAL,DUM,NSTPT,GAMMA,
2440	+ CODE,RES,DUM
2441	WRITE(4) Q1,Q2,Q3,Q4
2442	WRITE(4) RESD
2443	WRITE(4) PSUR
2444	WRITE(4) CF
2445	WRITE(4) CLB,CDPH
2446	WRITE(4) CMU
2447	WRITE(4) FY
2448	WRITE(4) TK
2449	WRITE(4) TE
2450	RETURN
2451	END

LINE # SOURCE TEXT

```

2452 SUBROUTINE OUTNT(NOUT,NSTPP,TIME,REREAL)
2453 PARAMETER (IX=180,KX=60)
2454 COMMON/GRID1/X(IX,K),Z(IX,KX)
2455 COMMON/PAR/GAMMA,REYREF,ALFA,ALFA1,REDFRE,AMINF,ALFAI
2456 COMMON/DGRID/DT,IMAX,KMAX,ITEL,ITEU
2457 COMMON/FLOW/Q1(IX,KX),Q2(IX,KX),Q3(IX,KX),Q4(IX,KX)
2458 ITN = NSTPP
2459 PI = 4.*ATAN(1.)
2460 ALFAD=ALFA*(180./PI)
2461 IF( ITN .EQ. 1*NOUT ) THEN
2462 REWIND 31
2463 WRITE (31) IMAX , KMAX
2464 WRITE (31) ( ( X(I,K), I=1,IMAX ), K=1,KMAX )
2465 WRITE (31) ( ( Z(I,K), I=1,IMAX ), K=1,KMAX )
2466 WRITE (31) IMAX , KMAX
2467 WRITE (31) AMINF, ALFAD, REREAL, TIME
2468 WRITE (31) ( ( Q1(I,K), I=1,IMAX ), K=1,KMAX )
2469 WRITE (31) ( ( Q2(I,K), I=1,IMAX ), K=1,KMAX )
2470 WRITE (31) ( ( Q3(I,K), I=1,IMAX ), K=1,KMAX )
2471 WRITE (31) ( ( Q4(I,K), I=1,IMAX ), K=1,KMAX )
2472 REWIND 31
2473 END IF
2474 IF( ITN .EQ. 2*NOUT ) THEN
2475 REWIND 32
2476 WRITE (32) IMAX , KMAX
2477 WRITE (32) ( ( X(I,K), I=1,IMAX ), K=1,KMAX )
2478 WRITE (32) ( ( Z(I,K), I=1,IMAX ), K=1,KMAX )
2479 WRITE (32) IMAX , KMAX
2480 WRITE (32) AMINF, ALFAD, REREAL, TIME
2481 WRITE (32) ( ( Q1(I,K), I=1,IMAX ), K=1,KMAX )
2482 WRITE (32) ( ( Q2(I,K), I=1,IMAX ), K=1,KMAX )
2483 WRITE (32) ( ( Q3(I,K), I=1,IMAX ), K=1,KMAX )
2484 WRITE (32) ( ( Q4(I,K), I=1,IMAX ), K=1,KMAX )
2485 REWIND 32
2486 END IF
2487 IF( ITN .EQ. 3*NOUT ) THEN
2488 REWIND 33
2489 WRITE (33) IMAX , KMAX
2490 WRITE (33) ( ( X(I,K), I=1,IMAX ), K=1,KMAX )
2491 WRITE (33) ( ( Z(I,K), I=1,IMAX ), K=1,KMAX )
2492 WRITE (33) IMAX , KMAX
2493 WRITE (33) AMINF, ALFAD, REREAL, TIME
2494 WRITE (33) ( ( Q1(I,K), I=1,IMAX ), K=1,KMAX )
2495 WRITE (33) ( ( Q2(I,K), I=1,IMAX ), K=1,KMAX )
2496 WRITE (33) ( ( Q3(I,K), I=1,IMAX ), K=1,KMAX )
2497 WRITE (33) ( ( Q4(I,K), I=1,IMAX ), K=1,KMAX )
2498 REWIND 33
2499 END IF
2500 IF( ITN .EQ. 4*NOUT ) THEN
2501 REWIND 34
2502 WRITE (34) IMAX , KMAX
2503 WRITE (34) ( ( X(I,K), I=1,IMAX ), K=1,KMAX )
2504 WRITE (34) ( ( Z(I,K), I=1,IMAX ), K=1,KMAX )
2505 WRITE (34) IMAX , KMAX
2506 WRITE (34) AMINF, ALFAD, REREAL, TIME
2507 WRITE (34) ( ( Q1(I,K), I=1,IMAX ), K=1,KMAX )
2508 WRITE (34) ( ( Q2(I,K), I=1,IMAX ), K=1,KMAX )
2509 WRITE (34) ( ( Q3(I,K), I=1,IMAX ), K=1,KMAX )
2510 WRITE (34) ( ( Q4(I,K), I=1,IMAX ), K=1,KMAX )
2511 REWIND 34
2512 END IF
2513 IF( ITN .EQ. 5*NOUT ) THEN
2514 REWIND 35
2515 WRITE (35) IMAX , KMAX
2516 WRITE (35) ( ( X(I,K), I=1,IMAX ), K=1,KMAX )
2517 WRITE (35) ( ( Z(I,K), I=1,IMAX ), K=1,KMAX )
2518 WRITE (35) IMAX , KMAX
2519 WRITE (35) AMINF, ALFAD, REREAL, TIME
2520 WRITE (35) ( ( Q1(I,K), I=1,IMAX ), K=1,KMAX )
2521 WRITE (35) ( ( Q2(I,K), I=1,IMAX ), K=1,KMAX )
2522 WRITE (35) ( ( Q3(I,K), I=1,IMAX ), K=1,KMAX )
2523 WRITE (35) ( ( Q4(I,K), I=1,IMAX ), K=1,KMAX )
2524 REWIND 35
2525 END IF
2526 IF( ITN .EQ. 6*NOUT ) THEN
2527 REWIND 36
2528 WRITE (36) IMAX , KMAX
2529 WRITE (36) ( ( X(I,K), I=1,IMAX ), K=1,KMAX )
2530 WRITE (36) ( ( Z(I,K), I=1,IMAX ), K=1,KMAX )
2531 WRITE (36) IMAX , KMAX
2532 WRITE (36) AMINF, ALFAD, REREAL, TIME
2533 WRITE (36) ( ( Q1(I,K), I=1,IMAX ), K=1,KMAX )
2534 WRITE (36) ( ( Q2(I,K), I=1,IMAX ), K=1,KMAX )
2535 WRITE (36) ( ( Q3(I,K), I=1,IMAX ), K=1,KMAX )
2536 WRITE (36) ( ( Q4(I,K), I=1,IMAX ), K=1,KMAX )
2537 REWIND 36
2538 END IF
2539 IF( ITN .EQ. 7*NOUT ) THEN
2540 REWIND 37
2541 WRITE (37) IMAX , KMAX
2542 WRITE (37) ( ( X(I,K), I=1,IMAX ), K=1,KMAX )
2543 WRITE (37) ( ( Z(I,K), I=1,IMAX ), K=1,KMAX )
2544 WRITE (37) IMAX , KMAX
2545 WRITE (37) AMINF, ALFAD, REREAL, TIME
2546 WRITE (37) ( ( Q1(I,K), I=1,IMAX ), K=1,KMAX )
2547 WRITE (37) ( ( Q2(I,K), I=1,IMAX ), K=1,KMAX )
2548 WRITE (37) ( ( Q3(I,K), I=1,IMAX ), K=1,KMAX )
2549 WRITE (37) ( ( Q4(I,K), I=1,IMAX ), K=1,KMAX )
2550 REWIND 37
2551 END IF
2552 IF( ITN .EQ. 8*NOUT ) THEN
2553 REWIND 38
2554 WRITE (38) IMAX , KMAX
2555 WRITE (38) ( ( X(I,K), I=1,IMAX ), K=1,KMAX )
2556 WRITE (38) ( ( Z(I,K), I=1,IMAX ), K=1,KMAX )
2557 WRITE (38) IMAX , KMAX
2558 WRITE (38) AMINF, ALFAD, REREAL, TIME
2559 WRITE (38) ( ( Q1(I,K), I=1,IMAX ), K=1,KMAX )
2560 WRITE (38) ( ( Q2(I,K), I=1,IMAX ), K=1,KMAX )
2561 WRITE (38) ( ( Q3(I,K), I=1,IMAX ), K=1,KMAX )
2562 WRITE (38) ( ( Q4(I,K), I=1,IMAX ), K=1,KMAX )
2563 REWIND 38
2564 END IF
2565 IF( ITN .EQ. 9*NOUT ) THEN
2566 REWIND 39
2567 WRITE (39) IMAX , KMAX
2568 WRITE (39) ( ( X(I,K), I=1,IMAX ), K=1,KMAX )
2569 WRITE (39) ( ( Z(I,K), I=1,IMAX ), K=1,KMAX )
2570 WRITE (39) IMAX , KMAX
2571 WRITE (39) AMINF, ALFAD, REREAL, TIME

```

LINE # SOURCE TEXT

```

2572 WRITE (39) ( ( Q1(I,K), I=1,IMAX ), K=1,KMAX )
2573 WRITE (39) ( ( Q2(I,K), I=1,IMAX ), K=1,KMAX )
2574 WRITE (39) ( ( Q3(I,K), I=1,IMAX ), K=1,KMAX )
2575 WRITE (39) ( ( Q4(I,K), I=1,IMAX ), K=1,KMAX )
2576 END IF
2577 IF( ITN .EQ. 10*NOUT ) THEN
2578 REWIND 40
2579 WRITE (40) IMAX , KMAX
2580 WRITE (40) ( ( X(I,K), I=1,IMAX ), K=1,KMAX )
2581 WRITE (40) ( ( Z(I,K), I=1,IMAX ), K=1,KMAX )
2582 WRITE (40) IMAX , KMAX
2583 WRITE (40) AMINF, ALFAD, REREAL, TIME
2584 WRITE (40) ( ( Q1(I,K), I=1,IMAX ), K=1,KMAX )
2585 WRITE (40) ( ( Q2(I,K), I=1,IMAX ), K=1,KMAX )
2586 WRITE (40) ( ( Q3(I,K), I=1,IMAX ), K=1,KMAX )
2587 WRITE (40) ( ( Q4(I,K), I=1,IMAX ), K=1,KMAX )
2588 END IF
2589 IF( ITN .EQ. 11*NOUT ) THEN
2590 REWIND 41
2591 WRITE (41) IMAX , KMAX
2592 WRITE (41) ( ( X(I,K), I=1,IMAX ), K=1,KMAX )
2593 WRITE (41) ( ( Z(I,K), I=1,IMAX ), K=1,KMAX )
2594 WRITE (41) IMAX , KMAX
2595 WRITE (41) AMINF, ALFAD, REREAL, TIME
2596 WRITE (41) ( ( Q1(I,K), I=1,IMAX ), K=1,KMAX )
2597 WRITE (41) ( ( Q2(I,K), I=1,IMAX ), K=1,KMAX )
2598 WRITE (41) ( ( Q3(I,K), I=1,IMAX ), K=1,KMAX )
2599 WRITE (41) ( ( Q4(I,K), I=1,IMAX ), K=1,KMAX )
2600 END IF
2601 IF( ITN .EQ. 12*NOUT ) THEN
2602 REWIND 42
2603 WRITE (42) IMAX , KMAX
2604 WRITE (42) ( ( X(I,K), I=1,IMAX ), K=1,KMAX )
2605 WRITE (42) ( ( Z(I,K), I=1,IMAX ), K=1,KMAX )
2606 WRITE (42) IMAX , KMAX
2607 WRITE (42) AMINF, ALFAD, REREAL, TIME
2608 WRITE (42) ( ( Q1(I,K), I=1,IMAX ), K=1,KMAX )
2609 WRITE (42) ( ( Q2(I,K), I=1,IMAX ), K=1,KMAX )
2610 WRITE (42) ( ( Q3(I,K), I=1,IMAX ), K=1,KMAX )
2611 WRITE (42) ( ( Q4(I,K), I=1,IMAX ), K=1,KMAX )
2612 END IF
2613 IF( ITN .EQ. 13*NOUT ) THEN
2614 REWIND 43
2615 WRITE (43) IMAX , KMAX
2616 WRITE (43) ( ( X(I,K), I=1,IMAX ), K=1,KMAX )
2617 WRITE (43) ( ( Z(I,K), I=1,IMAX ), K=1,KMAX )
2618 WRITE (43) IMAX , KMAX
2619 WRITE (43) AMINF, ALFAD, REREAL, TIME
2620 WRITE (43) ( ( Q1(I,K), I=1,IMAX ), K=1,KMAX )
2621 WRITE (43) ( ( Q2(I,K), I=1,IMAX ), K=1,KMAX )
2622 WRITE (43) ( ( Q3(I,K), I=1,IMAX ), K=1,KMAX )
2623 WRITE (43) ( ( Q4(I,K), I=1,IMAX ), K=1,KMAX )
2624 END IF
2625 IF( ITN .EQ. 14*NOUT ) THEN
2626 REWIND 44
2627 WRITE (44) IMAX , KMAX
2628 WRITE (44) ( ( X(I,K), I=1,IMAX ), K=1,KMAX )
2629 WRITE (44) ( ( Z(I,K), I=1,IMAX ), K=1,KMAX )
2630 WRITE (44) IMAX , KMAX
2631 WRITE (44) AMINF, ALFAD, REREAL, TIME
2632 WRITE (44) ( ( Q1(I,K), I=1,IMAX ), K=1,KMAX )
2633 WRITE (44) ( ( Q2(I,K), I=1,IMAX ), K=1,KMAX )
2634 WRITE (44) ( ( Q3(I,K), I=1,IMAX ), K=1,KMAX )
2635 WRITE (44) ( ( Q4(I,K), I=1,IMAX ), K=1,KMAX )
2636 END IF
2637 RETURN
2638 END

```

LINE # SOURCE TEXT

```

1 PROGRAM AIRFGRID
2 PARAMETER (IX=100,KX=100)
3 COMMON/GRID1/X(IX,KX),Z(IX,KX)
4 COMMON/DGRID/DT,IMAX,KMAX,ITEL,ITEU
5 LOGICAL VISCOUS
6 READ(5,10)
7 READ(5,100) IMAX,KMAX
8 READ(5,10)
9 READ(5,100) ITEL,ITEU
10 READ(5,10)
11 READ(5,200) VISCOUS
12 READ(5,10)
13 READ(5,300) DMIN
14 READ(5,10)
15 READ(5,*) AORAT , AOEXP , sdispl
16 ILE = ( ITEU + ITEL ) / 2
17 IUP = ( ITEU - ITEL ) / 2
18 WRITE(6,1000) IMAX,KMAX,ITEL,ITEU,ILE,IUP,DMIN,AORAT
19 1000 FORMAT('Imax = ',I10,10x,'kmax = ',I10,5x,/,
20 1 'Trailing edge lower = ',I10,/,
21 2 'Trailing edge upper = ',I10,/,
22 2 'Leading edge = ',I10,/,
23 2 'Iupper = Ilower = ',I10,/,
24 3 'Distance of the first point = ',F20,10,/,
25 4 'Stretching ratio = ',F20,10,/)
26 CALL AIRFOL( AORAT , AOEXP , sdispl )
27 IF( VISCOUS ) CALL CLUSTR( DMIN )
28 C
29 WRITE(6,1100)
30 1100 FORMAT(//,'GRID BOUNDARIES',/)
31 RTEOUT = ABS( X(1,1) - X(ITEL,1) )
32 RLEIN = ABS( X(ILE,KMAX) - X(ILE,1) )
33 IUP = ILE + ( ITEU - ILE ) / 2
34 RUP = ABS( Z(IUP,KMAX) - Z(IUP,1) )
35 WRITE(6,1200) RTEOUT , RLEIN , RUP
36 1200 FORMAT(5X,'Distance between trailing edge ans outflow = ',F20,10,/,
37 1 5x,'Distance " leading edge and inflow = ',F20,10,/,
38 2 5x,'Distance of the body from the upper boudary = ',F20,10,/)
39 REWIND 21
40 WRITE (21) IMAX,KMAX
41 WRITE (21) (( X(I,K), I=1,IMAX), K=1,KMAX ),
42 1 (( Z(I,K), I=1,IMAX), K=1,KMAX )
43 STOP
44 10 FORMAT(1X)
45 100 FORMAT(2I5)
46 200 FORMAT(3L5)
47 300 FORMAT(4F10,0)
48 END

```

LINE #	SOURCE TEXT
49	SUBROUTINE METRIC
50	C.....
51	C*
52	C*
53	C*
54	C.....
55	PARAMETER (IX=300,KX=100)
56	COMMON/FIX/OMEGA,HDOT
57	COMMON/DGRID/DT,IMAX,KMAX,ITEL,ITEU
58	COMMON/GRID1/X(IX,KX),Z(IX,KX)
59	COMMON/GRID/YACOB(IX,KX)
60	COMMON/MTRIX/XIX(IX,KX),XIZ(IX,KX),ZETAX(IX,KX),ZETAZ(IX,KX),
61	XIT(IX,KX),ZETAT(IX,KX)
62	C
63	C*** THE SUBROUTINE METRIC COMPUTES THE METRICS IN ALL THE TWO DIRECTIONS AND
64	C THE UNSTEADY COEFFICIENTS ETAT ETC.
65	C
66	DO 1000 K = 1 , KMAX
67	DO 1000 I = 1 , IMAX
68	XTAU = OMEGA * Z(I,K)
69	YTAU = OMEGA * (-X(I,K))- HDOT
70	C*** PRESENT SET UP IS FOR FLOW PAST AN AIRFOIL.
71	C
72	IF(I.EQ.1.OR.I.EQ.IMAX) GO TO 10
73	XXI = .5 * (X(I+1,K)-X(I-1,K))
74	ZXI = .5 * (Z(I+1,K)-Z(I-1,K))
75	GO TO 15
76	10 IF(I.EQ.IMAX) GO TO 16
77	XXI = 1.0 * (X(2,K) - X(1,K))
78	ZXI = 1.0 * (Z(2,K) - Z(1,K))
79	GO TO 15
80	16 XXI = 1.0 * (X(IMAX,K) - X(IMAX-1,K))
81	ZXI = 1.0 * (Z(IMAX,K) - Z(IMAX-1,K))
82	15 CONTINUE
83	IF(K.EQ.1.OR.K.EQ.KMAX) GO TO 17
84	XZET = .5 * (X(1,K+1)-X(1,K-1))
85	ZZET = .5 * (Z(1,K+1)-Z(1,K-1))
86	GO TO 20
87	17 IF(K.EQ.KMAX) GO TO 18
88	XZET = 2. * X(1,2)-1.5 * X(1,1) - .5 * X(1,3)
89	ZZET = 2. * Z(1,2) - 1.5 * Z(1,1) - .5 * Z(1,3)
90	GO TO 20
91	18 XZET = 1.5 * X(1,KMAX)-2. * X(1,KMAX-1)+.5*X(1,KMAX-2)
92	ZZET = 1.5 * Z(1,KMAX)-2. * Z(1,KMAX-1)+.5*Z(1,KMAX-2)
93	20 CONTINUE
94	YACOB1 = XXI * ZZET - XZET * ZXI
95	YACOB(I,K) = 1. / YACOB1
96	XIX(I,K) = ZZET * YACOB(I,K)
97	XIZ(I,K) = -XZET * YACOB(I,K)
98	XTAU = OMEGA * Z(I,K)
99	YTAU = - OMEGA * X(I,K)- HDOT
100	XIT(I,K) = - XIX(I,K) * XTAU - XIZ(I,K) * YTAU
101	ZETAX(I,K) = -ZXI * YACOB(I,K)
102	ZETAZ(I,K) = XXI * YACOB(I,K)
103	ZETAT(I,K) = - ZETAX(I,K) * XTAU - ZETAZ(I,K) * YTAU
104	1000 CONTINUE
105	RETURN
106	END

LINE #	SOURCE TEXT
107	SUBROUTINE WRAP(II,JJ,XSING,YSING,XP,YP,S0,A0,Y0)
108
109	C.....
110	C* SUBROUTINE WRAP
111	C*.....
112	C.....
113	PARAMETER (IX=300,KX=100)
114	DIMENSION S0(IX,4),Y0(IX,4),A0(IX,4),XP(1),YP(1)
115	
116	THIS SUBROUTINE UNWRAPS THE AIRFOIL AND STORES THE UNWRAPPED
117	SURFACE IN ARRAYS A0 AND S0. IT ALSO DETERMINES THE STRETCHING
118	IN THE ETA DIRECTION.
119	
120	IMID = (II + 1) / 2
121	DY = .8 / (JJ - 2)
122	DO 1 J = 2, JJ
123	Y = FLOAT(J-2) * DY
124	1 Y0(J,1) = 1.25 * Y / (1. - Y * Y)
125	Y0(1,1) = - Y0(3,1)
126	PI = 4. * ATAN (1.)
127	ANGL = PI + PI
128	U = XP(1) - XSING
129	V = YP(1) - YSING
130	U = 1.
131	V = 0
132	IIM1 = II - 1
133	DO 2 I = 1, IIM1
134	X11 = XP(I) - XSING
135	Y11 = YP(I) - YSING
136	ANGL = ANGL + ATAN2((U*Y11-V*X11),(U*X11+V*Y11))
137	R = SQRT(X11**2 + Y11**2)
138	U = X11
139	V = Y11
140	R = SQRT(R)
141	A0(I,1) = R * COS(.5 * ANGL)
142	2 S0(I,1) = R * SIN(.5 * ANGL)
143	C WRITE (6,1000)
144	C WRITE (6,2000) (I,A0(I,1),S0(I,1),I = 1, IIM1)
145	C RETURN
146	1000 FORMAT(1X,'UNWRAPPED COORDINATES IN THE TRANSFORMED PLANE')
147	2000 FORMAT(15, 2F20.8)
148	END

LINE #	SOURCE TEXT
149	SUBROUTINE TABINT(XP,YP,XSING,YSING,N,sdispl)
150	C*****
151	C*
152	C*
153	C*
154	C*****
155	PARAMETER (IX=300,KX=100)
156	DIMENSION XP(IX),YP(IX),SO(IX),AO(IX),DTHXI(IX),DXW(IX),DX(IX)
157	COMMON/DGRID/DT,IMAX,KMAX,ITEL,ITEU,ILE
158	PI = 4.*ATAN(1.)
159	U = XP(1) - XSING
160	V = YP(1) - YSING
161	U = 1.
162	V = 0.
163	ANGL = 8. * ATAN(1.)
164	DO 1 I = 1,N
165	X11 = XP(I) - XSING
166	Y11 = YP(I) - YSING
167	ANGL = ANGL + ATAN2((U*Y11-V*X11),(U*X11+V*Y11))
168	R = SQRT(X11**2 + Y11 ** 2)
169	U = X11
170	V = Y11
171	R = SQRT(R)
172	AO(I) = R * COS(ANGL * .5)
173	1 SO(I) = R * SIN(ANGL * .5)
174	C
175	AO1 = AO(N) - AO(1)
176	DXWS = 0.0
177	C
178	AOST = AO(1)
179	idiv = 1 + (iteu - itel)
180	C
181	THDX = 0.
182	DTHXI(1) = 0.
183	DTHXI(2) = pi* SDISPL/2.
184	DTHXI = (1.- SDISPL) * PI / (IDIV-1)
185	DO 9 I= 3,IDIV
186	9 DTHXI(I) = DTHXI(I-1) + DTHXI
187	DO 10 I = 1,IDIV
188	THDX = (I-1)*DTHXI
189	if(i .eq. 2 .or. i .eq. idiv) then
190	if(i .eq. 2)
191	if(i .eq. idiv)
192	else
193	thdx = tdx
194	endif
195	THDX = DTHXI(I)
196	thdx = (180/pi)*thdx
197	C
198	write(6,*) I, thdx
199	DXW(I) = abs (SIN(THDX))
200	10 DXWS = DXWS + DXW(I)
201	DO 20 I = 1,IDIV
202	20 DX(I) = DXW(I) * AO1 / DXWS
203	DXI = 0.
204	DO 3 I = 1 , IDIV
205	DXI = DXI + DX(I)
206	XX = DXI + AOST
207	CALL TAIN(TA0,SO,XX,YY,N,3,NER,MON)
208	XP(I) = XX * XX - YY * YY + XSING
209	3 YP(I) = 2. * XX * YY + YSING
210	RETURN
211	END

LINE # SOURCE TEXT

```
211 C
212 SUBROUTINE TAIN(TAB,FTAB,X,FX,N,E,NER,MON)
213 C.....
214 C
215 SUBROUTINE TAIN
216 C.....
217 C
218 PARAMETER (IX=300,EX=100)
219 DIMENSION TAB(1),FTAB(1),T(10),C(10)
220 C
221 NASA - AMES SUBROUTINE FOR POLYNOMIAL INTERPOLATION
222 OF A TABULATED FUNCTION
223 C
224 IF(N-E) 1, 1, 2
225 1 NER = 2
226 RETURN
227 2 IF(K-9) 3,3,1
228 3 IF(MON) 4,4,5
229 5 IF(MON-2) 6,7,4
230 4 J = 0
231 NML = N - 1
232 DO 8 I = 1, NML
233 IF(TAB(I) - TAB(I+1)) 9,11,10
234 11 NER = 3
235 RETURN
236 9 J = J-1
237 GO TO 8
238 10 J = J+1
239 8 CONTINUE
240 MON = 1
241 IF(J) 12, 6, 6
242 12 MON = 2
243 7 DO 13 I = 1, N
244 IF(X - TAB(I)) 14,14,13
245 14 J = I
246 GO TO 18
247 13 CONTINUE
248 GO TO 15
249 6 DO 16 I = 1, N
250 IF(X-TAB(I)) 16,17,17
251 17 J = I
252 GO TO 18
253 16 CONTINUE
254 15 J = N
255 18 J = J - (K-1) / 2
256 IF(J) 19,19,20
257 19 J = 1
258 20 M = J + K
259 IF(M - N) 21,21,22
260 22 J = J - 1
261 GO TO 20
262 21 KP1 = K + 1
263 JSAVE = J
264 26 DO 23 L = 1, KP1
265 C(L) = X - TAB(J)
266 T(L) = FTAB(J)
267 23 J = J+1
268 DO 24 J = 1,K
269 I = J+1
270 25 T(I) = (C(J)*T(I)-C(I)*T(J))/(C(J)-C(I))
271 I = I+1
272 IF(I-EP1) 25,25,24
273 24 CONTINUE
274 FX = T(KP1)
275 NER = 1
276 RETURN
277 END
```

LINE #	SOURCE TEXT
278	SUBROUTINE SING(N2,N,X,Z,XLE,YLE,TEA,TES,XSING,YSING,CHD)
279	C*****
280	C*
281	C* SUBROUTINE SING
282	C*
283	C*****
284	PARAMETER (IX=300,KX=100)
285	C
286	C
287	C THIS SUBROUTINE COMPUTES SINGULAR POINT LOCATIONS.
288	C
289	DIMENSION X(2) , Z(2)
290	NU = N2
291	N1 = N2 + 1
292	N3 = N2 - 1
293	X1 = X(N1)
294	Z1 = Z(N1)
295	X2 = X(N2)
296	Z2 = Z(N2)
297	X3 = X(N3)
298	Z3 = Z(N3)
299	D1 = X2 ** 2 - X1 ** 2
300	D2 = Z2 ** 2 - Z1 ** 2
301	D3 = X2 - X1
302	D4 = Z2 - Z1
303	D5 = X3 ** 2 - X1 ** 2
304	D6 = Z3 ** 2 - Z1 ** 2
305	D7 = X3 - X1
306	D8 = Z3 - Z1
307	B = (D7 * (D1 + D2) - D3*(D5+D6))/(2.*(D7*D4-D3*D8))
308	IF(ABS(D3).LT.ABS(D7)) GO TO 10
309	A = (D1 + D2 - 2. * B * D4) / (2. * D3)
310	GO TO 20
311	10 A = (D5 + D6 - 2. * B * D8) / (2. * D7)
312	20 CONTINUE
313	R = SQRT((X2-A)** 2 + (Z2-B)**2)
314	XLE = X(NU)
315	YLE = Z(NU)
316	CHD = X(1) - X(NU)
317	A2 = (Z(2)-Z(1))/(X(2) - X(1))
318	A1 = (Z(N)-Z(N-1))/(X(N)-X(N-1))
319	TES = .5 * (A1 + A2)
320	TEA = A2 - A1
321	TEA = TEA + 57.29578
322	XSING = (A+XLE) /2.
323	YSING = (B+YLE) / 2.
324	RETURN
325	END

LINE # SOURCE TEXT

```

326 SUBROUTINE AIRPOL( AORAT , a0exp ,edispl)
327 C.....
328 C* SUBROUTINE AIRPOL
329 C.....
330 PARAMETER (IX=300,KX=100)
331 COMMON/GRID1/X(IX,KX),Z(IX,KX)
332 COMMON/DGRID/DT,IMAX,KMAX,ITEL,ITEU
333 COMMON/YSYM/ISYM
334 DIMENSION SO(IX,4),AO(IX,4),YO(IX,4),XP(IX),YP(IX),
335 1E(IX),F(IX),B0(IX)
336 DIMENSION XL(IX),XU(IX),YL(IX),YU(IX),
337 2 XX(IX),YY(IX)
338
339 DATA (B0(I),I=1,32)/1.,1.0414,1.0836,1.1270,1.1715,1.2175,1.2651,
340 11.3145,1.3659,1.4199,1.4755,1.5349,1.5973,1.6636,1.7342,1.8099,
341 21.8914,1.9799,2.0764,2.1829,2.3012,2.4341,2.5853,2.7597,2.9646,
342 33.2106,3.5141,3.9019,4.4219,5.1687,6.3632,8.6809/
343
344 READ(5,*) ISYM, IBMAX
345 IF( ISYM .EQ. 1 ) THEN
346 DO 101 I=1,IBMAX
347 READ(5,*) XU(I), YU(I)
348 ELSE
349 DO 102 I=1,IBMAX
350 READ(5,*) XU(I), YU(I), YL(I)
351 102 CONTINUE
352 ENDDIF
353 IF( ISYM .EQ. 1 ) THEN
354 DO 103 I=1,IBMAX
355 103 YL(I) = - YU(I)
356 ENDDIF
357 C
358 DO 1000 I=1,IBMAX
359 IU = I + IBMAX
360 IX(IU) = XU(I)
361 YY(IU) = YU(I)
362 IL = IBMAX - I + 1
363 IX(IL) = XU(IL)
364 YY(IL) = YL(IL)
365 1000 CONTINUE
366 C
367 IBMAX2 = 2*IBMAX
368 DO 1010 I=1,IBMAX2
369 XP(I) = XX(I)
370 YP(I) = YY(I)
371 1010 CONTINUE
372 FNU = IBMAX
373 FNL = IBMAX
374 C
375 THIS SUBROUTINE GENERATES SHEAR PARABOLIC C-GRID
376 C THE FOLLOWING SUBROUTINES ARE RELATED TO THE GRID GENERATION
377 C WRAP SING
378 C TABINT CLUSTR
379 C TAINI STRIC
380 C
381 AO(1,1) = 1.
382 DO 8 I = 2 , IBMAX
383 8 AO(I,1) = ( AO(I-1,1) * AORAT )**AOEXP
384 PI = 4. * ATAN(1.)
385 NU = FNU
386 NL = FNL
387 N = NU + NL
388 IT = ITEL
389 IE = ITEU
390 ILE = ( ITEL + ITEU ) / 2
391 II = IMAX
392 JJ = KMAX-1
393 IIP1 = II + 1
394 IIM1 = II - 1
395 IIJJ = II * JJ
396 IIJJ2 = II * ( JJ-2)
397 C
398 SCALE = 1. / ( XP(1) - XP(NL) )
399 DO 3333 I=1,N
400 XP(I) = XP(I) * SCALE
401 YP(I) = YP(I) * SCALE
402 3333 CONTINUE
403 CALL SING(NU,N,XP,YP,XLE,ZLE,TEA,TES,XSING,YSING,CBD)
404 CALL TABINT(XP,YP,XSING,YSING,N,edispl)
405 NBODY = IE + 1 - IT
406 DO 6791 I = 1 , NBODY
407 L = I - 1
408 E(IT+L) = XP(I)
409 6791 F(IT+L) = YP(I)
410 IEP1 = IE + 1
411 SLOPT = TES * .75
412 DO 438 I = IEP1 , II
413 II = I + 1 - IE
414 E(I) = AO(II,1)
415 DXI = 1. / 48.
416 D = 4. / 3. * (E(I) - .25)
417 F(I) = F(IE) + SLOPT * ALOG(D) / D
418 L = IIP1 - I
419 E(L) = E(I)
420 F(L) = F(IT) + SLOPT * ALOG(D)/D
421 C
422 WRITE (6,439)
423 439 FORMAT(2X,3H I,19X,19X,19X)
424 C
425 WRITE (6,37) (I,E(I),F(I),I = 1 , II)
426 CALL WRAP(II,JJ,XSING,YSING,E,F,SO,AO,YO)
427 DO 10 J = 2 , JJ
428 DO 10 I = 1 , II
429 X(I,J-1) = AO(I,1)**2 - (SO(I,1)*YO(J,1))**2
430 Z(I,J-1) = 2. * AO(I,1) * (SO(I,1)*YO(J,1))
431 RETURN
432 37 FORMAT(15,F20.8)
433 END

```

```
LINE #      SOURCE TEXT
432      SUBROUTINE CLUSTR(DS)
433      C-----
434      C*
435      C*      SUBROUTINE CLUSTR
436      C*
437      C-----
438      PARAMETER (IX=300,KX=100)
439      COMMON/GRID1/X(IX,KX),Z(IX,KX)
440      COMMON/DGRID/DT,IMAX,KMAX,ITEL,ITEU
441      DIMENSION S(IX),XP(IX),YP(IX),R(IX)
442
443      C
444      C      THIS SUBROUTINE CLUSTERS A GIVEN X,Z GRID SUCH THAT THE FIRST POINT IS AT
445      C
446      DO 100 I = 1 , IMAX
447      S(I) = 0.
448      XP(I) = X(I,1)
449      YP(I) = Z(I,1)
450      DO 10 K = 2 , KMAX
451      XP(K) = X(I,K)
452      YP(K) = Z(I,K)
453      10 S(K) = SQRT((XP(K)-XP(K-1))**2+(YP(K)-YP(K-1))**2)
454      1+S(K-1)
455      SUMDX = S(KMAX)
456      CALL STATCH(SUMDX,DS,F1,KMAX,FACTOR)
457      C
458      WRITE (6,200) I,FACTOR
459      R(1) = 0.
460      DR = DS
461      DO 20 K = 2 , KMAX
462      R(K) = R(K-1) + DR
463      DR = DR * FACTOR
464      20 CONTINUE
465      RLAST = 1. / R(KMAX)
466      DO 30 K = 2 , KMAX
467      R1 = R(K) * RLAST * S(KMAX)
468      CALL TAIN(T,S,XP,R1,XP1,KMAX,3,NER,MON)
469      X(I,K) = XP1
470      CALL TAIN(T,S,YP,R1,Y1,Y1,KMAX,3,NER,MON)
471      Z(I,K) = Y1
472      30 CONTINUE
473      100 CONTINUE
474      C
475      WRITE (6,115)
476      DO 110 I = 1 , IMAX
477      DX = X(I,2) - X(I,1)
478      DY = Z(I,2) - Z(I,1)
479      DN = SQRT(DX*DX+DY*DY)
480      C
481      WRITE(6,120) I , DX , DY , DN
482      110 CONTINUE
483      RETURN
484      115 FORMAT(5X,6HNORMAL,1X,8HDISTANCE,3H AT,4H THE,5H WALL,/,
485      1,5H 1,8X,2HDX,8X,2HDY,8X,2HDN,/)
486      120 FORMAT(15,3F10.5)
487      200 FORMAT(15,F10.5)
488      END
```

LINE #	SOURCE TEXT
--------	-------------

485	SUBROUTINE STRTCH(SUMDX,DX1,F1,N1,R)
486	C*****
487	C*
488	C* SUBROUTINE STRTCH
489	C*
490	C*****
491	PARAMETER (IX=300,KX=100)
492	C
493	C THIS SUBROUTINE DETERMINES A GEOMETRIC
494	C PROGRESSION OF GRID SPACING BETWEEN 1 AND N1 SUCH THAT
495	C SUMSDX) EQUALS SUMDX. THE RATIO BETWEEN SUCCESSIVE
496	C SPACINGS IS R.
497	N = N1 - 1
498	R = 1.5
499	E1 = 1.E-04
500	E2 = 1.E-04
501	DO 10 I = 1, 50
502	F = (R-1) * SUMDX - DX1*(R**N-1)
503	FP = SUMDX - DX1 * FLOAT(N) * R ** (N-1)
504	RITER = R - F/ FP
505	C IF(1.E-02.LT.RITER.AND.RITER.LT.1.) RITER = 1.
506	C IF(1. LT.RITER.AND.RITER.LT.100.) RITER=.01
507	IF(ABS(R-RITER).LT. R*E1) GO TO 1
508	R = RITER
509	10 CONTINUE
510	R = 1.0001
511	C DX1 = DETOT/FLOAT(N1-1)
512	RETURN
513	1 R= RITER
514	RETURN
515	END

LINE # SOURCE TEXT

```
516 SUBROUTINE ROTGRID(INAX,KMAX,DALFA)
517 C*****
518 C*
519 C* SUBROUTINE ROTGRID
520 C*
521 C*****
522 PARAMETER (IX=300,KI=100)
523 C ROTATE GRID IN THE CLOCKWISE DIRECTION BY AN AMOUNT DALFA
524 COMMON/GRID1/X(IX,KI),Z(IX,KI)
525 CA = COS(DALFA)
526 SA = - SIN(DALFA)
527 DO 20 K = 1 , KMAX
528 DO 20 I = 1 , INAX
529 X1 = X(I,K)
530 Z1 = Z(I,K)
531 X(I,K) = X1 * CA - Z1 * SA
532 20 Z(I,K) = Z1 * CA + X1 * SA
533 RETURN
534 END
```


20. Ms. L. Cowles 1
Naval Air Development Center
Street Road
Warminster, PA 18974-5000
21. Dr. W. Tseng 1
Naval Air Development Center
Street Road
Warminster, PA 18974-5000
22. Mr. D. Findlay 1
Naval Air Development Center
Street Road
Warminster, PA 18974-5000
23. Mr. M. Walters 1
Naval Air Development Center
Street Road
Warminster, PA 18974-5000
24. Mr. W. J. King 1
Technology Area Manager, Aircraft
Code 212
Office of Naval Technology
Arlington, VA 22217-5000
25. Dr. T. Cebeci 1
Professor and Chairman
Dept. of Aerospace Engineering
California State University
Long Beach, CA 90840
26. Capt. H. Helin 1
Program Manager, Directorate of Aerospace Sciences
AFOSRNA
Bolling AFB
Washington, D.C. 20332-6448
27. Dr. T. L. Doligalski 1
Chief, Fluid Mechanics Division
Army Research Office
P.O. Box 1221
Research Triangle Park, NC 27709-2211
29. Lt. Col. Steven Grohsmeyer 2
P.O. Box 732
Venice, FL 34284

10. Dr. R. M. Howard 1
Dept. of Aeronautics and Astronautics, Code 67H0
Naval Postgraduate School
Monterey, CA 93943
11. Dr. S. K. Hebbar 1
Dept. of Aeronautics and Astronautics, Code 67HB
Naval Postgraduate School
Monterey, CA 93943
12. Dr. M. S. Chandrasekhara 1
NASA Ames Research Center (M.S. 260-1)
Moffet Field, CA 94035
13. Dr. L. W. Carr 1
NASA Ames Research Center (M.S. 260-1)
Moffet Field, CA 94035
14. Dr. L. E. Schiff 1
NASA Ames Research Center (M.S. 258-1)
Moffet Field, CA 94035
15. Mr. D. P. Bencze 1
Chief, Applied Aerodynamics Branch
NASA Ames Research Center (M.S. 227-6)
Moffet Field, CA 94035
16. Dr. S. Davis 1
NASA Ames Research Center (M.S. 260-1)
Moffet Field, CA 94035
17. Mr. T. S. Momiyama 1
Director, Aircraft Division
Code AIR-931
Naval Air Systems Command
Washington, D.C. 20631-9320
18. Mr. B. Neuman 1
Aircraft Division
Code AIR-931
Naval Air Systems Command
Washington, D.C. 20631-9320
19. Mr. G. Derderian 1
Aircraft Division
Code AIR-931
Naval Air Systems Command
Washington, D.C. 20631-9320

INITIAL DISTRIBUTION LIST

	No. Copies
1. Commandant of the Marine Corps Code TE 06 Headquarters, U.S. Marine Corps Washington, D.C. 20380-0001	1
2. Library, Code 52 Naval Postgraduate School Monterey, CA 93943-5002	2
3. Dr. J. A. Ekaterinaris NASA Ames Research Center (M.S. 260-1) Moffet Field, CA 94035	5
4. Defense Technical Information Center Cameron Station Alexandria, VA 22304-6145	2
5. Dr. E. R. Wood Chairman Dept. of Aeronautics and Astronautics, Code 67WD Naval Postgraduate School Monterey, CA 93943-5002	1
6. Dr. M. F. Platzler Dept. of Aeronautics and Astronautics, Code 67PL Naval Postgraduate School Monterey, CA 93943-5002	5
7. Dr. L. V. Schmidt Dept. of Aeronautics and Astronautics, Code 67SC Naval Postgraduate School Monterey, CA 93943-5002	1
8. Dr. R. P. Shreeve Dept. of Aeronautics and Astronautics, Code 67SF Naval Postgraduate School Monterey, CA 93943-5002	1
9. Dr. R. Kolar Dept. of Aeronautics and Astronautics, Code 67KJ Naval Postgraduate School Monterey, CA 93943-5002	1